



UiT The Arctic University of Norway

Faculty of Health Sciences

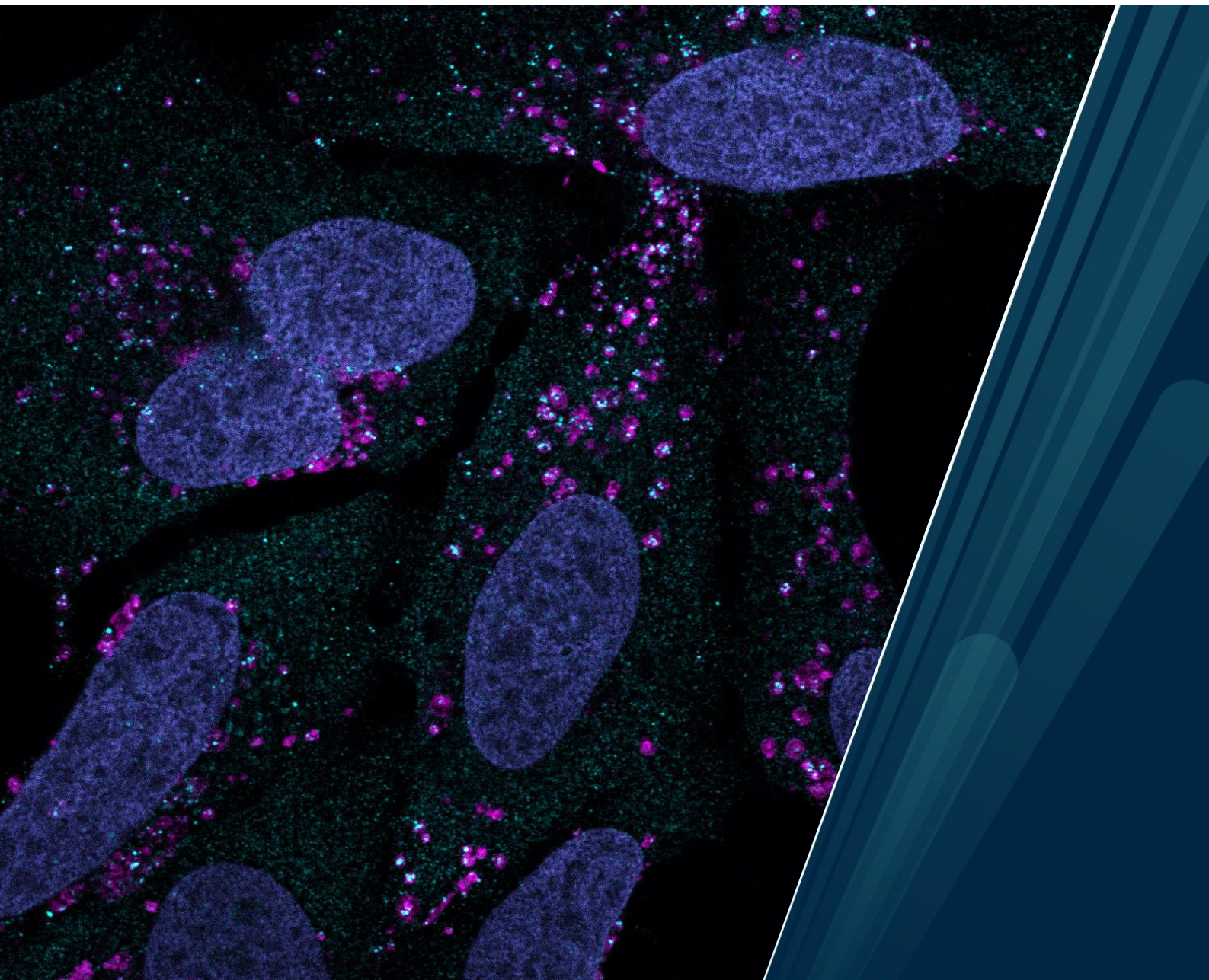
Department of Medical Biology

All roads lead to the lysosome: Exploring the degradation of TNIP1 by selective autophagy

Nikoline Lander Rasmussen

A dissertation for the degree of Philosophiae Doctor

January 2023



All roads lead to the lysosome: Exploring the degradation of TNIP1 by selective autophagy

Nikoline Lander Rasmussen

A dissertation for the degree of Philosophiae Doctor



UiT – The Arctic University of Norway

Faculty of Health Sciences

Department of Medical Biology

Autophagy Research Group

January 2023

© Nikoline Lander Rasmussen, 2023

Front page image: Confocal image of U2OS cells stained for TNIP1 (cyan) and LAMP1 (magenta) after 5 hours of Bafilomycin A1 treatment. Nuclei in blue.

Acknowledgements

The work presented in this thesis was performed at the Department of Medical Biology, Faculty of Health Sciences, UiT – the Arctic University of Norway, as part of the Autophagy Research Group (ARG).

First and foremost, I would like to thank my main supervisor Terje Johansen, for giving me the opportunity to perform this work in such a knowledgeable and resourceful lab. I appreciate all the feedback and opportunities you have given me over the course of this PhD journey. I am also grateful for the support and feedback from my co-supervisor Trond Lamark, who always had his door open for questions and discussions. The same goes for my second co-supervisor, Hallvard Olsvik, with whom I could always discuss ideas with and help to formulate research questions – and the methods to find the answers.

I also want to thank both past and present members of ARG: Anne, Anthimi, Aud, Birendra, Eva, Gry, Hanne, Jana, Juncal, Katrine, Marcus, Mireia, Mutugi, Pradip, Thanasis, Yakubu and Yu. One of the best things about this PhD has been to get to know all of you. I want to highlight Thanasis, Mireia, Juncal and Anthimi for their friendship, support, and encouragement also outside the lab. A special thank you to Gry and Aud for their valuable help in the lab, particularly during these last few critical months. And thank you to Jianwen Zhou and Jörn Dengjel for the great collaboration.

Finally, a big thank you to friends and family, especially: my 8th floor friends May-Britt, Kjersti and Susannah; Unn Beate for her long-distance support; fellow knitters from the geology department for inviting me along for some “stitch and bitch”; my parents, especially my mom for always being available for some “bæl og brok”; and of course Fredrik, who despite having his own PhD to go through, always had the time to lift me up and light up my day even during the darkest days of winter.

Nikoline Lander Rasmussen

January 2023

Table of Contents

Abbreviations	I
Summary	III
List of papers	IV
Introduction	1
Protein degradation systems	1
General autophagy	2
The many steps of autophagosome formation	4
Selective autophagy	8
Sequestosome-1-like receptors	9
LIR-ATG8 interactions	11
SAR-mediated autophagy induction	14
Other forms of autophagy	16
Chaperone-mediated autophagy	16
Microautophagy	17
Non-canonical autophagy pathways	18
“Non-canonical” lipidation	18
SARs bypassing the need for ATG8s in autophagy	19
Interplay between autophagy and immunity	20
Innate immune signaling	21
Toll-like receptor signaling and autophagy	21
TBK1 in autophagy and immunity	23
TNIP1	25
Aims of the study	31
Summary of papers	32
Discussion	34
Identification of TNIP1 as an autophagy substrate	34
Identification of LIRs and FIR in TNIP1	35
LIR-dependent degradation of TNIP1 upon inflammatory signaling	36
Role of TNIP1 degradation upon inflammatory stimuli: substrate or receptor?	38
LIR-independent basal degradation of TNIP1	41

Evolving selectivity in selective autophagy: NBR1 and TNIP1	43
Conclusions	44
Methodological considerations	45
Cell lines as model systems.....	45
CRISPR-Cas9 gene knockout	46
In vitro interaction studies.....	46
Transient and stable protein expression	47
Poly(I:C)-induced TLR3 signaling.....	48
Western blotting	48
References	50

Abbreviations

ABIN	A20-binding inhibitor of NF-kappa-B activation
AHD	ABIN homology domain
ATG	Autophagy-related genes
CALCOCO	Calcium-binding and coiled-coil domain-containing protein
CC	Coiled-coil
CMA	Chaperome-mediated autophagy
CRISPR	Clustered regularly interspaced short palindromic repeats
DAMP	Danger-associated molecular patterns
dsRNA/DNA	Double-stranded RNA/DNA
ER	Endoplasmic reticulum
ESCRT	Endosomal sorting complexes required for transport
FIP200	FAK family kinase-interacting protein of 200 kDa
FIR	FIP200-interacting region
FYCO1	FYVE and coiled-coil domain-containing protein 1
GABARAP	Gamma-aminobutyric acid receptor-associated protein
HSC70	Heat shock cognate 71 kDa protein
IKK	I-kappa-B kinase
ILV	Intraluminal vesicle
IRAK1/4	Interleukin-1 receptor-associated kinase 1
IRF3	Interferon regulatory factor 3
LAMP2A	Lysosome-associated membrane protein type 2A
LAP	LC3-associated phagocytosis
LDS	LIR-docking site
LIR	LC3-interacting region
LPS	Lipopolysaccharide
MAP1LC3	Microtubule-associated proteins 1A/1B light chain 3
MAPK	Mitogen-activated protein kinase
mPAS	Mammalian phagophore assembly site
mTOR	Mechanistic target of rapamycin
MVB	Multivesicular body
MyD88	Myeloid differentiation primary response protein 88
NBR1	Neighbor-of-BRCA 1
NCOA4	Nuclear receptor coactivator 4
NDP52	Nuclear dot protein 52
NEMO	NF-kappa-B essential modulator
NF-kB	Nuclear factor-kappa-B
OPTN	Optineurin
PAMP	Pathogen-associated molecular pattern
PB1	Phox and Bem1
PE	Phosphatidylethanolamine
Poly(I:C)	Polyinosinic-polycytidylic acid
PRR	Pattern recognition receptor

RIPK	Receptor-interacting serine/threonine-protein kinase
SAR	Selective autophagy receptor
SKICH	SKIP carboxyl homology
SLR	Sequestosome-1-like receptor
ssRNA/DNA	Single-stranded RNA/DNA
SQSTM1	Sequestosome-1
TAX1BP1	Tax1-binding protein 1
TBK1	TANK-binding kinase 1
TLR	Toll-like receptor
TNF α	Tumor necrosis factor α
TNIP1	TNFAIP3-interacting protein
TRAF3/6	TNF receptor-associated factor 3
TRIF	TIR-domain-containing adapter-inducing interferon- β
TSG101	Tumor susceptibility gene 101
UBAN	Ubiquitin-binding domain of ABIN proteins and NEMO
ULK1	Unc-51-like kinase 1

Summary

Selective autophagy is important for maintaining cellular homeostasis. Generally, autophagy is considered cytoprotective and anti-inflammatory, acting to limit infection and accumulation of deleterious material. Key to this function is the ability to select cargo to be degraded, and here, selective autophagy receptors play a central role.

In this thesis, we show that the anti-inflammatory and pro-survival adaptor protein TNIP1 is a selective autophagy substrate. Moreover, we identify two LIR motifs in TNIP1, designated LIR1 and LIR2, of which LIR2 is primarily responsible for direct binding to ATG8 proteins. While TNIP1 is constitutively degraded by autophagy in resting cells, inflammatory signaling via TLR3 resulted in increased degradation of TNIP1. Specifically, activation of the kinase TBK1 was demonstrated to directly phosphorylate LIR2 in TNIP1, leading to enhanced ATG8 interaction and increased TNIP1 degradation by ATG7-dependent macroautophagy. The degradation of TNIP1 correlated with the increased activation of downstream inflammatory signaling. This suggests that the reduction of TNIP1 protein levels by autophagy upon inflammatory stimuli occurs to allow the mounting of a robust inflammatory response.

Many studies of TNIP1 function have been done using mouse models. We found that human LIR1 is impaired by the presence of a proline, making LIR2 the main functional LIR in human TNIP1. In mice, however, LIR1 can augment binding to LC3A in conjunction with LIR2. Nonetheless, we discover that the constitutive turnover of human and mouse TNIP1 occurs independently of LIRs, contrary to the inflammation-induced degradation by macroautophagy. Instead, we show that a part of TNIP1 that binds directly to TAX1BP1 and NBR1 is required for lysosomal degradation. Our study of the constitutive turnover of TNIP1 highlights the existence of alternative routes to the lysosome beyond canonical macroautophagy.

Finally, we provide an overview of the ancestral selective autophagy receptor NBR1. Here, we explore the evolution of NBR1 and selective autophagy, and discuss the role of NBR1 in different forms of selective autophagy.

List of papers

Paper I

TBK1 phosphorylation activates LIR-dependent degradation of the inflammation repressor TNIP1

Zhou, J. *, Rasmussen, N.L. *, Olsvik, H.L., Akimov V., Hu Z., Evjen G., Kaeser-Pebernard S., Sankar, D.S., Roubaty, C., Verlhac, P., van de Beck, N., Reggiori F., Abudu, Y.P., Blagoev, B., Lamark, T., Johansen, T. and Dengjel, J. (2023). *J. Cell Biol.* 222 (2): e202108144.

<https://doi.org/10.1083/jcb.202108144>; PMID: 36574265

*Contributed equally to this paper

Paper II

TNIP1 is a constitutive autophagy substrate independent of ATG8 lipidation and LIRs

Rasmussen, N.L., Olsvik, H.L., Evjen, G., Øvervatn A., Lamark, T., and Johansen, T. (2023)

Manuscript

Paper III

NBR1: The archetypal selective autophagy receptor

Rasmussen, N.L., Kournoutis, A., Lamark, T. and Johansen, T. (2022). *J. Cell Biol.* 221 (11): e202208092. <https://doi.org/10.1083/jcb.202208092>; PMID: 36255390

Introduction

Protein degradation systems

There are two major systems for the degradation of cytoplasmic material within the cell, namely the ubiquitin-proteasome system and the process of autophagy (Pohl and Dikic, 2019). The ubiquitin-proteasome system facilitates the degradation of single proteins by the action of a barrel-like protein complex known as the proteasome (Coux et al., 1996). Autophagy (greek for “self-eating”) involves delivery of cytoplasmic material to lysosomes and is commonly used to degrade larger structures, such as protein complexes, aggregates and organelles (Bento et al., 2016). Upon macroautophagy, the most studied type of autophagy, cytoplasmic material is engulfed by the formation of a double-membrane vesicle that subsequently fuses with lysosomes, where the contents become degraded. The handling and removal of surplus or damaged material is pivotal for maintaining cell homeostasis. Therefore, it is not surprising that the process of autophagy plays important roles in human health and disease and is linked either directly or indirectly to a multitude of cellular processes.

Both the ubiquitin-proteasome system and the process of autophagy are guided by the ubiquitin code. Ubiquitin is a small 76-amino acid protein that can be covalently attached via its C-terminal glycine to lysines (K) on other proteins, through a process called ubiquitination (Komander and Rape, 2012). The attachment of ubiquitin to a substrate is catalyzed by an enzymatic cascade involving E1, E2 and E3 enzymes (Figure 1) (Komander and Rape, 2012). The addition of a single ubiquitin protein to a substrate is known as monoubiquitination. Furthermore, ubiquitin itself contains lysine residues to which other ubiquitin proteins can be attached to form polyubiquitin chains. Polyubiquitin chains can be formed through either of the 7 internal lysines, as well as the N-terminal methionine (M): K6, K11, K27, K29, K33, K48, K63 and M1 (Figure 1) (Komander and Rape, 2012). The many combinations of polyubiquitin types and lengths make up the ubiquitin code, as different ubiquitin modifications can be recognized by specific proteins and lead to distinct outcomes. For instance, K48-linked polyubiquitination predominantly acts as a signal for proteasomal degradation, while M1-linked (also known as linear) polyubiquitination is used for mediating signal transduction upon inflammatory stimuli (Yau and Rape, 2016). K63-linked polyubiquitination is involved in forming protein complexes, and can also mark substrates for autophagosomal degradation (Yau and Rape, 2016). However, K63-linked polyubiquitination is not an exclusive signal for autophagy, as other chain types have been implicated in autophagy as well.

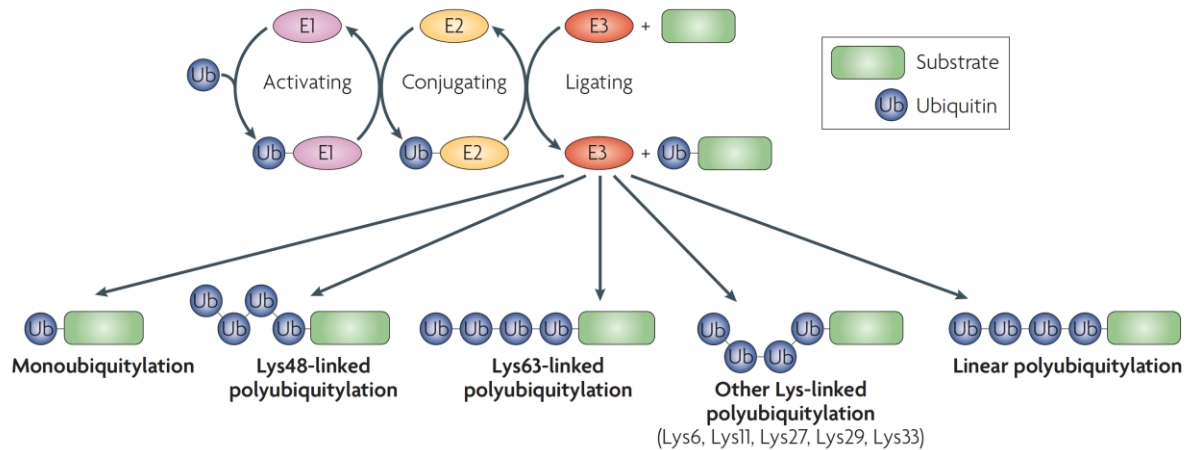


Figure 1: Overview of the process of ubiquitination. Ubiquitination is a stepwise process mediated by an activating E1 enzyme, followed by a conjugating E2 enzyme, and finally attached to a substrate by the E3 ligase. The attachment of a single moiety of ubiquitin is called monoubiquitylation, while the different polyubiquitin chains can also be formed as shown. Figure from (Dikic et al., 2009).

General autophagy

The uncovering of the process of autophagy can be said to have begun with the discovery of the lysosome by Christian de Duve in 1955 (Ohsumi, 2014, De Duve et al., 1955). The lysosome is an acidic organelle containing hydrolytic enzymes that can degrade biological polymers (Bonam et al., 2019). In a way, the lysosome can be considered as the stomach of the cell, as it can break down proteins and organelles into single units that can subsequently be reused. However, at the time of its discovery, it was unclear how the cell could deliver cytoplasmic material to the lysosome for degradation. Because of the acidic nature of lysosomes, it would likely be lethal to the cell if their contents weren't completely sealed off from the rest of the cytoplasm. This was also the reason why de Duve referred to them as "suicide bags" (De Duve, 1965). Taking advantage of the revelatory electron microscope, one was able to observe characteristic double-membrane structures in different stages of enclosing cytoplasmic material (Figure 2) (Arstila and Trump, 1968). It was eventually established that these structures were engulfing material and subsequently fusing with lysosomes, delivering the contents for degradation. The term "autophagy" was coined to describe the process of engulfing and delivering cytoplasmic material to lysosomes – directly translating to "self-eating" (Ohsumi, 2014).



Figure 2: Electron micrograph of autophagic vacuoles (AV) taken by (Arstila and Trump, 1968) showing the characteristic double membrane. Magnification x106,500.

In the decades since its discovery, there has been an astounding advancement in our understanding of the complex steps involved in the process of autophagy. Indeed, several types of autophagy have been uncovered. The previously described engulfment of cytoplasmic material by a double-membrane structure is known as macroautophagy. In addition, material can be taken up directly into lysosomes or endosomes by invagination of the lysosomal or endosomal membrane, referred to as microautophagy (Galluzzi et al., 2017). A third process, called chaperone-mediated autophagy, involves the transfer of material into the lysosome with the help of chaperone proteins and the lysosomal membrane protein LAMP2A (Kaushik and Cuervo, 2018).

The many steps of autophagosome formation

The process of macroautophagy involves multiple steps: the initiation and nucleation of the double-membrane structure, the sequestration of cargo and expansion of the double-membrane, eventually leading to the sealing and subsequent maturation and fusion with lysosomes (Figure 3) (Dikic and Elazar, 2018). Each step requires the action of several proteins and/or protein complexes. These proteins include a group of autophagy-related proteins (ATGs), which make up the core autophagic machinery (Mizushima et al., 2011). Several of these genes were first identified in yeast by the pioneering work of Yoshinori Ohsumi's laboratory, paving the way for further understanding of the regulation and execution of autophagy in higher eukaryotes as well (Ohsumi, 2014). In addition to the ATGs, the portfolio of proteins involved in the regulation of autophagy is yet expanding.

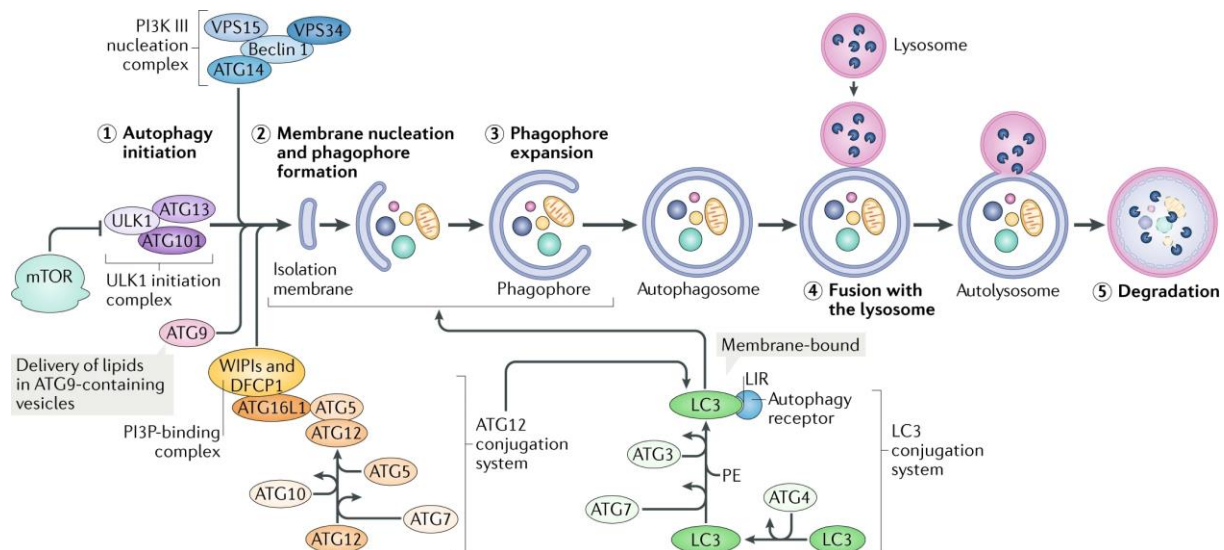


Figure 3: Overview of the different steps of macroautophagy. For details, see main text. Figure was modified from (Hansen et al., 2018)

Initiation and nucleation

The major initiator of autophagy is the **Unc-51-like kinase 1 (ULK1) complex**, which consists of the ULK1 kinase, ATG13, ATG101 and FAK family interacting protein of 200 kDa (FIP200, also known as retinoblastoma 1-inducible coiled-coil 1 (RB1CC1)) (Figure 3) (Bento et al., 2016). One of the most studied pathways for ULK1 complex activation is starvation. Upon nutrient deprivation, the kinase mechanistic target of rapamycin (mTOR) is inactivated, which alleviates an inhibitory phosphorylation of ULK1 by mTOR (Hosokawa et al., 2009, Jung et al., 2009). This allows ULK1 to dissociate from mTOR and phosphorylate targets that initiate

the further steps of autophagosome formation. Activated ULK1 complex marks the mammalian phagophore assembly site (mPAS) (Dikic and Elazar, 2018). This is usually localized at the endoplasmic reticulum (ER), a site called the omegasome (Dikic and Elazar, 2018, Axe et al., 2008).

A central target of ULK1 is Beclin-1, which is recruited by the ULK1 complex to what will become the site of phagophore nucleation (Russell et al., 2013). Beclin-1 forms the **phosphoinositide 3-kinase (PI3K) class III complex 1** along with VPS34, VPS15, and ATG14L, which mediate nucleation of the phagophore by inducing the production of phosphatidylinositol-3-phosphate (PI3P) (Figure 3) (Mizushima et al., 2011). PI3P is recognized by WD-repeat protein interacting with phosphoinositides (WIPI)1-4 and double-FYVE-containing protein 1 (DFCP1), which are needed for the further expansion of the phagophore (Axe et al., 2008, Polson et al., 2010).

Expansion and sealing

WIPI1-4 mediate the recruitment of the **ATG12-ATG5-ATG16L1 complex**, which facilitates the conjugation of ATG8 family proteins to phosphatidylethanolamine (PE) (Figure 3) (Bento et al., 2016). The ATG8 family of proteins are small, ubiquitin-like proteins that consists of 6 members in humans, divided into two subfamilies: the microtubule associated protein light chain 1 (MAP1LC3) subfamily (LC3A, LC3B and LC3C); and the GABA type A receptor-associated protein (GABARAP) subfamily (GABARAP, GABARAPL1 and GABARAPL2) (Figure 4). Yeast, where the name ATG8 stems from, only have a single ATG8 protein. All ATG8 proteins are expressed as precursors, which become cleaved to expose a C-terminal glycine that can be conjugated to PE (Johansen and Lamark, 2020). When conjugated to PE, the ATG8 family proteins are incorporated into the growing phagophore membrane, where they play important roles in the further elongation of the phagophore, as well as the selection and recruitment of cargo. For instance, several core autophagy components bind lipidated ATG8 proteins in the phagophore (Birgisdottir et al., 2019, Wirth et al., 2019, Alemu et al., 2012, Bozic et al., 2020, Skytte Rasmussen et al., 2017). This way, ATG8 proteins help scaffold the different complexes involved in phagophore expansion. Specifically, the LC3 subfamily is important for elongation of the phagophore, while the GABARAP subfamily is implicated in the initiation and closure of the autophagosome (Weidberg et al., 2010). The role and biochemistry of ATG8 family proteins in cargo selection will be elaborated further in later sections.

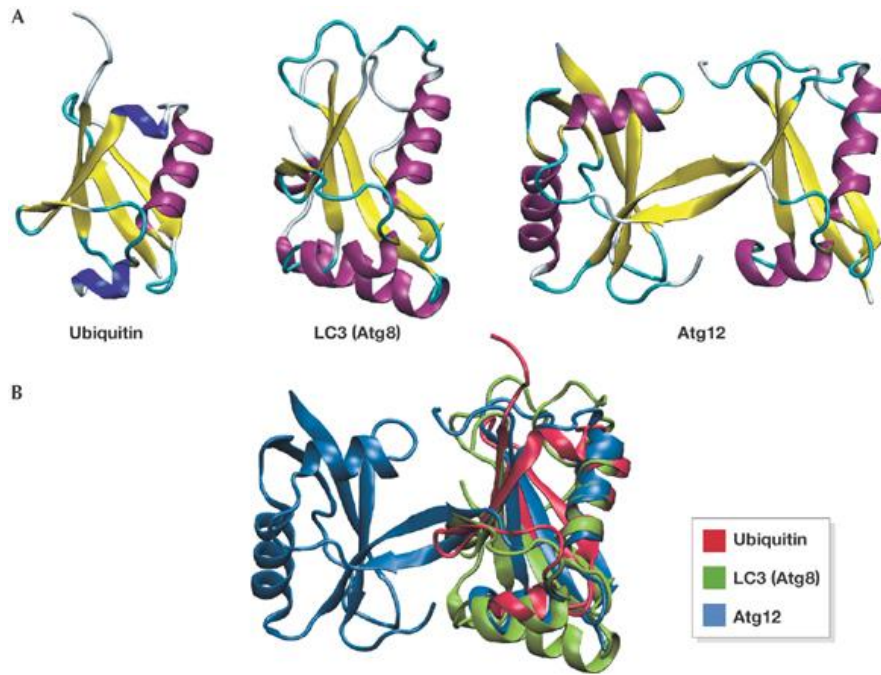


Figure 4: (A) Structural comparison and (B) superimposition of ubiquitin and the ubiquitin-like proteins LC3 (mammalian Atg8) and *Arabidopsis thaliana* Atg12. Figure from (Geng and Klionsky, 2008)

The lipidation of ATG8 family proteins and their incorporation into the growing phagophore membrane requires the activity of two ubiquitin-like conjugation processes: ATG12-conjugation and ATG8-modification (Tanida et al., 2004). ATG12 is a ubiquitin-like protein that can be conjugated to substrates via its C-terminal glycine, reminiscent of the process of protein ubiquitination (Figure 4). The first step involves ATG7, an E1-like enzyme, which activates the C-terminal glycine of ATG12, followed by the attachment of ATG12 to ATG10, an E2-like enzyme. ATG10 subsequently transfers ATG12 to ATG5, which couples with ATG16L1 to form the ATG12-ATG5-ATG16L1 complex (Mizushima et al., 1998, Tanida et al., 2004). This complex then acts as an E3-like ligase which couples ATG8 to PE (Hanada et al., 2007). However, before ATG8 proteins can be attached to PE, the ATG8 precursor must be cleaved by ATG4 to expose the C-terminal glycine, which is then activated by ATG7. ATG7 attaches the activated ATG8 protein to the E2-like enzyme ATG3, which then, together with the ATG12-ATG5-ATG16L1 complex, mediates attachment of ATG8 to PE (Tanida et al., 2004). In addition to being important for ATG8 lipidation, ATG4 can also deconjugate ATG8 from PE to limit phagophore expansion, and allow the reuse of ATG8 proteins (Satoo et al., 2009).

A critical protein involved in the formation of autophagosomes is ATG9A. ATG9A, and its isoform ATG9B, are the only membrane-spanning ATG proteins (Bento et al., 2016).

ATG9A is generally found embedded in small vesicles that are speculated to act as lipid sources for the growing phagophore (Figure 4) (Bento et al., 2016). These vesicles are believed to originate from the plasma membrane, recycling endosomes and the Golgi (Puri et al., 2013, Young et al., 2006, Imai et al., 2016). Nonetheless, the ER is considered a major source of membrane for phagophore expansion (Bento et al., 2016). Recent structural and mechanistic studies are beginning to shed light on the mechanisms that mediate the transfer of lipids from the ER to the growing phagophore. First, several labs successively reported that ATG2 is a lipid transferase that can transfer lipids from one membrane to another (Valverde et al., 2019, Osawa et al., 2019, Maeda et al., 2019). Second, it was recently discovered that ATG9 is a lipid scramblase, meaning it can transfer phospholipids between the leaflets of a lipid bilayer (Matoba et al., 2020, Maeda et al., 2020). This has culminated in a model in which ATG2 is suggested to transfer lipids from the ER to the phagophore, where ATG9 mediates the distribution of lipids in the growing phagophore membrane (Ghanbarpour et al., 2021, van Vliet et al., 2022).

The mechanisms behind the sealing of the phagophore to form an autophagosome are still poorly understood. Interaction between GABARAP and ATG2A/B has been reported to be required for phagophore expansion and closure (Bozic et al., 2020). Endosomal sorting complex required for transport (ESCRT) proteins have also been shown to be involved in the steps leading to the sealing of the phagophore (Zhen et al., 2020, Takahashi et al., 2019).

Maturation and fusion with lysosomes

Once an autophagosome fuses with a lysosome, forming an autolysosome, the lysosomal hydrolases start to break down the cargo into its primary building blocks. Autophagosomes can either fuse directly with lysosomes, forming an autolysosome, or with late endosomes, resulting in an amphisome that subsequently fuses with lysosomes (Figure 4) (Lőrincz and Juhász, 2020, Gordon and Seglen, 1988). A number of proteins and complexes have been implicated in the process of autophagosome-lysosome fusion, including Rab GTPases, membrane tethering factors and soluble N-ethylmaleimide-sensitive factor attachment protein receptors (SNAREs) (Lőrincz and Juhász, 2020). The SNARE syntaxin 17 (Stx17) is inserted into the closed autophagosome and mediates fusion by interacting with synaptosomal-associated protein 29 (SNAP-29), vesicle-associated membrane protein 8 (VAMP8) and the homotypic fusion and protein sorting (HOPS) complex on lysosomes (Itakura et al., 2012, Jiang et al., 2014).

ATG8 proteins are shown to be involved in maturation and fusion steps as well. FYVE and coiled-coil domain-containing protein 1 (FYCO1), an adaptor protein involved in transport along microtubules, interacts with LC3-proteins to mediate transport of autophagosomes (Olsvik et al., 2015, Pankiv et al., 2010). GABARAP subfamily proteins are proposed to be important for fusion with lysosomes, as knockout of these proteins result in severely impaired autophagosome-lysosome fusion (Vaites et al., 2018, Nguyen et al., 2016).

Selective autophagy

Initially, autophagy was described as a bulk process where autophagosomes are formed to engulf parts of the cytoplasm in an unselective manner (Zaffagnini and Martens, 2016). This may be the case upon nutrient deprivation, where cells can utilize autophagy to acquire building blocks to maintain the most essential components needed to survive. However, autophagy is triggered by a wide range of stressors and can be utilized accordingly to degrade substrates in a more targeted approach – a process known as selective autophagy (Lamark and Johansen, 2021, Johansen and Lamark, 2011). Upon selective autophagy, specific cargoes such as proteins, protein complexes and organelles, become engulfed and degraded depending on the needs of the cell. There are many types of selective autophagy, often named after the component being degraded. Examples include mitophagy, the degradation of mitochondria; pexophagy, degradation of peroxisomes; aggrephagy, degradation of protein aggregates; xenophagy, degradation of intracellular pathogens and their components; and ERphagy, degradation of the ER, to name a few (Galluzzi et al., 2017). Specific proteins and protein complexes can also be degraded by selective autophagy, for instance to disrupt signaling pathways.

Specific cargo is targeted for selective autophagy by a group of adaptor proteins known as selective autophagy receptors (SARs) (Lamark and Johansen, 2021). To function as a SAR, these proteins must interact with both the cargo as well as the phagophore. The latter is mediated through interaction with ATG8 family proteins embedded in the phagophore membrane and is achieved through so-called LC3-interacting regions (LIRs) of the SARs (Johansen and Lamark, 2011, Johansen and Lamark, 2020). SARs can either be soluble and interact with cargo through specific domains, or integral to the membrane of specific organelles. The category of membrane-associated SARs mediate the degradation of the organelle in which they are embedded, and have been described for mitophagy, ERphagy and pexophagy (Lamark and Johansen, 2021). The most studied group of soluble receptors are the Sequestosome-1-like receptors (SLRs, see below), which largely interact with cargo through ubiquitin-binding

domains (Lamark and Johansen, 2021). In addition, other soluble SARs that bind cargo independent of ubiquitin-binding domains have been identified, including calcium-binding and coiled-coil domain-containing protein 1 (CALCOCO1), nuclear receptor coactivator 4 (NCOA4) and tripartite motif-containing protein 5 (TRIM5 α) (Mandell et al., 2014, Mancias et al., 2014, Nthiga et al., 2020, Lamark and Johansen, 2021) .

Sequestosome-1-like receptors

The Sequestosome-1-like receptors, or SLRs, are characterized by their similarity to the first identified SAR: p62/SQSTM1 (Deretic, 2012, Bjørkøy et al., 2005). This group of SARs contain ubiquitin-binding domains for cargo interaction, domains for oligomerization, and LIR(s) for interaction with ATG8 family proteins. An overview of the current known SLRs is shown in Figure 5.

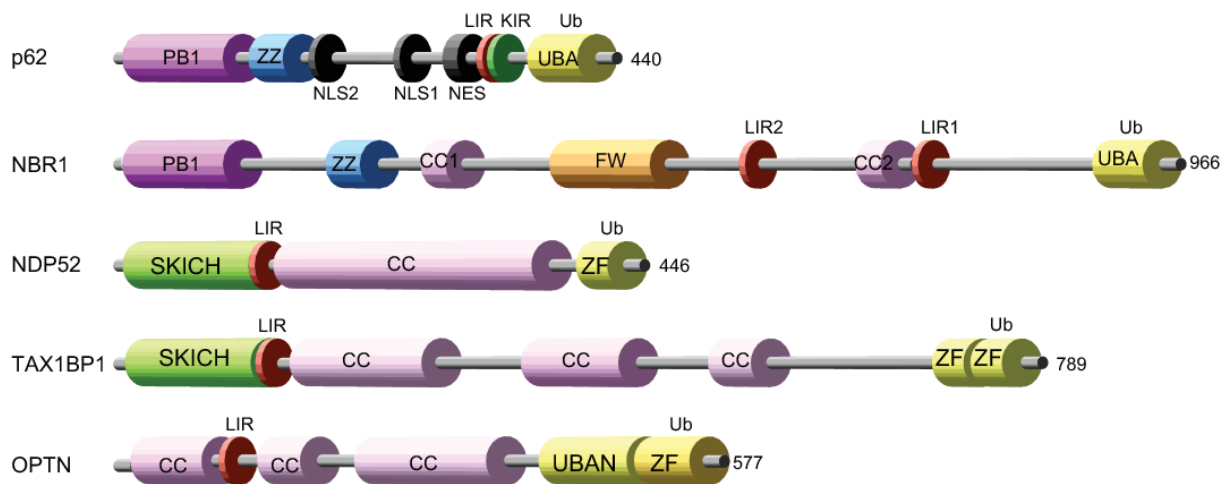


Figure 5: Overview of the domain architecture of the known SLRs. PB1: Phox and Bem1p; ZZ: ZZ-type zing finger; NLS: nuclear localization signal; NES: nuclear export signal; LIR: LC3-interacting region; KIR: Keap1-interacting region; UBA: Ubiquitin-binding domain; ZF: zinc-finger; SKICH: SKIP carboxyl homology domain; CC: coiled-coil domain; FW: four tryptophan domain; UBAN: ubiquitin-binding domain of ABIN proteins and NEMO. Figure from (Birgisdottir Å et al., 2013).

p62 and NBR1

p62 was the first identified mammalian SAR and has since been shown to be involved in several forms of selective autophagy. In particular, p62 is important for the clearance of polyubiquitinated protein aggregates by aggrephagy (Zaffagnini et al., 2018, Bjørkøy et al., 2005, Pankiv et al., 2007). In addition to a ubiquitin-binding domain that binds polyubiquitin, p62 contains a Phox and Bem1 (PB1)-domain that together allows oligomerization and formation of so-called p62 bodies (Sun et al., 2018, Wurzer et al., 2015, Bjørkøy et al., 2005).

p62-bodies are dynamic liquid-liquid phase separated structures that are believed to serve as platforms for signaling and protein degradation by autophagy (Kageyama et al., 2021). In addition to aggrephagy, p62 is involved in mitophagy, xenophagy, regulating oxidative stress response, nuclear factor- κ B (NF- κ B) and mTOR signaling, and more (reviewed in (Sánchez-Martín et al., 2019)).

Another PB1 domain containing protein that acts as an SLR is neighbor of BRCA1 gene 1 (NBR1), which is genetically related to p62 (Lamark et al., 2003). Evolutionary analysis of NBR1 and p62 suggests that NBR1 may be the ancestral SAR, and that p62 resulted from a gene duplication during metazoan evolution (Svenning et al., 2011). There appears to be a close relationship between p62 and NBR1, due to their interaction with each other via their PB1 domains (Lamark et al., 2003). NBR1 aids in forming p62 bodies, where p62 and NBR1 collaborate in clearing protein aggregates by aggrephagy (Turco et al., 2021). While many studies have focused on NBR1 in relation to p62 function, evidence of unique roles for NBR1 are emerging, as reviewed in paper III of this thesis.

NDP52 and TAX1BP1

Nuclear dot protein 52 kDa (NDP52, also known as CALCOCO2) was first identified as an SLR involved in the autophagic degradation of ubiquitin-coated *Salmonella* bacteria (Thurston et al., 2009). NDP52 contains an N-terminal SKIP carboxyl homology (SKICH) domain, a coiled-coil (CC) domain, a C-terminal ubiquitin-binding domain made up of two zinc fingers and a noncanonical LIR for ATG8 binding (von Muhlinen et al., 2012, Thurston et al., 2009). NDP52 is primarily involved in xenophagy, mitophagy and lysophagy (Lamark and Johansen, 2021).

Before being identified as an SLR, the NDP52 homolog Tax1-binding protein 1 (TAX1BP1) was initially studied as a regulator of immune signaling. This was attributed to TAX1BP1 acting as an adaptor for the anti-inflammatory ubiquitin-editing enzyme A20 (also known as tumor necrosis factor alpha-induced protein 3 (TNFAIP3)), allowing A20 to terminate NF- κ B and jun-kinase 1 (JNK1) signaling (Shembade et al., 2007). TAX1BP1 knockout mice are hypersensitive to pro-inflammatory stimuli (Iha et al., 2008). Similar to NDP52, TAX1BP1 contains an N-terminal SKICH domain, three coiled-coil (CC) domains, and two C-terminal ubiquitin-binding zinc fingers (Figure 5) (Kirkin and Rogov, 2019). Eventually, it was discovered that TAX1BP1 is an autophagy substrate and receptor, with two ATG8-interacting LIRs (Newman et al., 2012). Since then, TAX1BP1 has been implicated in

several forms of selective autophagy that affects immunity, including aggrephagy, xenophagy and autophagy of immune signaling components (White et al., 2022). Furthermore, emerging evidence suggests TAX1BP1 may play an important role in mediating lysosomal degradation of substrates through other pathways than canonical macroautophagy. This will be described in more detail in later sections.

Optineurin

Optineurin (OPTN) has several coiled-coil (CC) domains for oligomerization, a LIR located near its N-terminus, and C-terminal ubiquitin-binding domains: a ubiquitin-binding domain of ABIN proteins and NEMO (UBAN) and a zinc-finger domain (Figure 5) (Kirkin and Rogov, 2019). The UBAN is also found in the pro-inflammatory adaptor NF- κ B essential modulator (NEMO), and the anti-inflammatory adaptors ABIN1-3 (also known as TNIP1-3) (Herhaus et al., 2019). OPTN has been found to accumulate in pathological inclusions associated with several types of diseases, including Parkinson's and Alzheimer's disease, and amyotrophic lateral sclerosis (Osawa et al., 2011). Mutations in OPTN are risk factors for Paget's disease of bone, familial and sporadic forms of amyotrophic lateral sclerosis and Crohn's disease (Ryan and Tumbarello, 2018).

Like TAX1BP1, OPTN has been implicated as a negative regulator of innate immune signaling, by interacting with several pro-inflammatory proteins (Ryan and Tumbarello, 2018). As an SLR, OPTN is particularly studied for its important roles in mitophagy, xenophagy and aggrephagy (Ryan and Tumbarello, 2018). Here, there is a close interplay between OPTN and the TANK-binding kinase 1 (TBK1). OPTN interacts with TBK1 through the OPTN N-terminal CC domain and the C-terminal domain of TBK1 (Li et al., 2016). The affinity of OPTN against ubiquitin and ATG8s is enhanced by TBK1-mediated phosphorylation of the UBAN domain and the LIR, respectively (Richter et al., 2016, Wild et al., 2011). In this way, TBK1 has been shown to promote OPTN-mediated degradation of mitochondria and cytosolic bacteria. Interestingly, mutations in TBK1, OPTN and p62 have been identified as risk genes for amyotrophic lateral sclerosis, suggesting a role for these autophagy related proteins in disease development (Cirulli et al., 2015).

LIR-ATG8 interactions

Central to the known SARs is the presence of one or more LIRs that allow for interaction with ATG8 proteins embedded in the phagophore. The first LIR to be described was found in the pioneer autophagy receptor p62 (Pankiv et al., 2007). Over the years, numerous LIRs in

different SARs have been identified. A canonical LIR motif is made up of the “core” sequence of $[W/F/Y]_0-X_1-X_2-[I/L/V]_3$, where X can be any amino acid (Johansen and Lamark, 2020). The part of the ATG8 protein that interacts with the LIR motif of the SAR is called the LIR-docking site, or LDS. The LDS contains two hydrophobic pockets, in which the aromatic (W/F/Y) and the hydrophobic residue (I/L/V) of the core LIR can dock (Figure 6) (Noda et al., 2008, Ichimura et al., 2008).

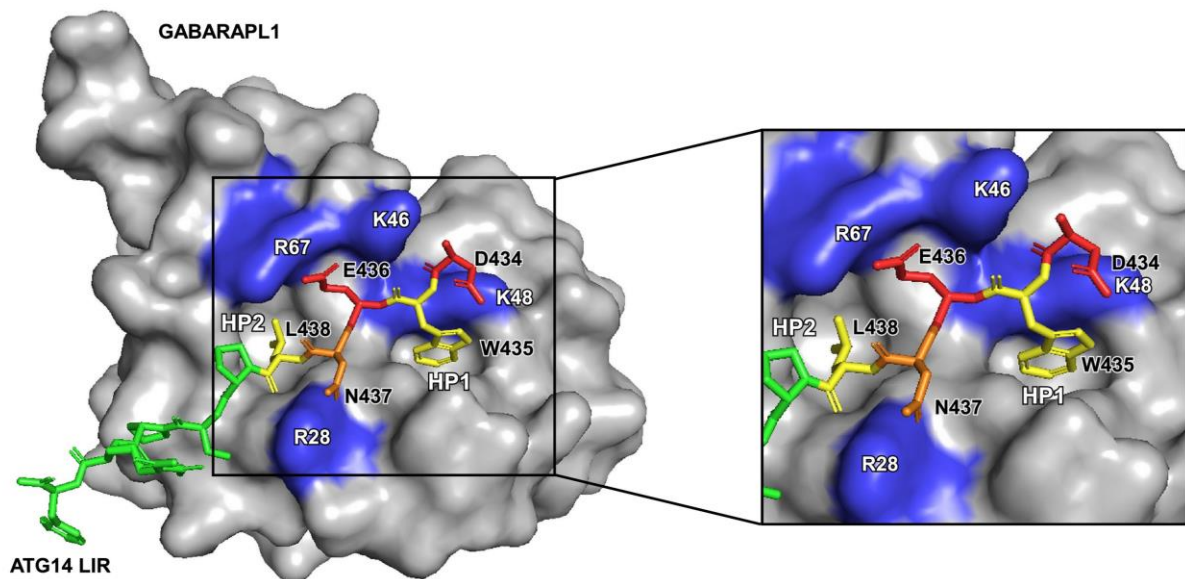


Figure 6: Structural model showing ATG14 LIR in the LDS of GABARAPL1. The side chains of the aromatic tryptophane (W435) and the hydrophobic leucine (L438) of ATG14 LIR dock inside the hydrophobic pockets of the LDS. The residues (D434, E436) engage in electrostatic interactions with the basic residues of GABARAPL1 (highlighted in blue). Figure from (Johansen and Lamark, 2020).

It is becoming increasingly clear that the residues flanking the core LIR, both N-terminal and C-terminal, can affect the interaction strength and specificity of a LIR towards the ATG8 proteins. Comparison of 100 different identified LIR motifs show that there is a higher frequency of acidic residues (aspartate (D), glutamate (E)) or residues that can be phosphorylated (serine (S), threonine (T)), immediately N-terminal, and to a degree also C-terminal, to the core LIR (Figure 7) (Johansen and Lamark, 2020). This can be explained by the LDS having a generally basic surface, which can promote electrostatic interaction with the negatively charged acidic and phosphorylated residues surrounding the core LIR, thereby strengthening the interaction (Figure 6) (Johansen and Lamark, 2020). While the residues in positions X_1 and X_2 can in theory be any amino acid, the basic surface of the LDS appears to select against the presence of the basic residues arginine (R) and lysine (K) (Alemu et al., 2012). Glycine (G) and proline (P) are also selected against in these positions, as they may interfere with the structure of the LIR (Johansen and Lamark, 2020, Alemu et al., 2012).

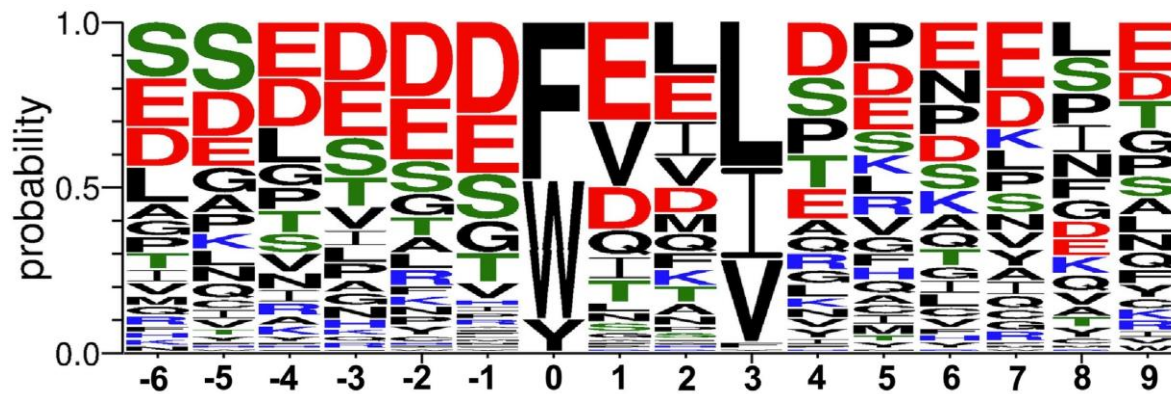


Figure 7: Sequence comparison of 100 known LIRs. The size of the lettering indicates the probability of finding the amino acid in the given position relative to the hydrophobic residue of the LIR (position 0). Figure from (Johansen and Lamark, 2020)

Despite the structural similarities between the ATG8-family proteins, not all LIRs bind equally well to all members. Structural and functional studies indicate that residues within the core LIR, and the flanking N- and C-terminal sequences, can participate in the specificity. For instance, LIRs with preference for GABARAP over LC3 family members, termed GABARAP-interaction motifs (GIMs), often carry the core consensus sequence of $[W/F]_0-[I/V]_1-X_2-V_3$ (Rogov et al., 2017a). Further analysis of LIRs with preference for GABARAP, show that key residues in the flanking C-terminal can select against LC3 binding, and favor GABARAP (Wirth et al., 2019). FYCO1, FAM134B and ankyrin B and G (AnkB/G) LIRs show particularly strong ATG8-binding, due to the presence of a C-terminal amphipathic α -helix that stabilizes the interaction (Li et al., 2018). In the case of FYCO1, this extended LIR also imposes selectivity towards LC3 proteins, while the extended LIR of AnkB and AnkG results in selectivity towards GABARAP (Olsvik et al., 2015, Li et al., 2018).

Post-translational regulation of LIR-LDS interaction

In addition to the intrinsic nature of the LIR directly influencing LDS affinity, examples of post-translational regulation of LIRs are emerging. Several LIRs have serines and/or threonines in close vicinity that may be subject to phosphorylation. Phosphorylation of such residues will impose a negative charge that can interact with basic residues in the LDS (Johansen and Lamark, 2020). Post-translational regulation of LIRs adds another level of complexity to selective autophagy, providing a mechanism for cells to regulate degradation of substrates depending on stimuli, intrinsic and extrinsic conditions, and cell type.

The LIR of OPTN was shown early on to be phosphorylated by TBK1 on the serine at the X-1 position upon *Salmonella* infection (Wild et al., 2011, Rogov et al., 2013). This TBK1-mediated phosphorylation enhances OPTN binding to ATG8-proteins, which promotes the

OPTN-mediated autophagic clearance of *Salmonella* bacteria. Furthermore, TBK1 and ULK1 have been demonstrated to phosphorylate the LIR of the Golgi protein SCOC, increasing affinity for the ATG8-proteins (Wirth et al., 2021). Phosphorylation of LIRs also regulate mitophagy: phosphorylation of activating molecule in BECN1-regulated autophagy protein 1 (AMBRA1) LIR enhances mitophagy, as does phosphorylation of the LIRs of the mitochondrial SARs BCL2/adenovirus E1B 19 kDa protein-interacting protein 3 (BNIP3), BNIP3L and FUN14 domain-containing protein 1 (FUNDC1) (Zhu et al., 2013, Wu et al., 2014b, Rogov et al., 2017b, Di Rita et al., 2018). In the case of FUNDC1, phosphorylation of and near the LIR can both enhance and inhibit mitophagy. While phosphorylation of serine at the X₋₁ position of the LIR enhances interaction with ATG8-proteins and mitophagy, phosphorylation of serine at the X₋₅ position and of the tyrosine within the core LIR inhibits mitophagy (Liu et al., 2012, Wu et al., 2014a). Regulation of LIRs by phosphorylation has also been suggested based on mutational studies. Mutation of serine or threonine to glutamate or aspartate imposes a negative charge that mimics phosphorylation. Phosphomimic mutations of known phosphorylation sites in the LIRs of VPS34 and Beclin-1 strongly enhance binding to ATG8-proteins (Birgisdottir et al., 2019). It is likely that regulation of LIRs by phosphorylation is widespread, and that more examples will emerge.

SAR-mediated autophagy induction

Increasing evidence supports that SARs not only act as bridges between cargo and the phagophore, but also induce selective macroautophagy by recruiting core autophagy machinery components to the cargo. As is often the case in autophagy research, studies in yeast have paved the way for our understanding of similar processes in mammalian cells. In yeast, phosphorylation of the autophagy receptor Atg19 promotes interaction with Atg11, the yeast ortholog of FIP200 (Tanaka et al., 2014, Pfaffenwimmer et al., 2014). Atg19 thereby links the cargo to the autophagic machinery, where Atg11 further recruits Atg1, the homolog of ULK1 (Kamber et al., 2015, Torggler et al., 2016). This then allows the induction of selective degradation of the receptor-bound cargo.

In mammals, SAR-mediated autophagy induction has been demonstrated for mitophagy (Lazarou et al., 2015, Vargas et al., 2019), xenophagy (Ravenhill et al., 2019), ERphagy (Smith et al., 2018) and aggrephagy (Turco et al., 2019). NDP52 and OPTN induce mitophagy by recruiting ULK1, DFCP1 and WIPI1 to mitochondria (Lazarou et al., 2015, Vargas et al., 2019). Phosphorylation of NDP52 by TBK1 mediates the binding to FIP200 and subsequent

recruitment of ULK1 (Vargas et al., 2019). Upon *Salmonella* infection, NDP52 also recruits FIP200-ULK1 to induce xenophagy (Ravenhill et al., 2019). The recently identified ERphagy receptor cell-cycle progression gene 1 (CCPG1) binds both ATG8 proteins and FIP200 to initiate ERphagy (Smith et al., 2018). During aggrephagy, p62, NBR1 and TAX1BP1 are all able to interact with FIP200, yet TAX1BP1 appears to be mainly responsible for FIP200-recruitment and aggrephagy induction (Turco et al., 2021). Intriguingly, a common theme is SAR-mediated recruitment of ULK1 through direct FIP200-interaction by so called FIP200-interacting regions, or FIRs.

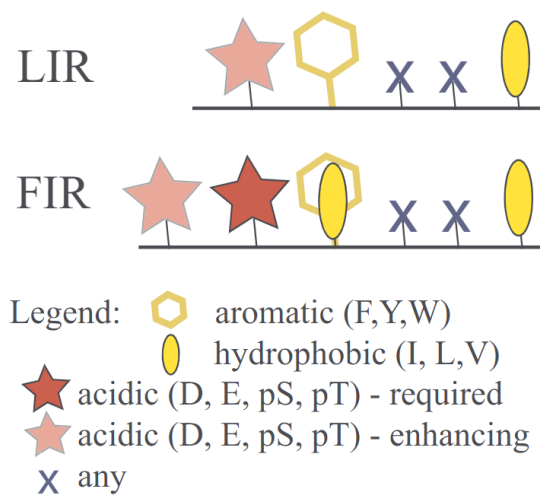


Figure 8: Comparison of the LIR motif and proposed FIR. Amino acid properties of a LIR and FIR, respectively, are indicated in the legend. Figure from (Popelka and Klionsky, 2022)

Alignment of the Atg11-interacting region of Atg19 with known FIP200-interacting proteins in humans, has led to the proposal of a core consensus FIR sequence that mediates interaction with the C-terminal region of FIP200 called the Claw domain (Zhou et al., 2021). In several instances, phosphorylation of the FIR increases the binding affinity, and for some SLRs the FIRs overlap with known LIRs. This is the case for OPTN, NDP52 and p62 (Zhou et al., 2021, Fu et al., 2021, Turco et al., 2019). For instance, TBK1-mediated phosphorylation of the OPTN LIR, which has been shown to promote ATG8-binding and mitophagy, strongly promotes binding between OPTN LIR and the FIP200 Claw (Zhou et al., 2021). The atypical LIR of NDP52 can interact with the Claw of FIP200, and again TBK1 promotes the interaction by phosphorylating a LIR-proximal residue (Fu et al., 2021). Interestingly, FIRs are also found in the two TBK1-adaptor proteins NAK-associated protein 1 (NAP1) and similar to NAP1 TBK1 adaptor (SINTBAD), which also interact with NDP52 and TAX1BP1 (Fu et al., 2021, Ravenhill et al., 2019). In p62, the FIR is also positively regulated by phosphorylation, yet the

kinase responsible remains to be determined (Turco et al., 2019). The FIR of p62 encompasses the LIR and results in competitive binding between LC3 and FIP200. Interaction between SARs and FIP200 can also occur through other means than consensus FIR-Claw interaction. Both TAX1BP1 and NDP52 can bind the coiled-coil domain of FIP200 through their SKICH domains (Fu et al., 2021, Ohnstad et al., 2020, Ravenhill et al., 2019), while NBR1 binds the FIP200 Claw through its CC2 domain (Turco et al., 2021). It appears that phosphorylation-induced interaction between SARs and FIP200 may represent an important mechanism for targeting selective autophagy induction.

Other forms of autophagy

Chaperone-mediated autophagy

Chaperone-mediated autophagy (CMA) involves the direct uptake of soluble cytosolic substrates into the lysosome, through the lysosomal membrane receptor lysosome-associated membrane protein type 2A (LAMP2A) (Figure 9) (Kaushik and Cuervo, 2018). Substrates are recognized by having a KFERQ-like motif which is bound by the chaperone heat shock cognate 71 kDa protein (HSC70) (Chiang et al., 1989). HSC70 directs the substrate to LAMP2A, where LAMP2A assembles into a multimeric channel complex (Rout et al., 2014). The substrate is unfolded prior to entering the lysosome, and aggregated proteins cannot be degraded by CMA (Salvador et al., 2000, Cuervo et al., 2004). LAMP2A has only been identified in mammals, birds, and recently fish (Tekirdag and Cuervo, 2018, Lescat et al., 2018). Studies suggest that CMA occurs at a resting state in multiple cell types, yet is also triggered by several stressors, including starvation, oxidative stress, and DNA damage (Koga et al., 2011, Park et al., 2015, Kiffin et al., 2004, Cuervo et al., 1995). Up to 40% of all proteins contain KFERQ-like motifs, and post-translational modifications can increase the number of potential substrates even further (Kaushik and Cuervo, 2018). How selection of substrates of CMA are spatiotemporally regulated is still unclear.

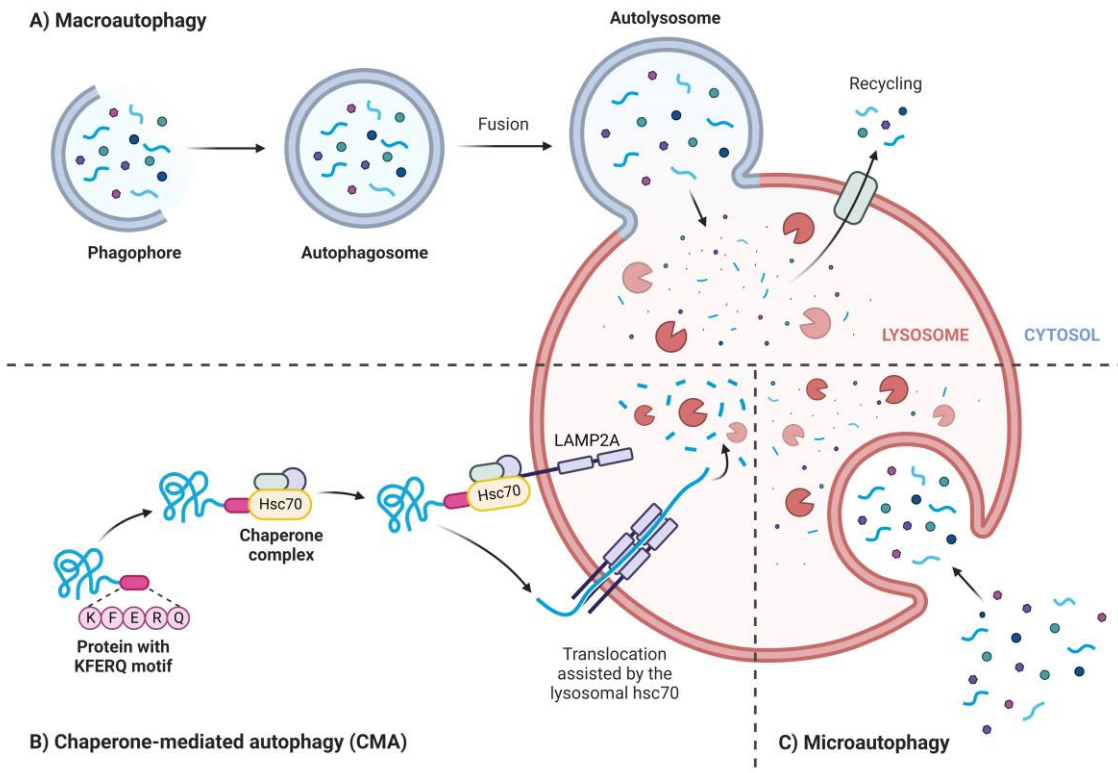


Figure 9: Destination: the lysosome. (A) Macroautophagy involves the formation of an autophagosome that fuses with the lysosome. (B) During chaperone-mediated autophagy, proteins with a KFERQ-like motif can be transported directly into lysosomes by the help of HSC70 and LAMP2A. (C) Microautophagy involves the direct uptake of material from the cytosol through invagination of the endosomal or lysosomal membrane. Figure is modified from BioRender.

Microautophagy

The term microautophagy encompasses several forms of autophagy that result in direct uptake of substrates into endosomes or lysosomes (Figure 9). Several substrates and mediators have been described, yet compared to macroautophagy and CMA, less is understood about the mechanisms behind microautophagy in mammals (Wang et al., 2022a). One type of microautophagy, known as endosomal microautophagy, shares similarities to CMA as it depends on HSC70 binding to a KFERQ-like motif within the substrate (Sahu et al., 2011). However, it does not require LAMP2A. Endosomal microautophagy is considered selective, and appears to be stimulus specific (Wang et al., 2022a). Upon invagination of the endosomal membrane, the substrate ends up inside endosomes to form multivesicular bodies (MVBs) and is degraded. The inward budding of the endosomal membrane to form intraluminal vesicles (ILVs) is one of the many processes mediated by the ESCRT machinery (Vietri et al., 2020). The ESCRT machinery consists of three protein complexes known as ESCRT-I, -II and -III, which are well studied for their role in sorting endocytosed plasma membrane receptors into ILVs for degradation. Furthermore, it appears that ESCRTs are involved in the process of

endosomal microautophagy as well, as this was shown to require ESCRT-I and -III (Sahu et al., 2011).

In *Schizosaccharomyces pombe*, the SAR Nbr1 (homologue of mammalian NBR1) mediates a type of microautophagy where substrates also end up in ILVs inside MVBs, which subsequently fuse with the yeast vacuole (Liu et al., 2015). This Nbr1-mediated vacuolar targeting (NVT) is independent of Atg proteins but requires the ESCRT machinery. Exactly how Nbr1 and its cargo is recruited to MVBs is still unclear. During the early stages of starvation in mammalian cells, several cytosolic proteins are taken up into endosomes by microautophagy and degraded (Mejlvang et al., 2018). It is estimated that around 2% of the total proteome within the cell was degraded during the first 2 hours of nutrient deprivation. Some of the most efficiently degraded substrates are the SLRs. This type of microautophagy is dependent on ATG8 lipidation and ESCRT-III, but not the activity of the ULK1- and PI3KC3 complexes, nor LAMP2A. Microautophagy has also been implicated in the Parkin-dependent removal of mitochondria in ATG5/7-deficient cells (Hammerling et al., 2017). This type of microautophagy is reported to occur in Rab5-positive early endosomes, as opposed to late endosomes. In this pathway, internalization of mitochondria in endosomes is dependent on the ESCRT machinery.

Non-canonical autophagy pathways

The process of macroautophagy described earlier is commonly referred to as “canonical” autophagy, as other routes to the lysosome – or “non-canonical” pathways – have been described as well. An exact definition of what constitutes *non-canonical autophagy* is lacking, yet the term is generally used to describe the formation of autophagosomes independent of one or more of the components of the core autophagy machinery, or instances where certain ATGs are involved in other processes not related to macroautophagy (Codogno et al., 2012).

“Non-canonical” lipidation

A type of non-canonical autophagy is LC3-associated phagocytosis (LAP). LAP involves ATG8-conjugation to single membranes that arise from the internalization of cell surface receptors, generally receptors that detect pathogens or debris from apoptotic cells (Sil et al., 2018). Unlike xenophagy, where a double membrane is formed around an intracellular pathogen, LAP results in a single-membrane vesicle with ATG8 proteins conjugated on the outside, called a LAPosome (Sil et al., 2018). Conjugation of ATG8 to form LAPosomes is required for fusion between the LAPosome and lysosome (Martinez et al., 2015). LAP has

proven to play an important role in innate immunity (Heckmann et al., 2017). Furthermore, conjugation of ATG8 proteins to single membranes has also been observed on endosomes in microglial cells (termed LANDO) and on Stimulator of interferon genes protein (STING)-containing vesicles (Heckmann et al., 2019, Fischer et al., 2020).

Upon conjugation to single membranes, ATG8 proteins can become coupled to phosphatidylserine (PS) as opposed to the exclusive conjugation to PE that occurs during canonical autophagy (Durgan et al., 2021). Adding another layer of complexity, it was recently reported that also ubiquitin can be covalently attached to PE on membranes, specifically endosomes (Sakamaki et al., 2022). Based on studies in yeast, it was proposed that lipidated ubiquitin may be involved in recruiting ESCRT proteins to endosomal membranes, and mediate uptake of substrates into intraluminal vesicles.

SARs bypassing the need for ATG8s in autophagy

The lipidation of ATG8, and thereby the components of the ATG8-conjugation system, was long considered essential for macroautophagy and autophagosome formation. This view was challenged when it was demonstrated that ATG5 and ATG7 deficient mouse cells, which are unable to lipidate ATG8 proteins, could still form autophagosomes and degrade substrates (Nishida et al., 2009). However, the autophagy flux in ATG8-conjugation deficient cells is highly reduced, likely due to their role in autophagosome closure (Tsuboyama et al., 2016, Vaitea et al., 2018, Nguyen et al., 2016).

A recent screen using a tandem fluorescent reporter system showed that not all autophagy receptors are equally affected by disruption of the ATG8-lipidation system (Shoemaker et al., 2019). Particularly, NBR1 is only partially dependent on the ATG8-lipidation system for degradation, and can be found inside double-membrane autophagosomes in ATG7 deficient cells (Ohnstad et al., 2020). Interestingly, the ATG8-independent degradation of NBR1 is mediated by TAX1BP1 and TBK1. TAX1BP1 interacts directly with NBR1 and can recruit FIP200 and TBK1 to induce local autophagosome formation independent of ATG8-lipidation (Ohnstad et al., 2020). Similarly, NDP52 can recruit FIP200 to mitochondria to induce ATG8-independent mitophagy, a process also promoted by TBK1 (Vargas et al., 2019).

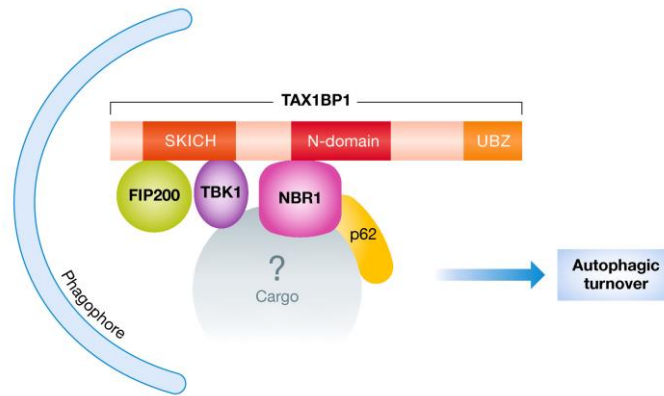


Figure 10: Proposed model for TAX1BP1-mediated autophagy independent of ATG8-lipidation. NBR1 recruits TAX1BP1 to the cargo, where TAX1BP1 together with TBK1 recruit FIP200 to mediate phagophore formation in an ATG8-independent process. Figure from (Nguyen and Lazarou, 2020)

TAX1BP1 has also been implicated as a driver of NCOA4 lysosomal degradation independent of ATG8-lipidation (Goodwin et al., 2017, Kuno et al., 2022). NCOA4 is a cargo receptor for ferritin, and thereby regulates iron homeostasis by mediating ferritin lysosomal degradation (Dowdle et al., 2014, Mancias et al., 2014). Degradation of NCOA4 and ferritin upon iron depletion does not require ATG8-conjugation, but depends on TAX1BP1, the ULK1/2-FIP200 complex, ATG9A, VPS34 and core ESCRT proteins (Goodwin et al., 2017). In the absence of FIP200, TBK1 can induce ferritin turnover in an ATG9-dependent manner. Here, TAX1BP1 is suggested to act as an adaptor for TBK1 recruitment. In iron replete cells, TAX1BP1 delivers iron-induced condensates of NCOA4-ferritin to lysosomes in a FIP200-dependent and ATG7-independent manner (Kuno et al., 2022, Ohshima et al., 2022). Based on these studies, it appears that TAX1BP1 may be an important mediator of lysosomal degradation upon defective ATG8-conjugation. The recruitment of FIP200 by TAX1BP1 or NDP52 appears to circumvent the need for ATG8 lipidation for selective autophagy, likely through the direct recruitment of FIP200.

Interplay between autophagy and immunity

Autophagy has been implicated in the regulation of both innate and adaptive immune processes and has cytoprotective and anti-inflammatory functions (Cadwell, 2016, Deretic, 2021). This is in part achieved through the removal of damaged organelles, pathogens and aggregates that could otherwise trigger inflammatory responses if not removed. Non-canonical autophagy in the form of LAP is also proving important for phagocytic immune cells to clear debris and pathogens (Heckmann et al., 2017). Autophagy can also influence immune signaling by targeting specific signaling components for degradation (Cadwell, 2016). A possible link between autophagy and immunity is revealed by a particular genetic variant of ATG16L1 that

is strongly associated with development of Crohn's disease, a type of inflammatory bowel disorder (Jostins et al., 2012). This variant causes a missense mutation (T300A), which results in destabilization of the ATG16L1 protein, and consequently compromised xenophagy and increased production of inflammatory modulators (Lassen et al., 2014, Murthy et al., 2014).

Innate immune signaling

Innate immune signaling is triggered by pathogen- and damage-associated molecular patterns (PAMPs and DAMPs, respectively) (Tang et al., 2012). Examples of PAMPs are molecules associated with invading pathogens, including bacterial membrane components such as lipopolysaccharide (LPS), and viral nucleic acids, including double-stranded RNA (dsRNA) (Tang et al., 2012). DAMPs, on the other hand, are endogenous molecules from damaged or dying cells that can trigger an inflammatory response in the absence of pathogenic infection (Tang et al., 2012). Examples of DAMPs can be the presence of specific nuclear proteins in the cytoplasm or DNA released from damaged mitochondria. Different PAMPs and DAMPs are recognized by specific pattern recognition receptors (PRRs), which exist either embedded in the plasma membrane or intracellular vesicles/organelles, or as soluble receptors (Tang et al., 2012). PRRs include Toll-like receptors (TLRs), which are membrane-embedded receptors found in the plasma membrane and in vesicular compartments, and the soluble cytosolic NOD-like receptors (NLRs) and RIG-I-like receptors (RLRs), which primarily detect cytosolic bacteria and viruses, respectively (Li and Wu, 2021). Upon activation, PRRs trigger downstream signaling pathways that ultimately lead to an inflammatory response, and in certain cases, autophagy (Tang et al., 2012).

Toll-like receptor signaling and autophagy

Toll-like receptors are found either on the cell surface or inside intracellular compartments, where they detect invading viruses and bacteria that are not exposed to the cytosol (Li and Wu, 2021). The TLR family includes 10 members in humans, designated TLR1-10. Different TLRs recognize distinct PAMPs associated with viruses and bacteria (Figure 11). For instance, TLR4 recognizes LPS on bacterial surfaces, while TLR3 recognizes viral double-stranded RNA genomes. When activated by PAMPs, TLRs mediate inflammatory signaling through the adaptors myeloid differentiation primary response protein 88 (MyD88) (except for TLR3) or TIR-domain-containing adapter-inducing interferon- β (TRIF) (Figure 11) (Li and Wu, 2021). MyD88 forms the Myddosome together with the kinases interleukin-1 receptor-associated kinase (IRAK) 1 and 4 (Kawasaki and Kawai, 2014). This leads to activation of IRAK1, which

further activates TGF β -activated kinase 1 (TAK1) through the E3 ligase TNF receptor-associated factor (TRAF) 6. TAK1, in turn, mediates activation of the mitogen activated protein kinase (MAPK) pathway, and the NF- κ B pathway. NF- κ B and MAPK signaling is important for activating inflammatory gene expression and regulating cell survival. TLR signaling through TRIF involves TRIF-mediated recruitment and activation of TRAF3 and -6. TRAF6 along with the receptor-interacting serine/threonine-protein kinase 1 (RIPK1), lead to activation of NF- κ B and MAPK signaling. Meanwhile, TRAF3 is responsible for activating the serine/threonine-protein kinases TBK1 and IKK ϵ , which in turn activate the transcription factor interferon regulatory factor 3 (IRF3). IRF3 induces the expression of type I interferons, which are small proteins that are released by cells to signal antiviral responses against viruses and other pathogens (Schneider et al., 2014).

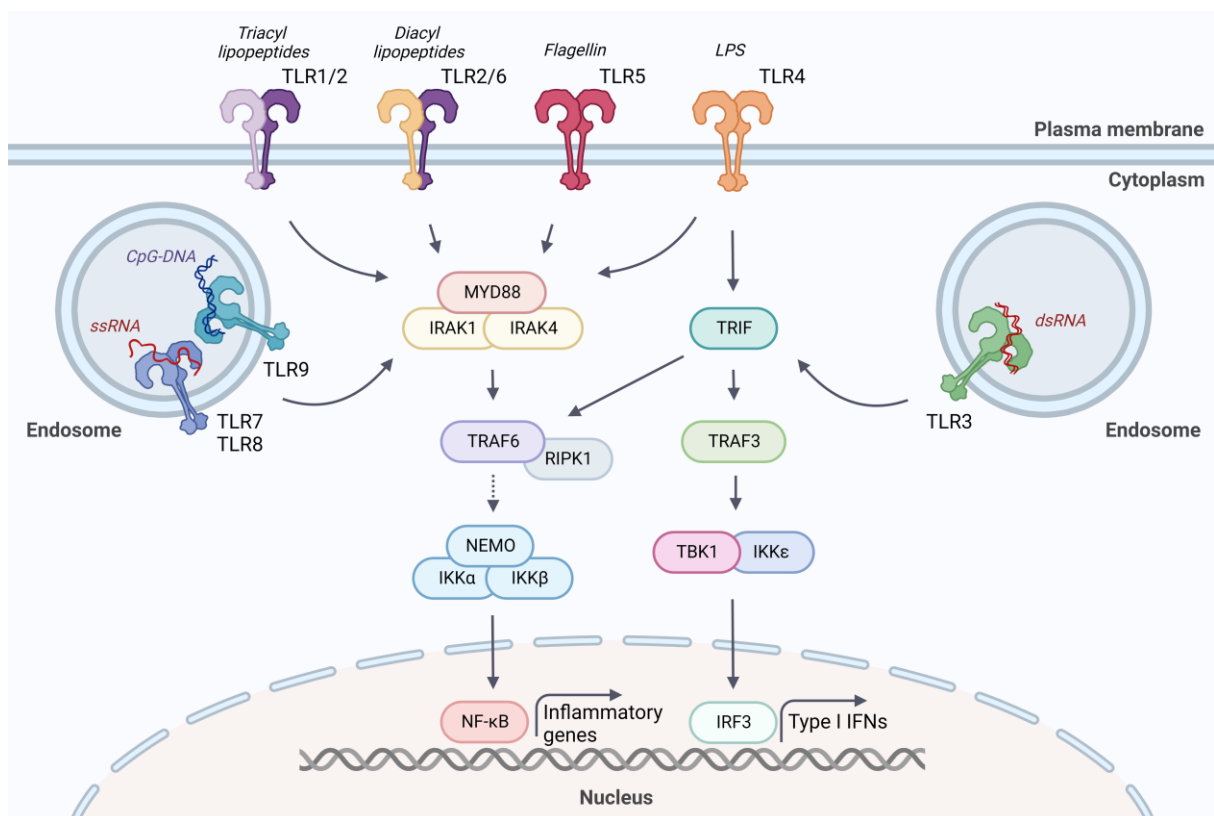


Figure 11: TLR signaling. Overview of the different TLRs, their main localization, agonists and downstream signaling events. All TLRs, except for TLR3, mediate signaling through MyD88. TLR4 can activate both MyD88 and TRIF, while TLR3 signals only through TRIF. MyD88 forms a complex with IRAK1 and IRAK4 called the Myddosome, which further leads to TRAF6 recruitment. TRAF6 and RIPK1 then further activate the IKK complex consisting of NEMO, IKK α and IKK β , ultimately leading to activation of NF- κ B-mediated gene transcription. Upon activation of TLR3 or TLR4, TRIF activates TRAF3, which further leads to the activation of the kinases TBK1 and IKK ϵ . This ultimately leads to activation of the IRF3 and the production of type I interferons. TRAF6/TAK1-induced activation of MAPK signaling is not included in the figure. Figure was made using BioRender.com

K63- and M1-linked polyubiquitination play essential roles in signal transduction through immune signaling pathways (Hu and Sun, 2016). For instance, signaling through MyD88 and TRIF requires TRAF3 and -6 mediated K63-linked polyubiquitination to activate downstream signaling (Kawasaki and Kawai, 2014). Activation of NF- κ B requires assembly of the I κ B kinase (IKK) complex, which consists of the kinases IKK α and IKK β , and the adaptor NEMO (Clark et al., 2013). This assembly and subsequent activation of NF- κ B depends on both K63- and M1-linked ubiquitin chains (Clark et al., 2013).

Several TLRs have been shown to activate autophagy, through both TRIF and MyD88 signaling (Xu et al., 2007, Delgado et al., 2008, Shi and Kehrl, 2008). MyD88 and TRIF-activated TRAF6 promotes K63-polyubiquitination of Beclin-1 to induce autophagy, while de-ubiquitination by the ubiquitin editing enzyme A20 blocks autophagy induction (Shi and Kehrl, 2010). Activation of autophagy by MyD88 in intestinal epithelium is important in protecting intestinal cells from bacterial invasion (Benjamin et al., 2013). Interestingly, TAX1BP1 mediates the selective autophagy of TRIF to attenuate pro-inflammatory signaling and excessive immune responses (Yang et al., 2017, Samie et al., 2018, Gentle et al., 2017). Furthermore, autophagy is important for cell survival upon TLR activation, as ATG16L1 deficient macrophages are more sensitive to TLR-induced cell death (Lim et al., 2019). These cells accumulate aggregated TRIF, RIPK1 and RIPK3, which are responsible for inducing cell death. Here, selective autophagy mediated by TAX1BP1 downstream of TRIF is important for survival (Lim et al., 2019).

TBK1 in autophagy and immunity

Historically, studies of TBK1 have largely focused on its function in mediating innate immune signaling. It is only recently that one has come to appreciate that TBK1 plays several roles in autophagy regulation as well.

In immune signaling, TBK1 is involved in signal transduction to induce interferon production by activating the transcription factor IRF3 (Figure 12) (Oakes et al., 2017). Interferon-production is triggered by PRRs that detect signs of viral or bacterial infection, such as the presence of viral genomes in vesicles or the cytosol. For instance, TLR3 can detect the presence of viral dsRNA in endosomes and induce TRIF-mediated signaling that leads to activation of TBK1 (Figure 12) (Kawasaki and Kawai, 2014). The soluble receptors retinoic acid-inducible gene 1 protein (RIG-1) and melanoma differentiation-associated protein 5 (MDA5) can detect dsRNA in the cytosol and activate TBK1 via the adaptor mitochondrial

antiviral-signaling protein (MAVS). Furthermore, TBK1 is activated upon sensing of dsDNA in the cytosol by the cyclic GMP-AMP synthase (cGAS)-STING pathway (Oakes et al., 2017).

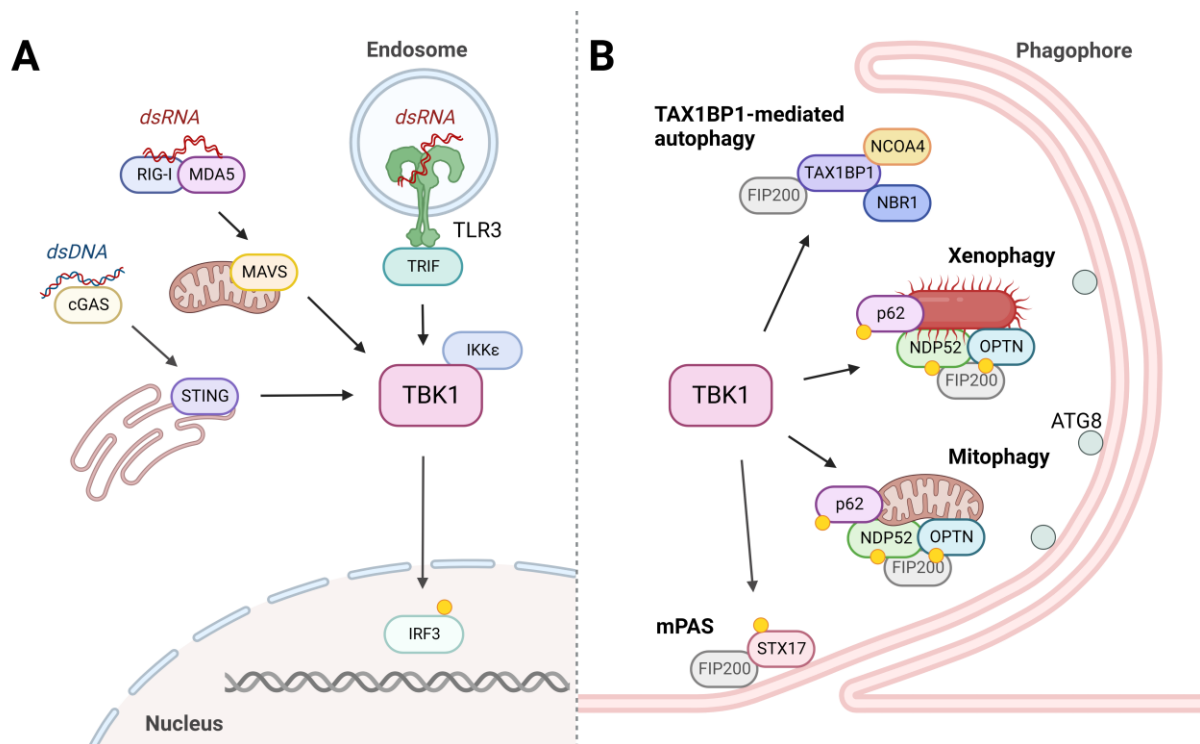


Figure 12: Overview of the role of TBK1 in autophagy and antiviral signaling. (A) Overview of the different signaling pathways that signal through TBK1 to activate the transcription factor IRF3. Detection of dsRNA through TLR3/TRIF or RIG-I/MDA5/MAVS, or cytosolic dsDNA by the cGAS/STING pathway leads to TBK1/IKKε activation. TBK1 in turn activates IRF3 transcription. Yellow dots show direct targets of TBK1 phosphorylation (B) Overview of known autophagic processes influenced by TBK1. TBK1 induces the degradation of NBR1 and NCOA4 by TAX1BP1/FIP200-mediated autophagy in the absence of ATG8 lipidation. Furthermore, TBK1-mediated phosphorylation of p62, NDP52 and OPTN promotes xenophagy and mitophagy. TBK1-induced phosphorylation of NDP52 and OPTN can recruit FIP200 directly to bacteria/mitochondria. Phosphorylation of STX17 by TBK1 can promote FIP200 recruitment and mPAS assembly. Figure was made using BioRender.

TBK1 has been implicated in mediating both induction and maturation of phagophores. Loss or inhibition of TBK1 results in reduced maturation of autophagosomes, yet the specific mechanisms for how TBK1 promotes maturation is not known (Pilli et al., 2012). Furthermore, TBK1 can phosphorylate syntaxin 17 (STX17) to promote mPAS assembly and autophagy induction at the Golgi (Figure 12) (Kumar et al., 2019). Cells deficient of TBK1 are unable to form FIP200 puncta upon autophagy induction by starvation (Kumar et al., 2019). In macrophages, IL-1β promotes autophagic killing of mycobacteria via TBK1 activation. (Pilli et al., 2012). TBK1 can phosphorylate the autophagy receptors OPTN, NDP52 and p62 to promote mitophagy or xenophagy (Figure 12) (Heo et al., 2015, Richter et al., 2016, Matsumoto et al., 2015, Wild et al., 2011, Pilli et al., 2012, Thurston et al., 2009). For OPTN, TBK1 phosphorylation can both enhance interaction with ATG8 proteins, polyubiquitin, and FIP200,

all which may participate in promoting mitophagy and xenophagy (Figure 12) (Richter et al., 2016, Wild et al., 2011, Zhou et al., 2021). Furthermore, TBK1 can phosphorylate p62 at S403 within the ubiquitin-binding domain, a modification that promotes the binding of p62 to ubiquitin, to promote xenophagy and mitophagy (Figure 12) (Matsumoto et al., 2011, Pilli et al., 2012, Matsumoto et al., 2015). As mentioned earlier, TBK1 also plays a role in TAX1BP1-mediated non-canonical autophagy of NCOA4 and NBR1 (Figure 12) (Ohnstad et al., 2020, Goodwin et al., 2017).

Regulation of TBK1 itself by autophagy receptors and other autophagy proteins has also been reported. NDP52 recruits both FIP200 and TBK1 via the adaptor proteins SINTBAD and NAP1 to induce phagophore formation around *Salmonella* bacteria (Ravenhill et al., 2019). Efficient activation of TBK1 at mitochondria during mitophagy depends on OPTN and NDP52-mediated recruitment (Heo et al., 2015). Furthermore, TAX1BP1 recruits TBK1 to p62-containing aggregates (Schlütermann et al., 2021). TBK1 activity is in itself regulated by autophagy, as autophagy is needed to limit excessive TBK1 activation (Schlütermann et al., 2021, Yang et al., 2016). Inefficient clearance of aggregates due to deficient autophagy, particularly loss of FIP200, results in accumulation of active TBK1 at these aggregates. Meanwhile, loss of FIP200 does not appear to affect TBK1 ability to promote interferon production upon TLR3/4 stimuli.

TNIP1

TNFAIP3-interacting protein 1 (TNIP1, also known as ABIN-1, Naf-1 and VAN) is an anti-inflammatory adaptor protein implicated in the negative regulation of inflammatory signaling and cell death (Shamilov and Aneskievich, 2018). Negative regulation of immune signaling is crucial to prevent excessive inflammation and development of disease. Cells deficient of TNIP1 show enhanced responses to TNF α and TLR activation, and TNIP1 deficient mice develop severe autoimmunity (Gao et al., 2011, Rudraiah et al., 2018, Su et al., 2019, Dziedzic et al., 2018, Oshima et al., 2009, Kuriakose et al., 2019). Numerous genome wide-association studies have identified genetic variants of TNIP1 to be associated with autoimmune pathologies, including systemic lupus erythematosus, lupus nephritis, psoriasis, rheumatoid arthritis, and systemic sclerosis (reviewed in (Shamilov and Aneskievich, 2018)).

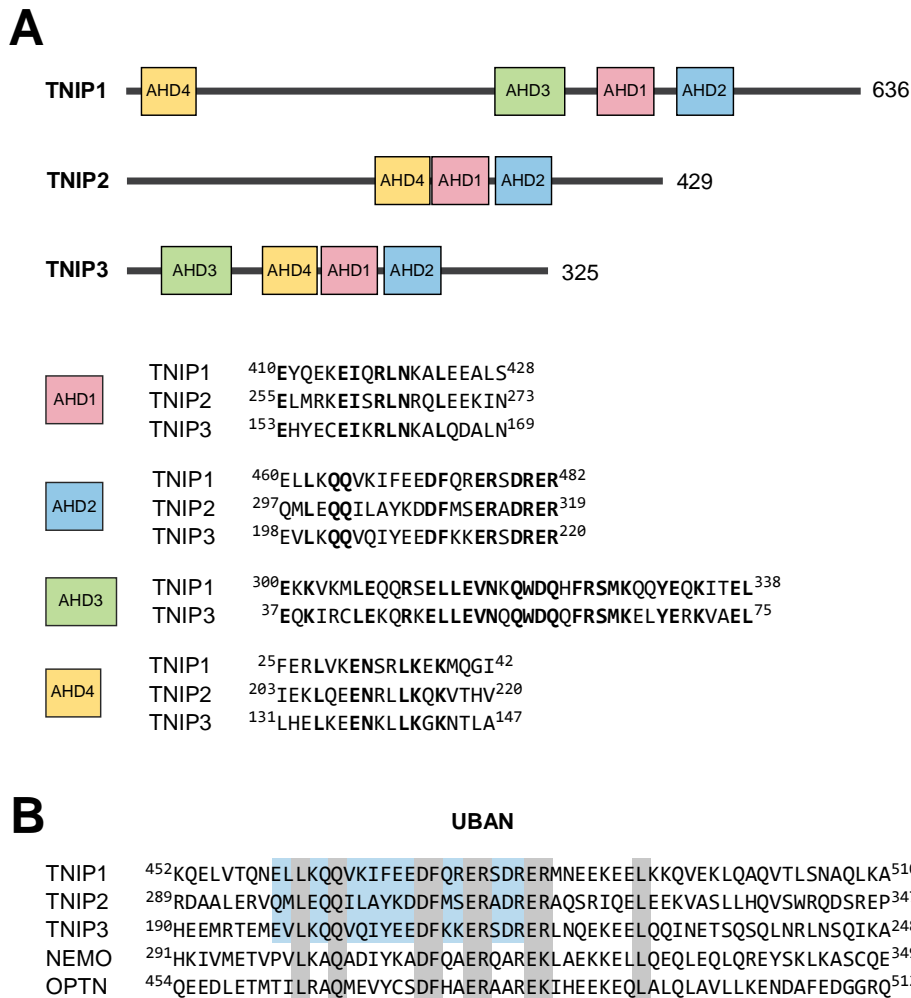


Figure 13: (A) Structural overview of TNIP family proteins, TNIP1-3. AHD1-4 are highlighted with respective colors, and sequence alignment showing the homology is shown in the lower panel. Conserved residues are highlighted in bold. (B) Sequence alignment shows the UBAN domains of TNIP1-3 compared to the UBAN domains of NEMO and Optineurin. Grey highlights fully conserved residues, blue shows the AHD2 in TNIP1-3. Figure was made based on (G'Sell et al., 2015)

TNIP1 is expressed in most tissues, but shows a higher expression level in skeletal muscle, peripheral blood lymphocytes and the spleen (Fukushi et al., 1999). TNIP1 belongs to a family of proteins consisting of three members: TNIP1, -2 and -3 (Figure 13A). Like TNIP1, TNIP2 and -3 also have anti-inflammatory functions (Clark et al., 2013). These proteins share sequences of homology designated ABIN homology domains (AHD) 1-4 (Figure 13A). All TNIP-proteins share the AHD2 domain that includes the ubiquitin-binding UBAN domain, which preferentially binds M1- and K63-linked polyubiquitin chains (Wagner et al., 2008, Nanda et al., 2011, Herhaus et al., 2019, Hong et al., 2021). The UBAN domain is also found in two other inflammatory regulators: OPTN and NEMO (Figure 13B) (Herhaus et al., 2019). A function for AHD3 and -4 in TNIP1 has not been established, while AHD1 is reported to be responsible for the interaction with the ubiquitin editing enzyme A20 (Heyninck et al., 2003, Mauro et al., 2006).

Mechanisms for negative regulation of immune signaling by TNIP1

Most functional studies of TNIP1 as an anti-inflammatory adaptor have focused on its ability to bind K63- and M1- polyubiquitinated substrates via its UBA1 domain. K63- and M1-linked polyubiquitination of proteins is particularly important for the complex assembly and signal transduction of immune-related signal pathways such as the NF- κ B pathway (Hu and Sun, 2016). Currently, there are two proposed hypotheses for how TNIP1 can negatively regulate inflammatory signaling through ubiquitin binding: (1) by competing for polyubiquitin binding and thereby blocking pro-inflammatory complex formation, or (2) through A20-dependent complex disruption (Shamilov and Aneskievich, 2018). A20 is a ubiquitin editing enzyme that can catalyze the removal of K63-linked polyubiquitin chains from substrates, yet also catalyze K48-linked polyubiquitination (Catrysse et al., 2014, Wertz et al., 2004). This way, A20 can disrupt inflammatory signaling complexes by removing K63-linked polyubiquitin chains, while also promoting the proteasomal degradation of substrates by marking them with K48-linked polyubiquitin. TNIP1 is a direct interactor of A20 and can thereby recruit A20 to polyubiquitinated pro-inflammatory mediators (Mauro et al., 2006, Heyninck et al., 2003). TNIP1 negatively regulates NF- κ B signaling by targeting A20 to NEMO to disrupt the IKK complex (Figure 14) (Mauro et al., 2006). However, overexpression of a TNIP1 deletion construct lacking the A20-interacting AHD1 is still able to counteract TNF α -induced NF- κ B activity, suggesting that TNIP1 can act independent of A20 on this pathway as well (Heyninck et al., 2003). Cooperation between TNIP1 and A20 is also demonstrated to inhibit interferon production upon viral infection (Figure 14) (Gao et al., 2011). Here, TNIP1 recruits A20 and TAX1BP1 to TBK1 and IKK ϵ to promote disruption of the TRAF3/TBK1/IKK ϵ complex and inhibit subsequent interferon production (Gao et al., 2011).

RIPK1 is a central regulator of inflammatory cell death, and its activity is controlled by post-translational modifications, including ubiquitination (Mifflin et al., 2020). Upon stimulation with TNF α , TNIP1 is critical for preventing RIPK1-induced necroptotic cell death (Dziedzic et al., 2018, Fauster et al., 2019). TNIP1 recruits A20 to RIPK1, where A20-mediated removal of K63-polyubiquitin inhibits RIPK1 activation (Figure 14) (Dziedzic et al., 2018). Interestingly, the combined loss of TNIP1 and A20 in the intestinal epithelium of mice leads to considerable cell death of intestinal epithelial cells (IECs), severe bowel inflammation, and early mortality (Kattah et al., 2018). However, mice with loss of TNIP1 or A20 alone survive to a similar extent as WT mice, suggesting that TNIP1 and A20 have independent functions that can prevent excessive cell death. IECs deficient of both TNIP1 and A20 are more

susceptible to cell death in response to TNF, microbial signals (dsRNA mimic polyinosinic-polycytidylic acid (poly(I:C)) and LPS) and lymphotoxin (Rusu et al., 2022). Cell death is partially rescued by TRIF deficiency, and completely rescued by MyD88 deficiency (Rusu et al., 2022).

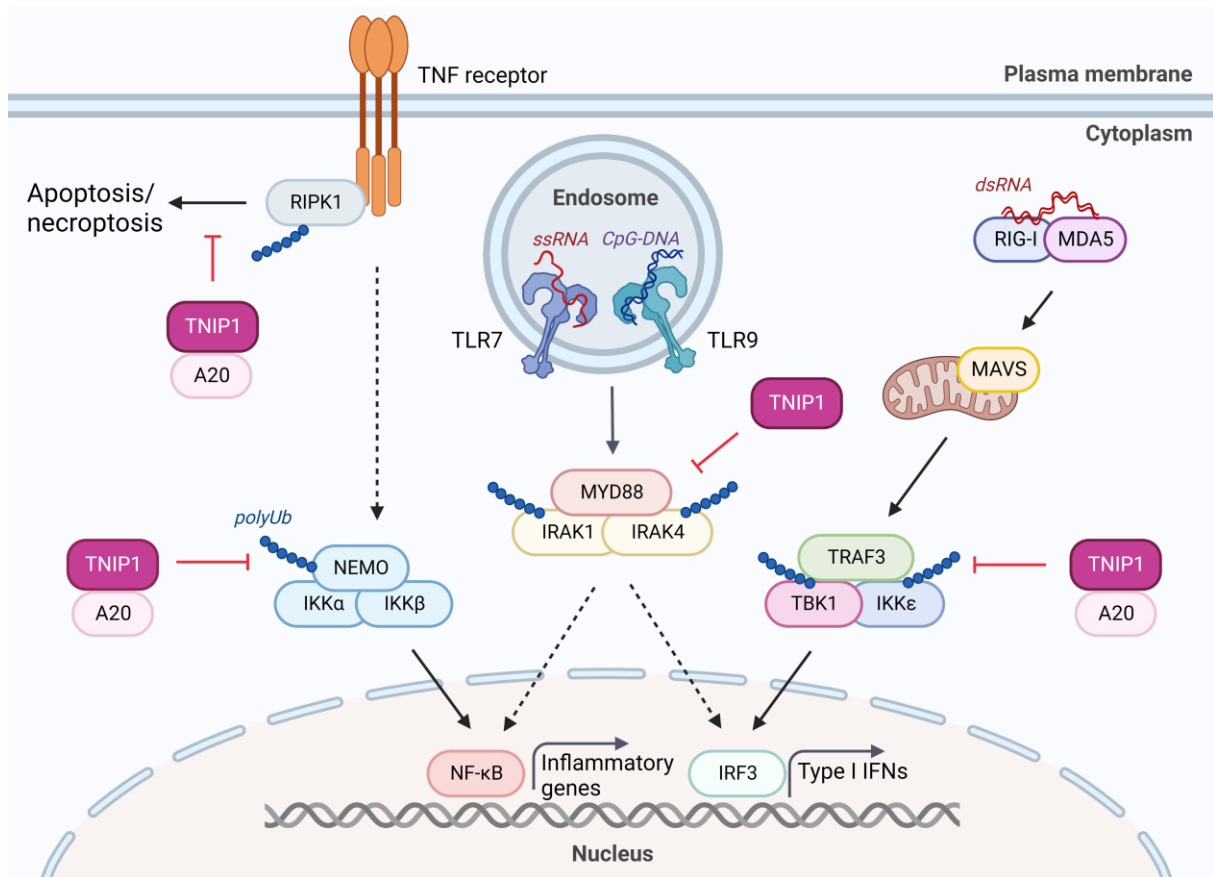


Figure 14: Overview of known pathways in which TNIP1 acts as an anti-inflammatory adaptor protein. Upon activation of the TNF receptor by TNF α , TNIP1 recruits A20 to RIPK1 to prevent the induction of apoptosis/necroptosis, and to NEMO to disrupt the IKK complex, through binding to ubiquitin via its UBAN domain. TNIP1 also prevents excessive activation of the Myddosome upon TLR signaling (specifically TLR4, TLR7/8 and TLR9), a process shown to depend on the UBAN domain. Furthermore, TNIP1 prevents IRF3 activation upon cytosolic viral infection detected via RIG-I/MDA5 and MAVS. Here, TNIP1, along with TAX1BP1 and A20 disrupts the TRAF3-TBK1-IKK ϵ complex required for IRF3 activation. Figure was made using BioRender.

Studies on TNIP1 deficient and mutant mice have shed further light on the mechanisms in which TNIP1 can affect autoimmunity. Only few mice deficient of TNIP1 survive to birth, as the majority die during embryogenesis due to excessive TNF α -induced liver apoptosis (Oshima et al., 2009). The mice that do survive develop severe autoimmune disease and die within 2-4 months (Zhou et al., 2011, Kuriakose et al., 2019). While TNF α signaling is the main driver of liver apoptosis in these mice, excessive TLR signaling through MyD88 promotes the development of autoimmunity, including glomerulonephritis, a sign of lupus nephritis (Kuriakose et al., 2019, Zhou et al., 2011). TNIP1 is recruited to the MyD88-IRAK1/4 complex

through ubiquitin binding (Figure 14) (Zhou et al., 2011, Nanda et al., 2011). Similar studies of mice expressing a ubiquitin-binding mutant of TNIP1 (D485N in mice, equivalent to D472N in humans) show that they are born at a seemingly healthy rate, yet develop severe autoimmune disease similar to that mice deficient of TNIP1, after around 3 months (Nanda et al., 2011, Nanda et al., 2019). Here, the development of disease is also demonstrated to be caused by TLR signaling through MyD88-IRAK1/4 (Nanda et al., 2016, Nanda et al., 2019).

Regulation of TNIP1 function

Generally, it is believed that TNIP1 recruitment to signaling complexes is primarily driven by the presence of polyubiquitin. OPTN, another UBAN containing protein, has a serine residue within the UBAN domain that is phosphorylated by TBK1 to enhance the affinity for ubiquitin upon specific stimuli (Figure 13B) (Herhaus et al., 2019, Richter et al., 2016). TNIP1, on the other hand, has an acidic glutamate in this position that enhances binding, but no obvious residues within the UBAN that allow for regulation by phosphorylation (Herhaus et al., 2019). Whether or not phosphorylation can regulate TNIP1 ubiquitin binding and recruitment to signaling complexes, is not known.

Recent studies have focused on the regulation of TNIP1 protein levels, and how this may relate to its function as a negative regulator of inflammation. For instance, NLR family pyrin domain containing 10 (NLRP10) can interact with and downregulate TNIP1 protein levels upon bacterial infection, through yet unknown mechanisms (Mirza et al., 2019). Activation of RIG-I/MDA5 signaling by cytoplasmic dsRNA mimic poly(I:C) also leads to a decline in TNIP1 protein levels, in a proposed A20-dependent manner (Su et al., 2019). Several recent proteomic screens have suggested a role for autophagy in the degradation of TNIP1. A proteomics screen of starvation-induced changes in protein expression done by our group found that TNIP1 protein levels were reduced upon starvation, alongside several known SLRs and LC3B (Mejlvang et al., 2018). A different proteomics screen of LPS-stimulated bone marrow derived macrophages deficient of ATG16L1, found that TNIP1 protein accumulates over time as compared to normal cells (Samie et al., 2018). TNIP1 has also been identified in a screen as a possible interactor of ATG16L1, alongside A20 (Slowicka et al., 2019). Interestingly, a proteomic analysis of senescent cells found that TNIP1 is degraded by OPTN-mediated selective autophagy upon induction of senescence (Lee et al., 2021). In the profiling of proteins found in autophagosomes-autolysosomes using proximity labelling of SARs and LC3B, TNIP1 was found together with p62, NBR1, NDP52, TAX1BP1 and OPTN as well as LC3B (Zellner et al., 2021) More recently, it was reported that mouse TNIP1 is degraded by autophagy upon

LPS-stimuli (Shinkawa et al., 2022). TLR4-activation led to phosphorylation of TNIP1 immediately N-terminal to an identified LIR motif, which increased binding to LC3A and the autophagic degradation of TNIP1 (Shinkawa et al., 2022). Meanwhile, TNIP1 is reported to be degraded by the proteasome in T cells upon T cell receptor activation, and upon interleukin-17 stimuli in fibroblasts, likely to allow the potent activation of downstream signaling (Yin et al., 2022, Cruz et al., 2017).

Aims of the study

TNIP1 is established as an anti-inflammatory and pro-survival adaptor protein and is associated with autoimmune diseases including systemic lupus erythematosus, rheumatoid arthritis and systemic sclerosis. Uncovering the mechanisms in which TNIP1 protects against excessive inflammation could help our understanding and management of such debilitating diseases. Based on indications that TNIP1 is an autophagy substrate, we hypothesized that selective autophagy of TNIP1 may act as a mechanism for the cell to regulate TNIP1 protein levels both basally and under inflammatory conditions. This, in turn, could further affect the output of inflammatory signaling. To this end, the following aims were put forward for this study:

- Identify TNIP1 as an autophagy substrate, and possibly an autophagy receptor
- Determine the mechanisms underlying TNIP1 autophagic degradation, through both ATG7-dependent and -independent pathways
- Examine the role of SLRs in TNIP1 degradation
- Examine the functional consequences of TNIP1 autophagic degradation on inflammatory signaling

Summary of papers

Paper I

TBK1 phosphorylation activates LIR-dependent degradation of the inflammation repressor TNIP1

Zhou, J.* , Rasmussen N.L.* , Olsvik, H.L., Akimov V., Hu Z., Evjen G., Kaeser-Pebernard S., Sankar, D.S., Roubaty, C., Verlhac, P., van de Beck, N., Reggiori F., Abudu, Y.P., Blagoev, B., Lamark, T., Johansen, T. and Dengjel, J. (2023). *J. Cell Biol.* 222 (2): e202108144.

<https://doi.org/10.1083/jcb.202108144>; PMID: 36574265

*Contributed equally to this paper

In this study, we establish TNIP1 as a constitutive autophagy substrate. Furthermore, we find that TNIP1 colocalizes with several SLRs and interacts directly with the ATG8 proteins. As a result, we identify two LIR motifs, designated LIR1 and LIR2, in which LIR2 is the primary LIR responsible for ATG8 binding. However, we find that the constitutive turnover of TNIP1 appears to depend on other SLRs and only partially on ATG8 lipidation. We further demonstrate that the autophagic degradation of TNIP1 is induced during the initial steps of TLR3 signaling by poly(I:C), in an ATG7- and LIR-dependent manner. The degradation of TNIP1 correlated with an enhancement of downstream TLR3 signaling, suggesting that autophagic degradation of TNIP1 occurs to remove its anti-inflammatory function. Mechanistically, the degradation of TNIP1 is induced through phosphorylation of residues immediately N-terminal to LIR2 by the kinase TBK1, which strongly promotes the interaction with all ATG8 proteins.

Paper II

TNIP1 is a constitutive autophagy substrate independent of ATG8 lipidation and LIRs

Rasmussen N.L., Olsvik, H.L., Evjen, G., Øvervatn A., Lamark, T., and Johansen, T. (2023).

Manuscript

In this study, we further explore the roles and biochemistry of the TNIP1 LIRs. Due to conflicting reports of the role of LIR1 in mouse and human TNIP1, we examined the potential differences in TNIP1 binding to ATG8s. We find that LIR2 is the key LIR in human TNIP1, while LIR1 in mouse TNIP1 can augment LC3A binding in conjunction with LIR2. This

difference is due to the presence of a proline in human LIR1, which disrupts binding to ATG8s. We further show that the constitutive degradation of TNIP1, as opposed to the TLR3-induced degradation described in paper I, is independent of LIRs and ATG8 lipidation. Instead, we find that TNIP1 can interact with several proteins implicated in autophagy independent of ATG8 lipidation, namely TAX1BP1, NBR1 and TSG101. Using tandem-tagged TNIP1 to assess lysosomal turnover, we find that the region of TNIP1 that interacts with TAX1BP1 and NBR1 is required for its constitutive turnover. We suggest that the basal turnover of TNIP1 can occur through a TAX1BP1-mediated autophagy pathway.

Paper III

NBR1: The archetypal selective autophagy receptor

Rasmussen, N.L., Kournoutis, A., Lamark, T. and Johansen, T. (2022). *J. Cell Biol.* 221 (11): e202208092. <https://doi.org/10.1083/jcb.202208092>; PMID: 36255390

In this review, we aim to present the current body of knowledge regarding the SLR NBR1, to bring it out of the shadow of its more famous cousin, p62. Evolutionary analysis suggests that NBR1 represents the archetypal autophagy receptor, and possibly the origin of selective autophagy. We further discuss that the yeast autophagy receptors Atg19 and Atg34 are likely NBR1 homologs. Nonetheless, the number of studies focusing on p62 are vastly greater than that of NBR1. Studies are revealing an important role for NBR1 in regulating p62 bodies, and the clearance of detrimental aggregates within the cell. Furthermore, NBR1 is the main mediator of the removal of peroxisomes by pexophagy. In plants, the NBR1 homolog is responsible for the clearance of several pathogens and pathogen components, yet in humans, NBR1 is not as centrally implicated in xenophagy as other SLRs have been. In recent years, studies have highlighted a role for NBR1 in disease, including cancer development and metastasis, highlighting the importance of increasing our understanding of the functions of NBR1, both as an autophagy receptor and beyond.

Discussion

Identification of TNIP1 as an autophagy substrate

Our exploration of TNIP1 as an autophagy substrate began as the results of two separate proteomics screens. Initially, TNIP1 showed up as a potential autophagy substrate upon starvation, based on a stable isotope labeling by amino acids in cell culture (SILAC) proteomics analysis performed in our lab (Mejlvang et al., 2018). Here, TNIP1 was one of several proteins, including known SLRs, that showed reduced protein levels upon acute amino acid starvation through a type of selective microautophagy (Mejlvang et al., 2018). In this analysis the authors did not study TNIP1 further than to show it was degraded upon starvation. As presented in paper I, in a subsequent screen for identifying new autophagy substrates based on protein ubiquitination, TNIP1 showed up again as a candidate autophagy substrate. This lay the grounds for us to further study TNIP1 as a candidate autophagy substrate.

In our proteomics screen of ubiquitinated autophagy substrates, we found that a ubiquitinated form of TNIP1 accumulated when lysosomal acidification was blocked, suggesting that TNIP1 may be ubiquitinated and degraded by autophagy. In support of our observations, accumulation of ubiquitinated TNIP1 was reported in a proteomics screen of ATG16L1 deficient macrophages infected with *Shigella flexneri* (Maculins et al., 2021). One of the ubiquitinated sites identified is K402, which is the mouse equivalent of human K389, which we identified as significantly ubiquitinated in our screen in paper I. We were, however, not able to pinpoint the exact importance of this ubiquitination for the turnover of TNIP1. Both modified and unmodified TNIP1 accumulated upon lysosomal blockage and mutating the identified lysine residues to arginine did not affect the autophagic turnover of TNIP1. TNIP1 contains several lysines surrounding the ones identified in this screen, and it is possible that the E3 ligase responsible for the ubiquitination can target these when i.e. K389 is mutated. We can therefore neither exclude nor confirm that ubiquitination of TNIP1 plays a role in TNIP1 degradation. Ubiquitination of TNIP1 may be involved in the formation of higher order structures that are involved in other signaling processes. It is also possible that ubiquitination allows for the interaction between TNIP1 and other SLRs, which are known to bind substrates through ubiquitin-binding domains (Lamark and Johansen, 2021). Proximity labeling of TNIP1 by LC3B, TAX1BP1, p62 and NBR1 is reduced upon blockage of protein ubiquitination, which indicates that the interaction between these proteins and TNIP1 is mediated by ubiquitination

(Zellner et al., 2021). However, it is also possible that these proteins are brought together through the binding to other ubiquitinated components.

Despite the undetermined role of TNIP1 ubiquitination, we were able to establish TNIP1 as an autophagy substrate. TNIP1 protein is stabilized by the V-ATPase inhibitors BafilomycinA1 (BafA1) and ConcanamycinA (ConA), and tandem-tagged TNIP1 showed clear formation of red-only dots, showing TNIP1 inside acidic vesicles. Staining for endogenous TNIP1, we could observe colocalization with several known SLRs, including p62 and TAX1BP1, as well as LAMP1, a marker for lysosomes, and LC3, a marker for autophagosomes. During this work, other studies have reported possible links between TNIP1 and autophagy as well. Combining proximity-labeling by SLRs with autophagosome/lysosome enrichment to profile for possible cargo of the different SLRs, TNIP1 showed up as a cargo candidate for NBR1, NDP52, TAX1BP1 and p62 (Zellner et al., 2021). Furthermore, TNIP1 was proximity labeled by LC3B and OPTN. However, the authors reported that TNIP1 did not show any significant BafA1 stabilization. The cells were treated with BafA1 for 2 hours and examined by western blotting, which in our experience may be too short a time to see a significant increase for TNIP1, which was also suggested by the authors (Zellner et al., 2021).

Structurally, TNIP1 carries some resemblance to OPTN, having a UBAN domain, coiled-coil domains and, as identified in this study, FIR/LIRs. OPTN has been thoroughly demonstrated to act as a TBK1-activated SAR for mitophagy and xenophagy (Ryan and Tumbarello, 2018). However, unlike TNIP1, OPTN does not appear to be an autophagy substrate upon acute starvation nor localize in Rab5-Q79L positive vesicles (Mejlvang et al., 2018). Another protein that shares the UBAN domain is NEMO, a pro-inflammatory adaptor protein in the NF- κ B pathway (Herhaus et al., 2019). Mammalian NEMO has been shown to not contain any LIR, while the NEMO homolog in *D. melanogaster*, Kenny, is a LIR-containing autophagy substrate (Tusco et al., 2017). The functional similarities and differences in the autophagic degradation of these proteins could shed light on important immune regulatory mechanisms.

Identification of LIRs and FIR in TNIP1

We identified two LIRs in TNIP1, designated LIR1 and LIR2, and demonstrate that LIR2 binding to ATG8s is enhanced by the phosphorylation of two adjacent serine residues by TBK1. Based on our in vitro studies of human and mouse TNIP1, we determined that LIR2 is the main LIR responsible for binding ATG8 proteins. Human LIR1 is disrupted by the presence of a

proline in the X₂ position of the LIR. Comparison of numerous established LIRs and mutational peptide array studies indicate that proline is selected against in the X₁ and X₂ positions of the core LIR (Johansen and Lamark, 2020, Alemu et al., 2012, Wirth et al., 2019). However, mouse LIR1 can augment binding to LC3A, in conjunction with an intact LIR2. So, while LIR1 appears to play a negligible role in human TNIP1, mouse LIR1 may play a more active role in ATG8 interaction. Nonetheless, human TNIP1 is, despite the lack of LIR1 cooperation, able to bind LC3A more strongly than mouse TNIP1, suggesting that ATG8 binding of human TNIP1 has been largely restricted to LIR2. This could potentially allow a more targeted regulation of the ATG8 interaction by post-translational modifications, for instance by TBK1.

In addition to identifying LIRs, we also found that LIR2 in TNIP1 acts as a FIR when phosphorylated. Others have also recently reported an interaction between TNIP1 and FIP200 that is LIR dependent (Le Guerroué et al., 2022, preprint). Several SLRs are reported to contain FIRs that overlap with LIRs, including NDP52, p62 and OPTN (Fu et al., 2021, Zhou et al., 2021, Turco et al., 2019). The phosphorylation-induced interaction between the TNIP1 LIR and FIP200 is reminiscent of the OPTN LIR, which upon phosphorylation shows both enhanced binding to LC3 proteins, and interaction with the C-terminal region of FIP200 (Wild et al., 2011, Rogov et al., 2013, Zhou et al., 2021). For p62, phosphorylation-induced binding to FIP200 competes with LC3 binding (Turco et al., 2019). It is possible that there may be a competition between LC3 and FIP200-binding by TNIP1 LIR2. Functionally, the overlapping LIR and FIR may somehow allow spatiotemporal regulation of these interactions. FIP200 is involved in the earlier steps of autophagy, followed by the lipidation of ATG8 proteins (Lamark and Johansen, 2021). It was suggested for p62 that the accumulation of lipidated ATG8s in the phagophore may outcompete any interaction with FIP200 as the formation of the phagophore progresses (Turco et al., 2019). On the other hand, TAX1BP1 and NBR1 are reported to interact with FIP200 through the SKICH and CC2 domain, respectively (Turco et al., 2021, Ohnstad et al., 2020). These interactions are likely LIR-independent.

LIR-dependent degradation of TNIP1 upon inflammatory signaling

In paper I, we find that TNIP1 LIR2 is phosphorylated by TBK1 upon TLR3-induced inflammatory signaling, which in turn results in the enhanced affinity for ATG8 proteins, and increased autophagic degradation of TNIP1. As TNIP1 has previously been shown to be involved in negatively regulating the immune response to several types of inflammatory stimuli, we examined the response of TNIP1 to TLR3-induced signaling (Gao et al., 2011,

Nanda et al., 2011, Dziedzic et al., 2018, Yin et al., 2022). Here, we observed that TNIP1 protein was degraded upon TLR3-induced signaling, in an ATG7- and LIR-dependent manner. Multiplex proteomic profiling of ATG16L1 KO bone-marrow derived macrophages showed that TNIP1 accumulates upon induction of TLR4 signaling, suggesting that TNIP1 is normally degraded by macroautophagy upon such stimuli (Samie et al., 2018). While the authors did not pursue to further verify TNIP1 as an autophagy substrate, it is in support of our findings that inflammatory stimuli can induce the degradation of TNIP1 by macroautophagy. This is also supported in a recent study, that shows the phosphorylation-induced autophagic degradation of TNIP1 upon TLR4 and TLR1/2 signaling in MEFs (Shinkawa et al., 2022). In another recent publication, it was shown that TNIP1 is degraded by autophagy in an ATG7- and OPTN-dependent manner upon induction of senescence, to allow an inflammatory response (Lee et al., 2021). The interaction between TNIP1 and OPTN was mapped to be between the AHD4 of TNIP1 and a NEMO-like domain of OPTN. In paper II, we were unable to demonstrate in vitro interaction between TNIP1 and OPTN, suggesting that there may be other factors involved in this interaction, such as post-translational modifications or indirect interaction.

Instead, we showed that the degradation of TNIP1 upon TLR3 stimuli was induced by TBK1-mediated phosphorylation of LIR2, which led to a strong increase in ATG8 binding by TNIP1. We observed that TNIP1 formed dots that to a large degree colocalized with active TBK1 upon TLR3 activation. Several instances of phosphorylation-based regulation of LIRs have been demonstrated (Birgisdottir et al., 2019, Wirth et al., 2021, Zhu et al., 2013, Wu et al., 2014b, Di Rita et al., 2018, Wild et al., 2011). In the case of SCOC LIR, phosphorylation of a serine at the X₂ position of the LIR results in an increased affinity for LC3 family proteins (Wirth et al., 2021). Also, TBK1-mediated phosphorylation of the OPTN LIR is demonstrated to enhance the affinity for LC3 proteins, which further promotes the autophagic degradation of OPTN (Rogov et al., 2013, Wild et al., 2011). This is reminiscent of the effect we observed when exchanging the serines in the X₂ and X₃ position with phosphomimic glutamate residues in the TNIP1 LIR2. Shinkawa et al. (2022) further report that phosphorylation of LIR1 in mouse TNIP1 is responsible for inducing the degradation of TNIP1 upon TLR4 and TLR1/2 activation. Whether TBK1 is involved in this process, and whether human TNIP1 LIR1 is also regulated by phosphorylation, remains to be determined.

The possible interaction between phosphorylated TNIP1 LIR2 and FIP200 adds another interesting layer of complexity to the function of the LIRs upon inflammatory stimuli. Recruitment of FIP200 through direct interaction with certain SARs has been demonstrated as

a mechanism for inducing selective autophagy (Fu et al., 2021, Ohnstad et al., 2020, Turco et al., 2019, Ravenhill et al., 2019). In several cases, the interaction with FIP200 is promoted by TBK1-mediated phosphorylation. Our observations of the interaction between TNIP1 and FIP200 raises the possibility that TNIP1 can be involved in initiating autophagy and is dependent on phosphorylation of LIR2.

Role of TNIP1 degradation upon inflammatory stimuli: substrate or receptor?

The presence of LIRs and ubiquitin-binding domains are hallmarks of the members of the SLR family of SARs (Lamark and Johansen, 2021). We therefore speculated if TNIP1 is an autophagy receptor, or merely an autophagy substrate. Previous studies of TNIP1 indicate that it acts negatively on inflammatory signaling by outcompeting other ubiquitin-binding proteins to block signal transduction (Shamilov and Aneskievich, 2018). In light of TNIP1 being an autophagy substrate, it raises the question of whether autophagy is utilized to regulate TNIP1 levels and thereby its ability to outcompete other ubiquitin-binding proteins, or if TNIP1 may act as a receptor that brings pro-inflammatory components for degradation. The autophagic degradation of TNIP1 may also have different functions depending on context and stimuli.

Several of the identified SLRs were originally studied for their roles in immune signaling, prior to them being identified as autophagy receptors (Deretic, 2012). This highlights the potential role of selective autophagy in regulating immune signaling. According to Shinkawa et al. (2022), TNIP1 acts a receptor that mediates autophagic degradation of the Myddosome upon TLR4 and TLR1/2 signaling. We have not yet identified any substrate of TNIP1 upon TLR3 signaling, which does not involve the Myddosome and this would be important to address in future studies (Yamamoto et al., 2003). The timing of TNIP1 degradation upon TLR3-signaling prompted us to speculate that the induced degradation of TNIP1 occurs to allow establishment of an inflammatory response during the early stages of TLR3 activation. The level of TNIP1 protein inversely correlates with the level of TBK1 activation. As TBK1 is an important mediator of TLR3-signaling, it is possible that TNIP1 is degraded to remove the negative effect on signaling. Interestingly, as TNIP1 levels increase again at later stages, the activation of TBK1 goes down, while in TNIP1 deficient cells, TBK1 activity is sustained and increased over time. Inflammatory signaling is often oscillatory, displaying peaks of signal activation, followed by reduction due to negative feedback (Tian et al., 2005). TNIP1 is established as a late NF- κ B activated gene, and its increased expression is related to the negative feedback of NF- κ B activation (Tian et al., 2005). This could support the

hypothesis that autophagy is utilized to limit the amount of TNIP1 in early stages of inflammation, followed by an increase in expression at later stages to inhibit signaling. Autophagy is generally considered anti-inflammatory, because of its homeostatic roles involving removal of damaged organelles such as mitochondria, and invading pathogens (reviewed in (Deretic, 2021)). However, we observed that the induction of ISG15 expression was delayed upon TLR3 activation in cells expressing LIR1+2 mutant TNIP1, suggesting that autophagic degradation of TNIP1 has a pro-inflammatory effect. We have not been able to establish if the autophagic turnover of TNIP1 occurs during later stages of signaling, due to the induction of TNIP1 expression. If TNIP1 acts as an autophagy receptor, it is possible that its expression is induced at later stages to promote the degradation of signaling components to prevent sustained inflammatory signaling. This would be important to determine in future studies.

TNIP1 is involved in cell survival upon inflammatory stimuli, yet the details behind the regulation are unclear (Oshima et al., 2009, Dziejczak et al., 2018). Signal transduction upon inflammatory stimuli involves formation of higher-order protein assemblies, either solid-like supramolecular complexes, or liquid-like phase-separated condensates (Xia et al., 2021). Such higher-order assemblies are commonly promoted by M1- and K63-linked polyubiquitination of proteins to mediate signaling events, including the promotion of cell death (Gentle, 2019, Xia et al., 2021). The receptor homotypic interaction motif (RHIM)-containing proteins RIPK3 and TRIF play central roles in mediating TLR3-induced cell death, and RIPK1 and RIPK3 promote TNF-induced cell death (Kaiser et al., 2013, Annibaldi and Meier, 2018). Interestingly, autophagic degradation of supramolecular complexes of RIPK1, RIPK3 and TRIF is involved in limiting inflammation-induced cell death (Lim et al., 2019, Gentle et al., 2017). Cells deficient of ATG16L1 show accumulation of aggregated RIPK1, RIPK3 and TRIF structures upon stimuli of TLR3 and TLR4 and are consequently more sensitive to cell death (Lim et al., 2019). Of the SLRs tested, TAX1BP1 loss also sensitized cells to cell death, suggesting a role for TAX1BP1 in mediating degradation of higher-order immune signaling complexes. TNF α can induce cell death through three different TNF receptor (TNFR) complexes designated IIa and IIb, inducers of apoptosis; and the necrosome, inducer of necroptosis, depending on stimuli and cellular context (Grootjans et al., 2017). In a very recent paper, it was demonstrated that autophagy acts as a cell death check-point upon TNF α -induced cell death via complex IIa caspase-8 activation (Huyghe et al., 2022). Specifically, the components of the cell death inducing TNFR complex IIa, consisting of Fas-associated death domain (FADD), RIPK1 and

caspase-8, were degraded through a non-canonical autophagy pathway that is independent of ATG8 lipidation and ULK1, but requires ATG9A and the other ULK1 complex components, including FIP200 (Huyghe et al., 2022). Interestingly, TAX1BP1 was responsible for mediating the degradation, likely through direct recruitment of FIP200 through its SKICH domain. In another example of crosstalk between TNF-induced cell death and autophagy, it has been shown that ULK1 can directly phosphorylate RIPK1 to prevent TNFR complex IIb and necrosome-induced cell death (Wu et al., 2020). Furthermore, induction of TNF-induced necroptosis leads to dysregulated fusion of autophagosomes with lysosomes (Wu et al., 2021). Interestingly, TAX1BP1 and p62 were still degraded under these conditions, suggesting alternative routes to the lysosome than macroautophagy. Altogether, these studies indicate a role for both canonical and non-canonical autophagy during inflammation-induced cell death. TNIP1 has previously been implicated in preventing excessive TNF-induced apoptosis and necroptosis, by targeting both RIPK1 and caspase-8-induced cell death pathways (Dziedzic et al., 2018, Oshima et al., 2009). TNIP1 is recruited to RIPK1 via ubiquitin binding and mediates the further recruitment of A20 to prevent TNF-induced apoptosis and necroptosis. TNIP1 is also demonstrated to prevent caspase-8 recruitment to the TNF death inducing signaling complex (Oshima et al., 2009). Considering the emerging role of autophagy in regulating inflammatory cell death, the pro-survival role of TNIP1, and that TNIP1 is an autophagy substrate of both canonical and non-canonical autophagy, it is tempting to speculate that TNIP1 may be involved in the autophagic turnover of cell death related components. It would therefore be interesting to investigate whether autophagy is involved in the cell-survival function of TNIP1, possibly in conjunction with TAX1BP1.

Whether autophagy plays a role in the functional relationship between TNIP1 and A20, is not known. However, there are clues that could indicate that A20 may be an autophagy substrate as well. In the profiling of proteins found in autophagosomes-autolysosomes by proximity labelling of SARs, A20 was identified as a cargo candidate of NDP52 and p62 (Zellner et al., 2021). A20 has been reported to localize to lysosomes and mediates the lysosomal degradation of TRAF2 (Li et al., 2008, Li et al., 2009). A20 has also been observed in p62 bodies (Johansson et al., 2017). In addition, A20 has been linked to the negative regulation of autophagy, by deubiquitination of Beclin-1 and ATG9A (Shi and Kehrl, 2010, Wang et al., 2022b). If TNIP1 is involved in these processes is not known. It is possible that degradation of TNIP1 by autophagy indirectly regulates A20, by affecting its recruitment to

inflammatory complexes. Whether A20 plays a role in TNIP1 stability, or vice versa, remains to be determined.

LIR-independent basal degradation of TNIP1

In paper II, we find that unlike the inflammation-induced turnover of TNIP1, the basal degradation of TNIP1 does not require LIRs, ATG8 lipidation or ubiquitin binding. Our results support that the basal TNIP1 turnover is mediated primarily by lysosomal degradation. This was based on the formation of red-only dots with tandem-tagged TNIP1, and that inhibitors of lysosomal acidification led to accumulation of TNIP1 protein, as well as colocalization with LAMP1 and LC3. Furthermore, proteasomal inhibitors did not affect TNIP1 stability. However, we still observed lysosomal turnover of TNIP1 in ATG7 and ATG16L1 deficient cells. ATG7 and ATG16L1 are central in the conjugation of ATG8 proteins to PE, which is considered an essential step in the process of macroautophagy (Weidberg et al., 2010). This indicates that TNIP1 can be delivered to lysosomes by other means than classical macroautophagy. This could include CMA and microautophagy, in addition to other less defined processes that go under the umbrella term of non-canonical autophagy (Codogno et al., 2012, Wang et al., 2022a, Kaushik and Cuervo, 2018). ESCRT proteins have been linked to forms of microautophagy (Mejlvang et al., 2018, Liu et al., 2015). Our observation that TNIP1 interacts with TSG101 *in vitro*, as well as the presence of TNIP1 in Rab5-Q79L positive vesicles could suggest involvement of microautophagy. The TSG101 interaction occurred through the N-terminal part of TNIP1 (1-260). The TNIP family member TNIP2 interacts directly with TSG101 via a conserved ESCRT and Alix binding region (EABR) (Banks et al., 2016). However, we did not identify any such region when examining the amino acid sequence of TNIP1, suggesting that the interaction with TSG101 is different from that of TNIP2. However, further studies are required to examine the functional significance of this interaction. Based on our tandem-tag assay using deletion constructs of TNIP1, the N-terminal region that binds TSG101 is not sufficient for lysosomal degradation.

The SLR NBR1 contains LIRs and is normally turned over in a LIR-dependent manner (Kirkin et al., 2009). However, it was recently shown that in ATG7-deficient cells, NBR1 could still be degraded by the help of another SLR, TAX1BP1 (Ohnstad et al., 2020). TNIP1 has previously been reported to interact in a complex with TAX1BP1 and A20 in the regulation of IRF3 activation by TBK1 and IKK ϵ (Gao et al., 2011). We observed direct *in vitro* interaction between TNIP1 and TAX1BP1 and NBR1, via a region of TNIP1 encompassing the AHD3.

Furthermore, we show that the region encompassing AHD3 can mediate TNIP1 turnover in unstimulated cells. This suggests that the ATG8-independent basal turnover of TNIP1 may be mediated by similar mechanisms as that of TAX1BP1 and NBR1. However, we cannot exclude that several mechanisms are at play during the basal turnover of TNIP1. Loss of TAX1BP1 alone does not perturb the accumulation of TNIP1 upon BafA1 treatment. It is possible that the turnover can involve LIRs and ATG8 conjugation, or be mediated by other SLRs, and that a form of non-canonical autophagy mediated by TAX1BP1 can compensate for loss of ATG8 conjugation. It is also possible that the interaction with FIP200 may play a role in an ATG7/ATG16L1/ATG8 deficient setting, while the turnover of LIR mutant TNIP1 (which cannot bind ATG8s or FIP200) is mediated by TAX1BP1 and/or other SLRs in ATG8 lipidation competent cells. To determine this, one would have to disrupt both pathways. The possibility that multiple pathways can lead to TNIP1 lysosomal degradation makes it challenging to pinpoint the required components and mechanisms involved. Our results suggest that the AHD3 region is involved in the lysosomal localization of TNIP1. If this is due to the interaction with TAX1BP1 would be relevant to investigate in future studies. For instance, if the interaction could be disrupted by a point mutation or a smaller deletion, one could test the ability of such a construct to be degraded in lysosomes. Interestingly, we have observed endogenous TNIP1 clustering around TAX1BP1 positive aggregates which form in ATG8- or FIP200-deficient cells (**Figure 15**). We have not been able to investigate the functional significance of this observation, but it supports the presence of an interaction between TNIP1 and TAX1BP1 upon impaired macroautophagy.

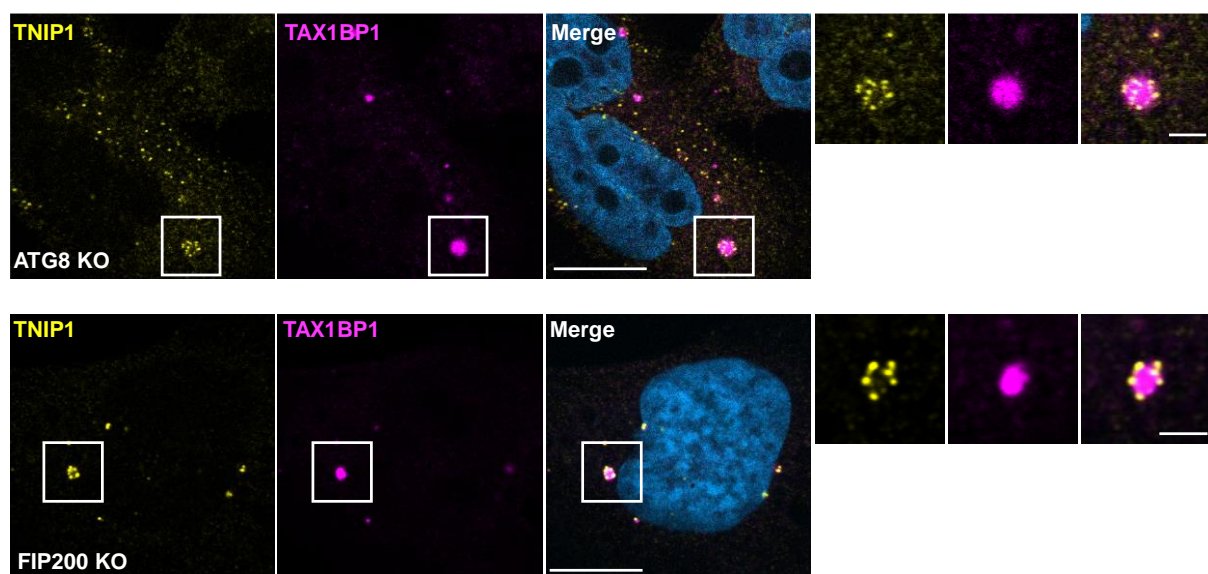


Figure 15: Staining of endogenous TNIP1 (yellow) and TAX1BP1 (purple) in HeLa FlpIn ATG8 deficient cells (top) and U2OS FIP200 deficient cells (bottom). Scale bar in main image = 10 μ m, scale bar in crops = 2 μ m. Images were taken with Zeiss LSM800, with a 63 \times NA1.4 oil immersion lens. The crop for FIP200 KO cell was acquired using Airyscan, followed by deconvolution.

The other TNIP family members TNIP2 and TNIP3 do not appear to have LIRs based on their amino acid sequences, and it is not known whether they are autophagy substrates. However, TNIP3 contains both AHD1 and AHD3, and one may speculate whether TNIP3 can undergo similar autophagic degradation as TNIP1. In contrast, TNIP2 lacks the AHD3. Whether autophagy can play a role in regulating the function of TNIP2 or TNIP3, either directly or indirectly, would be interesting to examine in future studies.

Evolving selectivity in selective autophagy: NBR1 and TNIP1

In paper III, we review the autophagy receptor NBR1. Evolutionary analysis suggests that NBR1 may be the ancestral soluble SAR, representing the possible origin of selective autophagy. A subsequent gene duplication during the development of early multicellular organisms (metazoa) likely gave rise to p62 (Svenning et al., 2011). Furthermore, homologs of the CALCOCO-family of SARs, with TAX1BP1 most resembling the ancestral gene, also exist in primitive metazoans (Tumbarello et al., 2015). Curiously, some species have lost the CALCOCO homologs, and this coincides with the loss of the NBR1 gene as well. This is potentially interesting considering the central role for TAX1BP1 in mediating lysosomal degradation of substrates independent of canonical autophagy, including the degradation of NBR1 (Ohnstad et al., 2020, Goodwin et al., 2017). Here, one may speculate if the CALCOCO family represents the development of an alternative pathway for autophagic clearance, while p62 developed into a central mediator of selective autophagy through canonical macroautophagy. It would be interesting to know if ancestral CALCOCO homologs interact with NBR1, and can mediate its degradation similar to what has been observed in humans (Ohnstad et al., 2020).

TNIP1 has been traced to amphioxus, the closest living invertebrate relative of vertebrates (Holland et al., 2004, Yuan et al., 2014). The TNIP1 homolog in *Branchiostoma belcheri tsingtauense* was demonstrated to cooperate with amphioxus A20 in targeting NEMO for degradation (Yuan et al., 2014). This homolog of TNIP1 shows conservation of the AHD1-4 and binds ubiquitin via a UBAN - yet this homolog lacks any sequence resembling a classical LIR (Yuan et al., 2014). A search for TNIP1 homologs in other amphioxus species reveals that *B. lanceolatum* (NCBI sequence CAH1246196.1), *B. floridae* (NCBI sequence

XP_035669761.1) and *B. belcheri* (NCBI sequence XP_019619449.1) all have TNIP1-like homologs that contain a sequence that resembles the LIR. Interestingly, we found that the TBK1 phosphorylation sites (S122, S123) of LIR2 in TNIP1 are preserved to cartilaginous fishes, which is believed to be the earliest species to develop an adaptive immune system (Flajnik and Kasahara, 2010). This could suggest that the regulation of LIR2 by phosphorylation emerged as part of the specialization of innate and adaptive immune responses.

Conclusions

Determining the mechanisms behind the anti-inflammatory and pro-survival function of TNIP1 can prove valuable for our understanding of the development of complex autoimmune disorders associated with TNIP1 polymorphisms. Here, we show that TNIP1 is an autophagy substrate under both basal and inflammatory conditions. Upon inflammatory stimuli, TNIP1 degradation by ATG7-dependent macroautophagy is induced by the TBK1-mediated phosphorylation of TNIP1 LIR2. We propose that the increased degradation of TNIP1 is to remove the inhibitory function of TNIP1 on inflammatory signaling to allow a robust cellular defense against infection. It is also possible that TNIP1 acts as a SAR for yet unidentified substrates, which will be relevant to address in future studies. Under basal conditions, however, we find that TNIP1 lysosomal degradation occurs independent of ATG8 lipidation, TNIP1 LIRs/FIR and ubiquitin-binding. Instead, it appears that TNIP1 turnover is regulated by SLRs. TNIP1 can interact directly with TAX1BP1, NBR1 and TSG101, which have been implicated in autophagy independent of ATG8-lipidation. While we were unable to determine the exact mechanisms of the ATG8-independent turnover of TNIP1, our observations highlight the need to uncover the mechanisms behind the alternative routes to the lysosome upon compromised macroautophagy.

Methodological considerations

Cell lines as model systems

There are many considerations to make when choosing cell lines for cell-based studies. Many of the cell biological results presented in this thesis were acquired using HeLa cells, a well-established model system in cell-based biomedical research. HeLa cells were established in 1951 from a cervical adenocarcinoma from the patient Henrietta Lacks (Lucey et al., 2009). In the many decades since, HeLa cells have been extensively used in biomedical research across the world. Because of their wide use, there are consequently many tools based on HeLa cells, such as established knockout clones. In both our lab and our collaborators lab, we had several established HeLa cell clones available that were deficient of autophagy genes that were relevant for our study. Therefore, it was an advantage to establish our methods for studying TNIP1 degradation in HeLa cells, as we had further tools to study the role of autophagy in this response.

However, another consequence of the wide use of HeLa cells globally, is the divergence of genetic variants. Being a cancer cell line, HeLa cells have a high level of genetic instability, resulting in the accumulation of variations and clonal selection over the decades (Frattini et al., 2015, Liu et al., 2019). An extensive multi-omics analysis of HeLa variants from different laboratories showed that there are indeed significant heterogeneity between HeLa cells originating from different labs (Liu et al., 2019). Furthermore, passaging time can influence reproducibility, as the cells can accumulate genetic alterations across passages (Liu et al., 2019). Therefore, it would be ideal to perform the same experiments in different HeLa variants as well as other cell lines to confirm if results are reproducible. For the studies of basal TNIP1 turnover, we also used U2OS cells, a human osteosarcoma cell line, where we saw similar results as observed for HeLa cells. However, U2OS reportedly show a poor TLR3 response, so we did not use this cell line for studying induced TNIP1 degradation (Laredj and Beard, 2011). Because TNIP1 is involved in immune signaling, it would be relevant to examine if similar TNIP1 degradation occurs in immune cell lines as well. Nonetheless, antiviral signaling through TLR3 is an important defense mechanism not only in immune cells, but also in epithelial tissues. As is pointed out in paper II, there is also inter-species differences in TNIP1, which is also something to consider when using cell lines such as MEFs.

CRISPR-Cas9 gene knockout

For studying TNIP1 mutants, we generated TNIP1 knockout cells using the CRISPR-Cas9 technology. CRISPR-Cas9 has revolutionized biomedical research since it was established as a genome editing tool, as it allows for the permanent silencing of genes (Ran et al., 2013). To target the TNIP1 gene specifically, we designed single guide RNAs (sgRNA) using the bioinformatics tools made by the Feng Zhang group (Ran et al., 2013). The sgRNAs guide the Cas9 enzyme to the target gene sequence, where Cas9 introduces double-stranded cuts in the DNA. However, there is a possibility of off-target effects, in which unintended mutations can occur in other sites of the genome (Fu et al., 2013). One should also keep in mind that KO cells arise from single clones. Within a population of the mother cell line, cells will have varying protein expression levels and metabolism, meaning that measured effects in a KO clone could instead be a clonal effect. There are several approaches that can be made to avoid the risk of off-target effects affecting the interpretation of observed phenotypes: 1) one can validate the phenotype using more than one knockout clone, 2) re-introduce the knockout gene to verify that the phenotype is reversed, 3) perform whole genome sequencing or sequencing of areas identified as having similarity with the sgRNA to identify potential off-target mutations. For studying the effects of TNIP1 KO on autophagy flux in paper I, we used two different clones to examine the effect of TNIP1 loss on autophagy flux and antiviral signal induction. For subsequent reconstitution studies, we decided to focus on a single clone. Here, we saw that TNIP1 loss resulted in increased abundance in pro-inflammatory proteins, and reconstitution was able to counteract this effect, suggesting it is indeed caused by TNIP1 loss, and not an off-target effect.

In vitro interaction studies

In vitro GST pulldown assays were performed in a candidate screen for interaction partners of TNIP1. An advantage with this method is that it is done in a cell-free system and allows for detailed biochemical studies of direct interactions between proteins and affinity assessment. On the other hand, the fact that it is cell-free could mean bringing together two proteins that may in fact never physically meet in a cellular context. For instance, if one protein is always found in the cytosol, while the other is confined inside peroxisomes, they may interact in vitro, but never actually encounter each other in a physiologically relevant context. Furthermore, specific post-translational modifications can be involved in interactions in a cellular context that may not occur in vitro, and in vitro translated protein may fold differently than it would within a cell. Notably, ubiquitination of proteins has been reported to occur in the rabbit reticulocyte

lysate based in vitro translation system used in our studies (Pridgeon et al., 2003). These factors could lead to false negative or positive results. Therefore, such in vitro GST pulldown studies should ideally be accompanied by other assays that can assess interaction in a cellular context, such as immunofluorescent microscopy assessed colocalization, proximity labeling or co-immunoprecipitation. A drawback with co-immunoprecipitation is that it doesn't discern direct interactions and indirect interactions through complexes. In addition, cell lysis may expose proteins that are otherwise confined to separate subcellular compartments. In the case of our reported interaction with ATG8 proteins and TAX1BP1, we have observed TAX1BP1 and LC3 in both immunoprecipitation-based proteomics screens, colocalization between endogenously stained proteins by immunofluorescent microscopy, and in vitro GST pulldown. For NBR1, TSG101 and FIP200, we have so far only established interaction in vitro, in addition to others reporting NBR1 (Van Quickelberghe et al., 2018, Zellner et al., 2021) and TSG101 (Huttlin et al., 2021, Luck et al., 2020) from large-scale screens. Future studies will be required to assess these interactions in a cellular context.

Transient and stable protein expression

To study TNIP1 degradation and effect of mutations and deletions, we utilized both stable and transient protein expression. Transient transfection of cells is a simple and fast method, but a drawback is that the expression is only temporary, and the protein expression levels are difficult to regulate, leading to overexpression compared to endogenous expression of the protein. We managed to achieve lower expression levels with stable expression of TNIP1, though the expression was still higher than endogenous levels. Furthermore, stably expressed TNIP1 is not under the control of its endogenous promoter, so its transcription is not regulated in the same way as the endogenous protein. This makes it difficult to assess the long-term physiological effects of TLR3-induced signaling on stably expressed exogenous TNIP1, as its expression will not be induced in the same way as the endogenous gene.

Transient transfection was used to express tandem-tagged TNIP1. Here, we observed that cells expressing very high levels of mCherry-EYFP-TNIP1, would accumulate TNIP1 in large yellow aggregates. To assess red-only dot formation, we therefore selected cells that showed lower expression levels. However, we cannot exclude that overexpression itself may induce the high levels of TNIP1 turnover observed with this method. Furthermore, the presence of two large protein tags (mCherry and EYFP) can potentially affect TNIP1 behavior and localization. Another factor to consider is that transient transfection involves introducing DNA

into the cell in the form of a plasmid, which can inadvertently be recognized as a PAMP and lead to a stress response. Since TNIP1 is involved in responses to immunogenic stimuli, this could itself affect the turnover we observe.

Poly(I:C)-induced TLR3 signaling

One of the challenges encountered when studying the effect of TLR3-induced autophagic degradation of TNIP1, was that many of the inhibitors used to block autophagy also affected TLR3 signaling. For instance, the activation of TLR3 in endosomes requires endosomal acidification (de Bouteiller et al., 2005), so blocking autophagy with V-ATPase inhibitors such as BafA1 and ConA also disrupts TLR3 signaling. Proteolytic cleavage of TLR3 by proteases has also been reported to be required for signaling, while others have reported that it is important for TLR3 stability and localization, and not essential for signaling (Garcia-Cattaneo et al., 2012, Qi et al., 2012). However, we found that inhibition of lysosomal proteases by E64d and pepstatin A also disrupted TLR3-signaling. We therefore used several cell lines deficient of different autophagy genes to assess the contribution of autophagy on TNIP1 degradation upon TLR3 signaling. TLR3 signal induction was determined based on the induction of ISG15 and CCL5 expression, which are target genes of IRF3 (Lin et al., 1999, Daly and Reich, 1995). While ISG15 and CCL5 were each successfully induced in cells deficient of various autophagy genes, we cannot exclude that there may be differences in the response of these cells to TLR3 signaling that could influence the effect observed on TNIP1 degradation. The same can be said by the observation that TBK1 inhibition prevents TNIP1 degradation upon TLR3 activation. While our data strongly indicate that TBK1 phosphorylates TNIP1 directly, it may be that TBK1 activity is necessary to activate other components involved in TNIP1 degradation.

Western blotting

Western blotting was employed to determine protein levels under different cellular conditions and treatments. Western blotting is a widely used technique, which involves the separation of proteins by sodium dodecyl sulfate-polyacrylamide gel electrophoresis (SDS-PAGE), followed by transfer to a nitrocellulose or polyvinylidene fluoride (PVDF) membrane. Proteins are subsequently detected using primary antibodies against the protein of interest, followed by secondary antibodies containing a probe, for instance horseradish peroxidase or a fluorophore (Mahmood and Yang, 2012). The technique involves many steps at which variations or errors can occur. Varying techniques for sample preparation, electrophoresis, buffers, transfer systems, immunolabeling and detection can all affect the obtained results. Consequently,

comparison of results between different labs, individual researchers and even individual experiments can sometimes prove challenging.

Despite these caveats, western blotting is often used as a means for quantifying protein levels and achieving statistically significant results. Because of the many variables affecting the obtained results by western blotting, it is generally considered a semi-quantitative method (Mahmood and Yang, 2012). This means that it allows for relative comparison of protein levels within a membrane but does not give an absolute value of protein quantity. Relative protein levels are normalized against housekeeping genes. However, the dynamic range of the housekeeping genes may differ from the protein of interest, and as a result the amount of protein loaded can affect the accuracy of the normalization (Pillai-Kastoori et al., 2020). The method used for immunodetection also impacts the reliability of quantification (Mathews et al., 2009). In our lab, we have two systems for detection: chemiluminescent and near-infrared detection. Chemiluminescent detection is achieved by an enzymatic reaction between a substrate and the horseradish peroxidase attached to the secondary antibody. Here, the rate of the reaction, and thereby the signal detected, depends on the concentration of substrate and enzyme, and the rate is not necessarily linear (Pillai-Kastoori et al., 2020). Uneven distribution of substrate across the blot can also affect the signal. Furthermore, highly expressed proteins may result in a too strong signal and use up the substrate, thereby “burning” the membrane. Near-infrared detection relies on the direct detection of fluorophores and does not require addition of substrate (Mathews et al., 2009). Furthermore, it allows detection of two proteins at the same time, by using fluorophores with different emission spectra. This reduces some of the variabilities from chemiluminescent detection, making the detection more reliable and quantifiable.

In our lab, near-infrared detection was the standard whenever the goal was to achieve quantifiable results. However, we occasionally experienced that some antibodies did not work well with this method. When this was the case, chemiluminescent detection was used. In paper I, our collaborators used only chemiluminescent detection of western blots. For quantification of western blots, at least 3 individual experiments were performed and quantified, to increase confidence in the obtained results. However, the values obtained only give an approximation of the changes in protein levels, and we cannot exclude that the sources of variation and error discussed here, could affect interpretation of results.

References

- ALEMU, E. A., LAMARK, T., TORGENSEN, K. M., BIRGISDOTTIR, A. B., LARSEN, K. B., JAIN, A., OLSVIK, H., ØVERVATN, A., KIRKIN, V. & JOHANSEN, T. 2012. ATG8 family proteins act as scaffolds for assembly of the ULK complex: sequence requirements for LC3-interacting region (LIR) motifs. *J Biol Chem*, 287, 39275-90.
- ANNIBALDI, A. & MEIER, P. 2018. Checkpoints in TNF-Induced Cell Death: Implications in Inflammation and Cancer. *Trends Mol Med*, 24, 49-65.
- ARSTILA, A. U. & TRUMP, B. F. 1968. Studies on cellular autophagocytosis. The formation of autophagic vacuoles in the liver after glucagon administration. *Am J Pathol*, 53, 687-733.
- AXE, E. L., WALKER, S. A., MANIFAVA, M., CHANDRA, P., RODERICK, H. L., HABERMANN, A., GRIFFITHS, G. & KTISTAKIS, N. T. 2008. Autophagosome formation from membrane compartments enriched in phosphatidylinositol 3-phosphate and dynamically connected to the endoplasmic reticulum. *J Cell Biol*, 182, 685-701.
- BANKS, C. A. S., BOANCA, G., LEE, Z. T., EUBANKS, C. G., HATTEM, G. L., PEAK, A., WEEMS, L. E., CONKRIGHT, J. J., FLORENS, L. & WASHBURN, M. P. 2016. TNIP2 is a hub protein in the NF- κ B network with both protein and RNA mediated interactions. *Mol Cell Proteomics*, 15, 3435-3449.
- BENJAMIN, J. L., SUMPTER, R., JR., LEVINE, B. & HOOPER, L. V. 2013. Intestinal epithelial autophagy is essential for host defense against invasive bacteria. *Cell Host Microbe*, 13, 723-34.
- BENTO, C. F., RENNA, M., GHISLAT, G., PURI, C., ASHKENAZI, A., VICINANZA, M., MENZIES, F. M. & RUBINSZTEIN, D. C. 2016. Mammalian Autophagy: How Does It Work? *Annu Rev Biochem*, 85, 685-713.
- BIRGISDOTTIR, Å. B., LAMARK, T. & JOHANSEN, T. 2013. The LIR motif - crucial for selective autophagy. *J Cell Sci*, 126, 3237-47.
- BIRGISDOTTIR, Å. B., MOUILLERON, S., BHUJABAL, Z., WIRTH, M., SJØTTEM, E., EVJEN, G., ZHANG, W., LEE, R., O'REILLY, N., TOOZE, S. A., LAMARK, T. & JOHANSEN, T. 2019. Members of the autophagy class III phosphatidylinositol 3-kinase complex I interact with GABARAP and GABARAPL1 via LIR motifs. *Autophagy*, 15, 1333-1355.
- BJØRKØY, G., LAMARK, T., BRECH, A., OUTZEN, H., PERANDER, M., ØVERVATN, A., STENMARK, H. & JOHANSEN, T. 2005. p62/SQSTM1 forms protein aggregates degraded by autophagy and has a protective effect on huntingtin-induced cell death. *J Cell Biol*, 171, 603-14.
- BONAM, S. R., WANG, F. & MULLER, S. 2019. Lysosomes as a therapeutic target. *Nat Rev Drug Discov*, 18, 923-948.
- BOZIC, M., VAN DEN BEKEROM, L., MILNE, B. A., GOODMAN, N., ROBERSTON, L., PRESCOTT, A. R., MACARTNEY, T. J., DAWE, N. & MCEWAN, D. G. 2020. A conserved ATG2-GABARAP family interaction is critical for phagophore formation. *EMBO Rep*, 21, e48412.
- CADWELL, K. 2016. Crosstalk between autophagy and inflammatory signalling pathways: balancing defence and homeostasis. *Nat Rev Immunol*, 16, 661-675.
- CATRYSSSE, L., VEREECKE, L., BEYAERT, R. & VAN LOO, G. 2014. A20 in inflammation and autoimmunity. *Trends Immunol*, 35, 22-31.
- CHIANG, H. L., TERLECKY, S. R., PLANT, C. P. & DICE, J. F. 1989. A role for a 70-kilodalton heat shock protein in lysosomal degradation of intracellular proteins. *Science*, 246, 382-5.
- CIRULLI, E. T., LASSEIGNE, B. N., PETROVSKI, S., SAPP, P. C., DION, P. A., LEBLOND, C. S., COUTHOUIS, J., LU, Y.-F., WANG, Q. & KRUEGER, B. J. 2015. Exome sequencing in amyotrophic lateral sclerosis identifies risk genes and pathways. *Science*, 347, 1436-1441.
- CLARK, K., NANDA, S. & COHEN, P. 2013. Molecular control of the NEMO family of ubiquitin-binding proteins. *Nat Rev Mol Cell Biol*, 14, 673-685.
- CODOGNO, P., MEHRPOUR, M. & PROIKAS-CEZANNE, T. 2012. Canonical and non-canonical autophagy: variations on a common theme of self-eating? *Nat Rev Mol Cell Biol*, 13, 7-12.

- COUX, O., TANAKA, K. & GOLDBERG, A. L. 1996. Structure and functions of the 20S and 26S proteasomes. *Annu Rev Biochem*, 65, 801-47.
- CRUZ, J. A., CHILDS, E. E., AMATYA, N., GARG, A. V., BEYAERT, R., KANE, L. P., ANESKIEVICH, B. J., MA, A. & GAFFEN, S. L. 2017. Interleukin-17 signaling triggers degradation of the constitutive NF-kappaB inhibitor ABIN-1. *Immunohorizons*, 1, 133-141.
- CUERVO, A. M., KNECHT, E., TERLECKY, S. R. & DICE, J. F. 1995. Activation of a selective pathway of lysosomal proteolysis in rat liver by prolonged starvation. *Am J Physiol*, 269, C1200-8.
- CUERVO, A. M., STEFANIS, L., FREDENBURG, R., LANSBURY, P. T. & SULZER, D. 2004. Impaired degradation of mutant alpha-synuclein by chaperone-mediated autophagy. *Science*, 305, 1292-5.
- DALY, C. & REICH, N. C. 1995. Characterization of specific DNA-binding factors activated by double-stranded RNA as positive regulators of Interferon alpha/beta-stimulated Genes. *J Biol Chem*, 270, 23739-23746.
- DE BOUTELLER, O., MERCK, E., HASAN, U. A., HUBAC, S., BENGUIGUI, B., TRINCHIERI, G., BATES, E. E. M. & CAUX, C. 2005. Recognition of double-stranded RNA by human Toll-like receptor 3 and downstream receptor signaling requires multimerization and an acidic pH. *J Biol Chem*, 280, 38133-38145.
- DE DUVE, C. 1965. The separation and characterization of subcellular particles. *Harvey Lect*, 59, 49-87.
- DE DUVE, C., PRESSMAN, B. C., GIANETTO, R., WATTIAUX, R. & APPELMANS, F. 1955. Tissue fractionation studies. 6. Intracellular distribution patterns of enzymes in rat-liver tissue. *Biochem J*, 60, 604-17.
- DELGADO, M. A., ELMAOUED, R. A., DAVIS, A. S., KYEI, G. & DERETIC, V. 2008. Toll-like receptors control autophagy. *EMBO J*, 27, 1110-1121.
- DERETIC, V. 2012. Autophagy as an innate immunity paradigm: expanding the scope and repertoire of pattern recognition receptors. *Curr Opin Immunol*, 24, 21-31.
- DERETIC, V. 2021. Autophagy in inflammation, infection, and immunometabolism. *Immunity*, 54, 437-453.
- DI RITA, A., PESCHIAROLI, A., D'ACUNZO, P., STROBBE, D., HU, Z., GRUBER, J., NYGAARD, M., LAMBRUGHI, M., MELINO, G., PAPALEO, E., DENGJEL, J., EL ALAOUI, S., CAMPANELLA, M., DÖTSCH, V., ROGOV, V. V., STRAPPAZZON, F. & CECCONI, F. 2018. HUWE1 E3 ligase promotes PINK1/PARKIN-independent mitophagy by regulating AMBRA1 activation via IKK α . *Nat Commun*, 9, 3755.
- DIKIC, I. & ELAZAR, Z. 2018. Mechanism and medical implications of mammalian autophagy. *Nat Rev Mol Cell Biol*, 19, 349-364.
- DIKIC, I., WAKATSUKI, S. & WALTERS, K. J. 2009. Ubiquitin-binding domains — from structures to functions. *Nat Rev Mol Cell Biol*, 10, 659-671.
- DOWDLE, W. E., NYFELER, B., NAGEL, J., ELLING, R. A., LIU, S., TRIANTAFELLOW, E., MENON, S., WANG, Z., HONDA, A., PARDEE, G., CANTWELL, J., LUU, C., CORNELLA-TARACIDO, I., HARRINGTON, E., FEKKES, P., LEI, H., FANG, Q., DIGAN, M. E., BURDICK, D., POWERS, A. F., HELLIWELL, S. B., D'AQUIN, S., BASTIEN, J., WANG, H., WIEDERSCHAIN, D., KUERTH, J., BERGMAN, P., SCHWALB, D., THOMAS, J., UGWONALI, S., HARBINSKI, F., TALLARICO, J., WILSON, C. J., MYER, V. E., PORTER, J. A., BUSSIÈRE, D. E., FINAN, P. M., LABOW, M. A., MAO, X., HAMANN, L. G., MANNING, B. D., VALDEZ, R. A., NICHOLSON, T., SCHIRLE, M., KNAPP, M. S., KEANEY, E. P. & MURPHY, L. O. 2014. Selective VPS34 inhibitor blocks autophagy and uncovers a role for NCOA4 in ferritin degradation and iron homeostasis in vivo. *Nat Cell Biol*, 16, 1069-79.
- DURGAN, J., LYSTAD, A. H., SLOAN, K., CARLSSON, S. R., WILSON, M. I., MARCASSA, E., ULFERTS, R., WEBSTER, J., LOPEZ-CLAVIJO, A. F., WAKELAM, M. J., BEALE, R., SIMONSEN, A., OXLEY, D. & FLOREY, O. 2021. Non-canonical autophagy drives alternative ATG8 conjugation to phosphatidylserine. *Mol Cell*, 81, 2031-2040.e8.
- DZIEDZIC, S. A., SU, Z., JEAN BARRETT, V., NAJAFOV, A., MOOKHTIAR, A. K., AMIN, P., PAN, H., SUN, L., ZHU, H., MA, A., ABBOTT, D. W. & YUAN, J. 2018. ABIN-1 regulates

- RIPK1 activation by linking Met1 ubiquitylation with Lys63 deubiquitylation in TNF-RSC. *Nat Cell Biol*, 20, 58-68.
- FAUSTER, A., REBSAMEN, M., WILLMANN, K. L., CÉSAR-RAZQUIN, A., GIRARDI, E., BIGENZAHN, J. W., SCHISCHLIK, F., SCORZONI, S., BRUCKNER, M., KONECKA, J., HÖRMANN, K., HEINZ, L. X., BOZTUG, K. & SUPERTI-FURGA, G. 2019. Systematic genetic mapping of necroptosis identifies SLC39A7 as modulator of death receptor trafficking. *Cell Death Differ*, 26, 1138-1155.
- FISCHER, T. D., WANG, C., PADMAN, B. S., LAZAROU, M. & YOULE, R. J. 2020. STING induces LC3B lipidation onto single-membrane vesicles via the V-ATPase and ATG16L1-WD40 domain. *J Cell Biol*, 219.
- FLAJNIK, M. F. & KASAHARA, M. 2010. Origin and evolution of the adaptive immune system: genetic events and selective pressures. *Nat Rev Genet*, 11, 47-59.
- FRATTINI, A., FABBRI, M., VALLI, R., DE PAOLI, E., MONTALBANO, G., GRIBALDO, L., PASQUALI, F. & MASERATI, E. 2015. High variability of genomic instability and gene expression profiling in different HeLa clones. *Sci Rep*, 5, 15377.
- FU, T., ZHANG, M., ZHOU, Z., WU, P., PENG, C., WANG, Y., GONG, X., LI, Y., WANG, Y., XU, X., LI, M., SHEN, L. & PAN, L. 2021. Structural and biochemical advances on the recruitment of the autophagy-initiating ULK and TBK1 complexes by autophagy receptor NDP52. *Sci Adv*, 7.
- FU, Y., FODEN, J. A., KHAYTER, C., MAEDER, M. L., REYON, D., JOUNG, J. K. & SANDER, J. D. 2013. High-frequency off-target mutagenesis induced by CRISPR-Cas nucleases in human cells. *Nat Biotechnol*, 31, 822-6.
- FUKUSHI, M., DIXON, J., KIMURA, T., TSURUTANI, N., DIXON, M. J. & YAMAMOTO, N. 1999. Identification and cloning of a novel cellular protein Naf1, Nef-associated factor 1, that increases cell surface CD4 expression. *FEBS Lett*, 442, 83-8.
- G'SELL, R. T., GAFFNEY, P. M. & POWELL, D. W. 2015. A20-binding inhibitor of NF- κ B activation 1 is a physiologic inhibitor of NF- κ B: a molecular switch for inflammation and autoimmunity. *Arthritis Rheumatol*, 67, 2292-302.
- GALLUZZI, L., BAEHRECKE, E. H., BALLABIO, A., BOYA, P., BRAVO-SAN PEDRO, J. M., CECCONI, F., CHOI, A. M., CHU, C. T., CODOGNO, P., COLOMBO, M. I., CUERVO, A. M., DEBNATH, J., DERETIC, V., DIKIC, I., ESKELINEN, E.-L., FIMIA, G. M., FULDA, S., GEWIRTZ, D. A., GREEN, D. R., HANSEN, M., HARPER, J. W., JÄÄTTELÄ, M., JOHANSEN, T., JUHASZ, G., KIMMELMAN, A. C., KRAFT, C., KTISTAKIS, N. T., KUMAR, S., LEVINE, B., LOPEZ-OTIN, C., MADEO, F., MARTENS, S., MARTINEZ, J., MELENDEZ, A., MIZUSHIMA, N., MÜNZ, C., MURPHY, L. O., PENNINGER, J. M., PIACENTINI, M., REGGIORI, F., RUBINSZTEIN, D. C., RYAN, K. M., SANTAMBROGIO, L., SCORRANO, L., SIMON, A. K., SIMON, H.-U., SIMONSEN, A., TAVERNARAKIS, N., TOOZE, S. A., YOSHIMORI, T., YUAN, J., YUE, Z., ZHONG, Q. & KROEMER, G. 2017. Molecular definitions of autophagy and related processes. *EMBO J*, 36, 1811-1836.
- GAO, L., COOPE, H., GRANT, S., MA, A., LEY, S. C. & HARHAJ, E. W. 2011. ABIN1 protein cooperates with TAX1BP1 and A20 proteins to inhibit antiviral signaling. *J Biol Chem*, 286, 36592-602.
- GARCIA-CATTANEO, A., GOBERT, F. X., MÜLLER, M., TOSCANO, F., FLORES, M., LESCURE, A., DEL NERY, E. & BENARROCH, P. 2012. Cleavage of Toll-like receptor 3 by cathepsins B and H is essential for signaling. *Proc Natl Acad Sci U S A*, 109, 9053-8.
- GENG, J. & KLIONSKY, D. J. 2008. The Atg8 and Atg12 ubiquitin-like conjugation systems in macroautophagy. *EMBO Rep*, 9, 859-864.
- GENTLE, I. E. 2019. Supramolecular complexes in cell death and inflammation and their regulation by autophagy. *Front Cell Dev Biol*, 7, 73.
- GENTLE, I. E., MCHENRY, K. T., WEBER, A., METZ, A., KRETZ, O., PORTER, D. & HÄCKER, G. 2017. TIR-domain-containing adapter-inducing interferon- β (TRIF) forms filamentous structures, whose pro-apoptotic signalling is terminated by autophagy. *FEBS J*, 284, 1987-2003.

- GHANBARPOUR, A., VALVERDE, D. P., MELIA, T. J. & REINISCH, K. M. 2021. A model for a partnership of lipid transfer proteins and scramblases in membrane expansion and organelle biogenesis. *Proc Natl Acad Sci U S A*, 118, e2101562118.
- GOODWIN, J. M., DOWDLE, W. E., DEJESUS, R., WANG, Z., BERGMAN, P., KOBYLARZ, M., LINDEMAN, A., XAVIER, R. J., MCALLISTER, G., NYFELER, B., HOFFMAN, G. & MURPHY, L. O. 2017. Autophagy-independent lysosomal targeting regulated by ULK1/2-FIP200 and ATG9. *Cell Rep*, 20, 2341-2356.
- GORDON, P. B. & SEGLEN, P. O. 1988. Prelysosomal convergence of autophagic and endocytic pathways. *Biochem Biophys Res Commun*, 151, 40-7.
- GROOTJANS, S., VANDEN BERGHE, T. & VANDENABEELE, P. 2017. Initiation and execution mechanisms of necroptosis: an overview. *Cell Death & Differentiation*, 24, 1184-1195.
- HAMMERLING, B. C., NAJOR, R. H., CORTEZ, M. Q., SHIRES, S. E., LEON, L. J., GONZALEZ, E. R., BOASSA, D., PHAN, S., THOR, A., JIMENEZ, R. E., LI, H., KITSIS, R. N., DORN, G. W., SADOSHIMA, J., ELLISMAN, M. H. & GUSTAFSSON, Å. B. 2017. A Rab5 endosomal pathway mediates Parkin-dependent mitochondrial clearance. *Nat Commun*, 8, 14050.
- HANADA, T., NODA, N. N., SATOMI, Y., ICHIMURA, Y., FUJIOKA, Y., TAKAO, T., INAGAKI, F. & OHSUMI, Y. 2007. The Atg12-Atg5 conjugate has a novel E3-like activity for protein lipidation in autophagy. *J Biol Chem*, 282, 37298-302.
- HANSEN, M., RUBINSZTEIN, D. C. & WALKER, D. W. 2018. Autophagy as a promoter of longevity: insights from model organisms. *Nat Rev Mol Cell Biol*, 19, 579-593.
- HECKMANN, B. L., BOADA-ROMERO, E., CUNHA, L. D., MAGNE, J. & GREEN, D. R. 2017. LC3-Associated Phagocytosis and Inflammation. *J Mol Biol*, 429, 3561-3576.
- HECKMANN, B. L., TEUBNER, B. J. W., TUMMERS, B., BOADA-ROMERO, E., HARRIS, L., YANG, M., GUY, C. S., ZAKHARENKO, S. S. & GREEN, D. R. 2019. LC3-associated endocytosis facilitates β -amyloid clearance and mitigates neurodegeneration in murine Alzheimer's disease. *Cell*, 178, 536-551.e14.
- HEO, J.-M., ORDUREAU, A., PAULO, JOAO A., RINEHART, J. & HARPER, J. W. 2015. The PINK1-PARKIN mitochondrial ubiquitylation pathway drives a program of OPTN/NDP52 recruitment and TBK1 activation to promote mitophagy. *Mol Cell*, 60, 7-20.
- HERHAUS, L., VAN DEN BEDEM, H., TANG, S., MASLENNIKOV, I., WAKATSUKI, S., DIKIC, I. & RAHIGHI, S. 2019. Molecular recognition of M1-Linked ubiquitin chains by native and phosphorylated UBA1 domains. *J Mol Biol*, 431, 3146-3156.
- HEYINCK, K., KREIKE, M. M. & BEYAERT, R. 2003. Structure-function analysis of the A20-binding inhibitor of NF-kappa B activation, ABIN-1. *FEBS Lett*, 536, 135-40.
- HOLLAND, L. Z., LAUDET, V. & SCHUBERT, M. 2004. The chordate amphioxus: an emerging model organism for developmental biology. *Cell Mol Life Sci*, 61, 2290-308.
- HONG, J. Y., LIN, S. C., KUO, B. J. & LO, Y. C. 2021. Structural and biochemical basis for higher-order assembly between A20-binding inhibitor of NF- κ B 1 (ABIN1) and M1-linked ubiquitins. *J Mol Biol*, 433, 167116.
- HOSOKAWA, N., HARA, T., KAIZUKA, T., KISHI, C., TAKAMURA, A., MIURA, Y., IEMURA, S., NATSUME, T., TAKEHANA, K., YAMADA, N., GUAN, J. L., OSHIRO, N. & MIZUSHIMA, N. 2009. Nutrient-dependent mTORC1 association with the ULK1-Atg13-FIP200 complex required for autophagy. *Mol Biol Cell*, 20, 1981-91.
- HU, H. & SUN, S.-C. 2016. Ubiquitin signaling in immune responses. *Cell Research*, 26, 457-483.
- HUTTLIN, E. L., BRUCKNER, R. J., NAVARRETE-PEREA, J., CANNON, J. R., BALTIER, K., GEBREAB, F., GYGI, M. P., THORNOCK, A., ZARRAGA, G., TAM, S., SZPYT, J., GASSAWAY, B. M., PANOV, A., PARZEN, H., FU, S., GOLBAZI, A., MAENPAA, E., STRICKER, K., GUHA THAKURTA, S., ZHANG, T., RAD, R., PAN, J., NUSINOW, D. P., PAULO, J. A., SCHWEPPE, D. K., VAITES, L. P., HARPER, J. W. & GYGI, S. P. 2021. Dual proteome-scale networks reveal cell-specific remodeling of the human interactome. *Cell*, 184, 3022-3040.e28.
- HUYGHE, J., PRIEM, D., VAN HOVE, L., GILBERT, B., FRITSCH, J., UCHIYAMA, Y., HOSTE, E., VAN LOO, G. & BERTRAND, M. J. M. 2022. ATG9A prevents TNF cytotoxicity by an unconventional lysosomal targeting pathway. *Science*, 378, 1201-1207.

- ICHIMURA, Y., KUMANOMIDOU, T., SOU, Y.-S., MIZUSHIMA, T., EZAKI, J., UENO, T., KOMINAMI, E., YAMANE, T., TANAKA, K. & KOMATSU, M. 2008. Structural basis for sorting mechanism of p62 in selective autophagy. *Journal of Biological Chemistry*, 283, 22847-22857.
- IHA, H., PELOPONESE, J. M., VERSTREPEN, L., ZAPART, G., IKEDA, F., SMITH, C. D., STAROST, M. F., YEDAVALLI, V., HEYNINCK, K., DIKIC, I., BEYAERT, R. & JEANG, K. T. 2008. Inflammatory cardiac valvulitis in TAX1BP1-deficient mice through selective NF-kappaB activation. *EMBO J*, 27, 629-41.
- IMAI, K., HAO, F., FUJITA, N., TSUJI, Y., OE, Y., ARAKI, Y., HAMASAKI, M., NODA, T. & YOSHIMORI, T. 2016. Atg9A trafficking through the recycling endosomes is required for autophagosome formation. *J Cell Sci*, 129, 3781-3791.
- ITAKURA, E., KISHI-ITAKURA, C. & MIZUSHIMA, N. 2012. The hairpin-type tail-anchored SNARE syntaxin 17 targets to autophagosomes for fusion with endosomes/lysosomes. *Cell*, 151, 1256-69.
- JIANG, P., NISHIMURA, T., SAKAMAKI, Y., ITAKURA, E., HATTA, T., NATSUME, T. & MIZUSHIMA, N. 2014. The HOPS complex mediates autophagosome-lysosome fusion through interaction with syntaxin 17. *Mol Biol Cell*, 25, 1327-37.
- JOHANSEN, T. & LAMARK, T. 2011. Selective autophagy mediated by autophagic adapter proteins. *Autophagy*, 7, 279-96.
- JOHANSEN, T. & LAMARK, T. 2020. Selective autophagy: ATG8 family proteins, LIR motifs and cargo receptors. *J Mol Biol*, 432, 80-103.
- JOHANSSON, I., SERGIN, I., KJØBLI, E., DAMÅS, J. K., RAZANI, B., FLO, T. H. & BJØRKØY, G. 2017. N-3 PUFAs induce inflammatory tolerance by formation of KEAP1-containing SQSTM1/p62-bodies and activation of NFE2L2. *Autophagy*, 13, 1664-1678.
- JOSTINS, L., RIPKE, S., WEERSMA, R. K., DUERR, R. H., MCGOVERN, D. P., HUI, K. Y., LEE, J. C., SCHUMM, L. P., SHARMA, Y., ANDERSON, C. A., ESSERS, J., MITROVIC, M., NING, K., CLEYNEN, I., THEATRE, E., SPAIN, S. L., RAYCHAUDHURI, S., GOYETTE, P., WEI, Z., ABRAHAM, C., ACHKAR, J. P., AHMAD, T., AMININEJAD, L., ANANTHAKRISHNAN, A. N., ANDERSEN, V., ANDREWS, J. M., BAIDOO, L., BALSCHUN, T., BAMPTON, P. A., BITTON, A., BOUCHER, G., BRAND, S., BÜNING, C., COHAIN, A., CICHON, S., D'AMATO, M., DE JONG, D., DEVANEY, K. L., DUBINSKY, M., EDWARDS, C., ELLINGHAUS, D., FERGUSON, L. R., FRANCHIMONT, D., FRANSEN, K., GEARRY, R., GEORGES, M., GIEGER, C., GLAS, J., HARITUNIAN, T., HART, A., HAWKEY, C., HEDL, M., HU, X., KARLSEN, T. H., KUPCINSKAS, L., KUGATHASAN, S., LATIANO, A., LAUKENS, D., LAWRENCE, I. C., LEES, C. W., LOUIS, E., MAHY, G., MANSFIELD, J., MORGAN, A. R., MOWAT, C., NEWMAN, W., PALMIERI, O., PONSIOEN, C. Y., POTOCNIK, U., PRESCOTT, N. J., REGUEIRO, M., ROTTER, J. I., RUSSELL, R. K., SANDERSON, J. D., SANS, M., SATSANGI, J., SCHREIBER, S., SIMMS, L. A., SVENTORAITYTE, J., TARGAN, S. R., TAYLOR, K. D., TREMELLING, M., VERSPAGET, H. W., DE VOS, M., WIJMENGA, C., WILSON, D. C., WINKELMANN, J., XAVIER, R. J., ZEISSIG, S., ZHANG, B., ZHANG, C. K., ZHAO, H., SILVERBERG, M. S., ANNESE, V., HAKONARSON, H., BRANT, S. R., RADFORD-SMITH, G., MATHEW, C. G., RIOUX, J. D., SCHADT, E. E., et al. 2012. Host-microbe interactions have shaped the genetic architecture of inflammatory bowel disease. *Nature*, 491, 119-24.
- JUNG, C. H., JUN, C. B., RO, S. H., KIM, Y. M., OTTO, N. M., CAO, J., KUNDU, M. & KIM, D. H. 2009. ULK-Atg13-FIP200 complexes mediate mTOR signaling to the autophagy machinery. *Mol Biol Cell*, 20, 1992-2003.
- KAGEYAMA, S., GUDMUNDSSON, S. R., SOU, Y.-S., ICHIMURA, Y., TAMURA, N., KAZUNO, S., UENO, T., MIURA, Y., NOSHIRO, D., ABE, M., MIZUSHIMA, T., MIURA, N., OKUDA, S., MOTOHASHI, H., LEE, J.-A., SAKIMURA, K., OHE, T., NODA, N. N., WAGURI, S., ESKELINEN, E.-L. & KOMATSU, M. 2021. p62/SQSTM1-droplet serves as a platform for autophagosome formation and anti-oxidative stress response. *Nat Commun*, 12, 16.

- KAISER, W. J., SRIDHARAN, H., HUANG, C., MANDAL, P., UPTON, J. W., GOUGH, P. J., SEHON, C. A., MARQUIS, R. W., BERTIN, J. & MOCARSKI, E. S. 2013. Toll-like receptor 3-mediated necrosis via TRIF, RIP3, and MLKL. *J Biol Chem*, 288, 31268-31279.
- KAMBER, ROARKE A., SHOEMAKER, CHRISTOPHER J. & DENIC, V. 2015. Receptor-bound targets of selective autophagy use a scaffold protein to activate the Atg1 kinase. *Mol Cell*, 59, 372-381.
- KATTAH, M. G., SHAO, L., ROSLI, Y. Y., SHIMIZU, H., WHANG, M. I., ADVINCULA, R., ACHACOSO, P., SHAH, S., DUONG, B. H., ONIZAWA, M., TANBUN, P., MALYNN, B. A. & MA, A. 2018. A20 and ABIN-1 synergistically preserve intestinal epithelial cell survival. *J Exp Med*, 215, 1839-1852.
- KAUSHIK, S. & CUERVO, A. M. 2018. The coming of age of chaperone-mediated autophagy. *Nat Rev Mol Cell Biol*, 19, 365-381.
- KAWASAKI, T. & KAWAI, T. 2014. Toll-Like Receptor Signaling Pathways. *Front Immunol*, 5.
- KIFFIN, R., CHRISTIAN, C., KNECHT, E. & CUERVO, A. M. 2004. Activation of chaperone-mediated autophagy during oxidative stress. *Mol Biol Cell*, 15, 4829-40.
- KIRKIN, V., LAMARK, T., SOU, Y. S., BJØRKØY, G., NUNN, J. L., BRUUN, J. A., SHVETS, E., MCEWAN, D. G., CLAUSEN, T. H., WILD, P., BILUSIC, I., THEURILLAT, J. P., ØVERVATN, A., ISHII, T., ELAZAR, Z., KOMATSU, M., DIKIC, I. & JOHANSEN, T. 2009. A role for NBR1 in autophagosomal degradation of ubiquitinated substrates. *Mol Cell*, 33, 505-16.
- KIRKIN, V. & ROGOV, V. V. 2019. A diversity of selective autophagy receptors determines the specificity of the autophagy pathway. *Mol Cell*, 76, 268-285.
- KOGA, H., MARTINEZ-VICENTE, M., MACIAN, F., VERKHUSHA, V. V. & CUERVO, A. M. 2011. A photoconvertible fluorescent reporter to track chaperone-mediated autophagy. *Nat Commun*, 2, 386.
- KOMANDER, D. & RAPE, M. 2012. The Ubiquitin Code. *Annu Rev Biochem*, 81, 203-229.
- KUMAR, S., GU, Y., ABUDU, Y. P., BRUUN, J.-A., JAIN, A., FARZAM, F., MUDD, M., ANONSEN, J. H., RUSTEN, T. E., KASOF, G., KTISTAKIS, N., LIDKE, K. A., JOHANSEN, T. & DERETIC, V. 2019. Phosphorylation of syntaxin 17 by TBK1 controls autophagy initiation. *Dev Cell*, 49, 130-144.e6.
- KUNO, S., FUJITA, H., TANAKA, Y. K., OGRA, Y. & IWAI, K. 2022. Iron-induced NCOA4 condensation regulates ferritin fate and iron homeostasis. *EMBO Rep*, 23, e54278.
- KURIAKOSE, J., REDECKE, V., GUY, C., ZHOU, J., WU, R., IPPAGUNTA, S. K., TILLMAN, H., WALKER, P. D., VOGEL, P. & HÄCKER, H. 2019. Patrolling monocytes promote the pathogenesis of early lupus-like glomerulonephritis. *J Clin Invest*, 129, 2251-2265.
- LAMARK, T. & JOHANSEN, T. 2021. Mechanisms of selective autophagy. *Annu Rev Cell Dev Biol*, 37, 143-169.
- LAMARK, T., PERANDER, M., OUTZEN, H., KRISTIENSEN, K., ØVERVATN, A., MICHAELSEN, E., BJØRKØY, G. & JOHANSEN, T. 2003. Interaction codes within the family of mammalian Phox and Bem1p domain-containing proteins. *J Biol Chem*, 278, 34568-81.
- LAREDJ, L. N. & BEARD, P. 2011. Adeno-associated virus activates an innate immune response in normal human cells but not in osteosarcoma cells. *J Virol*, 85, 13133-43.
- LASSEN, K. G., KUBALLA, P., CONWAY, K. L., PATEL, K. K., BECKER, C. E., PELOQUIN, J. M., VILLABLANCA, E. J., NORMAN, J. M., LIU, T. C., HEATH, R. J., BECKER, M. L., FAGBAMI, L., HORN, H., MERCER, J., YILMAZ, O. H., JAFFE, J. D., SHAMJI, A. F., BHAN, A. K., CARR, S. A., DALY, M. J., VIRGIN, H. W., SCHREIBER, S. L., STAPPENBECK, T. S. & XAVIER, R. J. 2014. Atg16L1 T300A variant decreases selective autophagy resulting in altered cytokine signaling and decreased antibacterial defense. *Proc Natl Acad Sci U S A*, 111, 7741-6.
- LAZAROU, M., SLITER, D. A., KANE, L. A., SARRAF, S. A., WANG, C., BURMAN, J. L., SIDERIS, D. P., FOGEL, A. I. & YOULE, R. J. 2015. The ubiquitin kinase PINK1 recruits autophagy receptors to induce mitophagy. *Nature*, 524, 309-314.
- LE GUERROUË, F., WERNER, A., WANG, C. & YOULE, R. 2022. TNIP1 inhibits Mitophagy via interaction with FIP200 and TAX1BP1. *bioRxiv*, 2022.03.14.484269.

- LEE, Y., KIM, J., KIM, M. S., KWON, Y., SHIN, S., YI, H., KIM, H., CHANG, M. J., CHANG, C. B., KANG, S. B., KIM, V. N., KIM, J. H., KIM, J. S., ELLEDGE, S. J. & KANG, C. 2021. Coordinate regulation of the senescent state by selective autophagy. *Dev Cell*, 56, 1512-1525.e7.
- LESCAT, L., HERPIN, A., MOUROT, B., VÉRON, V., GUIGUEN, Y., BOBE, J. & SEILIEZ, I. 2018. CMA restricted to mammals and birds: myth or reality? *Autophagy*, 14, 1267-1270.
- LI, D. & WU, M. 2021. Pattern recognition receptors in health and diseases. *Signal Transduct Target Ther* 6, 291.
- LI, F., XIE, X., WANG, Y., LIU, J., CHENG, X., GUO, Y., GONG, Y., HU, S. & PAN, L. 2016. Structural insights into the interaction and disease mechanism of neurodegenerative disease-associated optineurin and TBK1 proteins. *Nat Commun*, 7, 12708.
- LI, J., ZHU, R., CHEN, K., ZHENG, H., ZHAO, H., YUAN, C., ZHANG, H., WANG, C. & ZHANG, M. 2018. Potent and specific Atg8-targeting autophagy inhibitory peptides from giant ankyrins. *Nat Chem Biol*, 14, 778-787.
- LI, L., HAILEY, D. W., SOETANDYO, N., LI, W., LIPPINCOTT-SCHWARTZ, J., SHU, H. B. & YE, Y. 2008. Localization of A20 to a lysosome-associated compartment and its role in NFkappaB signaling. *Biochim Biophys Acta*, 1783, 1140-9.
- LI, L., SOETANDYO, N., WANG, Q. & YE, Y. 2009. The zinc finger protein A20 targets TRAF2 to the lysosomes for degradation. *Biochim Biophys Acta Mol Cell Res*, 1793, 346-353.
- LIM, J., PARK, H., HEISLER, J., MACULINS, T., ROOSE-GIRMA, M., XU, M., MCKENZIE, B., VAN LOOKEREN CAMPAGNE, M., NEWTON, K. & MURTHY, A. 2019. Autophagy regulates inflammatory programmed cell death via turnover of RHIM-domain proteins. *eLife*, 8, e44452.
- LIN, R., HEYLBROECK, C., GENIN, P., PITHA, P. M. & HISCOTT, J. 1999. Essential role of interferon regulatory factor 3 in direct activation of RANTES chemokine transcription. *Mol Cell Biol*, 19, 959-66.
- LIU, L., FENG, D., CHEN, G., CHEN, M., ZHENG, Q., SONG, P., MA, Q., ZHU, C., WANG, R., QI, W., HUANG, L., XUE, P., LI, B., WANG, X., JIN, H., WANG, J., YANG, F., LIU, P., ZHU, Y., SUI, S. & CHEN, Q. 2012. Mitochondrial outer-membrane protein FUNDC1 mediates hypoxia-induced mitophagy in mammalian cells. *Nat Cell Biol*, 14, 177-185.
- LIU, X. M., SUN, L. L., HU, W., DING, Y. H., DONG, M. Q. & DU, L. L. 2015. ESCRTs cooperate with a selective autophagy receptor to mediate vacuolar targeting of soluble cargos. *Mol Cell*, 59, 1035-42.
- LIU, Y., MI, Y., MUELLER, T., KREIBICH, S., WILLIAMS, E. G., VAN DROGEN, A., BOREL, C., FRANK, M., GERMAIN, P.-L., BLUDAU, I., MEHNERT, M., SEIFERT, M., EMMENLAUER, M., SORG, I., BEZRUKOV, F., BENA, F. S., ZHOU, H., DEHIO, C., TESTA, G., SAEZ-RODRIGUEZ, J., ANTONARAKIS, S. E., HARDT, W.-D. & AEBERSOLD, R. 2019. Multi-omic measurements of heterogeneity in HeLa cells across laboratories. *Nat Biotechnol*, 37, 314-322.
- LUCEY, B. P., NELSON-REES, W. A. & HUTCHINS, G. M. 2009. Henrietta Lacks, HeLa cells, and cell culture contamination. *Arch Pathol Lab Med*, 133, 1463-1467.
- LUCK, K., KIM, D. K., LAMBOURNE, L., SPIROHN, K., BEGG, B. E., BIAN, W., BRIGNALL, R., CAFARELLI, T., CAMPOS-LABORIE, F. J., CHARLOTEAUX, B., CHOI, D., COTÉ, A. G., DALEY, M., DEIMLING, S., DESBULEUX, A., DRICOT, A., GEBBIA, M., HARDY, M. F., KISHORE, N., KNAPP, J. J., KOVÁCS, I. A., LEMMENS, I., MEE, M. W., MELLOR, J. C., POLLIS, C., PONS, C., RICHARDSON, A. D., SCHLABACH, S., TEEKING, B., YADAV, A., BABOR, M., BALCHA, D., BASHA, O., BOWMAN-COLIN, C., CHIN, S. F., CHOI, S. G., COLABELLA, C., COPPIN, G., D'AMATA, C., DE RIDDER, D., DE ROUCK, S., DURAN-FRIGOLA, M., ENNAJDAOUI, H., GOEBELS, F., GOEHRING, L., GOPAL, A., HADDAD, G., HATCHI, E., HELMY, M., JACOB, Y., KASSA, Y., LANDINI, S., LI, R., VAN LIESHOUT, N., MACWILLIAMS, A., MARKEY, D., PAULSON, J. N., RANGARAJAN, S., RASLA, J., RAYHAN, A., ROLLAND, T., SANMIGUEL, A., SHEN, Y., SHEYKHKARIMLI, D., SHEYNKMAN, G. M., SIMONOVSKY, E., TAŞAN, M., TEJEDA, A., TROPEPE, V., TWIZERE, J. C., WANG, Y., WEATHERITT, R. J., WEILE, J., XIA, Y., YANG, X., YEGER-LOTEM, E., ZHONG, Q., ALOY, P.,

- BADER, G. D., DE LAS RIVAS, J., GAUDET, S., HAO, T., RAK, J., TAVERNIER, J., HILL, D. E., VIDAL, M., ROTH, F. P. & CALDERWOOD, M. A. 2020. A reference map of the human binary protein interactome. *Nature*, 580, 402-408.
- LŐRINCZ, P. & JUHÁSZ, G. 2020. Autophagosome-Lysosome Fusion. *J Mol Biol*, 432, 2462-2482.
- MACULINS, T., VERSCHUEREN, E., HINKLE, T., CHOI, M., CHANG, P., CHALOUNI, C., RAO, S., KWON, Y., LIM, J., KATAKAM, A. K., KUNZ, R. C., ERICKSON, B. K., HUANG, T., TSAI, T.-H., VITEK, O., REICHEL, M., SENBABA OGLU, Y., MCKENZIE, B., ROHDE, J. R., DIKIC, I., KIRKPATRICK, D. S. & MURTHY, A. 2021. Multiplexed proteomics of autophagy-deficient murine macrophages reveals enhanced antimicrobial immunity via the oxidative stress response. *eLife*, 10, e62320.
- MAEDA, S., OTOMO, C. & OTOMO, T. 2019. The autophagic membrane tether ATG2A transfers lipids between membranes. *eLife*, 8, e45777.
- MAEDA, S., YAMAMOTO, H., KINCH, L. N., GARZA, C. M., TAKAHASHI, S., OTOMO, C., GRISHIN, N. V., FORLI, S., MIZUSHIMA, N. & OTOMO, T. 2020. Structure, lipid scrambling activity and role in autophagosome formation of ATG9A. *Nat Struct Mol Biol*, 27, 1194-1201.
- MAHMOOD, T. & YANG, P. C. 2012. Western blot: technique, theory, and trouble shooting. *N Am J Med Sci*, 4, 429-34.
- MANCIAS, J. D., WANG, X., GYGI, S. P., HARPER, J. W. & KIMMELMAN, A. C. 2014. Quantitative proteomics identifies NCOA4 as the cargo receptor mediating ferritinophagy. *Nature*, 509, 105-109.
- MANDELL, M. A., JAIN, A., ARKO-MENSAH, J., CHAUHAN, S., KIMURA, T., DINKINS, C., SILVESTRI, G., MÜNCH, J., KIRCHHOFF, F., SIMONSEN, A., WEI, Y., LEVINE, B., JOHANSEN, T. & DERETIC, V. 2014. TRIM proteins regulate autophagy and can target autophagic substrates by direct recognition. *Dev Cell*, 30, 394-409.
- MARTINEZ, J., MALIREDDI, R. K. S., LU, Q., CUNHA, L. D., PELLETIER, S., GINGRAS, S., ORCHARD, R., GUAN, J.-L., TAN, H., PENG, J., KANNEGANTI, T.-D., VIRGIN, H. W. & GREEN, D. R. 2015. Molecular characterization of LC3-associated phagocytosis reveals distinct roles for Rubicon, NOX2 and autophagy proteins. *Nat Cell Biol*, 17, 893-906.
- MATHEWS, S. T., PLAISANCE, E. P. & KIM, T. 2009. Imaging systems for westerns: chemiluminescence vs. infrared detection. *Methods Mol Biol*, 536, 499-513.
- MATOBA, K., KOTANI, T., TSUTSUMI, A., TSUJI, T., MORI, T., NOSHIRO, D., SUGITA, Y., NOMURA, N., IWATA, S., OHSUMI, Y., FUJIMOTO, T., NAKATOGAWA, H., KIKKAWA, M. & NODA, N. N. 2020. Atg9 is a lipid scramblase that mediates autophagosomal membrane expansion. *Nat Struct Mol Biol*, 27, 1185-1193.
- MATSUMOTO, G., SHIMOGORI, T., HATTORI, N. & NUKINA, N. 2015. TBK1 controls autophagosomal engulfment of polyubiquitinated mitochondria through p62/SQSTM1 phosphorylation. *Hum Mol Genet*, 24, 4429-4442.
- MATSUMOTO, G., WADA, K., OKUNO, M., KUROSAWA, M. & NUKINA, N. 2011. Serine 403 phosphorylation of p62/SQSTM1 regulates selective autophagic clearance of ubiquitinated proteins. *Mol Cell*, 44, 279-89.
- MAURO, C., PACIFICO, F., LAVORGNA, A., MELLONE, S., IANNETTI, A., ACQUAVIVA, R., FORMISANO, S., VITO, P. & LEONARDI, A. 2006. ABIN-1 binds to NEMO/IKKgamma and co-operates with A20 in inhibiting NF-kappaB. *J Biol Chem*, 281, 18482-8.
- MEJLVANG, J., OLSVIK, H., SVENNING, S., BRUUN, J. A., ABUDU, Y. P., LARSEN, K. B., BRECH, A., HANSEN, T. E., BRENNE, H., HANSEN, T., STENMARK, H. & JOHANSEN, T. 2018. Starvation induces rapid degradation of selective autophagy receptors by endosomal microautophagy. *J Cell Biol*, 217, 3640-3655.
- MIFFLIN, L., OFENGEIM, D. & YUAN, J. 2020. Receptor-interacting protein kinase 1 (RIPK1) as a therapeutic target. *Nat Rev Drug Discov*, 19, 553-571.
- MIRZA, N., SOWA, A. S., LAUTZ, K. & KUFER, T. A. 2019. NLRP10 affects the stability of Abin-1 to control inflammatory responses. *J Immunol*, 202, 218-227.
- MIZUSHIMA, N., NODA, T., YOSHIMORI, T., TANAKA, Y., ISHII, T., GEORGE, M. D., KLIONSKY, D. J., OHSUMI, M. & OHSUMI, Y. 1998. A protein conjugation system essential for autophagy. *Nature*, 395, 395-398.

- MIZUSHIMA, N., YOSHIMORI, T. & OHSUMI, Y. 2011. The role of Atg proteins in autophagosome formation. *Annu Rev Cell Dev Biol*, 27, 107-132.
- MURTHY, A., LI, Y., PENG, I., REICHEL, M., KATAKAM, A. K., NOUBADE, R., ROOSE-GIRMA, M., DEVOSS, J., DIEHL, L., GRAHAM, R. R. & VAN LOOKEREN CAMPAGNE, M. 2014. A Crohn's disease variant in Atg16l1 enhances its degradation by caspase 3. *Nature*, 506, 456-462.
- NANDA, S. K., LOPEZ-PELAEZ, M., ARTHUR, J. S., MARCHESI, F. & COHEN, P. 2016. Suppression of IRAK1 or IRAK4 catalytic activity, but not type 1 IFN signaling, prevents Lupus Nephritis in mice expressing a ubiquitin binding-defective mutant of ABIN1. *J Immunol*, 197, 4266-4273.
- NANDA, S. K., PETROVA, T., MARCHESI, F., GIERLINSKI, M., RAZSOLKOV, M., LEE, K. L., WRIGHT, S. W., RAO, V. R., COHEN, P. & ARTHUR, J. S. C. 2019. Distinct signals and immune cells drive liver pathology and glomerulonephritis in ABIN1[D485N] mice. *Life Sci Alliance*, 2.
- NANDA, S. K., VENIGALLA, R. K., ORDUREAU, A., PATTERSON-KANE, J. C., POWELL, D. W., TOTH, R., ARTHUR, J. S. & COHEN, P. 2011. Polyubiquitin binding to ABIN1 is required to prevent autoimmunity. *J Exp Med*, 208, 1215-28.
- NEWMAN, A. C., SCHOLEFIELD, C. L., KEMP, A. J., NEWMAN, M., MCIVER, E. G., KAMAL, A. & WILKINSON, S. 2012. TBK1 kinase addiction in lung cancer cells is mediated via autophagy of Tax1bp1/Ndp52 and non-canonical NF- κ B signalling. *PLoS One*, 7, e50672.
- NGUYEN, T. N. & LAZAROU, M. 2020. Rebellious autophagy proteins bypass ATG8 lipidation, taking their own path to autophagic degradation. *EMBO J*, 39, e106990.
- NGUYEN, T. N., PADMAN, B. S., USHER, J., OORSCHOT, V., RAMM, G. & LAZAROU, M. 2016. Atg8 family LC3/GABARAP proteins are crucial for autophagosome-lysosome fusion but not autophagosome formation during PINK1/Parkin mitophagy and starvation. *J Cell Biol*, 215, 857-874.
- NISHIDA, Y., ARAKAWA, S., FUJITANI, K., YAMAGUCHI, H., MIZUTA, T., KANASEKI, T., KOMATSU, M., OTSU, K., TSUJIMOTO, Y. & SHIMIZU, S. 2009. Discovery of Atg5/Atg7-independent alternative macroautophagy. *Nature*, 461, 654-658.
- NODA, N. N., KUMETA, H., NAKATOGAWA, H., SATOO, K., ADACHI, W., ISHII, J., FUJIOKA, Y., OHSUMI, Y. & INAGAKI, F. 2008. Structural basis of target recognition by Atg8/LC3 during selective autophagy. *Genes Cells*, 13, 1211-1218.
- NTHIGA, T. M., KUMAR SHRESTHA, B., SJØTTEM, E., BRUUN, J. A., BOWITZ LARSEN, K., BHUJABAL, Z., LAMARK, T. & JOHANSEN, T. 2020. CALCOCO1 acts with VAMP-associated proteins to mediate ER-phagy. *Embo j*, 39, e103649.
- OAKES, J. A., DAVIES, M. C. & COLLINS, M. O. 2017. TBK1: a new player in ALS linking autophagy and neuroinflammation. *Mol Brain*, 10, 5.
- OHNSTAD, A. E., DELGADO, J. M., NORTH, B. J., NASA, I., KETTENBACH, A. N., SCHULTZ, S. W. & SHOEMAKER, C. J. 2020. Receptor-mediated clustering of FIP200 bypasses the role of LC3 lipidation in autophagy. *EMBO J*, 39, e104948.
- OHSHIMA, T., YAMAMOTO, H., SAKAMAKI, Y., SAITO, C. & MIZUSHIMA, N. 2022. NCOA4 drives ferritin phase separation to facilitate macroferritinophagy and microferritinophagy. *J Cell Biol*, 221, e202203102.
- OHSUMI, Y. 2014. Historical landmarks of autophagy research. *Cell Research*, 24, 9-23.
- OLSVIK, H. L., LAMARK, T., TAKAGI, K., LARSEN, K. B., EVJEN, G., ØVERVATN, A., MIZUSHIMA, T. & JOHANSEN, T. 2015. FYCO1 Contains a C-terminally Extended, LC3A/B-preferring LC3-interacting Region (LIR) Motif Required for Efficient Maturation of Autophagosomes during Basal Autophagy. *J Biol Chem*, 290, 29361-74.
- OSAWA, T., KOTANI, T., KAWAOKA, T., HIRATA, E., SUZUKI, K., NAKATOGAWA, H., OHSUMI, Y. & NODA, N. N. 2019. Atg2 mediates direct lipid transfer between membranes for autophagosome formation. *Nat Struct Mol Biol*, 26, 281-288.
- OSAWA, T., MIZUNO, Y., FUJITA, Y., TAKATAMA, M., NAKAZATO, Y. & OKAMOTO, K. 2011. Optineurin in neurodegenerative diseases. *Neuropathology*, 31, 569-74.
- OSHIMA, S., TURER, E. E., CALLAHAN, J. A., CHAI, S., ADVINCULA, R., BARRERA, J., SHIFRIN, N., LEE, B., BENEDICT YEN, T. S., WOO, T., MALYNN, B. A. & MA, A. 2009.

- ABIN-1 is a ubiquitin sensor that restricts cell death and sustains embryonic development. *Nature*, 457, 906-9.
- PANKIV, S., ALEMU, E. A., BRECH, A., BRUUN, J. A., LAMARK, T., OVERVATN, A., BJØRKØY, G. & JOHANSEN, T. 2010. FYCO1 is a Rab7 effector that binds to LC3 and PI3P to mediate microtubule plus end-directed vesicle transport. *J Cell Biol*, 188, 253-69.
- PANKIV, S., CLAUSEN, T. H., LAMARK, T., BRECH, A., BRUUN, J.-A., OUTZEN, H., ØVERVATN, A., BJØRKØY, G. & JOHANSEN, T. 2007. p62/SQSTM1 binds directly to Atg8/LC3 to facilitate degradation of ubiquitinated protein aggregates by autophagy. *J Biol Chem*, 282, 24131-24145.
- PARK, C., SUH, Y. & CUERVO, A. M. 2015. Regulated degradation of Chk1 by chaperone-mediated autophagy in response to DNA damage. *Nat Commun*, 6, 6823.
- PFÄFFENWIMMER, T., REITER, W., BRACH, T., NOGELLOVA, V., PAPINSKI, D., SCHUSCHNIG, M., ABERT, C., AMMERER, G., MARTENS, S. & KRAFT, C. 2014. Hrr25 kinase promotes selective autophagy by phosphorylating the cargo receptor Atg19. *EMBO Rep*, 15, 862-870.
- PILLAI-KASTOORI, L., SCHUTZ-GESCHWENDER, A. R. & HARFORD, J. A. 2020. A systematic approach to quantitative Western blot analysis. *Anal Biochem*, 593, 113608.
- PILLI, M., ARKO-MENSAH, J., PONPUAK, M., ROBERTS, E., MASTER, S., MANDELL, M. A., DUPONT, N., ORNATOWSKI, W., JIANG, S., BRADFUTE, S. B., BRUUN, J. A., HANSEN, T. E., JOHANSEN, T. & DERETIC, V. 2012. TBK-1 promotes autophagy-mediated antimicrobial defense by controlling autophagosome maturation. *Immunity*, 37, 223-34.
- POHL, C. & DIKIC, I. 2019. Cellular quality control by the ubiquitin-proteasome system and autophagy. *Science*, 366, 818-822.
- POLSON, H. E., DE LARTIGUE, J., RIGDEN, D. J., REEDIJK, M., URBÉ, S., CLAGUE, M. J. & TOOZE, S. A. 2010. Mammalian Atg18 (WIPI2) localizes to omegasome-anchored phagophores and positively regulates LC3 lipidation. *Autophagy*, 6, 506-22.
- PEPELKA, H. & KLIONSKY, D. J. 2022. The RB1CC1 Claw-binding motif: a new piece in the puzzle of autophagy regulation. *Autophagy*, 18, 237-239.
- PRIDGEON, J. W., GEETHA, T. & WOOTEN, M. W. 2003. A method to identify p62's UBA domain interacting proteins. *Biol Proced Online*, 5, 228-237.
- PURI, C., RENNA, M., BENTO, CARLA F., MOREAU, K. & RUBINSZTEIN, DAVID C. 2013. Diverse autophagosome membrane sources coalesce in recycling endosomes. *Cell*, 154, 1285-1299.
- QI, R., SINGH, D. & KAO, C. C. 2012. Proteolytic processing regulates Toll-like receptor 3 stability and endosomal localization. *J Biol Chem*, 287, 32617-29.
- RAN, F. A., HSU, P. D., WRIGHT, J., AGARWALA, V., SCOTT, D. A. & ZHANG, F. 2013. Genome engineering using the CRISPR-Cas9 system. *Nat Protoc*, 8, 2281-2308.
- RAVENHILL, B. J., BOYLE, K. B., VON MUHLINEN, N., ELLISON, C. J., MASSON, G. R., OTTEN, E. G., FOEGLEIN, A., WILLIAMS, R. & RANDOW, F. 2019. The cargo deceptor NDP52 initiates selective autophagy by recruiting the ULK complex to cytosol-invading bacteria. *Mol Cell*, 74, 320-329.e6.
- RICHTER, B., SLITER, D. A., HERHAUS, L., STOLZ, A., WANG, C., BELI, P., ZAFFAGNINI, G., WILD, P., MARTENS, S., WAGNER, S. A., YOULE, R. J. & DIKIC, I. 2016. Phosphorylation of OPTN by TBK1 enhances its binding to Ub chains and promotes selective autophagy of damaged mitochondria. *Proc Natl Acad Sci U S A*, 113, 4039-44.
- ROGOV, V. V., STOLZ, A., RAVICHANDRAN, A. C., RIOS-SZWED, D. O., SUZUKI, H., KNISS, A., LÖHR, F., WAKATSUKI, S., DÖTSCH, V., DIKIC, I., DOBSON, R. C. & MCEWAN, D. G. 2017a. Structural and functional analysis of the GABARAP interaction motif (GIM). *EMBO Rep*, 18, 1382-1396.
- ROGOV, VLADIMIR V., SUZUKI, H., FISKIN, E., WILD, P., KNISS, A., ROZENKNOP, A., KATO, R., KAWASAKI, M., MCEWAN, DAVID G., LÖHR, F., GÜNTERT, P., DIKIC, I., WAKATSUKI, S. & DÖTSCH, V. 2013. Structural basis for phosphorylation-triggered autophagic clearance of Salmonella. *Biochem J*, 454, 459-466.

- ROGOV, V. V., SUZUKI, H., MARINKOVIĆ, M., LANG, V., KATO, R., KAWASAKI, M., BULJUBAŠIĆ, M., ŠPRUNG, M., ROGOVA, N., WAKATSUKI, S., HAMACHER-BRADY, A., DÖTSCH, V., DIKIC, I., BRADY, N. R. & NOVAK, I. 2017b. Phosphorylation of the mitochondrial autophagy receptor Nix enhances its interaction with LC3 proteins. *Sci Rep*, 7, 1131.
- ROUT, A. K., STRUB, M.-P., PISZCZEK, G. & TJANDRA, N. 2014. Structure of transmembrane domain of lysosome-associated membrane protein type 2a (LAMP-2A) reveals key features for substrate specificity in chaperone-mediated autophagy. *J Biol Chem*, 289, 35111-35123.
- RUDRAIAH, S., SHAMILOV, R. & ANESKIEVICH, B. J. 2018. TNIP1 reduction sensitizes keratinocytes to post-receptor signalling following exposure to TLR agonists. *Cell Signal*, 45, 81-92.
- RUSSELL, R. C., TIAN, Y., YUAN, H., PARK, H. W., CHANG, Y. Y., KIM, J., KIM, H., NEUFELD, T. P., DILLIN, A. & GUAN, K. L. 2013. ULK1 induces autophagy by phosphorylating Beclin-1 and activating VPS34 lipid kinase. *Nat Cell Biol*, 15, 741-50.
- RUSU, I., MENNILLO, E., BAIN, J. L., LI, Z., SUN, X., LY, K. M., ROSLI, Y. Y., NASER, M., WANG, Z., ADVINCULA, R., ACHACOSO, P., SHAO, L., RAZANI, B., KLEIN, O. D., MARSON, A., TURNBAUGH, J. A., TURNBAUGH, P. J., MALYNN, B. A., MA, A. & KATTAH, M. G. 2022. Microbial signals, MyD88, and lymphotoxin drive TNF-independent intestinal epithelial tissue damage. *J Clin Invest*, 132.
- RYAN, T. A. & TUMBARELLO, D. A. 2018. Optineurin: A coordinator of membrane-associated cargo trafficking and autophagy. *Front Immunol*, 9.
- SAHU, R., KAUSHIK, S., CLEMENT, C. C., CANNIZZO, E. S., SCHARF, B., FOLLENZI, A., POTOLICCHIO, I., NIEVES, E., CUERVO, A. M. & SANTAMBROGIO, L. 2011. Microautophagy of cytosolic proteins by late endosomes. *Dev Cell*, 20, 131-139.
- SAKAMAKI, J. I., ODE, K. L., KURIKAWA, Y., UEDA, H. R., YAMAMOTO, H. & MIZUSHIMA, N. 2022. Ubiquitination of phosphatidylethanolamine in organellar membranes. *Mol Cell*, 82, 3677-3692.e11.
- SALVADOR, N., AGUADO, C., HORST, M. & KNECHT, E. 2000. Import of a cytosolic protein into lysosomes by chaperone-mediated autophagy depends on its folding state. *J Biol Chem*, 275, 27447-56.
- SAMIE, M., LIM, J., VERSCHUEREN, E., BAUGHMAN, J. M., PENG, I., WONG, A., KWON, Y., SENBABA OGLU, Y., HACKNEY, J. A., KEIR, M., MCKENZIE, B., KIRKPATRICK, D. S., VAN LOOKEREN CAMPAGNE, M. & MURTHY, A. 2018. Selective autophagy of the adaptor TRIF regulates innate inflammatory signaling. *Nat Immunol*, 19, 246-254.
- SÁNCHEZ-MARTÍN, P., SAITO, T. & KOMATSU, M. 2019. p62/SQSTM1: 'Jack of all trades' in health and cancer. *FEBS J*, 286, 8-23.
- SATOO, K., NODA, N. N., KUMETA, H., FUJIOKA, Y., MIZUSHIMA, N., OHSUMI, Y. & INAGAKI, F. 2009. The structure of Atg4B-LC3 complex reveals the mechanism of LC3 processing and delipidation during autophagy. *EMBO J*, 28, 1341-50.
- SCHLÜTERMANN, D., BERLETH, N., DEITERSEN, J., WALLOT-HIEKE, N., FRIESEN, O., WU, W., STUHL DREIER, F., SUN, Y., BERNING, L., FRIEDRICH, A., MENDIBURO, M. J., PETER, C., WIEK, C., HANENBERG, H., STEFANSKI, A., STÜHLER, K. & STORK, B. 2021. FIP200 controls the TBK1 activation threshold at SQSTM1/p62-positive condensates. *Sci Rep*, 11, 13863.
- SCHNEIDER, W. M., CHEVILLOTTE, M. D. & RICE, C. M. 2014. Interferon-stimulated genes: a complex web of host defenses. *Annu Rev Immunol*, 32, 513-45.
- SHAMILOV, R. & ANESKIEVICH, B. J. 2018. TNIP1 in Autoimmune Diseases: Regulation of Toll-like Receptor Signaling. *J Immunol Res*, 2018, 3491269.
- SHEMBADE, N., HARHAJ, N. S., LIEBL, D. J. & HARHAJ, E. W. 2007. Essential role for TAX1BP1 in the termination of TNF-alpha-, IL-1- and LPS-mediated NF-kappaB and JNK signaling. *EMBO J*, 26, 3910-22.
- SHI, C.-S. & KEHRL, J. H. 2010. TRAF6 and A20 regulate lysine 63-linked ubiquitination of Beclin-1 to control TLR4-induced autophagy. *Sci Signal*, 3, ra42.
- SHI, C. S. & KEHRL, J. H. 2008. MyD88 and Trif target Beclin 1 to trigger autophagy in macrophages. *J Biol Chem*, 283, 33175-82.

- SHINKAWA, Y., IMAMI, K., FUSEYA, Y., SASAKI, K., OHMURA, K., ISHIHAMA, Y., MORINOBU, A. & IWAI, K. 2022. ABIN1 is a signal-induced autophagy receptor that attenuates NF- κ B activation by recognizing linear ubiquitin chains. *FEBS Lett*, 596, 1147-1164.
- SHOEMAKER, C. J., HUANG, T. Q., WEIR, N. R., POLYAKOV, N. J., SCHULTZ, S. W. & DENIC, V. 2019. CRISPR screening using an expanded toolkit of autophagy reporters identifies TMEM41B as a novel autophagy factor. *PLoS Biology*, 17, e2007044.
- SIL, P., MUSE, G. & MARTINEZ, J. 2018. A ravenous defense: canonical and non-canonical autophagy in immunity. *Curr Opin Immunol*, 50, 21-31.
- SKYTTE RASMUSSEN, M., MOUILLERON, S., KUMAR SHRESTHA, B., WIRTH, M., LEE, R., BOWITZ LARSEN, K., ABUDU PRINCELY, Y., O'REILLY, N., SJØTTEM, E., TOOZE, S. A., LAMARK, T. & JOHANSEN, T. 2017. ATG4B contains a C-terminal LIR motif important for binding and efficient cleavage of mammalian orthologs of yeast Atg8. *Autophagy*, 13, 834-853.
- SLOWICKA, K., SERRAMITO-GÓMEZ, I., BOADA-ROMERO, E., MARTENS, A., SZE, M., PETTA, I., VIKKULA, H. K., DE RYCKE, R., PARTHOENS, E., LIPPENS, S., SAVVIDES, S. N., WULLAERT, A., VEREECKE, L., PIMENTEL-MUIÑOS, F. X. & VAN LOO, G. 2019. Physical and functional interaction between A20 and ATG16L1-WD40 domain in the control of intestinal homeostasis. *Nat Commun*, 10, 1834.
- SMITH, M. D., HARLEY, M. E., KEMP, A. J., WILLS, J., LEE, M., ARENDS, M., VON KRIEGSHEIM, A., BEHREND, C. & WILKINSON, S. 2018. CCPG1 is a non-canonical autophagy cargo receptor essential for ER-phagy and pancreatic ER proteostasis. *Dev Cell*, 44, 217-232.e11.
- SU, Z., DZIEDZIC, S. A., HU, D., BARRETT, V. J., BROEKEMA, N., LI, W., QIAN, L., JIA, N., OFENGEIM, D., NAJAFOV, A., ZHU, H., KNIPE, D. M. & YUAN, J. 2019. ABIN-1 heterozygosity sensitizes to innate immune response in both RIPK1-dependent and RIPK1-independent manner. *Cell Death Differ*, 26, 1077-1088.
- SUN, D., WU, R., ZHENG, J., LI, P. & YU, L. 2018. Polyubiquitin chain-induced p62 phase separation drives autophagic cargo segregation. *Cell Research*, 28, 405-415.
- SVENNING, S., LAMARK, T., KRAUSE, K. & JOHANSEN, T. 2011. Plant NBR1 is a selective autophagy substrate and a functional hybrid of the mammalian autophagic adapters NBR1 and p62/SQSTM1. *Autophagy*, 7, 993-1010.
- TAKAHASHI, Y., LIANG, X., HATTORI, T., TANG, Z., HE, H., CHEN, H., LIU, X., ABRAHAM, T., IMAMURA-KAWASAWA, Y., BUCHKOVICH, N. J., YOUNG, M. M. & WANG, H.-G. 2019. VPS37A directs ESCRT recruitment for phagophore closure. *J Cell Biol*, 218, 3336-3354.
- TANAKA, C., TAN, L.-J., MOCHIDA, K., KIRISAKO, H., KOIZUMI, M., ASAI, E., SAKOH-NAKATOGAWA, M., OHSUMI, Y. & NAKATOGAWA, H. 2014. Hrr25 triggers selective autophagy-related pathways by phosphorylating receptor proteins. *J Cell Biol*, 207, 91-105.
- TANG, D., KANG, R., COYNE, C. B., ZEH, H. J. & LOTZE, M. T. 2012. PAMPs and DAMPs: signal 0s that spur autophagy and immunity. *Immunological Reviews*, 249, 158-175.
- TANIDA, I., UENO, T. & KOMINAMI, E. 2004. LC3 conjugation system in mammalian autophagy. *Int J Biochem Cell Biol*, 36, 2503-2518.
- TEKIRDAG, K. & CUERVO, A. M. 2018. Chaperone-mediated autophagy and endosomal microautophagy: Joint by a chaperone. *J Biol Chem*, 293, 5414-5424.
- THURSTON, T. L., RYZHAKOV, G., BLOOR, S., VON MUHLINEN, N. & RANDOW, F. 2009. The TBK1 adaptor and autophagy receptor NDP52 restricts the proliferation of ubiquitin-coated bacteria. *Nat Immunol*, 10, 1215-21.
- TIAN, B., NOWAK, D. E. & BRASIER, A. R. 2005. A TNF-induced gene expression program under oscillatory NF- κ B control. *BMC genomics*, 6, 137-137.
- TORGGLER, R., PAPINSKI, D., BRACH, T., BAS, L., SCHUSCHNIG, M., PFAFFENWIMMER, T., ROHRINGER, S., MATZHOLD, T., SCHWEIDA, D., BREZOVICH, A. & KRAFT, C. 2016. Two independent pathways within selective autophagy converge to activate Atg1 kinase at the vacuole. *Mol Cell*, 64, 221-235.

- TSUBOYAMA, K., KOYAMA-HONDA, I., SAKAMAKI, Y., KOIKE, M., MORISHITA, H. & MIZUSHIMA, N. 2016. The ATG conjugation systems are important for degradation of the inner autophagosomal membrane. *Science*, 354, 1036-1041.
- TUMBARELLO, D. A., MANNA, P. T., ALLEN, M., BYCROFT, M., ARDEN, S. D., KENDRICK-JONES, J. & BUSS, F. 2015. The autophagy receptor TAX1BP1 and the molecular motor myosin VI are required for clearance of *Salmonella Typhimurium* by autophagy. *PLoS Pathog*, 11, e1005174.
- TURCO, E., SAVOVA, A., GERE, F., FERRARI, L., ROMANOV, J., SCHUSCHNIG, M. & MARTENS, S. 2021. Reconstitution defines the roles of p62, NBR1 and TAX1BP1 in ubiquitin condensate formation and autophagy initiation. *Nat Commun*, 12, 5212.
- TURCO, E., WITT, M., ABERT, C., BOCK-BIERBAUM, T., SU, M. Y., TRAPANNONE, R., SZTACHO, M., DANIELI, A., SHI, X., ZAFFAGNINI, G., GAMPER, A., SCHUSCHNIG, M., FRACCHIOLLA, D., BERNKLAU, D., ROMANOV, J., HARTL, M., HURLEY, J. H., DAUMKE, O. & MARTENS, S. 2019. FIP200 Claw domain binding to p62 promotes autophagosome formation at ubiquitin condensates. *Mol Cell*, 74, 330-346.e11.
- TUSCO, R., JACOMIN, A.-C., JAIN, A., PENMAN, B. S., LARSEN, K. B., JOHANSEN, T. & NEZIS, I. P. 2017. Kenny mediates selective autophagic degradation of the IKK complex to control innate immune responses. *Nat Commun*, 8, 1264.
- VAITES, L. P., PAULO, J. A., HUTTLIN, E. L. & HARPER, J. W. 2018. Systematic analysis of human cells lacking ATG8 proteins uncovers roles for GABARAPs and the CCZ1/MON1 regulator C18orf8/RMC1 in macroautophagic and selective autophagic flux. *Mol Cell Biol*, 38.
- VALVERDE, D. P., YU, S., BOGGAVARAPU, V., KUMAR, N., LEES, J. A., WALZ, T., REINISCH, K. M. & MELIA, T. J. 2019. ATG2 transports lipids to promote autophagosome biogenesis. *J Cell Biol*, 218, 1787-1798.
- VAN QUICKELBERGHE, E., DE SUTTER, D., VAN LOO, G., EYCKERMAN, S. & GEVAERT, K. 2018. A protein-protein interaction map of the TNF-induced NF- κ B signal transduction pathway. *Sci Data*, 5, 180289.
- VAN VLIET, A. R., CHIDUZA, G. N., MASLEN, S. L., PYE, V. E., JOSHI, D., DE TITO, S., JEFFERIES, H. B. J., CHRISTODOULOU, E., ROUSTAN, C., PUNCH, E., HERVÁS, J. H., O'REILLY, N., SKEHEL, J. M., CHEREPANOV, P. & TOOZE, S. A. 2022. ATG9A and ATG2A form a heteromeric complex essential for autophagosome formation. *Mol Cell*.
- VARGAS, J. N. S., WANG, C., BUNKER, E., HAO, L., MARIC, D., SCHIAVO, G., RANDOW, F. & YOULE, R. J. 2019. Spatiotemporal control of ULK1 activation by NDP52 and TBK1 during selective autophagy. *Mol Cell*, 74, 347-362.e6.
- VIETRI, M., RADULOVIC, M. & STENMARK, H. 2020. The many functions of ESCRTs. *Nat Rev Mol Cell Biol*, 21, 25-42.
- VON MUHLINEN, N., AKUTSU, M., RAVENHILL, B. J., FOEGLEIN, Á., BLOOR, S., RUTHERFORD, T. J., FREUND, S. M., KOMANDER, D. & RANDOW, F. 2012. LC3C, bound selectively by a noncanonical LIR motif in NDP52, is required for antibacterial autophagy. *Mol Cell*, 48, 329-42.
- WAGNER, S., CARPENTIER, I., ROGOV, V., KREIKE, M., IKEDA, F., LÖHR, F., WU, C. J., ASHWELL, J. D., DÖTSCH, V., DIKIC, I. & BEYAERT, R. 2008. Ubiquitin binding mediates the NF-kappaB inhibitory potential of ABIN proteins. *Oncogene*, 27, 3739-45.
- WANG, L., KLIONSKY, D. J. & SHEN, H.-M. 2022a. The emerging mechanisms and functions of microautophagy. *Nat Rev Mol Cell Biol*.
- WANG, Y. T., LIU, T. Y., SHEN, C. H., LIN, S. Y., HUNG, C. C., HSU, L. C. & CHEN, G. C. 2022b. K48/K63-linked polyubiquitination of ATG9A by TRAF6 E3 ligase regulates oxidative stress-induced autophagy. *Cell Rep*, 38, 110354.
- WEIDBERG, H., SHVETS, E., SHPILKA, T., SHIMRON, F., SHINDER, V. & ELAZAR, Z. 2010. LC3 and GATE-16/GABARAP subfamilies are both essential yet act differently in autophagosome biogenesis. *EMBO J*, 29, 1792-1802.
- WERTZ, I. E., O'ROURKE, K. M., ZHOU, H., EBY, M., ARAVIND, L., SESHAGIRI, S., WU, P., WIESMANN, C., BAKER, R., BOONE, D. L., MA, A., KOONIN, E. V. & DIXIT, V. M.

2004. De-ubiquitination and ubiquitin ligase domains of A20 downregulate NF- κ B signalling. *Nature*, 430, 694-699.
- WHITE, J., SUKLABAIDYA, S., VO, M. T., CHOI, Y. B. & HARHAJ, E. W. 2022. Multifaceted roles of TAX1BP1 in autophagy. *Autophagy*, 1-10.
- WILD, P., FARHAN, H., MCEWAN, D. G., WAGNER, S., ROGOV, V. V., BRADY, N. R., RICHTER, B., KORAC, J., WAIDMANN, O., CHOUDHARY, C., DÖTSCH, V., BUMANN, D. & DIKIC, I. 2011. Phosphorylation of the autophagy receptor optineurin restricts Salmonella growth. *Science*, 333, 228-33.
- WIRTH, M., MOUILLERON, S., ZHANG, W., SJØTTEM, E., PRINCELY ABUDU, Y., JAIN, A., LAURITZ OLSVIK, H., BRUUN, J. A., RAZI, M., JEFFERIES, H. B. J., LEE, R., JOSHI, D., O'REILLY, N., JOHANSEN, T. & TOOZE, S. A. 2021. Phosphorylation of the LIR domain of SCOC modulates ATG8 binding affinity and specificity. *J Mol Biol*, 433, 166987.
- WIRTH, M., ZHANG, W., RAZI, M., NYONI, L., JOSHI, D., O'REILLY, N., JOHANSEN, T., TOOZE, S. A. & MOUILLERON, S. 2019. Molecular determinants regulating selective binding of autophagy adapters and receptors to ATG8 proteins. *Nat Commun*, 10, 2055.
- WU, H., XUE, D., CHEN, G., HAN, Z., HUANG, L., ZHU, C., WANG, X., JIN, H., WANG, J., ZHU, Y., LIU, L. & CHEN, Q. 2014a. The BCL2L1 and PGAM5 axis defines hypoxia-induced receptor-mediated mitophagy. *Autophagy*, 10, 1712-1725.
- WU, W., TIAN, W., HU, Z., CHEN, G., HUANG, L., LI, W., ZHANG, X., XUE, P., ZHOU, C., LIU, L., ZHU, Y., ZHANG, X., LI, L., ZHANG, L., SUI, S., ZHAO, B. & FENG, D. 2014b. ULK1 translocates to mitochondria and phosphorylates FUNDC1 to regulate mitophagy. *EMBO Rep*, 15, 566-575.
- WU, W., WANG, X., BERLETH, N., DEITERSEN, J., WALLOT-HIEKE, N., BÖHLER, P., SCHLÜTERMANN, D., STUHL DREIER, F., COX, J., SCHMITZ, K., SEGGEWIB, S., PETER, C., KASOF, G., STEFANSKI, A., STÜHLER, K., TSCHAPEK, A., GÖDECKE, A. & STORK, B. 2020. The Autophagy-Initiating Kinase ULK1 Controls RIPK1-Mediated Cell Death. *Cell Rep*, 31, 107547.
- WU, W., WANG, X., SUN, Y., BERLETH, N., DEITERSEN, J., SCHLÜTERMANN, D., STUHL DREIER, F., WALLOT-HIEKE, N., JOSÉ MENDIBURO, M., COX, J., PETER, C., BERGMANN, A. K. & STORK, B. 2021. TNF-induced necroptosis initiates early autophagy events via RIPK3-dependent AMPK activation, but inhibits late autophagy. *Autophagy*, 17, 3992-4009.
- WURZER, B., ZAFFAGNINI, G., FRACCHIOLLA, D., TURCO, E., ABERT, C., ROMANOV, J. & MARTENS, S. 2015. Oligomerization of p62 allows for selection of ubiquitinated cargo and isolation membrane during selective autophagy. *eLife*, 4, e08941.
- XIA, S., CHEN, Z., SHEN, C. & FU, T. M. 2021. Higher-order assemblies in immune signaling: supramolecular complexes and phase separation. *Protein Cell*, 12, 680-694.
- XU, Y., JAGANNATH, C., LIU, X. D., SHARAFKHANEH, A., KOLODZIEJSKA, K. E. & EISSA, N. T. 2007. Toll-like receptor 4 is a sensor for autophagy associated with innate immunity. *Immunity*, 27, 135-44.
- YAMAMOTO, M., SATO, S., HEMMI, H., HOSHINO, K., KAISHO, T., SANJO, H., TAKEUCHI, O., SUGIYAMA, M., OKABE, M., TAKEDA, K. & AKIRA, S. 2003. Role of adaptor TRIF in the MyD88-independent Toll-like receptor signaling pathway. *Science*, 301, 640-643.
- YANG, Q., LIU, T. T., LIN, H., ZHANG, M., WEI, J., LUO, W. W., HU, Y. H., ZHONG, B., HU, M. M. & SHU, H. B. 2017. TRIM32-TAX1BP1-dependent selective autophagic degradation of TRIF negatively regulates TLR3/4-mediated innate immune responses. *PLoS Pathog*, 13, e1006600.
- YANG, S., IMAMURA, Y., JENKINS, R. W., CAÑADAS, I., KITAJIMA, S., AREF, A., BRANNON, A., OKI, E., CASTORENO, A., ZHU, Z., THAI, T., REIBEL, J., QIAN, Z., OGINO, S., WONG, K. K., BABA, H., KIMMELMAN, A. C., PASCA DI MAGLIANO, M. & BARBIE, D. A. 2016. Autophagy inhibition dysregulates TBK1 signaling and promotes pancreatic inflammation. *Cancer Immunol Res*, 4, 520-530.
- YAU, R. & RAPE, M. 2016. The increasing complexity of the ubiquitin code. *Nat Cell Biol*, 18, 579-586.

- YIN, H., KARAYEL, O., CHAO, Y. Y., SEEHOLZER, T., HAMP, I., PLETTENBURG, O., GEHRING, T., ZIELINSKI, C., MANN, M. & KRAPPMANN, D. 2022. A20 and ABIN-1 cooperate in balancing CBM complex-triggered NF- κ B signaling in activated T cells. *Cell Mol Life Sci*, 79, 112.
- YOUNG, A. R. J., CHAN, E. Y. W., HU, X. W., KÖCHL, R., CRAWSHAW, S. G., HIGH, S., HAILEY, D. W., LIPPINCOTT-SCHWARTZ, J. & TOOZE, S. A. 2006. Starvation and ULK1-dependent cycling of mammalian Atg9 between the TGN and endosomes. *J Cell Sci*, 119, 3888-3900.
- YUAN, S., DONG, X., TAO, X., XU, L., RUAN, J., PENG, J. & XU, A. 2014. Emergence of the A20/ABIN-mediated inhibition of NF-kappaB signaling via modifying the ubiquitinated proteins in a basal chordate. *Proc Natl Acad Sci U S A*, 111, 6720-5.
- ZAFFAGNINI, G. & MARTENS, S. 2016. Mechanisms of Selective Autophagy. *J Mol Biol*, 428, 1714-24.
- ZAFFAGNINI, G., SAVOVA, A., DANIELI, A., ROMANOV, J., TREMEL, S., EBNER, M., PETERBAUER, T., SZTACHO, M., TRAPANONE, R., TARAFDER, A. K., SACHSE, C. & MARTENS, S. 2018. p62 filaments capture and present ubiquitinated cargos for autophagy. *EMBO J*, 37, e98308.
- ZELLNER, S., SCHIFFERER, M. & BEHREND, C. 2021. Systematically defining selective autophagy receptor-specific cargo using autophagosome content profiling. *Mol Cell*, 81, 1337-1354.e8.
- ZHEN, Y., SPANGENBERG, H., MUNSON, M. J., BRECH, A., SCHINK, K. O., TAN, K.-W., SØRENSEN, V., WENZEL, E. M., RADULOVIC, M., ENGEDAL, N., SIMONSEN, A., RAIBORG, C. & STENMARK, H. 2020. ESCRT-mediated phagophore sealing during mitophagy. *Autophagy*, 16, 826-841.
- ZHOU, J., WU, R., HIGH, A. A., SLAUGHTER, C. A., FINKELSTEIN, D., REHG, J. E., REDECKE, V. & HÄCKER, H. 2011. A20-binding inhibitor of NF- κ B (ABIN1) controls Toll-like receptor-mediated CCAAT/enhancer-binding protein β activation and protects from inflammatory disease. *Proc Natl Acad Sci U S A*, 108, E998-1006.
- ZHOU, Z., LIU, J., FU, T., WU, P., PENG, C., GONG, X., WANG, Y., ZHANG, M., LI, Y., WANG, Y., XU, X., LI, M. & PAN, L. 2021. Phosphorylation regulates the binding of autophagy receptors to FIP200 Claw domain for selective autophagy initiation. *Nat Commun*, 12, 1570.
- ZHU, Y., MASSEN, S., TERENCE, M., LANG, V., CHEN-LINDNER, S., EILS, R., NOVAK, I., DIKIC, I., HAMACHER-BRADY, A. & BRADY, N. R. 2013. Modulation of serines 17 and 24 in the LC3-interacting region of Bnip3 determines pro-survival mitophagy versus apoptosis. *J Biol Chem*, 288, 1099-1113.

PAPER I

ARTICLE

TBK1 phosphorylation activates LIR-dependent degradation of the inflammation repressor TNIP1

Jianwen Zhou^{1*}, Nikoline Lander Rasmussen^{2*}, Hallvard Lauritz Olsvik², Vyacheslav Akimov³, Zehan Hu¹, Gry Evjen², Stéphanie Kaeser-Pebarnard¹, Devanarayanan Siva Sankar¹, Carole Roubaty¹, Pauline Verlhac⁴, Nicole van de Beck⁴, Fulvio Reggiori^{4,5,6}, Yakubu Princely Abudu², Blagoy Blagoev³, Trond Lamark², Terje Johansen², and Jörn Dengjel¹

Limitation of excessive inflammation due to selective degradation of pro-inflammatory proteins is one of the cytoprotective functions attributed to autophagy. In the current study, we highlight that selective autophagy also plays a vital role in promoting the establishment of a robust inflammatory response. Under inflammatory conditions, here TLR3-activation by poly(I:C) treatment, the inflammation repressor TNIP1 (TNFAIP3 interacting protein 1) is phosphorylated by Tank-binding kinase 1 (TBK1) activating an LIR motif that leads to the selective autophagy-dependent degradation of TNIP1, supporting the expression of pro-inflammatory genes and proteins. This selective autophagy efficiently reduces TNIP1 protein levels early (0–4 h) upon poly(I:C) treatment to allow efficient initiation of the inflammatory response. At 6 h, TNIP1 levels are restored due to increased transcription avoiding sustained inflammation. Thus, similarly as in cancer, autophagy may play a dual role in controlling inflammation depending on the exact state and timing of the inflammatory response.

Introduction

Macroautophagy, hereafter referred to as autophagy, is a primary cytoprotective process that leads to the removal and lysosomal degradation of non-functional and/or superfluous cytoplasmic material. Autophagy is a constitutive process but may also be triggered by various forms of cell stresses (Mizushima and Levine, 2020). It involves the formation of a double membrane vesicle known as autophagosome that enwraps portions of the cytoplasm, including organelles. The content of the autophagosome is then targeted for degradation through the lysosome. Constitutive autophagy is regarded as a non-selective, bulk process, whereas stress-induced autophagy is often selective, aiming at removing the causes of stress, e.g., depolarized mitochondria in oxidative stress (Youle, 2019). Selective autophagy is carried out either by direct interactions between cargo and lipidated human ATG8 family members (MAP1LC3-A, -B, -C, GABARAP, GABARAPL1, GABARAPL2, commonly referred to as LC3s) that are anchored to autophagosomal membranes or by indirect interactions in which so-called selective autophagy receptors (SARs) tether cargo to LC3s (Johansen and Lamark, 2020). Cargo and receptors are then both degraded within lysosomes (Morishita and Mizushima, 2019). p62/SQSTM1, which is considered the founding member

of the protein class of p62/SQSTM1-like receptors (SLRs), recognizes poly-ubiquitinated proteins/organelles destined for lysosomal degradation through its ubiquitin-associated (UBA) domain and interacts with lipidated LC3s through its LC3-interacting region (LIR) motif (Johansen and Lamark, 2020; Pankiv et al., 2007). SLRs are involved in the selective, autophagy-dependent degradation of a highly diverse set of substrates (Zellner et al., 2021).

The limitation of deleterious inflammatory responses is one of the cytoprotective functions attributed to autophagy (Deretic and Levine, 2018). The link between autophagy and tissue inflammation became obvious by genome-wide association studies that identified *ATG16L1* as susceptibility locus for Crohn's disease (Hampe et al., 2007). Since then several autophagy loci have been linked to inflammatory and autoimmune disorders (Mizushima and Levine, 2020). The selective degradation of inflammasome components, e.g., by p62/SQSTM1, is among the best-understood functions of autophagy in limiting tissue inflammation (Deretic and Levine, 2018; Samie et al., 2018). However, autophagy was also shown to support unconventional secretion of the pro-inflammatory cytokine IL1B (Dupont et al., 2011; Zhang et al., 2015), which argues for a fine-tuned and

¹Department of Biology, University of Fribourg, Fribourg, Switzerland; ²Autophagy Research Group, Department of Medical Biology, University of Tromsø—The Arctic University of Norway, Tromsø, Norway; ³Department of Biochemistry and Molecular Biology, Center for Experimental Bioinformatics, University of Southern Denmark, Odense, Denmark; ⁴Department of Biomedical Sciences of Cells and Systems, University of Groningen, University Medical Center Groningen, Groningen, Netherlands; ⁵Department of Biomedicine, Aarhus University, Aarhus, Denmark; ⁶Aarhus Institute of Advanced Studies (AIAS), Aarhus University, Aarhus, Denmark.

*J. Zhou and N.L. Rasmussen contributed equally to this paper. Correspondence to Jörn Dengjel: joern.dengjel@unifr.ch; Terje Johansen: terje.johansen@uit.no.

© 2022 Zhou et al. This article is distributed under the terms of an Attribution–Noncommercial–Share Alike–No Mirror Sites license for the first six months after the publication date (see <http://www.rupress.org/terms/>). After six months it is available under a Creative Commons License (Attribution–Noncommercial–Share Alike 4.0 International license, as described at <https://creativecommons.org/licenses/by-nc-sa/4.0/>).

balanced role of autophagy in regulating inflammatory responses.

TNIP1 (also known as ABIN-1, Naf1, and VAN) is a ubiquitin-binding adaptor protein that has been implicated as a negative regulator of inflammatory signaling and cytokine-induced cell death (Dziedzic et al., 2018; Gao et al., 2011; Oshima et al., 2009; Su et al., 2019; Zhou et al., 2011). Interestingly, recent studies linked TNIP1, either as cargo or as receptor, to autophagy-dependent protein degradation (Shinkawa et al., 2022). Selective autophagy-dependent degradation of TNIP1 through interaction with the SLR optineurin (OPTN) was reported, supporting senescence-associated inflammation (Lee et al., 2021). While TNIP1 itself shows no catalytic activity, its ability to bind linear polyubiquitin chains through its Ub-binding domain in ABIN proteins and NEMO (UBAN) is important for its anti-inflammatory function (Nanda et al., 2011; Wagner et al., 2008). A number of studies suggest that TNIP1 exerts its negative function by recruiting the ubiquitin-editing enzyme TNFAIP3 (also known as A20) to polyubiquitinated targets (Dziedzic et al., 2018; Gao et al., 2011; Mauro et al., 2006). However, the exact mechanism behind this negative regulation is not completely understood. Furthermore, TNIP1 shows activity independent of TNFAIP3 (Kattah et al., 2018; Oshima et al., 2009). The importance of TNIP1 as an anti-inflammatory signal transducer is highlighted by numerous studies implicating TNIP1 dysregulation in autoimmune disorders (Shamilov and Aneskievich, 2018). Uncovering the molecular function and dynamics of TNIP1 could, therefore, be valuable in understanding the mechanisms behind such complex disorders.

In the current study, we characterize TNIP1 as an autophagy substrate, which is selectively degraded at an early stage (0–4 h) under inflammatory conditions. We highlight that TNIP1 fulfills the structural characteristics of an autophagy receptor with an oligomerization domain, a ubiquitin-binding domain, and an LIR motif. Upon TLR3 activation, TNIP1 is phosphorylated by TBK1 on LIR proximal serine residues to increase binding to LC3s. Hence, TNIP1 is selectively degraded by autophagy in order to promote a competent initiation of pro-inflammatory signaling.

Results

TNIP1 is ubiquitinated and degraded within lysosomes

To identify new proteins potentially involved in autophagy regulation or autophagosomal targeting, we screened ubiquitination dynamics by quantitative mass spectrometry (MS)-based proteomics. U2OS and HeLa cells were differentially labeled by stable isotope labeling by amino acids in cell culture (SILAC), and autophagy was induced by inhibiting MTORC1 by rapamycin. In parallel, lysosomal degradation was blocked by concanamycin A (ConA), an inhibitor of lysosomal V-type ATPase (Klionsky et al., 2021). Respective cell lysates were mixed, proteins digested with the endoprotease LysC and ubiquitinated peptides were enriched using the UbiSite approach followed by MS-based identification and quantification (Akimov et al., 2018; Fig. 1 A). We identified more than 9,000 ubiquitination sites, of which more than 2,000 were quantified in minimally three biological replicates and could be localized clearly to specific

amino acid residues (class I sites, Fig. 1 B and Table S1; Olsen et al., 2006). These sites were used for further analyses. Comparing abundance changes of ubiquitination sites of cells treated with rapamycin with cells treated with rapamycin and ConA, 148 sites were identified as significantly regulated; the majority being more abundant in cells in which lysosomal degradation was inhibited by ConA (paired *t* test, FDR < 0.05, Fig. 1 C). As anticipated, we identified many proteins involved in autophagosomal biogenesis and target recruitment. Importantly, four central SLRs, p62/SQSTM1, NBR1, CALCOCO2/NDP52, and TAX1BP1 (Johansen and Lamark, 2020), were identified as being increasingly ubiquitinated (Fig. 1 C), indicating that our experimental strategy was successful.

One protein that caught our attention was TNIP1/ABIN-1, which was identified as significantly ubiquitinated on the amino acid residue Lys389 (Fig. 1 C). TNIP1 is a key repressor of inflammatory signaling (Shamilov and Aneskievich, 2018), and posttranslational mechanisms regulating its protein abundance are largely unknown. In a reverse affinity purification (AP), we used U2OS-StUbEx cells inducibly expressing 6xHis-FLAG-tagged ubiquitin (Akimov et al., 2014), treated cells with rapamycin, or starved for amino acids with and without ConA and used Ni-NTA beads to enrich ubiquitinated proteins. Anti-TNIP1 immunoblotting validated the MS findings and characterized TNIP1 as increasingly ubiquitinated in cells in which lysosomal degradation was inhibited (Fig. 1 D and Fig. S1 A).

As only a fraction of TNIP1 appeared to be ubiquitinated, we investigated whether ubiquitination of Lys389 is necessary for lysosomal targeting of TNIP1. We performed site-directed mutagenesis and analyzed the stability and ubiquitination of wild-type (TNIP1^{WT}) and respective TNIP1 variants. Next to Lys389, we also mutated the neighboring residue Lys371, which we identified in two out of the three SILAC experiments. The blockage of lysosomal degradation led to the accumulation of modified and non-modified variants of TNIP1, indicating that ubiquitination is not decisive for lysosomal degradation (Fig. S1 B). In addition, arginine-variants did neither exhibit alterations in their global ubiquitination pattern nor in their stability, indicating the presence of additional ubiquitination sites, which agrees with database entries (Fig. S1, B–F). Together, these results indicate that non-ubiquitinated and multi-ubiquitinated variants of TNIP1 accumulate upon the blockage of lysosomal acidification and that TNIP1 may be an autophagy substrate. Due to its importance in inflammation, we decided to study the regulation of TNIP1 protein abundance in more detail.

TNIP1 is degraded by autophagy

Because the blockage of lysosomal degradation by ConA led to an accumulation of non- and ubiquitinated TNIP1 variants, we examined whether TNIP1 is degraded by autophagy and whether proteasomal degradation also contributes to regulating TNIP1 protein abundance under basal conditions. TNIP1 behaved similarly as p62/SQSTM1 under basal and mTORC1 inhibited conditions using Torin-1, while the inhibition of lysosomal acidification by ConA led to a significant accumulation of TNIP1 protein, inhibition of the proteasome by MG132 did not (Fig. 2, A and B). Furthermore, confocal immunofluorescent imaging

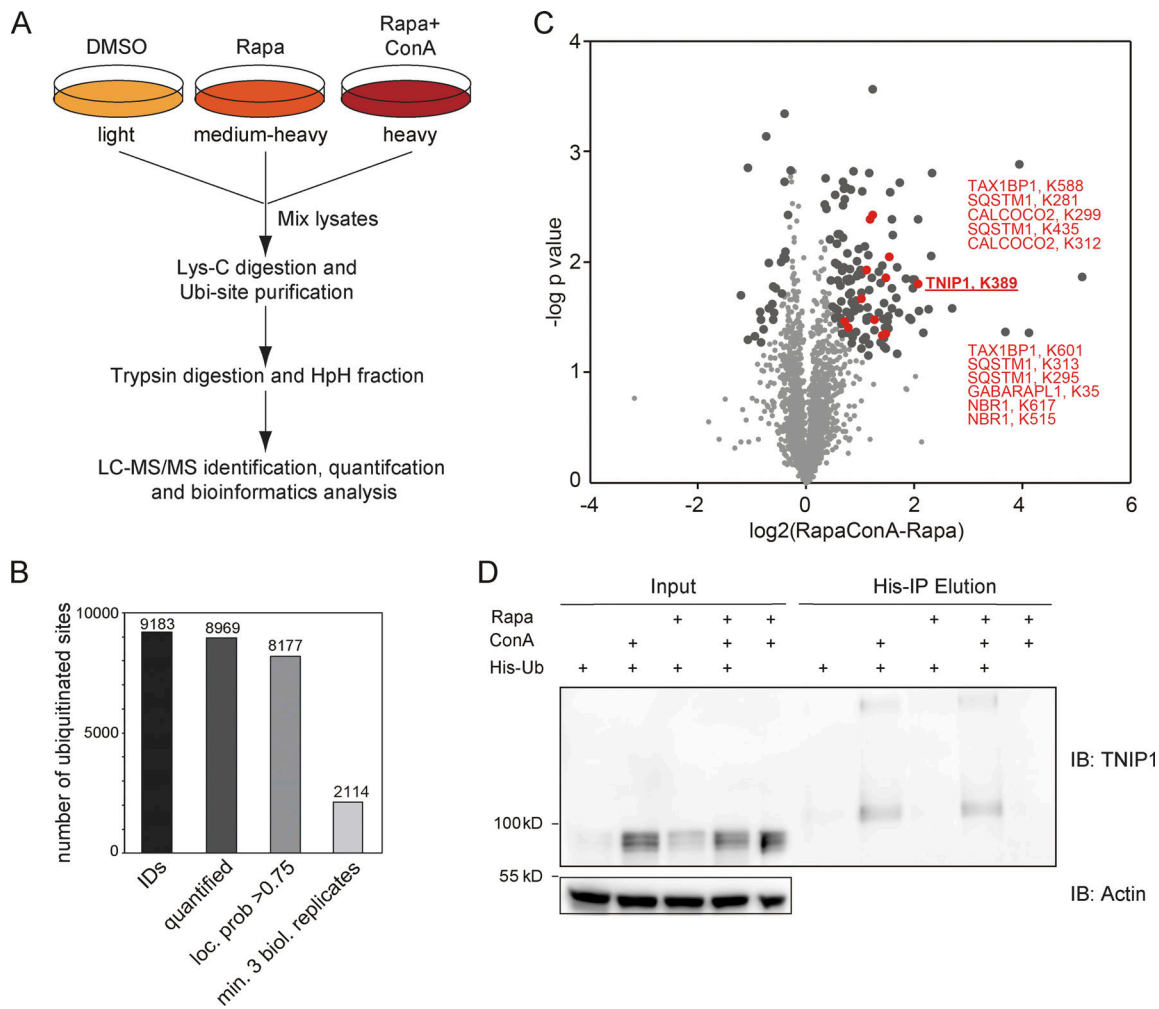


Figure 1. Ubiquitination and lysosomal degradation of TNIP1. (A) MS workflow to quantify ubiquitination sites potentially involved in autophagy-dependent lysosomal protein degradation. U2OS and HeLa cells were SILAC labeled and treated for 4 h with 100 nM rapamycin (Rapa), Rapa and 2 nM concanamycin A (ConA), or DMSO as control. After mixing of lysates, proteins were digested with Lys-C endoprotease and ubiquitinated peptides were enriched using the UbiSite approach (Akimov et al., 2018). Enriched peptides were digested with trypsin, followed by high-pH reversed phase fractionation (Batth and Olsen, 2016) and shotgun LC-MS/MS analysis. (B) Detected ubiquitination sites. In three biological replicates, 9,183 ubiquitination sites were identified of which 8,969 were quantified. (C) Volcano plot highlighting significantly regulated ubiquitination sites. Significantly regulated sites comparing Rapa with Rapa + ConA treated cells are highlighted in dark grey ($n = 3$, paired two-sided t test, $FDR < 0.05$, $S0 = 0.1$, 148 sites in total; see Table S1). Data distribution was assumed to be normal but this was not formally tested. Non-regulated sites are colored in light gray. Sites identified on known autophagy receptors are colored in red exemplifying data quality. The newly identified site on TNIP1, K389, is highlighted in bold red. (D) TNIP1 gets ubiquitinated and degraded in the lysosome. U2-OS-StUbEx cells inducibly expressing His-FLAG-tagged ubiquitin at endogenous levels were used to enrich ubiquitinated proteins (Akimov et al., 2014). Under control conditions as well as under 4 h 100 nM rapamycin treatment TNIP1 got ubiquitinated as shown by anti-TNIP1 immunoblots. Ubiquitinated TNIP1 was stabilized by the addition of concanamycin A indicating its lysosomal degradation in treated and nontreated cells. The same was observed for starved cells (HBSS treatment; see Fig. S1). Actin was used as loading control. Note: Due to the design of the experiment and the used gels, the molecular weight marker (PageRuler Plus, #26619; Thermo Fisher Scientific) and the Rapa+/ConA+ sample were run in the same lane. In the respective source data, an additional replicate is shown in which samples ran separately. Source data are available for this figure: SourceData F1.

showed endogenous TNIP1 accumulation upon Bafilomycin A1 (BafA1), another V-type ATPase inhibitor, treatment (Fig. S2). Importantly, under these conditions TNIP1 colocalized with LC3-positive structures, which also strongly overlapped with p62/SQSTM1. Using airyscan super-resolution confocal microscopy, we found that TNIP1 is located inside LAMP1- and LC3-positive structures in untreated cells, and that TNIP1 is accumulated within these structures upon BafA1 treatment (Fig. 2 C). Another way to test for lysosomal degradation is using a tandem tag autophagy flux reporter system (Pankiv et al., 2007), in which

TNIP1 is fused to a tandem mCherry-EYFP tag. While EYFP is sensitive to low pH and therefore quickly loses its fluorescence in acidic lysosomes, the mCherry tag is rather stable under these conditions. In neutral cytosol, both tags of mCherry-EYFP-TNIP1 will be visible, while in lysosomes, only the mCherry-tag will fluoresce and appear as red-only dots. Transient transfection of mCherry-EYFP-TNIP1 did indeed lead to the formation of many red-only dots per cell, supporting the notion that TNIP1 ends up in lysosomal structures (Fig. 2 D). Taken together, this suggests that TNIP1 is degraded by autophagy under basal conditions as

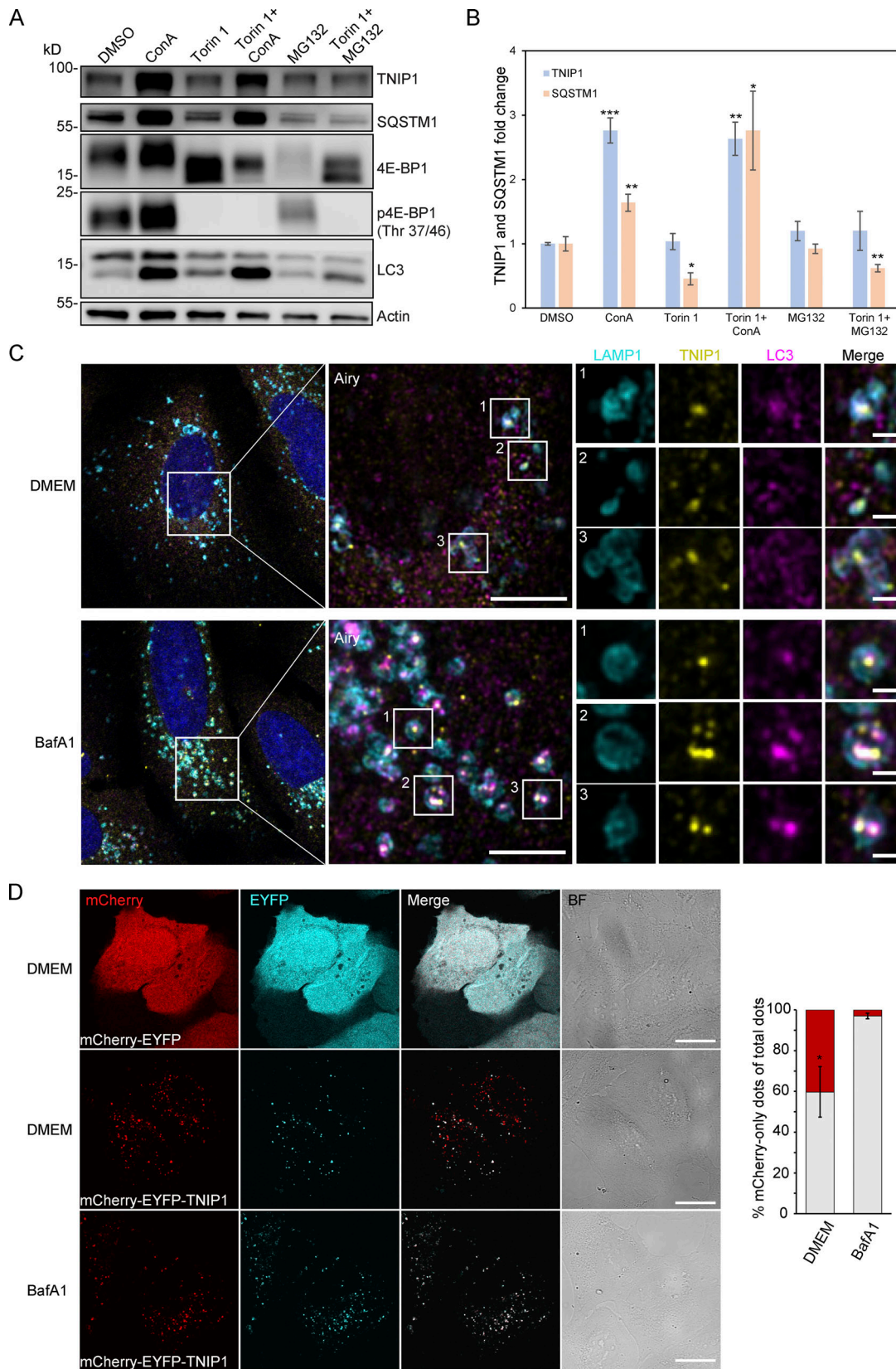


Figure 2. **TNIP1 is degraded by autophagy.** (A) U2OS cells were treated with 1 μ M Torin-1 for 4 h; proteasomal or lysosomal degradation were inhibited by 10 μ M MG132 or 2 nM ConA, respectively. Under fed conditions (DMSO) and in Torin-1 treated cells blockage of lysosomal acidification led to a significant increase of TNIP1 protein abundance. Shown are representative blots of three biological replicates. (B) Quantification of blots shown in A ($n = 3$). * = $P < 0.05$, ** = $P < 0.01$, *** = $P < 0.001$ unpaired, two-sided t test compared to DMSO treated samples. Error bars indicate SEM. (C) Confocal images showing

colocalization between endogenous TNIP1, LAMP1 and LC3 in U2OS cells treated for 5 h with either BafA1 or vehicle DMSO. Cells were immunostained against endogenous TNIP1 (yellow), LAMP1 (cyan), and LC3 (purple) and imaged by Airyscan using the Zeiss LSM880 confocal microscope. Inserts highlight TNIP1 localized in LAMP1- and LC3-positive structures. Due to BafA1 treatment leading to accumulation of the immunostained proteins, signal intensities in the DMSO image have been increased relative to the BafA1 treated image during post-processing. Scale bars are 5 μ m for the airyscan images and 1 μ m for the inserts. **(D)** U2OS cells were transiently transfected with either mCherry-EYFP or mCherry-EYFP-TNIP1. 24 h after transfection, cells were either left untreated or treated with BafA1 for 4 h. BF = bright field. Scale bars, 20 μ m. Quantification of red-only TNIP1 dots over total TNIP1 dots was done using Velocity software (PerkinElmer), with intensity cut-offs based on BafA1 intensity of red and green dots ($n = 3$). Around 2,000–3,000 dots were counted for each condition within each replicate. * = $P < 0.05$, unpaired, two-sided t test. Error bars indicates SD. In B and D, data distribution was assumed to be normal, but this was not formally tested. Source data are available for this figure: SourceData F2.

well as upon Torin-1 treatment, with proteasomal protein degradation playing a negligible role.

Next, we aimed to characterize the molecular events that led to autophagosomal recruitment of TNIP1. We immunoprecipitated HA-tagged TNIP1 and performed an MS analysis of its interactome. This screen identified a number of autophagy-related proteins as possible TNIP1 interactors, including p62/SQSTM1, TAX1BP1, OPTN, and TBK1 (Fig. 3, A and B and Table S2). The former two, p62/SQSTM1 and TAX1BP1, were also identified by MS as enriched in IPs of endogenous TNIP1 under basal conditions (Fig. S3 A). The interaction with p62/SQSTM1 was also observed by immunoprecipitation followed by Western blotting (Fig. 3 C). In ATG101 KO, FIP200 KO, and pentaKO HeLa cells (which do not express the SLRs p62/SQSTM1, NBR1, NDP52, TAX1BP1 and OPTN [Sarraf et al., 2020]) TNIP1 no longer showed stabilization upon lysosomal blockage (Fig. 3, D and E). This was also true for single KOs of p62 and OPTN (but not TAX1BP1), which also showed a reduction in TNIP1 abundance upon lysosomal blockage (Fig. S3, B and C). Taken together, this suggests that more than one SLR is mediating the basal autophagic turnover of TNIP1. The staining of endogenous TNIP1 in U2OS cells showed an increase in the number of TNIP1 puncta (Fig. 3, F and G) and increased colocalization between TNIP1 and the SLRs p62/SQSTM1, TAX1BP1, and NDP52 upon BafA1 treatment (Fig. 3 H). Thus, under basal conditions, TNIP1 interacts with SLRs, which target TNIP1 to autophagosomes for lysosomal degradation. To further investigate the basal turnover, we analyzed the autophagic flux using mCherry-EYFP-TNIP1 in U2OS cells KO for FIP200, ATG9, ATG7, and ATG16L1. As quantified in Fig. 3 I, FIP200 and ATG9 KO cells showed little to no red-only dots. This is consistent with the importance of these proteins in both ATG7-dependent and -independent autophagy (Goodwin et al., 2017). ATG7 and ATG16L1 KOs showed reduced formation of red-only dots, but not a complete loss, indicating that there may also be ATG7-independent degradation of TNIP1 under basal conditions. Altogether, these results suggest that autophagic degradation of TNIP1 under basal conditions is aided by SLRs, and that this turnover may be both ATG7-dependent and -independent.

TNIP1 interacts with human ATG8 family proteins through LIR motifs

Having established that TNIP1 colocalizes with several SLRs and is degraded by autophagy, we aimed to examine whether TNIP1 may also function independently of SLRs in autophagy. TNIP1 contains coiled-coil domains for oligomerization and a ubiquitin-binding UBAN domain similar to that of OPTN,

which preferentially binds K63- and M1-linked polyubiquitin chains (Fig. 4 A; Herhaus et al., 2019; Wagner et al., 2008). TNIP1 only needs an LIR motif interacting with ATG8 proteins to be able to function as a SAR itself. Hence, we performed a peptide array screen for potential LIR motifs in human TNIP1. The peptide array, containing overlapping 20-mer peptides of TNIP1 moved by increments of three amino acids to cover the 636 amino acids full-length sequence, was probed with GST-GABARAP and revealed two potential LIRs in TNIP1, with core sequences 83-FDPL-86 and 125-FEVV-128, respectively (Fig. 4 B). The N-terminal region harboring these LIR motifs is missing in the two other TNIP family members, TNIP2 and -3. Of these two candidates, only LIR2 is conserved in the evolution of vertebrates down to cartilaginous fishes, while LIR1 is only conserved down to marsupials and is not found in platypus (Fig. 4 C). LIR2 also has acidic- and phosphorylatable residues flanking the core LIR motif, making it a very strong candidate for a functional LIR that could be positively regulated by phosphorylation (Johansen and Lamark, 2020; Wirth et al., 2019). LIR1 has a proline within the core motif which is usually inhibitory to binding to the ATG8s (Alemu et al., 2012; Johansen and Lamark, 2020). We then further tested the interaction between TNIP1 and the six human ATG8 family proteins by GST-pulldown assays. GST and GST-tagged human LC3 and GABARAP proteins were used to pull down in vitro translated wild-type TNIP1. Here, we observed that TNIP1 bound very well to several of the human ATG8s, with the strongest interaction being with LC3A, LC3B, GABARAP, and GABARAPL1, and weak binding to LC3C and GABARAPL2 (Fig. 4, D and E). To test whether any of the two potential LIRs identified in the peptide array scan were responsible for this interaction, we mutated the conserved aromatic- and hydrophobic residues in each core LIR sequence to alanine, namely, F83A/L86A and F125A/V128A (Fig. 4 C). GST-pulldown assays with these mutants revealed that the F125A/V128A mutations in LIR2 strongly reduced the interaction between TNIP1 and the GST-ATG8s, while the F83A/L86A mutations in LIR1 had either no or a very minor effect compared to mutating LIR2 alone (Fig. 4, D and E). We also tested the influence of LIRs for in vivo interactions of TNIP1 with LC3s using HeLa cells expressing HA-TNIP1 variants by performing anti-HA affinity purifications (APs) followed by anti-LC3A/B Western blots (Fig. 4, F and G). In agreement with the in vitro observations, TNIP1 with both LIR motifs mutated (mLIR1+2) interacted significantly weaker with LC3A/B in vivo. Thus, TNIP1 fulfills all structural characteristics of being an SLR, with LIR2 being the motif mainly responsible for binding to ATG8s.

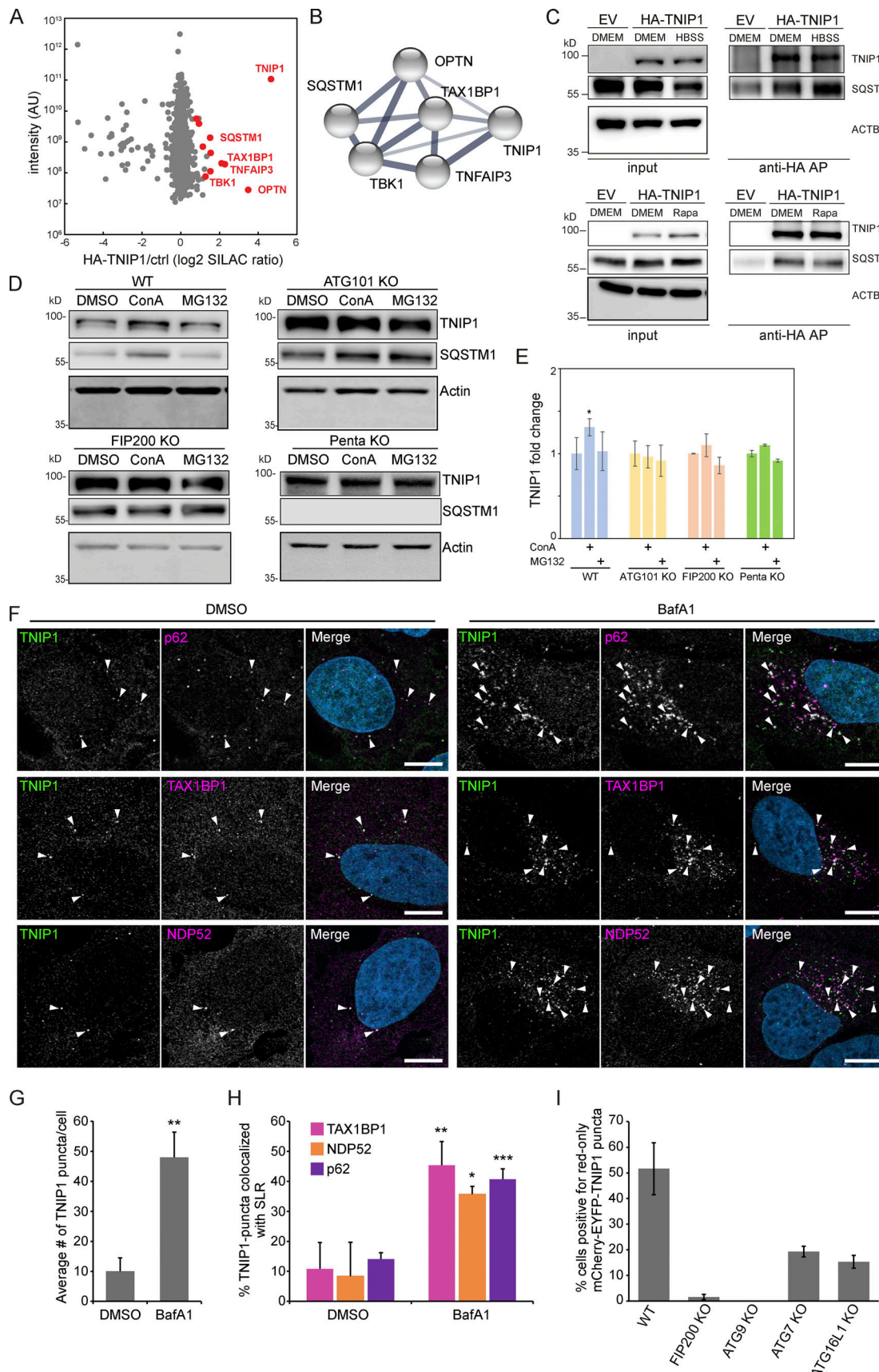


Figure 3. **TNIP1 localizes to p62 bodies.** (A) HA-TNIP1 affinity purification (AP)-MS highlights its interaction with autophagy receptors. HeLa cells expressing HA-TNIP1 and vector control cells (ctrl.) were differentially SILAC-labeled and anti-HA APs were performed under basal conditions, followed by quantitative MS

analyses ($n = 3$). Proteins that were significantly enriched in minimum two out of three replicates are highlighted in red ($P < 0.05$, BH corrected). Proteins with known functions in autophagy and inflammation are annotated. **(B)** TNIP1 interactome. STRING DB was used to highlight the TNIP1 interactome identified in A (Szklarczyk et al., 2019). Thickness of edges indicate confidence of interaction. **(C)** TNIP1 interacts with p62/SQSTM1. Anti-HA affinity purifications followed by Western blot analyses were performed to test for HA-TNIP1-p62/SQSTM1 interactions as identified in A in basal (DMEM), stress conditions (amino acid starvation, HBSS) and after rapamycin (Rapa) treatment each for 4 h. EV, empty vector. **(D and E)** TNIP1 is degraded in an autophagy- and SLR-dependent manner. Shown are representative blots of three biological replicates. HeLa WT cells, ATG101 KO cells, FIP200 KO cells and PentaKO cells were treated with 10 μ M MG132 or 2 nM ConA for 4 h. TNIP1 abundance was significantly increased in ConA-treated HeLa WT cells, while treatment had no effect in HeLa ATG101 KO, FIP200 KO, and pentaKO cells. E shows quantifications of D ($n = 3$). * = $P < 0.05$, unpaired, two-sided t test. Error bars indicates SEM. **(F)** U2OS cells were treated with either vehicle (DMSO) or BafA1 for 5 h and stained for endogenous TNIP1 (green) together with either endogenous p62, NDP52 or TAX1BP1. Representative images are shown. Colocalization between TNIP1 and respective SLRs are indicated by arrowheads. Scale bars, 10 μ m. **(G)** Quantification of the average number of TNIP1 puncta per cell imaged in F (>40 cells analyzed for each condition within each replicate [$n = 3$]). ** = $P < 0.01$, unpaired two-sided t test. Error bars indicate SD. **(H)** Quantification of percent TNIP1 puncta colocalizing with the indicated SLRs in F (>40 cells analyzed for each condition within each replicate [$n = 3$]). *** = $P < 0.001$, ** = $P < 0.01$, * = $P < 0.05$, unpaired, two-sided t test. Error bars indicate SD. **(I)** Transient transfection of mCherry-EGFP-TNIP1 in WT U2OS cells and indicated KO cell lines. The graph bars indicate the percentage of transfected cells containing >5 red-only puncta indicative of autophagic degradation. Each graph bar shows the mean value from three separate transfections ($n = 3$, >100 cells counted per transfection, unpaired, two-sided t test). Error bars indicate SD. In E and G–I, data distribution was assumed to be normal, but this was not formally tested. Source data are available for this figure: SourceData F3.

TNIP1 does not affect basal autophagy flux

We next asked whether TNIP1 was capable of regulating autophagy flux. For this, we compared the levels of several known SLRs as well as the ratio of LC3-I and II under basal and starvation conditions in WT HeLa and two TNIP1 KO clones. The ratio of LC3-I and LC3-II was not affected by TNIP1 KO, and neither was the conversion upon starvation by HBSS, suggesting that TNIP1 does not affect autophagic flux under the tested conditions (Fig. 5, A and B). With the exception of OPTN, the basal protein levels of several SLRs and their degradation upon starvation were also unaffected by TNIP1 KO. However, the basal protein levels of OPTN were elevated in both TNIP1 KO clones, indicating that OPTN might be involved in a compensatory response. Indeed, we identified an upregulation of OPTN mRNA in TNIP1 KO clones (Table S3).

As SLRs are themselves autophagy substrates, and as loss of TNIP1 was shown to lead to increased inflammatory signaling (Shamilov and Aneskievich, 2018), we next asked if loss of TNIP1 in our cell systems also led to an increase of pro-inflammatory proteins. Comparing gene expression by RNAseq and protein abundance by SILAC-based proteomics between WT and TNIP1 KO HeLa cells, we indeed observed an upregulation of a number of genes involved in inflammatory signaling in TNIP1 KO cells on mRNA and protein level, including TNFAIP3, ISG15, and GBP1 (Fig. 5, C and D; and Table S3). This was confirmed by gene set enrichment analyses (GSEA), which highlighted an activation of the inflammatory response in TNIP1 KO cells at both mRNA and protein level (Fig. 5, E and F). At the mRNA level, we identified several chemokines which were more abundant in TNIP1 KO cells, CCL5 being the most differentially regulated gene (Table S3 B). The upregulation of single proteins was also observed by Western blot analysis and was at least in part due to changes at the transcriptional level (Fig. 5, G and H). Importantly, re-expression of TNIP1 blunted this effect confirming that it was indeed the absence of TNIP1 that led to the observed changes of the respective proteins. The LIR motifs did not affect this response under basal conditions as expression of TNIP1-mLIR1+2 led to the same consequences as TNIP1-WT (Fig. 5 I). Taken together, whereas TNIP1 seemed not to affect autophagy flux under basal conditions, its loss led to an increased abundance of

pro-inflammatory proteins, indicating that selective autophagy may contribute to the tuning of inflammatory signaling by regulating TNIP1 protein levels. Thus, in this context, TNIP1 is a bona fide autophagy substrate whose protein level is critical for the regulation of inflammatory signaling.

Pro-inflammatory signaling induces LIR-dependent, autophagic degradation of TNIP1

So far, we characterized TNIP1 as a constitutive autophagic cargo as we did not observe changes in autophagosomal recruitment and lysosomal degradation based on the metabolic status of cells. To test whether inflammatory signaling could lead to specific effects, we treated cells with the double-stranded RNA mimic poly(I:C), which mimics viral infection and elicits a TLR3 signaling response (Glavan and Pavelic, 2014). After 4 h of poly(I:C) treatment, we observed a significant decrease in endogenous TNIP1 levels, followed by an increase after 6 h (Fig. 6, A and B). Parallel to the observed decrease of TNIP1, an increase in pro-inflammatory proteins like ISG15 and the chemokine CCL5 was observed (Fig. 6 A and Fig. S4 A). The decrease of TNIP1 was dependent on canonical autophagy, as loss of ATG7, ATG101, and FIP200 inhibited the response, but independent of SLRs, as loss of the SLRs p62/SQSTM1, NBR1, NDP52, TAX1BP1, and OPTN in a pentaKO cell line did not inhibit the response (Fig. 6, A and B). In agreement, lysosomal inhibition by ConA could block this decrease in WT and pentaKO cells but had no effect on the autophagy incompetent cell lines (Fig. S4 B). Proteasomal inhibition by MG132 did not stabilize TNIP1 levels in any of the cell lines (Fig. S4 B). The observed increase at 6 h of treatment is due to transcriptional upregulation of TNIP1 (Fig. 6 C). Hence, TNIP1 is itself specifically targeted to autophagosomes under poly(I:C) treatment. Confocal imaging showed that upon poly(I:C) treatment in WT cells, endogenous TNIP1 changes from being mostly diffuse to forming dots in the cytoplasm (Fig. 6, D and E). The formation of TNIP1 dots in response to poly(I:C) was also observed in ATG7- and pentaKO cells (Fig. 6, D and E). In ATG7 KO cells, there was an increased amount of TNIP1 dots already at the basal level, which increased even further upon poly(I:C) treatment. In pentaKO cells, we observed an increased diffuse TNIP1 staining of cells at the basal

tagged human ATG8s. Bound myc-TNIP1 WT and LIR mutants were detected by autoradiography (AR). **(E)** Quantification of GST-pulldown from D. Relative % binding was quantified against 10% input ($n = 3$). * = $P < 0.05$, ** = $P < 0.01$, based on one-way ANOVA (post hoc Tukey test). Error bars indicate SEM. **(F)** LIR mutation impacts in vivo interaction with LC3A/B. Anti-HA AP of cells expressing HA-TNIP1^{WT} and HA-TNIP1^{mLIR1+2} were performed followed by Western blot against indicated proteins. LIR mutation reduced the interaction between TNIP1 and LC3A/B. **(G)** Quantification of blots exemplified in panel F ($n = 3$). Error bars indicate SEM. ** = $P < 0.01$, unpaired, two-sided *t* test. In E and G, data distribution was assumed to be normal, but this was not formally tested. Source data are available for this figure: SourceData F4.

level likely reflecting an increase in basal protein levels. Upon 4 h stimulation with poly(I:C) TNIP1 puncta increased also in pentaKO cells similarly as in ATG7 KO cells. Taken together, our data suggest that neither ATG7 nor SLRs are required for poly(I:C)-induced TNIP1 aggregation into dots. However, ATG7, but not SLRs, is necessary for TNIP1 degradation upon poly(I:C) stimulation.

Because our data suggested that TNIP1 is degraded specifically by autophagy upon poly(I:C) exposure, we investigated whether this was LIR-dependent. To this end, we observed that in cells reconstituted with HA-TNIP1-WT, 6 h of poly(I:C) treatment led to a significant decrease in TNIP1 levels, while we did not observe this decrease in cells expressing HA-TNIP1-mLIR1+2 (Fig. 6, F and G; and Fig. S4 C). ISG15 levels anti-correlated with HA-TNIP1 levels confirming the inhibitory role of TNIP1 in regulating ISG15 expression (Fig. 6, F and G; and Fig. S4 A). Importantly, the relative increase of ISG15 was significantly higher in HA-TNIP1-WT compared to HA-TNIP1-mLIR1+2 expressing cells, supporting the interpretation that LIR-dependent degradation of TNIP1 is critical for a stimulus- and time-dependent expression of pro-inflammatory genes. Note that the time-dependent increase of endogenous and exogenous TNIP1 after prolonged poly(I:C) treatment differed, indicating a long-term transcriptional and/or translational regulation next to the observed short-term autophagy-dependent effects (Fig. 6, F and G; and Fig. S4 D). TNIP1 expression has previously been shown to be transcriptionally regulated by NF- κ B, making it likely that prolonged poly(I:C) treatment can lead to the increased expression of TNIP1 (Tian et al., 2005). To further test the LIR-dependent recruitment of TNIP1 to autophagosomes under poly(I:C) treatment, we performed anti-GFP-LC3B IPs followed by anti-TNIP1 Western blotting. In these IP experiments, we observed a poly(I:C)-dependent increase in interaction of TNIP1 with LC3B in TNIP1 KO cells reconstituted with WT TNIP1, which was significantly reduced in KO cells reconstituted with TNIP1-mLIR1+2 (Fig. 6 H). Thus, pro-inflammatory signaling as exemplified by poly(I:C) treatment appears to lead to the specific, LIR-dependent degradation of TNIP1 by autophagy.

TBK1 positively regulates LIR-dependent interaction of OPTN with LC3B by phosphorylating the LIR motif of OPTN (Wild et al., 2011). In addition, TBK1 is an important mediator of TLR3-induced antiviral signaling (Louis et al., 2018). Since we identified TBK1 as a possible interaction partner of TNIP1 (Fig. 3 A), we tested whether TBK1 also plays a role in selective TNIP1 degradation. Indeed, confocal imaging showed that upon poly(I:C) treatment in WT cells, several of the observed endogenous TNIP1 dots colocalized with phosphorylated (Ser172), i.e., active, TBK1 (Fig. 7 A). Poly(I:C) treatment also led to a time-dependent activation of TBK1 as indicated by phosphorylation of Ser172

(Fig. 7 B). Interestingly, loss of TNIP1 led to an increased activation of TBK1 indicating a feedback regulatory mechanism.

With the TBK1-mediated regulation of the OPTN LIR in mind, we used MS-based phosphoproteomics to study whether TBK1 can phosphorylate serine and threonine residues located N-terminal to the core LIR sequence FEVV of LIR2 in TNIP1 (Fig. 4 C). Due to the surrounding amino acid sequence, we could not follow the standard workflow of bottom-up proteomics experiments using trypsin to generate respective peptides. Instead, we performed a multi-protease digestion protocol using Elastase or ProAlanase to generate optimal sequence coverage (Eisenhardt et al., 2016; Samodova et al., 2020). We were able to identify and quantify two phosphopeptide species which were phosphorylated within the TSS motif just in front of LIR2 (Fig. 7 C). Comparing cells treated or not with poly(I:C) and/or the TBK1 inhibitor MRT67307 clearly indicated that TBK1 phosphorylates TNIP1 in a stimulus-dependent manner (Fig. 7 C). To determine whether TNIP1 is a direct target of TBK1, we performed in vitro kinase assays and could recapitulate the in vivo observations characterizing TNIP1 as a bona fide TBK1 substrate (Fig. 7 D). To test the effect of phosphorylations of the evolutionary conserved S122 and S123 residues N-terminal to the core LIR motif (Fig. 4 C), we analyzed the binding of the phosphomimicking S122E/S123E TNIP1 mutant to ATG8 family proteins by GST pulldown. Strikingly, the phosphomimicking mutant displayed strongly increased binding to all ATG8 proteins. The binding increase was particularly evident for LC3B (3.4-fold), LC3C (4.4-fold) and GABARAPL2 (5.8-fold; Fig. 7 E). Finally, we tested the effects of poly(I:C) treatment and TBK1 inhibition on TNIP1-LC3B interaction by GFP-LC3B IP. Inhibition of TBK1 led to a decreased interaction of TNIP1-WT with GFP-LC3B indicating that TBK1-dependent phosphorylation of the TNIP1 LIR motif was responsible for the observed increased interaction between LC3 and TNIP1 (Fig. 7 F). In agreement, pharmacological and genetic inhibition of TBK1 led to a stabilization of TNIP1 under poly(I:C) treatment, i.e., interfered with its stimulus-dependent degradation (Fig. 7, G and H). Thus, whereas SLRs appear to support autophagy-dependent, basal turnover of TNIP1, activation of its LIR motif by TBK1 induces its selective, autophagy-dependent removal, supporting the mounting of a transcriptional program to induce a robust inflammation response (Fig. 8).

Discussion

Autophagy is largely regarded as a cytoprotective, anti-inflammatory response ensuring cell and organismal homeostasis (Deretic, 2021; Deretic and Levine, 2018). Several autophagy loci have been linked to genetic predispositions for chronic

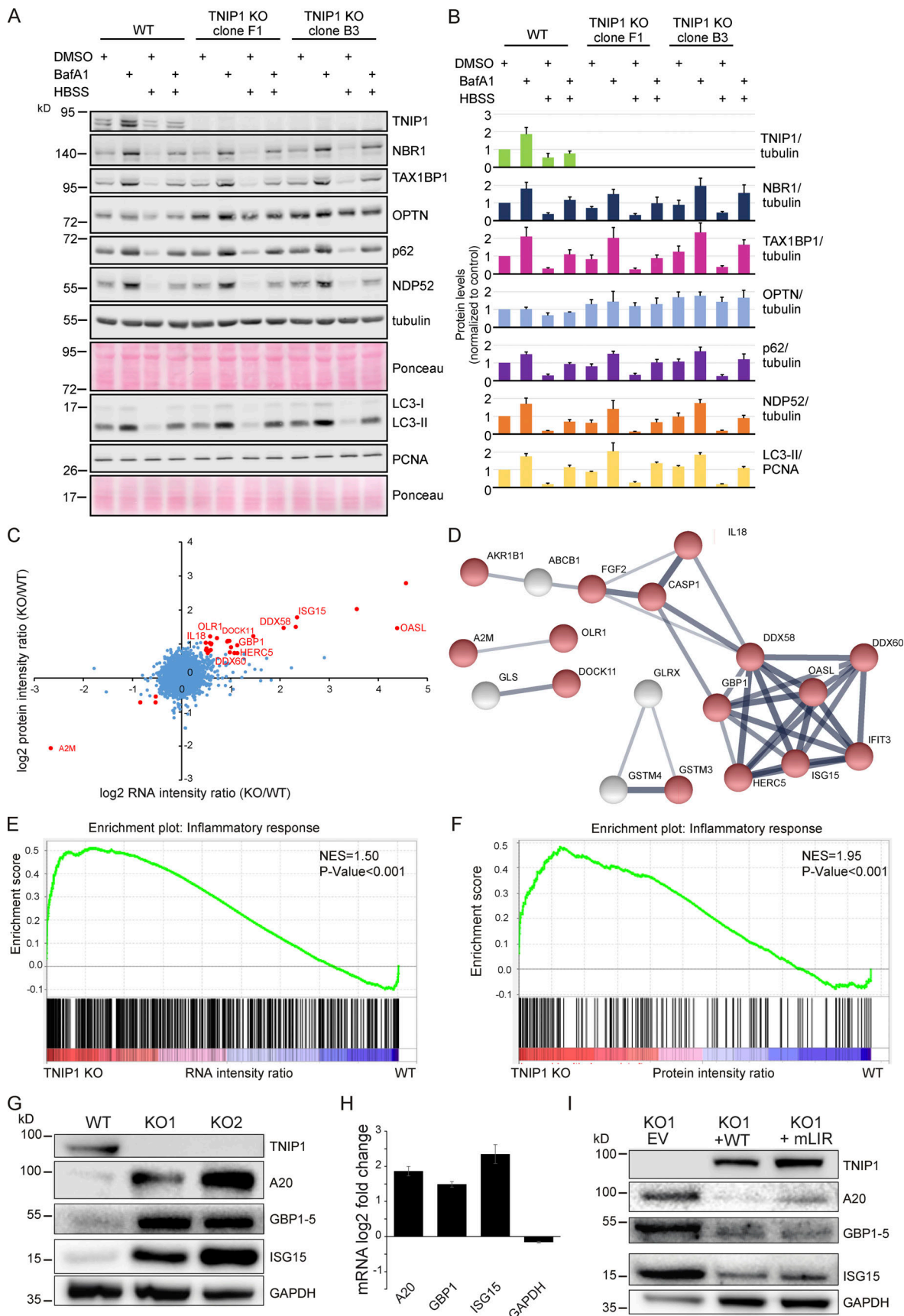


Figure 5. **Loss of TNIP1 leads to an increase in inflammatory proteins.** (A) Loss of TNIP1 does not alter autophagy flux under basal and starvation conditions. TNIP1 knock out HeLa cells generated by CRISPR/Cas9 were used to study its effect on autophagy. Wild-type HeLa cells and the two TNIP1

knockout clones denoted KO1 and KO2 were kept in either fed or starved (HBSS) conditions and treated with either vehicle (DMSO) or BafA1 for 8 h. Blots were probed for several known SLRs as well as LC3. **(B)** Quantification of blots shown in A ($n = 3$). Error bars indicate SD. **(C)** Loss of TNIP1 leads to an increased transcription of inflammatory genes. Fold changes of RNA and protein intensities of TNIP1 KO and WT cells were compared. Shown are average values of two KO clones compared to WT cells ($n = 3$ per cell type for RNAseq; $n = 5$ per cell type for proteomics). Genes that were significantly regulated on RNA and protein level are highlighted in red ($P < 0.01$). Genes linked to immune effector processes and interferon-stimulated genes are annotated. **(D)** Protein-protein interactions of significantly regulated proteins. Proteins highlighted in red in C were analyzed on known interactions using STRING DB (Szklarczyk et al., 2019). Interactions between 17 proteins were identified, of which 13 are linked to stress response (marked in red). Thickness of edges indicate confidence of interaction. **(E and F)** Gene set enrichment analysis of significantly dysregulated mRNAs and proteins identifies an increased transcription and translation of genes involved in inflammation. NES denotes normalized enrichment score. **(G–I)** TNIP1 represses translation of pro-inflammatory gene products. Whereas knockout of TNIP1 led to an increased abundance of indicated inflammatory proteins (G), which is likely due to transcriptional changes (H, $n = 3$, error bars indicate SEM), re-expression of TNIP1^{WT} or TNIP1^{mLIR1+2} blunted this phenotype (I). Source data are available for this figure: SourceData F5.

inflammatory and autoimmune diseases. This indicates that the lack of removal of damaged organelles may indirectly promote tissue destabilizing pro-inflammatory signaling. Autophagy may also contribute on a direct molecular level to limit excessive inflammatory signaling, e.g., by the selective degradation of inflammasome components by SARs, such as p62/SQSTM1 (Shi et al., 2012). Furthermore, by removing other endogenous pro-inflammatory sources including damaged organelles and components from viral and bacterial infections, SARs play an important role in anti-inflammatory responses (Deretic, 2021). The pro-inflammatory functions of autophagy were so far limited to its contribution to interleukin secretion and to senescence-associated inflammation (Dupont et al., 2011; Lee et al., 2021; Zhang et al., 2015). In the current article, we highlight that the role of autophagy in inflammation appears to be more complex than anticipated and that both processes appear to be more intimately intertwined on a molecular level.

As TNIP1 has no reported enzymatic activity itself, it was believed that its functions in inflammation were directly linked to its interaction with TNFAIP3 (also known as A20), a ubiquitin-editing enzyme that contains both ubiquitin ligase and deubiquitinase activities and that was shown to negatively interfere with NF- κ B signaling (Shamilov and Aneskievich, 2018; Song et al., 1996). Several recent studies, however, indicate that TNIP1 itself may function as a key repressor of inflammatory signaling, its dysregulation being linked to hyperinflammatory diseases like psoriasis (Nair et al., 2009), systemic lupus erythematosus (Gateva et al., 2009), systemic sclerosis (Allanore et al., 2011), and senescence (Lee et al., 2021). TNIP1 is thus a potential target for the design of anti-inflammatory therapeutics. It has also been suggested that TNIP1 can function by out-competing other pro-inflammatory mediators for polyubiquitin binding, thereby negatively affecting inflammatory signaling (Shamilov and Aneskievich, 2018).

Whereas single nucleotide polymorphisms were shown to alter TNIP1 expression and microRNAs to decrease TNIP1 mRNA levels (Shamilov and Aneskievich, 2018), posttranslational mechanisms regulating TNIP1 protein abundance are largely unknown. We and others localized TNIP1 to autophagosomes, but did so far not address underlying mechanisms and phenotypical consequences (Mejlvang et al., 2018; Shinkawa et al., 2022; Zellner et al., 2021). In the current study, we corroborate observations that TNIP1 can be regarded as a substrate for constitutive autophagosomal degradation. We did not identify changes in autophagy-dependent lysosomal degradation under fed and starved conditions, as well as under blocked mTORC1

signaling. The association of TNIP1 with SLRs and its colocalization with p62 bodies and LC3 puncta further supports this interpretation, indicating that ubiquitination of TNIP1 and direct protein-protein interactions lead to SLR-dependent lysosomal degradation (Fig. 8). Indeed, we could show that TNIP1 was still ubiquitinated even after mutating the two ubiquitination sites identified in this study. This is in agreement with www.phosphosite.org, which lists 11 ubiquitination sites of TNIP1, Lys389 being one of them (Akimov et al., 2018). In addition, also non-modified TNIP1 could be stabilized by lysosomal inhibition. Thus, TNIP1 appears to be constitutively degraded by autophagy, the role of ubiquitination being not entirely clear.

Interestingly, this changes under inflammatory conditions. Poly(I:C) treatment led to SLR-independent, selective removal of TNIP1 by autophagy dependent on its LIR motif. This suggests the existence of distinct TNIP1 pools within cells: non-modified TNIP1, phosphorylated and/or ubiquitinated TNIP1 (Fig. 8). This interpretation is supported by the observation that TNFAIP3 appeared to not be degraded by autophagy in a poly(I:C)-dependent manner, indicating that the pool of TNIP1 which interacts with TNFAIP3 under these conditions is also spared from degradation (see Fig. S4 A). The time-dependent regulation of TNIP1 protein levels indicates that autophagy-dependent degradation within the first 4 h of poly(I:C) treatment contributes to the establishment of a robust inflammatory response. At 6 h, TNIP1 levels rise again due to transcriptional upregulation starting already at 4 h. This regulation occurs to prevent excessive inflammatory signaling, which may lead to cell and tissue damage. In light of the model suggesting that TNIP1 can compete with pro-inflammatory proteins for ubiquitin binding (Shamilov and Aneskievich, 2018), it is possible that TNIP1 is degraded during the early stages of TLR3-activation to prevent this competition. The subsequent increase in TNIP1 at later stages of the signaling response could then be to outcompete other pro-inflammatory mediators in order to limit excessive signaling. In a recent study, OPTN was characterized as a direct, ubiquitination-independent binding partner of TNIP1 contributing to the specific, autophagy-dependent degradation of TNIP1 in senescent cells (Lee et al., 2021). The pathway characterized by us is different as TNIP1 degradation under inflammation conditions appears as SLR-independent (Fig. 8). OPTN and TNIP1 appear to function in parallel and to be positively linked on the transcriptional level since TNIP1 KO led to an upregulation of OPTN mRNA and protein levels, potentially in a compensatory fashion.

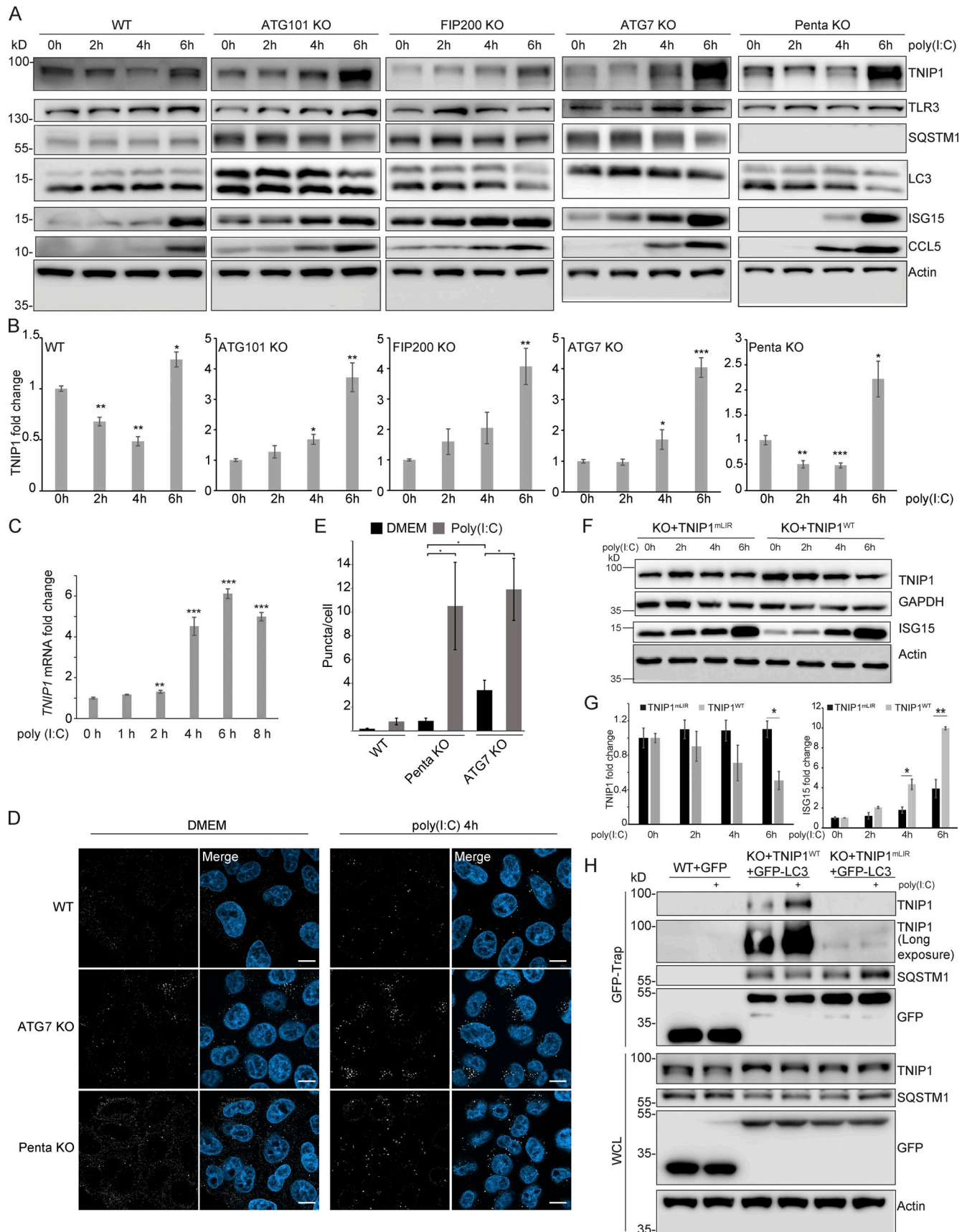


Figure 6. **Poly(I:C) stimulation induces LIR-dependent, specific degradation of TNIP1 by autophagy.** (A) Poly(I:C) treatment leads to time-dependent changes in TNIP1 abundance. Poly(I:C) stimulation leads to an autophagy dependent and SLR independent decrease of TNIP1 abundance within the first 4 h as

indicated by a block of degradation in ATG101, FIP200 and ATG7 KO cells. Autophagy receptors appear to have a minor influence as degradation still occurs in pentaKO cells. **(B)** Quantification of blots shown in A ($n = 3$). Error bars indicate SEM. * = $P < 0.05$, ** = $P < 0.01$, *** = $P < 0.001$ unpaired, two-sided t test compared to 0 h values of respective cell lines. **(C)** After 2–4 h of poly(I:C) treatment TNIP1 transcription is significantly upregulated. Bar diagrams show quantification of three biological replicates ($n = 3$), error bars: SEM. * = $P < 0.05$, ** = $P < 0.01$, *** = $P < 0.001$; unpaired, two-sided t test. **(D)** Representative immunofluorescent images showing endogenous TNIP1 response to poly(I:C) in WT, ATG7 KO, and pentaKO. Cells were either left untreated or treated with 5 $\mu\text{g/ml}$ poly(I:C) for 4 h. Scale bar = 10 μm . **(E)** Quantification of images shown in D, error bars indicate SEM. * = $P < 0.05$, unpaired two-sided t test. **(F and G)** The degradation of TNIP1 depends on functional LIR motifs. TNIP1 WT is degraded in a time-dependent fashion after poly(I:C) stimulation. The double LIR mutant TNIP1 (LIR1+2, TNIP1^{mLIR}) is spared from degradation. Note: Protein amounts of TNIP1 and ISG15 correlate inversely. Due to ectopic expression of TNIP1 variants regulation based on transcriptional/translational control as shown in A is lost. E shows quantification of blots exemplified in D ($n = 3$). Error bars indicate SEM. * = $P < 0.05$, unpaired, two-sided t test. KO1 cells were used for reconstitution. **(H)** Poly(I:C) induces a LIR-dependent interaction with LC3. Indicated HeLa cells expressing GFP-LC3 were used for anti-GFP AP. Cells expressing TNIP1^{mLIR} do not exhibit an increased interaction between TNIP1 and GFP-LC3 after poly(I:C) treatment, in contrast to cells expressing TNIP1^{WT}. KO1 cells were used for reconstitution. In B, C, E, and G, data distribution was assumed to be normal, but this was not formally tested. Source data are available for this figure: SourceData F6.

The canonical core LIR motif has the consensus sequence W/F/Y-X₁-X₂-L/I/V. The W/F/Y and the L/I/V occupy two hydrophobic pockets of the LIR docking site (LDS) of ATG8 family proteins. Additionally, acidic residues N-terminal, within and C-terminal, to the core motif, as found in the main LIR2 of TNIP1, increase binding affinity to the LDS which has a largely basic surface surrounding the two hydrophobic pockets (reviewed in Johansen and Lamark, 2020). The presence of serine or threonine residues N-terminal to the core motif which can be phosphorylated to increase the acidic nature of the LIR is a neat strategy for a switchable LIR-LDS interaction. It has been shown for a number of SARs, including OPTN and several mitophagy receptors, that phosphorylation of N-terminal residues flanking the core LIR enhances the LIR-LDS interaction (Di Rita et al., 2018; Rogov et al., 2017; Wild et al., 2011; Wu et al., 2014; Zhu et al., 2013). This is also found for Beclin1, VPS34, and SCOC LIR-ATG8 interactions (Birgisdottir et al., 2019; Wirth et al., 2021). In the case of OPTN, the LIR-proximal phosphorylation is mediated by TBK1, leading to the enhanced binding of OPTN to LC3 (Wild et al., 2011). In this study, we show that upon TLR3-activation, TNIP1 is phosphorylated at residues N-terminal to its main LIR-motif. Similar to OPTN, TNIP1 phosphorylation N-terminal of LIR2 enhances the interaction of TNIP1 with human LC3B. In vitro, phosphomimic S122E/S123E mutations of TNIP1 led to a strong increase in the binding to all of the human LC3 and GABARAP proteins, further supporting that LIR2 of TNIP1 is regulated by phosphorylation. Whether phosphorylation also influences the ubiquitination status of TNIP1 is currently not known, and a potential crosstalk between the two PTMs will have to be addressed in future studies.

During revision of our article, TNIP1 was reported as a potential SLR acting in the lipopolysaccharide (LPS)- and TLR1/TLR2-dependent degradation of MYD88 and IRAK1 (Shinkawa et al., 2022). In contrast to our data, this group reported LIR1 of murine TNIP1 as being responsive to TLR1/TLR2 activation by LPS (Shinkawa et al., 2022). In another very recent study, TNIP1 was shown to negatively interfere with mitophagy by interfering with ULK1 complex dynamics (Le Guerroue et al., 2022 Preprint). In accordance with our results, these authors reported that LIR2 mutation abolished all binding to ATG8 proteins, while LIR1 mutations had no effect on binding. As we noted, LIR2 is conserved in vertebrate evolution down to cartilaginous fishes, while LIR1 is only conserved down to marsupials (Fig. 4 A).

Our results strongly suggest that TBK1 is responsible for phosphorylation of the LIR2 proximal TSS motif. TBK1 is an important kinase in response to innate antiviral signaling. Upon TLR3-activation, TBK1 gets activated through TRIF and TRAF3 leading to the phosphorylation and activation of IRF3 and induction of type I interferons (Louis et al., 2018). TRIF itself may undergo autophagy-dependent degradation (Gentle et al., 2017; Inomata et al., 2012; Lim et al., 2019; Samie et al., 2018). How this anti-inflammatory effect of autophagy is coordinated with the described pro-inflammatory acting degradation of TNIP1 will be an interesting question to address in the future studies. TBK1 is also implicated in the regulation of autophagy and is known to phosphorylate several autophagy proteins (Oakes et al., 2017). It is possible that TBK1 promotes TNIP1 degradation in order to ensure the efficient activation of downstream interferon signaling. Our results indicate that TNIP1 may rely on the other SLRs for its basal turnover in unstimulated cells, but upon TBK1 activation in response to innate immune stimuli, the selective degradation of TNIP1 is promoted (Fig. 8). Interestingly, TNIP1 fulfills all characteristics of a SAR, having a UBD, LIR motif, and coiled-coil regions supporting multimerization. TLR1/2-induced degradation of TNIP1 was shown to mediate the degradation of MYD88 and IRAK1 (Shinkawa et al., 2022). Whether TLR3-activation leads to selective TNIP1-dependent degradation of specific cargo proteins will have to be addressed in future studies. The knockout of TNIP1 resulted in a basal increase in the expression and protein levels of several pro-inflammatory genes, even in the absence of pro-inflammatory signaling. This suggests that TNIP1 may have a role in preventing the induction of an inflammatory response even in untreated cells. Whether this is caused by TNIP1-mediated selective degradation of pro-inflammatory-mediators or -complexes will also be important to address in future studies.

Taken together, we identified TBK1-dependent phosphorylation sites immediately N-terminal to the core LIR motif of TNIP1 that lead to its selective degradation by autophagy under inflammatory conditions. Autophagy may contribute to the establishment of a potent inflammatory response before it limits excessive cytotoxic inflammatory signaling. Thus in addition to cancer, inflammation is another condition in which autophagy may have a dual role either supporting or inhibiting underlying processes depending on the exact cell state and timing.

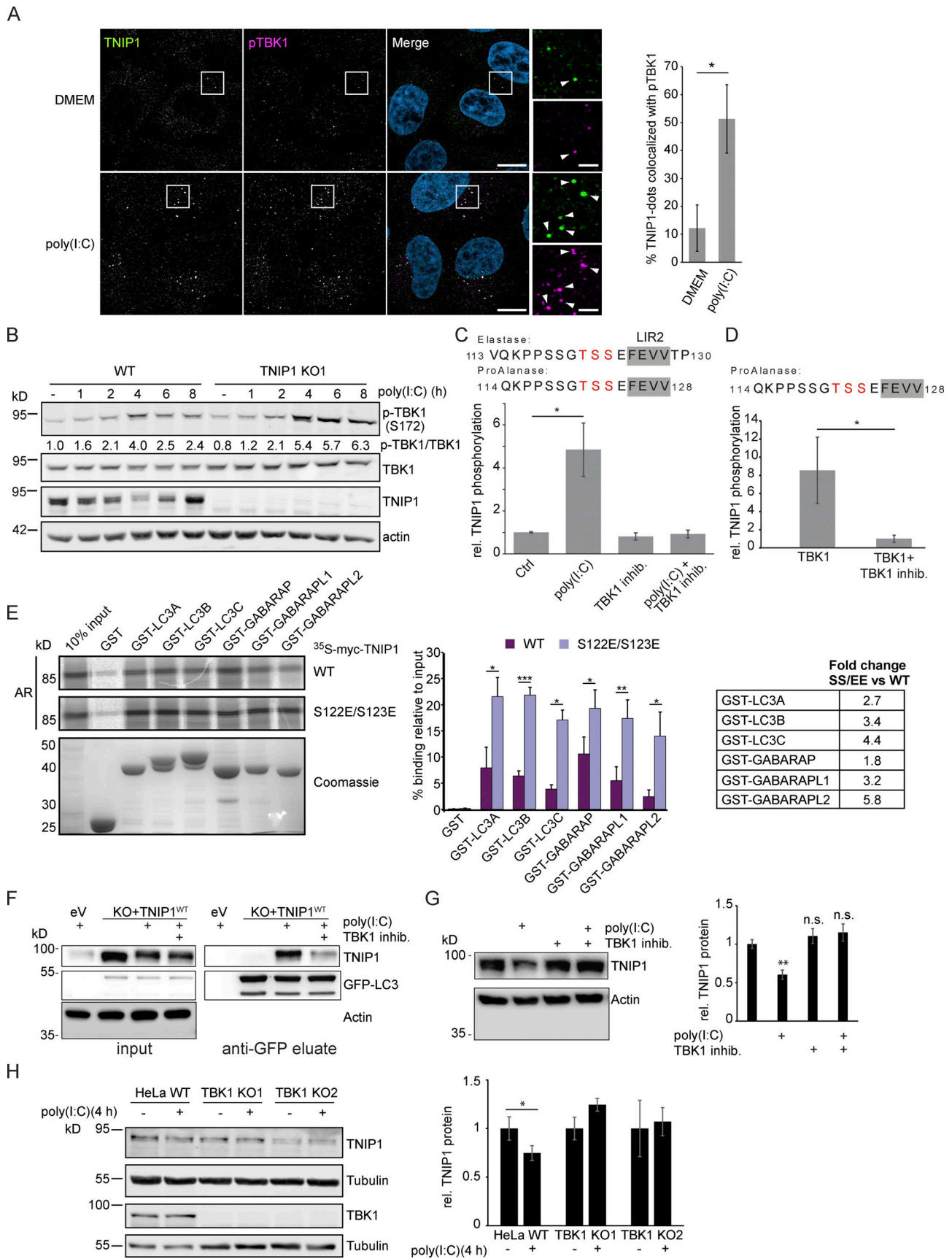


Figure 7. **Poly(I:C) stimulation induces TBK1-dependent, specific degradation of TNIP1 by autophagy.** (A) Immunofluorescence images showing co-localization between TNIP1 and pTBK1 upon poly(I:C) treatment. Cells were either left untreated or treated with 5 μ g/ml poly(I:C) for 4 h, and subsequently

stained for endogenous TNIP1 and pTBK1. Colocalization between TNIP1 and pTBK1 is indicated by arrowheads. Quantification of TNIP1 dots colocalizing with pTBK1 was done using Volocity software (PerkinElmer). Around 160–220 cells were counted for each condition in each independent experiment ($n = 3$). * = $P < 0.05$, unpaired two-sided t test. Error bars indicate SD. Scale bar in overview image is 10 μm , and scale bar in insert is 2 μm . **(B)** Time-course effect of poly(I:C) treatment on TBK1 activation and TNIP1. Representative blot and the corresponding quantification of the relative pTBK1 over total TBK1 levels are shown. **(C and D)** TBK1 phosphorylates TNIP1 N-terminal of LIR2. **(C)** In vivo phosphoproteomics using Elastase or ProAlanaase as proteolytic enzymes identified indicated phosphopeptides. The single phosphorylation site could not be unambiguously localized to one of the three amino acid residues highlighted in red. Inhibition of TBK1 blocked the respective phosphorylation event ($n \geq 3$). **(D)** In vitro kinase assay using purified TBK1 and TNIP1 coupled to phosphoproteomics indicates that TBK1 directly phosphorylates TNIP1 on one of the amino acid residues highlighted in red. * = $P < 0.05$, unpaired two-sided t test. Error bars indicate SEM. **(E)** In vitro GST-pulldown assay using ^{35}S -labeled myc-TNIP1 and myc-TNIP1-S122E/S123E against recombinant GST and GST-tagged human ATG8s. Bound myc-TNIP1 WT and S122E/S123E was detected using autoradiography (AR). Quantification and fold change of $n = 3$, * = $P < 0.05$, ** = $P < 0.01$, *** = $P < 0.001$; unpaired two-sided t test. Error bars indicate SD. **(F)** The interaction between TNIP1 and LC3B is regulated by TBK1. GFP-LC3B is purified using GFP trap beads. Bound TNIP1 is detected by Western blot. Inhibition of TBK1 by MRT67307 negatively regulates the poly(I:C)-dependent interaction of TNIP1 with LC3. KO1 cells were used for reconstitution. **(G)** Inhibition of TBK1 negatively interferes with poly(I:C)-dependent degradation of TNIP1. Western blots of whole cell lysate indicate TNIP1 stabilization by TBK1 inhibition. Actin was used as loading control ($n = 3$). Error bars indicate SEM. ** = $P < 0.01$, unpaired, two-sided t test. **(H)** TBK1 KO negatively interferes with poly(I:C)-dependent degradation of TNIP1. Western blots of whole cell lysate indicate TNIP1 stabilization by TBK1 KO in two independent cell lines. Tubulin was used as loading control ($n = 3$). Error bars indicate SD. ** = $P < 0.01$, unpaired, two-sided t test. In A, C, D, E, G, and H, data distribution was assumed to be normal, but this was not formally tested. Source data are available for this figure: SourceData F7.

Materials and methods

The reagents, antibodies, and plasmids used in this study are listed in Tables S4, S5, and S6, respectively.

Cell culture and cell treatments

HeLa cells and HEK293T cells were obtained from ATCC. U2OS cells were obtained from ECACC. StUbEx U2OS cells were a gift

from Blagoy Blagoev (Department of Biochemistry and Molecular Biology, University of Southern Denmark, Odense, Denmark; Akimov et al., 2014). HeLa CCL2.2, HeLa CCL2.2 ATG7 KO cells, and HeLa CCL2.2 pentaKO cells were a gift from Richard J. Youle (National Institutes of Health, Bethesda, MD; Sarraf et al., 2020). HeLa p62 KO cells have been described previously (Abudu et al., 2021). All cells were maintained in Dulbecco's

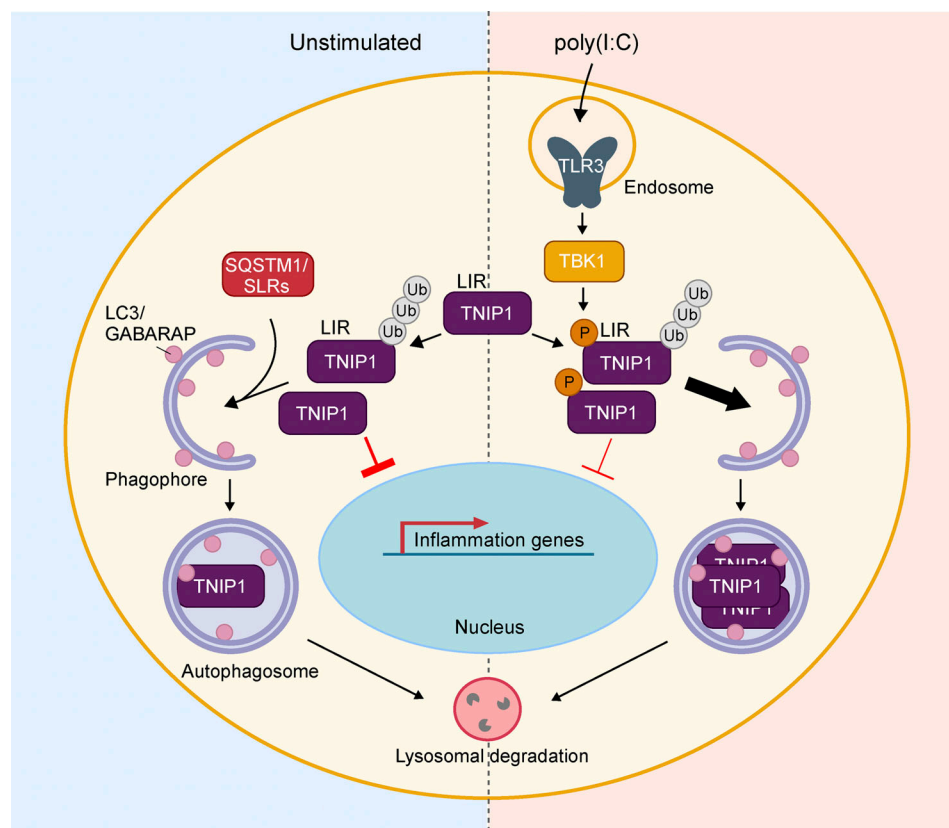


Figure 8. Model of TNIP1 regulation. Under basal, unstimulated conditions (left panel), TNIP1 functions as a negative regulator of inflammatory signaling and is subject to constitutive autophagic degradation through interaction with autophagy receptors such as p62/SQSTM1. Upon poly(I:C)-induced activation of TLR3 (right panel), activated TBK1 phosphorylates TNIP1 in the vicinity of its LIR, increasing TNIP1 affinity for human LC3 and GABARAP proteins. This, in turn, leads to a LIR-dependent increase in TNIP1 degradation through selective autophagy. The removal of TNIP1 relieves the negative effect on inflammatory signaling, allowing the establishment of a robust inflammatory response upon antiviral signaling.

modified Eagle's medium (DMEM) supplemented with 10% fetal calf serum, 2 mM L-glutamine, and 100 U/ml penicillin/streptomycin. For starvation experiments, cells were incubated with Hanks' Balanced Salt solution (HBSS) for the indicated times. Cells were treated with 100 nM rapamycin, 200 nM bafilomycin A1, 5 µg/ml Concanamycin A, 20 µg/ml cycloheximide, or 10 µM MG132, for the indicated time periods. For SILAC, cells were grown for >14 d in SILAC DMEM supplemented with dialyzed fetal calf serum, 2 mM L-glutamine, 100 U/ml penicillin, and "light" ($^{12}\text{C}_6^{14}\text{N}_2$ -Lysine and $^{12}\text{C}_6^{14}\text{N}_4$ -Arginine), "medium" (D_4 -Lysine and $^{13}\text{C}_6$ -Arginine), or "heavy" ($^{13}\text{C}_6^{15}\text{N}_2$ -Lysine and $^{13}\text{C}_6^{15}\text{N}_4$ -Arginine) stable isotope-labeled amino acids. For transient DNA transfection, subconfluent cells were transfected using TransIT LT1 transfection reagent according to the manufacturer's instructions.

Plasmid constructs

Plasmids used in this study are listed in Table S4. Cloning into pDest-vectors was performed using the Gateway cloning system (Invitrogen). QuickChange site-directed mutagenesis kit (Stratagene) was used to create desired point mutations, which were verified by DNA sequencing (BigDye Sequencing kits, Applied Biosystems). Oligonucleotides for mutagenesis and sequencing were from Invitrogen. TNIP1 cDNA was obtained from Genscript (NM_001252390), TNIP1 LIR mutation fragment was synthesized by IDT gBlocks Fragments (Integrated DNA Technologies). TNIP1 and TNIP1_mLIR were cloned into pDONR201 and pLenti CMV Blast DEST (706-1) by Gateway recombination cloning according to manufacturer's instructions. All plasmid constructs were verified by sequencing (BigDye; Applied Biosystems) and/or restriction digestion.

Generation of knockout (KO) and stable cell lines

The TNIP1 KO cells were generated by CRISPR/Cas9-mediated genome-editing tools provided by the F. Zhang laboratory (Broad Institute, MIT, Boston, MA). A target sequence in exon twenty of human TNIP1 was selected (sgTNIP1-1, 5'-CGTACCGATCTACGACCCT-3'; sgTNIP1-2, 5'-GGCCCTGGAGTTCAA CCGAC-3'; sgTNIP1-3, 5'-CACCCGACAGCGTGAGTACC-3'). The sgRNA oligos were cloned into the Bbs1 site of hSpCas9 plasmid. Lipofectamine LTX and Plus reagent (15338100; Invitrogen) were used to transfect hSpCas9-sgRNA into HeLa cells according to the manufacturer's instructions. Cells were selected with 2 µg/ml puromycin for 2 d and single cells were isolated by serial dilutions. TNIP1 deficiency was screened by immunoblotting.

CRISPR knockout of FIP200 and ATG101 in HeLa cells was performed using sgRNAs cloned into the plasmid pX330-U6-Chimeric_BB-CBh-hSpCas9 (#42230; Addgene): ATG101, 5'-ACCAGAAGAAGAAGTCTCGC-3' and 5'-GTTATCCACCTCCGACTGTG-3'; FIP200, 5'-GTAGTTTTAGGAATAGCAGG-3'. CRISPR plasmids and pEGFP-puromycin plasmid were co-transfected in HeLa cells using lipofectamine LTX reagent (15338030; Thermo Fisher Scientific), according to manufacturer's instructions. 24-h post-transfection, co-transfected cells were selected in culture medium supplemented with 3 µg/ml puromycin (Invivogen, ant-pr-1). Efficiently transfected cells were isolated to generate clonal lineages by single-cell cloning in 96-well plates; colonies

were all evaluated for KO efficiency by Western blotting against the targeted protein. The sgRNAs were designed using CHOP-CHOP CRISPR/gRNA algorithm (Labun et al., 2019).

Generation of HeLa CCL2.2 cells KO for OPTN and TAX1BP1 and HeLa KO for TBK1 was carried out as described previously (Abudu et al., 2021). The following gRNAs were used: sgOPTN: 5'-CCGACGAGAACAGTCTCCAC-3', sgTAX1BP1: 5'-AGACCTGCA TACTGCACGCT-3', sgTBK1: 5'-AACGTGGATGTACTTTAGGG-3'.

For generation of stable cell lines, lentiviral vectors were co-transfected with packaging (psPax2) and envelope plasmids (pMD2.G) in HEK293T cells using jetPRIME reagent (Polyplus transfection). Medium was changed to fresh DMEM 15 h after transfection. After 24 h incubation, the supernatant was harvested by filtration through 0.22-µm filter. Polybrene (8 µg/ml) was added before infection of recipient cells. To obtain stable cell lines, infected cells were cultured in the presence of 5 µg/ml blasticidin for 1 wk and monitored by immunoblotting.

Enrichment of ubiquitinated peptides

Ubiquitinated peptides were purified according to Akimov et al. (2018). Triple SILAC labeled U2OS and HeLa cells were treated with DMSO, Rapa, and Rapa + ConA. Cells were washed twice with cold PBS and lysed with 12 ml lysis buffer (8 M guanidine-HCl, 25 mM ammonium bicarbonate [ABC], pH 8.5). The lysates were sonicated to reduce viscosity and cleared by centrifugation at 15,000 RCF for 30 min. Protein concentration was determined by BCA protein assay kit (23225 and 23227 Pierce), and the same amount of proteins of each label were mixed. Proteins were reduced with 2 mM DTT for 30 min at room temperature and alkylated with 11 mM chloro acetamide in the dark for 30 min at room temperature. The concentration of guanidine-HCl was diluted to 2 M with 25 mM ammonium bicarbonate and filtrated with low binding 0.45-µm PVDF filters (Millipore). The Lys-C endopeptidase was added at a 1:100 enzyme-to-protein ratio to digest proteins at room temperature overnight. The peptide mixture was cleaned and purified using C18 cartridges (WATERS) and lyophilized for 24–36 h. The lyophilized peptides were dissolved in 12 ml of IAP buffer (50 mM MOPS, pH 7.2, 10 mM sodium phosphate, 50 mM NaCl, pH 7.5–8.0) plus 0.1% Triton X-100. Dissolved peptides were spun down and passed through low binding 0.45-µm PVDF filters and incubated with 500 µl of UbiSite conjugated matrix for 5 h at 4°C. The UbiSite matrix was washed three times with IAP buffer without detergent and three times with 150 mM NaCl. After the third wash, the matrix was transferred to a small Poly-Prep column (Bio-RAD). Enriched peptides were eluted with 250 µl 0.1% TFA three times, and each time incubated for 5 min. The eluted peptides were pooled and neutralized with 1 M ABC buffer to a final concentration at 25 mM, followed by trypsin digestion overnight at 37°C. The fractionation of tryptic peptides was performed as described previously (Akimov et al., 2018). The resulting peptides were lyophilized and cleaned by STAGE-tips.

Enrichment of ubiquitinated proteins by StUbEx

StUbEx U2OS cells were induced with doxycycline for 48 h and treated with Rapa and lysosomal degradation was blocked with

ConA. The cells were washed with cold PBS and lysed with binding buffer (6 M Guanidinium-HCl, 50 mM Na₂HPO₄/NaH₂PO₄, pH 8.0, 500 mM NaCl, 5 mM imidazole). Sample viscosity was reduced by sonication followed by centrifugation at 11,000 RCF for 30 min at room temperature. Protein concentration was determined by BCA assay. Ubiquitin conjugates were purified by cOmplete His-tag purification beads (Roth) for 4 h at room temperature, followed by washes with binding buffer and washing buffers 1–3 (WB1—8 M Urea, 50 mM Na₂HPO₄/NaH₂PO₄, pH 8.0, 500 mM NaCl, 0.1% Triton-X-100; WB2—same as WB1 but with 0.2% Triton X-100; WB3 -8 M Urea, 25 mM Tris, pH 8.0, 150 mM NaCl). The ubiquitin conjugates were finally eluted with three times elution buffer (150 mM NaCl, 50 mM Tris, pH 8.0, and 300 mM imidazole).

Immunoblotting

For immunoblot analysis, treated cells were harvested and lysed in modified RIPA buffer supplemented with 2% SDS and 0.1% benzonase Nuclease or 1× SDS buffer (50 mM Tris, pH 6.8, 2% SDS, and 10% glycerol). For cells harvested in modified RIPA buffer, lysates were centrifuged for 15 min at 11,000 RCF. For cells harvested in 1× SDS buffer, lysates were incubated at 100°C for 10 min. Protein concentration was measured using Pierce BCA Protein Assay Kit. Quantified cell lysates or AP elutes were either reduced with 2 mM DTT at 75°C for 10 min or 100 mM DTT at 100°C for 10 min and resolved on SDS-PAGE gels. Proteins were transferred to a PVDF or nitrocellulose membrane, and subsequently prepared for either fluorescent or chemiluminescent detection. For fluorescent detection, membranes were blocked in Intercept (PBS or TBS) Blocking Buffer, followed by overnight incubation at 4°C with primary antibody. Membranes were subsequently washed 4× in PBS or TBS containing 0.1% Tween (PBS-T/TBS-T), followed by incubation with secondary antibody diluted in Intercept Blocking Buffer. After 4× wash in PBS-T/TBS-T, a final wash was carried out in PBS/TBS without Tween. Fluorescent signal was detected using LiCOR Odyssey CLx imaging system. Chemiluminescent detection: membranes were blocked in either 5% milk or 5% bovine serum albumin in PBS-T or TBS-T, followed by incubation with primary antibody. Membranes were washed 3–4× in PBS-T/TBS-T followed by incubation with secondary antibody. After 3–4× washes in PBS-T/TBS-T, membranes were developed using SuperSignal West Pico Chemiluminescent Substrate on GE Fujifilm LAS4000 Luminescent image analyzer or Odyssey Fc reader (LI-COR Biosciences-GmbH). The densitometry of immunoblotting was performed by either ImageJ (National Institutes of Health) or ImageStudio software (LI-COR Biosciences-GmbH).

Immunofluorescence staining and confocal fluorescence microscopy

For imaging, cells were grown on #1.5 round 12-mm coverslips (#631-0150; VWR) for immunofluorescence staining or 8-well Lab-Tek chamber coverglass for double-tag analysis (#155411; Thermo Fisher Scientific), and fixed with 4% formaldehyde in PBS for 30 min. For immunofluorescence staining, cells were washed 3× with PBS and then permeabilized with either 0.1% Triton X-100 in PBS for 10 min, or ice-cold methanol for 10 min.

Next, cells were washed 5× with PBS or TBS, and blocked for 1 h in 5% BSA in PBS or TBS. Subsequently, cells were incubated with primary antibodies diluted in 1% BSA in PBS or TBS for 1–2 h at room temperature. After 5× wash in PBS or TBS, cells were incubated with Alexa Fluor secondary antibodies diluted in 1% BSA in PBS or TBS for 1 h at room temperature. After 5× wash in PBS or TBS, cell nuclei were stained with 1 µg/ml DAPI diluted in PBS for 5 min, followed by 2× final washes in PBS or TBS. Coverslips were mounted using ProLong Gold or ProLong Glass Antifade Mountant. Cells were imaged using Zeiss LSM800 or LSM880 (Carl Zeiss Microscopy) using a 63 × NA1.4 oil immersion lens for coverslips or a 40× NA1.2 water immersion lens for chambered coverglass. Images were collected in ZEN software (Zeiss). For Airyscan super-resolution images, optimal pixel size and z spacing as suggested by ZEN was used. Optimal excitation and emission settings were determined using the Smart Setup function. All fluorescence channels were recorded at non-saturating levels, and settings were kept identical between all samples within replicates used for comparisons or quantifications.

Image analysis

For quantification of red-only dots of mCherry-EYFP-TNIP1, transiently transfected cells with low expression of mCherry-EYFP-TNIP1 were visually selected and imaged. Cells with high levels of overexpression were excluded, as this resulted in the formation of large aggregates. All images within each replicate were taken using identical settings. For quantification of relative amounts of red-only dots versus total dots, mCherry and EYFP dot detection was performed using a custom-made measurement protocol using intensity thresholding, size exclusion, and noise filtering, based on signal intensity of the BafA1 control in Volocity software (PerkinElmer) ver. 6.3. The number of mCherry-only positive dots was counted by subtracting total EYFP dots from total mCherry dots for each experiment. For quantification of the number of cells positive for red-only mCherry-EYFP-TNIP1 dots, the images were analyzed manually by a subject that was blind to the analyzed conditions.

To quantify the number of TNIP1 dots and the colocalization between TNIP1 and SLRs/pTBK1, populations of objects representing fluorescent puncta in each channel were segmented using a custom-made protocol in Volocity ver. 6.3 (PerkinElmer). Detection of TNIP1, SLRs, and pTBK1 puncta was performed by intensity thresholding, size exclusion, and noise reduction. Overlap between TNIP1 and pTBK1 was identified by excluding TNIP1 objects not touching SLRs/pTBK1. The percentage of TNIP1 dots colocalizing with SLRs/pTBK1 was calculated by dividing the number of TNIP1 dots overlapping with SLRs/pTBK1 with the total number of TNIP1 dots. For line-profiles, the line-profile tool in Zen Blue software (Zeiss) was used to measure signal intensity across indicated lines.

SPOT synthesis and peptide array

TNIP1 peptide array was synthesized on cellulose membranes using MultiPrep peptide synthesizer (INTAVIS Bioanalytical Instruments AG). Membranes were blocked with 5% non-fat milk in TBS-T and peptide interactions were tested using GST-

GABARAP by overlaying the membrane with 1 $\mu\text{g}/\text{ml}$ recombinant protein for 2 h at room temperature. Membranes were washed three times in TBS-T. Bound GST-GABARAP was visualized with HRP-conjugated anti-GST antibody (Johansen et al., 2017). Putative LIR motifs in 20, 3 arrays (20-mer peptides moved a window of 3 residues along the protein sequence) were identified as 4–6 consecutive strong spots containing the core LIR consensus (W/F/Y)XX(L/I/V).

Recombinant protein production and GST-pulldown analysis

GST and GST-fusion proteins were expressed in *Escherichia coli* strain SoluBL21 (DE3; #C700200; Genlantis). Protein expression was induced by adding 50 $\mu\text{g}/\text{ml}$ isopropyl β -D-1-thiogalactopyranoside (IPTG). The bacterial cells were sonicated in lysis buffer (20 mM Tris-HCl, pH 7.5, 10 mM EDTA, 5 mM EGTA, 150 mM NaCl) and GST-fused proteins were immobilized on Glutathione Sepharose 4 Fast Flow beads (#17-5132-01; GE Healthcare) by incubating in a rotator at 4°C for 1 h. The beads containing GST-fusion proteins were subsequently used for pulling down in vitro translated proteins or cell lysates. For in vitro translated proteins, a pDest-myc-vector containing the protein of interest and a T7 promoter was used. In vitro translation was performed using the TNT T7 Reticulocyte Lysate System (Promega Corp.), in the presence of radioactive ^{35}S -methionine. In vitro translated protein was then precleared by incubation with empty Glutathione Sepharose beads in 100 μl of NETN buffer (50 mM Tris, pH 8.0, 150 mM NaCl, 1 mM EDTA, 0.5% NP-40) supplemented with cOmplete Mini EDTA-free protease inhibitor (Merck) for 30 min at 4°C. Precleared lysates were then incubated with GST-fusion protein bound beads for 1–2 h on a rotator at 4°C. Beads were then washed 5 \times with NETN-buffer, and resuspended in 2 \times SDS-PAGE gel loading buffer (125 mM Tris, pH 7.5, 4% SDS, 0.04% bromophenol blue, 20% glycerol, 100 mM dithiothreitol), boiled for 10 min, and resolved by SDS-PAGE. Gels were stained with Coomassie Brilliant Blue for protein visualization and then vacuum-dried. The radioactive signal was then detected on imaging plates with Fujifilm BAS-5000 (Fujifilm). Signals from ^{35}S -labeled proteins were measured in terms of unit of photostimulated luminescent (PSL) and quantified in comparison with 10% of the in vitro translated lysate (input) using the Image Gauge software (Fuji; Johansen et al., 2017).

Affinity purification

Cells were lysed in ice-cold modified RIPA buffer (25 mM Tris-HCl, pH 7.4, 150 mM NaCl, 1 mM EDTA, 1% NP-40, 0.1% Sodium deoxycholate) containing complete protease inhibitor cocktail and phosphatase inhibitor cocktail. Lysates were centrifuged for 15 min at 13,000 RCF and protein concentration was determined by BCA assay. GFP-tagged proteins were affinity purified by GFP-trap (ChromoTek) according to the manufacturer's instructions. HA-TNIP1 was affinity purified by anti-HA magnetic beads (Pierce). TNIP1 polyclonal antibody-coupled protein G dynabeads were used for affinity purification of endogenous TNIP1. For denaturing purification, the lysate was supplemented with 2% SDS and incubated for 30 min at room temperature to break protein-protein interaction, then diluted to 0.5% SDS with lysis buffer and incubated with HA or anti-TNIP1 antibody for affinity purification.

For TNIP1 interactome analysis by MS, HA-TNIP1 cells and empty vector cells were cultured in “heavy” and “light” SILAC medium, respectively. After 2 wk, cells were harvested and lysed in modified RIPA buffer containing complete protease inhibitor cocktail and phosphatase inhibitor cocktail. Protein concentration was determined by BCA assay, and protein amount was adjusted to equal concentration with lysis buffer, followed by affinity purification with anti-HA magnetic beads. The eluate of “heavy” and “light” samples was combined and fractionated by SDS-PAGE. Proteins were in-gel digested by trypsin and peptides were desalted by STAGE-tips prior to LC-MS/MS analysis.

Whole proteome analysis

For whole proteome analysis by MS, HeLa wild-type cells and TNIP1 KO cells were cultured in SILAC medium for 2 wk. Cells were harvested and lysed in modified RIPA buffer containing 2% SDS and 0.1% benzonase Nuclease. Protein concentration was determined by BCA assay and equal amounts of proteins in each label were mixed. Proteins were reduced with DTT and alkylated with IAA, followed with SDS-PAGE fractionation and trypsin in-gel digestion. Tryptic peptides were desalted by STAGE-tips prior LC-MS/MS analysis.

TNIP1 phosphorylation analysis

HA-TNIP1 cells were treated with poly(I:C) with or without TBK1 inhibitor MRT67307. Cells were harvested and lysed in modified RIPA buffer containing complete protease inhibitor cocktail and phosphatase inhibitor cocktail, 2% SDS was supplemented to break protein-protein interaction. The samples were diluted to 0.5% SDS with lysis buffer and subjected to affinity purification with anti-HA magnetic beads. After purification, the beads were transferred onto 10 kDa MW cut-off filter with 400 μl 8 M urea and 1 mM DTT. Proteins were digested by elastase or ProAlanaase using the FASP protocol (Wiśniewski et al., 2009). Digested peptides were eluted twice with 200 μl 50 mM ammonium bicarbonate into fresh tubes and acidified with TFA to a final concentration of 1%. Peptides were frozen and lyophilized prior to phosphopeptide enrichment. The lyophilized peptides were resuspended in 200 μl of 80% ACN, 0.1% TFA. Phosphopeptides enrichment was performed on Agilent AssayMAP Bravo platform according to manufacturer's instructions. The Agilent AssayMAP phosphopeptide enrichment v2.0 App was used for automated phosphopeptide enrichment using Fe (III)-NTA cartridges (Basel, Switzerland). Cartridges were primed with 100 μl of 50% ACN, 0.1% TFA using a high flow rate of 300 $\mu\text{l}/\text{min}$ and equilibrated using 80% ACN containing 0.1% TFA. Samples were loaded onto the cartridge using a low flow rate of 3 $\mu\text{l}/\text{min}$. The cartridges were washed twice with 200 μl 80% ACN containing 0.1% TFA and eluted with 50 μl of 1% ammonium hydroxide (pH 11) and 50 μl of 1% ammonium hydroxide in 80% ACN to a low-binding PCR tube containing 5 μl FA. The eluted peptides were lyophilized and resuspended in 20 μl of 0.1% FA for LC-MS/MS analysis.

In vitro kinase assay

HA-TNIP1 cells were harvested and lysed in ice-cold modified RIPA buffer containing complete protease inhibitor cocktail.

TNIP1 protein was enriched by anti-HA magnetic beads and dephosphorylated by lambda phosphatase with 1 mM MnCl₂ for 30 min at 30°C. Beads were washed with 2 × 10 ml of kinase buffer (50 mM Tris-HCl, pH 7.6, 10 mM MgCl₂, 150 mM NaCl and 1× PhosSTOP) to remove lambda phosphatase. Kinase buffer was added to a final volume of 800 μl with 1 μg TBK1 protein, for control sample, 10 μM TBK1 inhibitor MRT67307 was added. Kinase assays were performed on a rotor at 37°C for 1 h. Finally, reactions were quenched by addition of 8 M urea and 1 mM DTT. The beads were transferred onto 10 kD MW cut-off filter for the digestion with ProAlanaase, followed with phosphopeptide enrichment.

LC-MS/MS analyses

Solubilized peptides were injected into a 20 cm fused silica column with an inner diameter of 75 μm and in-house packed with C18 (ReproSil-Pur 120 C18-AQ, 1.9 μm, Dr. Maisch) for reverse phase fractionation by EasyLC 1200 nanoflow-HPLC system (Thermo Fisher Scientific). Peptides were loaded with solvent A (0.1% FA in water) at a max. pressure of 800 Bar and eluted with a step gradient of solvent B (0.1% FA in 80% ACN) from 2 to 25% within 85 min, from 25 to 60% within 5 min, followed by increasing to 100% in 2 min at a flow rate of 250 nl/min. MS/MS analysis was performed on a nano-electrospray ion source equipped QExactive HF-X mass spectrometer (Thermo Fisher Scientific). The spray voltage was set to 2.3 kV with a capillary temperature of 250°C. Mass spectrometer was operated in positive polarity mode and MS data were acquired in the data-dependent mode. The automatic gain control (AGC) target was set to 3 × 10⁶, the resolution was set to 120,000, and the ion injection time was set to 15 ms for the full scan at a mass range of $m/z = 370-1750$. 12 precursors were fragmented using normalized collisional energy (NCE) of 28 by higher-energy collisional dissociation (HCD). MS/MS scans were acquired with a resolution of 30,000, AGC target of 100,000 maximum IT of 54 ms, isolation window of 1.6 m/z , and dynamic exclusion window of 30 s. MS raw files were analyzed using MaxQuant software version 1.6.2.10 (Cox and Mann, 2008), data were searched against UniProt full-length homo sapiens database (21,033 entries, released March, 2016). Cysteine carbamidomethylation was set as a fixed modification, protein aminoterminal acetylation and methionine oxidation were set as variable modifications. Ubiquitination of lysine was set as a variable modification and digestion was specific to trypsin/P for Ubisite experiment. Serine-, threonine- and tyrosine-phosphorylation were set as a variable modification and digestion was set to unspecific or ProAlanaase for TNIP1 phosphorylation experiments. The analysis was carried out with “match-between-run” with a time window of 0.7 min. MaxQuant results were analyzed using Perseus (Tyanova et al., 2016).

Total RNA extraction and library construction

Four replicates of HeLa WT cells and TNIP1 KO cells (clone1 and clone2) were cultured in 10 cm dishes. The total RNA was extracted using RNeasy Mini Kit (Qiagen) according to the instructions of the manufacturer. Cells were lysed with 350 μl RLT buffer and homogenized by passing 5 times through a blunt 20-gauge needle. One volume of 70% ethanol was supplemented, the lysates were transferred to RNeasy spin column and

centrifuged at 8,000 × *g* to collect RNA. The RNA was washed once with 700 μl RW1 buffer and twice with 500 μl RPE buffer. After completely removing the RPE buffer, the RNA was eluted with 50 μl RNase-free water. The quality of RNA samples was analyzed by RNA screen tape (Agilent). The complementary DNA (cDNA) libraries were barcoded using Illumina primers and sequenced on one lane of an Illumina Novaseq 6000 instrument with 2 × 50 bp paired-end sequencing cycles. The sequence data were deposited at the European Nucleotide Archive (accession number: PRJEB45902). The output reads from multiple lanes were combined into single files and quality control was performed with FastQC v0.11.7 and cleaned with fastp v0.19.5 to removed polyG trails and keep only full-length reads (Chen et al., 2018). The human genome GRCh38.p13 (ENSEMBL) was used to remap the reads using STAR v2.5.3a (Dobin et al., 2013). The differential expression between WT and KO was analyzed by R software (R Core Team, 2014 <http://www.R-project.org/>) using the DESeq2 package (Love et al., 2014).

qRT-PCR

The total RNA were purified as above, 1 μg RNA was subjected to reverse transcription by Quantitect RT kit (Qiagen). Quantitative PCR was performed using the KAPA SYBR Fast (Universal) qPCR kit (Merck Millipore) according to the manufacturer’s recommendations. The qRT-PCR reaction was performed with a Rotor-GeneQ (Qiagen) and the same thermal profile conditions were set as 95°C for 10 min; then 40 cycles were performed of 10 s at 95°C, 20 s 60°C and 20 s 7°C. The following primer pairs were used: TNIP1 forward 5’-CTAGTGTGACGGCAGGTAAGG-3’, TNIP1 reverse 5’-GCTGCTTCATGGACCGGAA-3’; Actin forward 5’-GGACTTCGAGCAAGAGATGG-3’, Actin reverse 5’-AGCACTGTGTTGGCGTACAG-3’; HPRT1 forward 5’-TGACACTGGCAAACAATGCA-3’, HPRT1 reverse 5’-GGTCCTTTTCACCAGCAAGCT-3’; 18s rRNA forward 5’-CGGCGACGACCCATTGCAAC-3’, 18s rRNA reverse 5’-GAATCGAACCTGATTCCTCCGTC-3’.

Gene set enrichment analyses

Gene set enrichment analyses (GSEA) was performed using default setting weighted enrichment statics and signal2noise metric for ranking genes (Subramanian et al., 2005). Significantly regulated genes in transcriptome data and proteins in whole proteome data were listed in Table S3.

Quantification and statistical analyses

Significantly regulated ubiquitination sites were determined by two samples paired *t* test, FDR < 0.05, S0 = 0.1. In all other cases unpaired, two-sided *t* tests were used unless stated otherwise. In general, parametric test were used, and data distribution was assumed to be normal, but this was not formally tested. The interactome network was generated by the String database. The statistical analyses including standard deviations, error bars, and P values were performed using Excel (Microsoft), all the details were indicated in figure legends.

Online supplemental material

Fig. S1 shows TNIP1 gets ubiquitinated and degraded in the lysosome. Fig. S2 shows TNIP1 localizes to autophagosomes. Fig. S3

shows endogenous TNIP1 interacts with TAX1BP1 and p62/SQSTM1 under basal conditions. Fig. S4 shows regulation of TNIP1 protein abundance. Table S1 shows UbiSite-proteomics approach to identify ubiquitination sites on proteins being potentially involved in autophagy. Table S2 shows HA-TNIP1 interactome. Table S3 shows RNA-Proteome correlation comparing WT and TNIP1 KO HeLa clones. Table S4 shows chemical reagents used in this study. Table S5 shows antibodies used in this study. Table S6 lists plasmids used in this study.

Data availability

The mass spectrometry proteomics data have been deposited to the ProteomeXchange Consortium through the PRIDE (Perez-Riverol et al., 2019) partner repository with the dataset identifier PXD027163.

The RNA sequence data were deposited at the European Nucleotide Archive (accession no. PRJEB45902).

Acknowledgments

The technical assistance of Aud Øvervatn is greatly appreciated. We thank Laurent Falquet for RNAseq data analysis and Michael Stumpe and Dieter Kressler for proteomics support. We are grateful to Richard J. Youle for the generous gift of the pentaKO cells. We thank the bioimaging core facility, Department of Medical Biology, UiT—The Arctic University of Norway for expert assistance.

This work was funded by grants from: FRIBIOMED (grant 214448) and TOPPFORSK (grant 249884) programs of the Research Council of Norway to T. Johansen; the Danish National Research Foundation (grant no. 141 to ATLAS) and the Independent Research Fund Denmark (8022-00051) to Blagoy Blagoev; the Swiss National Science Foundation to J. Dengjel (310030_184781) and F. Reggiori (CRSII5_189952), the Canton and University of Fribourg, and the Novartis Foundation for Medical-Biological Research to J. Dengjel. This work was part of the SKINTEGRITY.CH collaborative research project.

Author contributions: J. Dengjel, T. Johansen, N.L. Rasmussen, and J. Zhou designed the experiments. J. Zou and N.L. Rasmussen performed most of the experiments. G. Evjen performed GST pulldown experiments and analyzed data. D.S. Sankar, P. Verlhac, N. van de Beck, F. Reggiori, and Y.P. Abudu generated cell lines. S. Kaeser-Pebernard and C. Roubaty performed expression analyses. V. Akimov and B. Blagoev performed and analyzed Ubi-Site experiments. Z. Hu performed phosphoproteomics. H.L. Olsvik assisted in supervision performed in vitro mutagenesis and analyzed data. T. Lamark analyzed data and assisted in supervision. T. Johansen and J. Dengjel supervised and coordinated the overall research, analyzed the data, and approved the final manuscript. J. Zou, N.L. Rasmussen, H.L. Olsvik, T. Johansen, and J. Dengjel wrote the manuscript with input from all authors.

Disclosures: The authors declare no competing financial interests.

Submitted: 1 September 2021

Revised: 24 June 2022

Zhou et al.

Degradation of TNIP1 by selective autophagy

Accepted: 17 August 2022

References

- Abudu, Y.P., B.K. Shrestha, W. Zhang, A. Palara, H.B. Brenne, K.B. Larsen, D.L. Wolfson, G. Dumitriu, C.I. Øie, B.S. Ahluwalia, et al. 2021. SAMM50 acts with p62 in piecemeal basal- and OXPHOS-induced mitophagy of SAM and MICOS components. *J. Cell Biol.* 220:220. <https://doi.org/10.1083/jcb.202009092>
- Akimov, V., I. Barrio-Hernandez, S.V.F. Hansen, P. Hallenborg, A.-K. Pedersen, D.B. Bekker-Jensen, M. Puglia, S.D.K. Christensen, J.T. Vanselow, M.M. Nielsen, et al. 2018. UbiSite approach for comprehensive mapping of lysine and N-terminal ubiquitination sites. *Nat. Struct. Mol. Biol.* 25:631–640. <https://doi.org/10.1038/s41594-018-0084-y>
- Akimov, V., J. Henningsen, P. Hallenborg, K.T. Rigbolt, S.S. Jensen, M.M. Nielsen, I. Kratchmarova, and B. Blagoev. 2014. StUbeX: Stable tagged ubiquitin exchange system for the global investigation of cellular ubiquitination. *J. Proteome Res.* 13:4192–4204. <https://doi.org/10.1021/pr500549h>
- Alemu, E.A., T. Lamark, K.M. Torgersen, A.B. Birgisdottir, K.B. Larsen, A. Jain, H. Olsvik, A. Øvervatn, V. Kirkin, and T. Johansen. 2012. ATG8 family proteins act as scaffolds for assembly of the ULK complex: Sequence requirements for LC3-interacting region (LIR) motifs. *J. Biol. Chem.* 287:39275–39290. <https://doi.org/10.1074/jbc.M112.378109>
- Allanore, Y., M. Saad, P. Dieudé, J. Avouac, J.H. Distler, P. Amouyel, M. Matucci-Cerinic, G. Riemekasten, P. Airo, I. Melchers, et al. 2011. Genome-wide scan identifies TNIP1, PSORS1C1, and RHOB as novel risk loci for systemic sclerosis. *PLoS Genet.* 7:e1002091. <https://doi.org/10.1371/journal.pgen.1002091>
- Batth, T.S., and J.V. Olsen. 2016. Offline High pH Reversed-Phase Peptide Fractionation for Deep Phosphoproteome Coverage. *Methods Mol Biol.* 1355:179–192. https://doi.org/10.1007/978-1-4939-3049-4_12
- Birgisdottir, A.B., S. Mouilleron, Z. Bhujabal, M. Wirth, E. Sjøttem, G. Evjen, W. Zhang, R. Lee, N. O'Reilly, S.A. Tooze, et al. 2019. Members of the autophagy class III phosphatidylinositol 3-kinase complex I interact with GABARAP and GABARAPL1 via LIR motifs. *Autophagy.* 15:1333–1355. <https://doi.org/10.1080/15548627.2019.1581009>
- Chen, S., Y. Zhou, Y. Chen, and J. Gu. 2018. fastp: An ultra-fast all-in-one FASTQ preprocessor. *Bioinformatics.* 34:i884–i890. <https://doi.org/10.1093/bioinformatics/bty560>
- Cox, J., and M. Mann. 2008. MaxQuant enables high peptide identification rates, individualized p.p.b.-range mass accuracies and proteome-wide protein quantification. *Nat. Biotechnol.* 26:1367–1372. <https://doi.org/10.1038/nbt.1511>
- Deretic, V. 2021. Autophagy in inflammation, infection, and immunometabolism. *Immunity.* 54:437–453. <https://doi.org/10.1016/j.immuni.2021.01.018>
- Deretic, V., and B. Levine. 2018. Autophagy balances inflammation in innate immunity. *Autophagy.* 14:243–251. <https://doi.org/10.1080/15548627.2017.1402992>
- Di Rita, A., A. Peschiaroli, P. D Acunzo, D. Strobbe, Z. Hu, J. Gruber, M. Nygaard, M. Lambrugh, G. Melino, E. Papaleo, et al. 2018. HUWE1 E3 ligase promotes PINK1/PARKIN-independent mitophagy by regulating AMBRA1 activation via IKKα. *Nat. Commun.* 9:3755. <https://doi.org/10.1038/s41467-018-05722-3>
- Dobin, A., C.A. Davis, F. Schlesinger, J. Drenkow, C. Zaleski, S. Jha, P. Batut, M. Chaisson, and T.R. Gingeras. 2013. STAR: Ultrafast universal RNA-seq aligner. *Bioinformatics.* 29:15–21. <https://doi.org/10.1093/bioinformatics/bts635>
- Dupont, N., S. Jiang, M. Pilli, W. Ornatowski, D. Bhattacharya, and V. Deretic. 2011. Autophagy-based unconventional secretory pathway for extracellular delivery of IL-1β. *EMBO J.* 30:4701–4711. <https://doi.org/10.1038/emboj.2011.398>
- Dziedzic, S.A., Z. Su, V. Jean Barrett, A. Najafav, A.K. Mookhtiar, P. Amin, H. Pan, L. Sun, H. Zhu, A. Ma, et al. 2018. ABIN-1 regulates RIPK1 activation by linking Met1 ubiquitylation with Lys63 deubiquitylation in TNF-RSC. *Nat. Cell Biol.* 20:58–68. <https://doi.org/10.1038/s41556-017-0003-1>
- Eisenhardt, A.E., A. Sprenger, M. Röring, R. Herr, F. Weinberg, M. Köhler, S. Braun, J. Orth, B. Diedrich, U. Lanner, et al. 2016. Phospho-proteomic analyses of B-Raf protein complexes reveal new regulatory principles. *Oncotarget.* 7:26628–26652. <https://doi.org/10.18632/oncotarget.8427>
- Gao, L., H. Coope, S. Grant, A. Ma, S.C. Ley, and E.W. Harhaj. 2011. ABIN1 protein cooperates with TAX1BP1 and A20 proteins to inhibit antiviral

- signaling. *J. Biol. Chem.* 286:36592–36602. <https://doi.org/10.1074/jbc.M111.283762>
- Gateva, V., J.K. Sandling, G. Hom, K.E. Taylor, S.A. Chung, X. Sun, W. Ortmann, R. Kosoy, R.C. Ferreira, G. Nordmark, et al. 2009. A large-scale replication study identifies TNIP1, PRDM1, JAZF1, UHRF1BP1 and IL10 as risk loci for systemic lupus erythematosus. *Nat. Genet.* 41:1228–1233. <https://doi.org/10.1038/ng.468>
- Gentile, I.E., K.T. McHenry, A. Weber, A. Metz, O. Kretz, D. Porter, and G. Häcker. 2017. TIR-domain-containing adapter-inducing interferon- β (TRIF) forms filamentous structures, whose pro-apoptotic signalling is terminated by autophagy. *FEBS J.* 284:1987–2003. <https://doi.org/10.1111/febs.14091>
- Glavan, T.M., and J. Pavelic. 2014. The exploitation of Toll-like receptor 3 signaling in cancer therapy. *Curr. Pharm. Des.* 20:6555–6564. <https://doi.org/10.2174/1381612820666140826153347>
- Goodwin, J.M., W.E. Dowdle, R. DeJesus, Z. Wang, P. Bergman, M. Kobylarz, A. Lindeman, R.J. Xavier, G. McAllister, B. Nyfeler, et al. 2017. Autophagy-independent lysosomal targeting regulated by ULK1/2-FIP200 and ATG9. *Cell Rep.* 20:2341–2356. <https://doi.org/10.1016/j.celrep.2017.08.034>
- Hampe, J., A. Franke, P. Rosenstiel, A. Till, M. Teuber, K. Huse, M. Albrecht, G. Mayr, F.M. De La Vega, J. Briggs, et al. 2007. A genome-wide association scan of nonsynonymous SNPs identifies a susceptibility variant for Crohn disease in ATG16L1. *Nat. Genet.* 39:207–211. <https://doi.org/10.1038/ng1954>
- Herhaus, L., H. van den Bedem, S. Tang, I. Maslennikov, S. Wakatsuki, I. Dikic, and S. Rahighi. 2019. Molecular recognition of M1-linked ubiquitin chains by native and phosphorylated UBAN domains. *J. Mol. Biol.* 431:3146–3156. <https://doi.org/10.1016/j.jmb.2019.06.012>
- Inomata, M., S. Niida, K. Shibata, and T. Into. 2012. Regulation of Toll-like receptor signaling by NDP52-mediated selective autophagy is normally inactivated by A20. *Cell. Mol. Life Sci.* 69:963–979. <https://doi.org/10.1007/s00018-011-0819-y>
- Johansen, T., A.B. Birgisdottir, J. Huber, A. Kniss, V. Dötsch, V. Kirkin, and V.V. Rogov. 2017. Methods for studying interactions between Atg8/LC3/GABARAP and LIR-containing proteins. *Methods Enzymol.* 587:143–169. <https://doi.org/10.1016/bs.mie.2016.10.023>
- Johansen, T., and T. Lamark. 2020. Selective autophagy: ATG8 family proteins, LIR motifs and cargo receptors. *J. Mol. Biol.* 432:80–103. <https://doi.org/10.1016/j.jmb.2019.07.016>
- Kattah, M.G., L. Shao, Y.Y. Rosli, H. Shimizu, M.I. Whang, R. Advincula, P. Achacoso, S. Shah, B.H. Duong, M. Onizawa, et al. 2018. A20 and ABIN-1 synergistically preserve intestinal epithelial cell survival. *J. Exp. Med.* 215:1839–1852. <https://doi.org/10.1084/jem.20180198>
- Klionsky, D.J., A.K. Abdel-Aziz, S. Abdelfatah, M. Abdellatif, A. Abdoli, S. Abel, H. Abellovich, M.H. Abildgaard, Y.P. Abudu, A. Acevedo-Arozena, et al. 2021. Guidelines for the use and interpretation of assays for monitoring autophagy. *Autophagy.* 8:445–544. <https://doi.org/10.4161/auto.19496>
- Labun, K., T.G. Montague, M. Krause, Y.N. Torres Cleuren, H. Tjeldnes, and E. Valen. 2019. CHOPCHOP v3: Expanding the CRISPR web toolbox beyond genome editing. *Nucleic Acids Res.* 47:W171–W174. <https://doi.org/10.1093/nar/gkz365>
- Le Guerroue, F., A. Werner, C. Wang, and R. Youle. 2022. TNIP1 inhibits Mitophagy via interaction with FIP200 and TAX1BP1. *bioRxiv*. (Preprint posted March 14, 2022). <https://doi.org/10.1101/2022.03.14.484269>
- Lee, Y., J. Kim, M.S. Kim, Y. Kwon, S. Shin, H. Yi, H. Kim, M.J. Chang, C.B. Chang, S.B. Kang, et al. 2021. Coordinate regulation of the senescent state by selective autophagy. *Dev. Cell.* 56:1512–1525.e7. <https://doi.org/10.1016/j.devcel.2021.04.008>
- Lim, J., H. Park, J. Heisler, T. Maculins, M. Roose-Girma, M. Xu, B. Mckenzie, M. van Lookeren Campagne, K. Newton, and A. Murthy. 2019. Autophagy regulates inflammatory programmed cell death via turnover of RHIM-domain proteins. *Elife.* 8:e44452. <https://doi.org/10.7554/eLife.44452>
- Louis, C., C. Burns, and I. Wicks. 2018. TANK-binding kinase 1-dependent responses in health and autoimmunity. *Front. Immunol.* 9:434. <https://doi.org/10.3389/fimmu.2018.00434>
- Love, M.I., W. Huber, and S. Anders. 2014. Moderated estimation of fold change and dispersion for RNA-seq data with DESeq2. *Genome Biol.* 15:550. <https://doi.org/10.1186/s13059-014-0550-8>
- Mauro, C., F. Pacifico, A. Lavorgna, S. Mellone, A. Iannetti, R. Acquaviva, S. Formisano, P. Vito, and A. Leonardi. 2006. ABIN-1 binds to NEMO/IKKgamma and co-operates with A20 in inhibiting NF-kappaB. *J. Biol. Chem.* 281:18482–18488. <https://doi.org/10.1074/jbc.M601502200>
- Mejlvang, J., H. Olsvik, S. Svenning, J.A. Bruun, Y.P. Abudu, K.B. Larsen, A. Brech, T.E. Hansen, H. Brenne, T. Hansen, et al. 2018. Starvation induces rapid degradation of selective autophagy receptors by endosomal microautophagy. *J. Cell Biol.* 217:3640–3655. <https://doi.org/10.1083/jcb.201711002>
- Mizushima, N., and B. Levine. 2020. Autophagy in human diseases. *N. Engl. J. Med.* 383:1564–1576. <https://doi.org/10.1056/NEJMr2022774>
- Morishita, H., and N. Mizushima. 2019. Diverse cellular roles of autophagy. *Annu. Rev. Cell Dev. Biol.* 35:453–475. <https://doi.org/10.1146/annurev-cellbio-100818-125300>
- Nair, R.P., K.C. Duffin, C. Helms, J. Ding, P.E. Stuart, D. Goldgar, J.E. Gudjonsson, Y. Li, T. Tejasvi, B.J. Feng, et al. 2009. Genome-wide scan reveals association of psoriasis with IL-23 and NF-kappaB pathways. *Nat. Genet.* 41:199–204. <https://doi.org/10.1038/ng.311>
- Nanda, S.K., R.K. Venigalla, A. Ordureau, J.C. Patterson-Kane, D.W. Powell, R. Toth, J.S. Arthur, and P. Cohen. 2011. Polyubiquitin binding to ABIN1 is required to prevent autoimmunity. *J. Exp. Med.* 208:1215–1228. <https://doi.org/10.1084/jem.20102177>
- Oakes, J.A., M.C. Davies, and M.O. Collins. 2017. TBK1: A new player in ALS linking autophagy and neuroinflammation. *Mol. Brain.* 10:5. <https://doi.org/10.1186/s13041-017-0287-x>
- Olsen, J.V., B. Blagoev, F. Gnab, B. Macek, C. Kumar, P. Mortensen, and M. Mann. 2006. Global, in vivo, and site-specific phosphorylation dynamics in signaling networks. *Cell.* 127:635–648. <https://doi.org/10.1016/j.cell.2006.09.026>
- Oshima, S., E.E. Turer, J.A. Callahan, S. Chai, R. Advincula, J. Barrera, N. Shifrin, B. Lee, T.S. Benedict Yen, T. Woo, et al. 2009. ABIN-1 is a ubiquitin sensor that restricts cell death and sustains embryonic development. *Nature.* 457:906–909. <https://doi.org/10.1038/nature07575>
- Pankiv, S., T.H. Clausen, T. Lamark, A. Brech, J.A. Bruun, H. Outzen, A. Øvervatn, G. Bjørkøy, and T. Johansen. 2007. p62/SQSTM1 binds directly to Atg8/LC3 to facilitate degradation of ubiquitinated protein aggregates by autophagy. *J. Biol. Chem.* 282:24131–24145. <https://doi.org/10.1074/jbc.M702824200>
- Perez-Riverol, Y., A. Csordas, J. Bai, M. Bernal-Llinares, S. Hewapathirana, D.J. Kundu, A. Inuganti, J. Griss, G. Mayer, M. Eisenacher, et al. 2019. The PRIDE database and related tools and resources in 2019: Improving support for quantification data. *Nucleic Acids Res.* 47:D442–D450. <https://doi.org/10.1093/nar/gky1106>
- Rogov, V.V., H. Suzuki, M. Marinković, V. Lang, R. Kato, M. Kawasaki, M. Buljubašić, M. Šprung, N. Rogova, S. Wakatsuki, et al. 2017. Phosphorylation of the mitochondrial autophagy receptor Nix enhances its interaction with LC3 proteins. *Sci. Rep.* 7:1131. <https://doi.org/10.1038/s41598-017-01258-6>
- Samie, M., J. Lim, E. Verschueren, J.M. Baughman, I. Peng, A. Wong, Y. Kwon, Y. Senbabaoglu, J.A. Hackney, M. Keir, et al. 2018. Selective autophagy of the adaptor TRIF regulates innate inflammatory signaling. *Nat. Immunol.* 19:246–254. <https://doi.org/10.1038/s41590-017-0042-6>
- Samodova, D., C.M. Hosfield, C.N. Cramer, M.V. Giuli, E. Cappellini, G. Franciosa, M.M. Rosenblatt, C.D. Kelstrup, and J.V. Olsen. 2020. ProAlanase is an effective alternative to trypsin for proteomics applications and disulfide bond mapping. *Mol. Cell. Proteomics.* 19:2139–2157. <https://doi.org/10.1074/mcp.TIR120.002129>
- Sarraf, S.A., H.V. Shah, G. Kanfer, A.M. Pickrell, L.A. Holtzclaw, M.E. Ward, and R.J. Youle. 2020. Loss of TAX1BP1-directed autophagy results in protein aggregate accumulation in the brain. *Mol. Cell.* 80:779–795.e10. <https://doi.org/10.1016/j.molcel.2020.10.041>
- Shamilov, R., and B.J. Aneskievich. 2018. TNIP1 in autoimmune diseases: Regulation of toll-like receptor signaling. *J. Immunol. Res.* 2018:3491269. <https://doi.org/10.1155/2018/3491269>
- Shi, C.S., K. Shenderov, N.N. Huang, J. Kabat, M. Abu-Asab, K.A. Fitzgerald, A. Sher, and J.H. Kehrl. 2012. Activation of autophagy by inflammatory signals limits IL-1 β production by targeting ubiquitinated inflammasomes for destruction. *Nat. Immunol.* 13:255–263. <https://doi.org/10.1038/ni.2215>
- Shinkawa, Y., K. Imami, Y. Fuseya, K. Sasaki, K. Ohmura, Y. Ishihama, A. Morinobu, and K. Iwai. 2022. ABIN1 is a signal-induced autophagy receptor that attenuates NF- κ B activation by recognizing linear ubiquitin chains. *FEBS Lett.* 596:1147–1164. <https://doi.org/10.1002/1873-3468.14323>
- Song, H.Y., M. Rothe, and D.V. Goeddel. 1996. The tumor necrosis factor-inducible zinc finger protein A20 interacts with TRAF1/TRAF2 and inhibits NF-kappaB activation. *Proc. Natl. Acad. Sci. USA.* 93:6721–6725. <https://doi.org/10.1073/pnas.93.13.6721>

- Su, Z., S.A. Dziedzic, D. Hu, V.J. Barrett, N. Broekema, W. Li, L. Qian, N. Jia, D. Ofengeim, A. Najafov, et al. 2019. ABIN-1 heterozygosity sensitizes to innate immune response in both RIPK1-dependent and RIPK1-independent manner. *Cell Death Differ.* 26:1077-1088. <https://doi.org/10.1038/s41418-018-0215-3>
- Subramanian, A., P. Tamayo, V.K. Mootha, S. Mukherjee, B.L. Ebert, M.A. Gillette, A. Paulovich, S.L. Pomeroy, T.R. Golub, E.S. Lander, and J.P. Mesirov. 2005. Gene set enrichment analysis: A knowledge-based approach for interpreting genome-wide expression profiles. *Proc. Natl. Acad. Sci. USA.* 102:15545-15550. <https://doi.org/10.1073/pnas.0506580102>
- Szklarczyk, D., A.L. Gable, D. Lyon, A. Junge, S. Wyder, J. Huerta-Cepas, M. Simonovic, N.T. Doncheva, J.H. Morris, P. Bork, et al. 2019. STRING v11: protein-protein association networks with increased coverage, supporting functional discovery in genome-wide experimental datasets. *Nucleic Acids Res.* 47:D607-D613. <https://doi.org/10.1093/nar/gky1131>
- Tian, B., D.E. Nowak, M. Jamaluddin, S. Wang, and A.R. Brasier. 2005. Identification of direct genomic targets downstream of the nuclear factor-kappaB transcription factor mediating tumor necrosis factor signaling. *J. Biol. Chem.* 280:17435-17448. <https://doi.org/10.1074/jbc.M500437200>
- Tyanova, S., T. Temu, and J. Cox. 2016. The MaxQuant computational platform for mass spectrometry-based shotgun proteomics. *Nat. Protoc.* 11: 2301-2319. <https://doi.org/10.1038/nprot.2016.136>
- Wagner, S., I. Carpentier, V. Rogov, M. Kreike, F. Ikeda, F. Löhr, C.J. Wu, J.D. Ashwell, V. Dötsch, I. Dikic, and R. Beyaert. 2008. Ubiquitin binding mediates the NF-kappaB inhibitory potential of ABIN proteins. *Oncogene.* 27:3739-3745. <https://doi.org/10.1038/sj.onc.1211042>
- Wild, P., H. Farhan, D.G. McEwan, S. Wagner, V.V. Rogov, N.R. Brady, B. Richter, J. Korac, O. Waidmann, C. Choudhary, et al. 2011. Phosphorylation of the autophagy receptor optineurin restricts *Salmonella* growth. *Science.* 333:228-233. <https://doi.org/10.1126/science.1205405>
- Wirth, M., S. Mouilleron, W. Zhang, E. Sjøttem, Y. Princely Abudu, A. Jain, H. Lauritz Olsvik, J.A. Bruun, M. Razi, H.B.J. Jefferies, et al. 2021. Phosphorylation of the LIR domain of SCOC modulates ATG8 binding affinity and specificity. *J. Mol. Biol.* 433:166987. <https://doi.org/10.1016/j.jmb.2021.166987>
- Wirth, M., W. Zhang, M. Razi, L. Nyoni, D. Joshi, N. O'Reilly, T. Johansen, S.A. Tooze, and S. Mouilleron. 2019. Molecular determinants regulating selective binding of autophagy adapters and receptors to ATG8 proteins. *Nat. Commun.* 10:2055. <https://doi.org/10.1038/s41467-019-10059-6>
- Wiśniewski, J.R., A. Zougman, N. Nagaraj, and M. Mann. 2009. Universal sample preparation method for proteome analysis. *Nat. Methods.* 6: 359-362. <https://doi.org/10.1038/nmeth.1322>
- Wu, W., W. Tian, Z. Hu, G. Chen, L. Huang, W. Li, X. Zhang, P. Xue, C. Zhou, L. Liu, et al. 2014. ULK1 translocates to mitochondria and phosphorylates FUNDC1 to regulate mitophagy. *EMBO Rep.* 15:566-575. <https://doi.org/10.1002/embr.201438501>
- Youle, R.J. 2019. Mitochondria-Striking a balance between host and endosymbiont. *Science.* 365:365. <https://doi.org/10.1126/science.aaw9855>
- Zellner, S., M. Schifferer, and C. Behrends. 2021. Systematically defining selective autophagy receptor-specific cargo using autophagosome content profiling. *Mol. Cell.* 81:1337-1354.e8. <https://doi.org/10.1016/j.molcel.2021.01.009>
- Zhang, M., S.J. Kenny, L. Ge, K. Xu, and R. Schekman. 2015. Translocation of interleukin-1 β into a vesicle intermediate in autophagy-mediated secretion. *Elife.* 4:e11205. <https://doi.org/10.7554/eLife.11205>
- Zhou, J., R. Wu, A.A. High, C.A. Slaughter, D. Finkelstein, J.E. Rehg, V. Redecke, and H. Häcker. 2011. A20-binding inhibitor of NF- κ B (ABIN1) controls Toll-like receptor-mediated CCAAT/enhancer-binding protein β activation and protects from inflammatory disease. *Proc. Natl. Acad. Sci. USA.* 108:E998-E1006. <https://doi.org/10.1073/pnas.1106232108>
- Zhu, Y., S. Massen, M. Terenzio, V. Lang, S. Chen-Lindner, R. Eils, I. Novak, I. Dikic, A. Hamacher-Brady, and N.R. Brady. 2013. Modulation of serines 17 and 24 in the LC3-interacting region of Bnip3 determines pro-survival mitophagy versus apoptosis. *J. Biol. Chem.* 288:1099-1113. <https://doi.org/10.1074/jbc.M112.399345>

Supplemental material

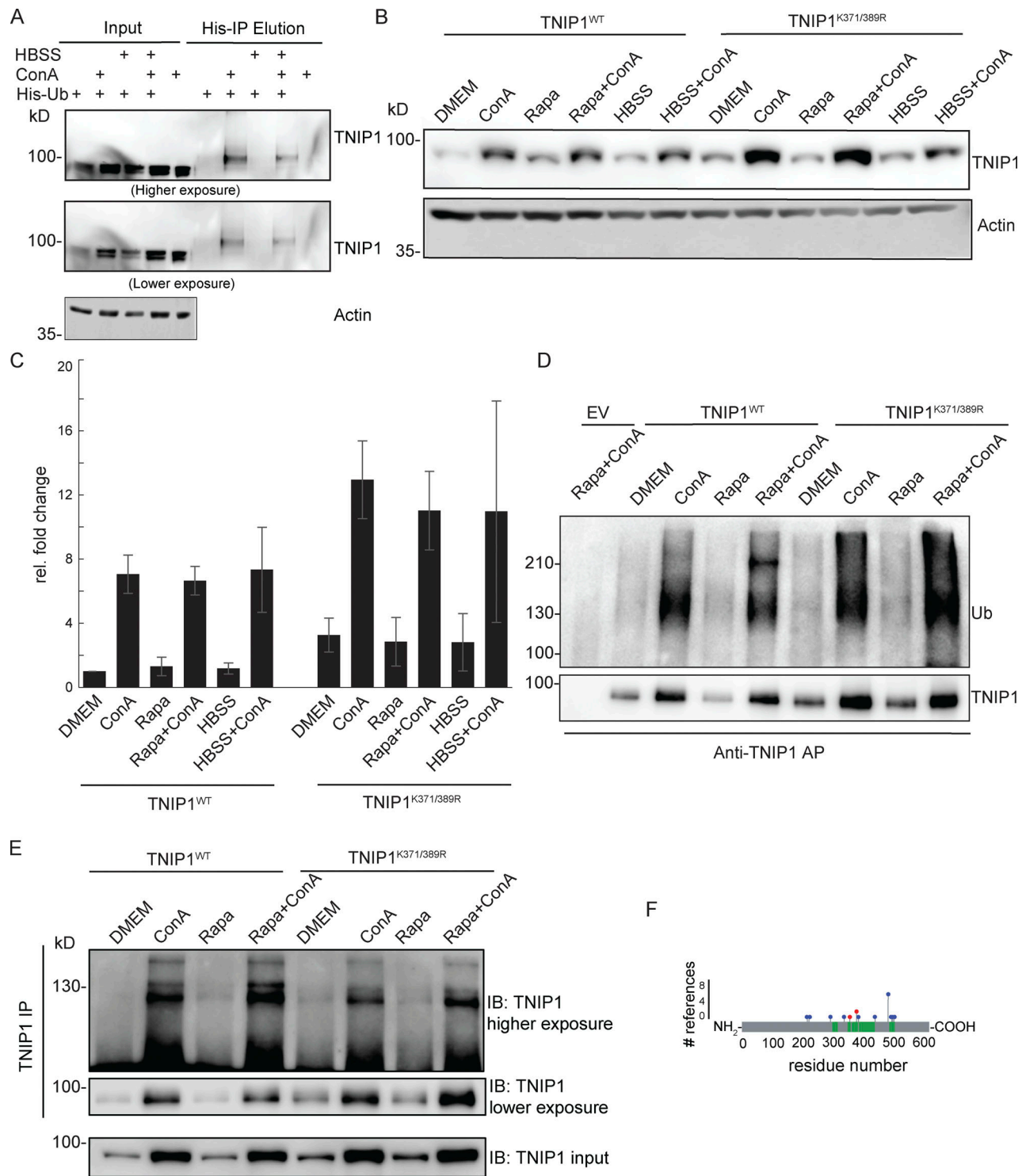


Figure S1. **TNIP1 gets ubiquitinated and degraded in the lysosome.** (A) U2-OS-StUbEx cells inducibly expressing His-FLAG-tagged ubiquitin at endogenous levels were used to enrich ubiquitinated proteins (Akimov et al., 2014). Under control conditions as well as under starvation treatment (HBSS), TNIP1 gets ubiquitinated as shown by anti-TNIP1 immunoblots. Ubiquitinated TNIP1 was stabilized by the addition of concanamycin A (ConA) indicating its lysosomal degradation in treated and nontreated cells. Actin was used as loading control. (B and C) Mutations of identified TNIP1 ubiquitination sites do not lead to reduced lysosomal degradation as indicated by stabilized protein amounts by ConA treatment. This is the case for fed control conditions (DMEM) as well as under active autophagy (Rapa and HBSS treatment). C shows quantification of blots exemplified in B ($n = 3$, error bars indicate SD). (D and E) Mutated TNIP1^{K371/389R} is still getting ubiquitinated as indicated by anti-TNIP1 IP followed by anti-ubiquitin (D) and anti-TNIP1 (E) Western blot. The addition of ConA leads in all cases to a stabilization of non-ubiquitinated and polyubiquitinated protein variants. (F) Identified ubiquitination sites according to PhosphoSitePlus database and this study. Gray bar depicts the amino acid sequence of TNIP1. Sections in green mark tryptic peptides identified in this study, i.e., sequence coverage of TNIP1. Amino acids marked in blue highlight published ubiquitination sites, number of references shown on y-axis. Amino acids marked in red were identified in this study. Source data are available for this figure: SourceData FS1.

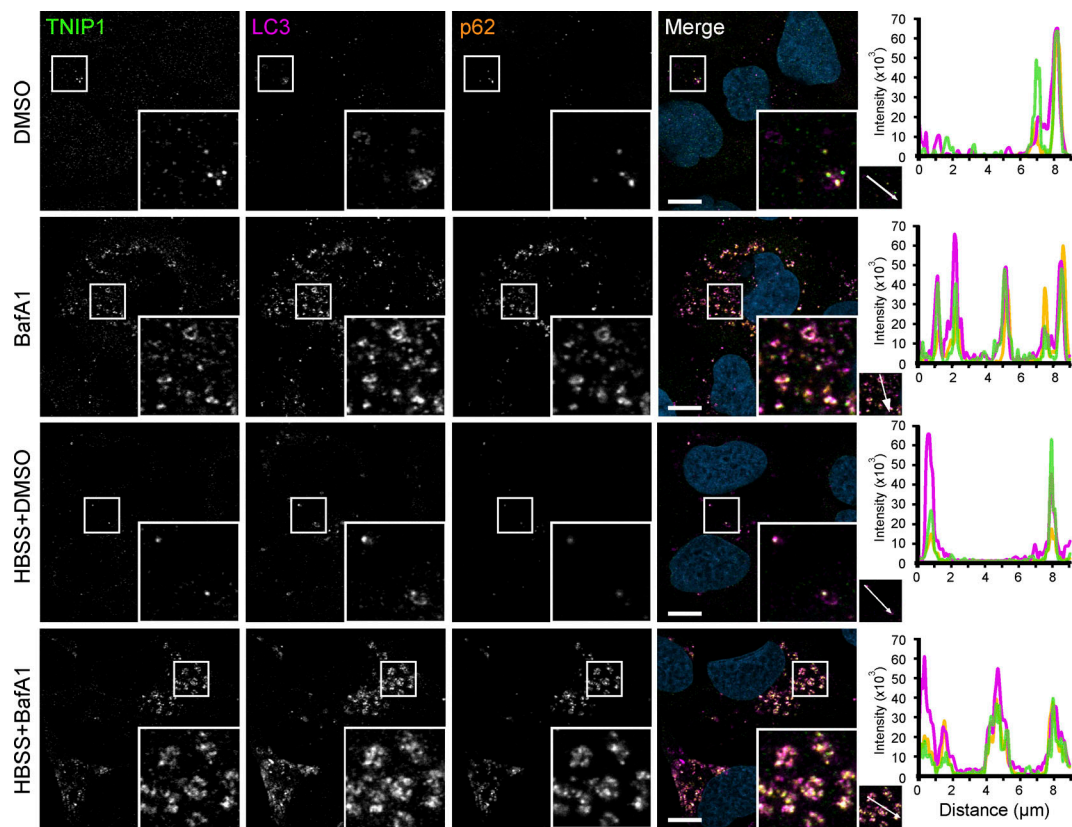


Figure S2. **TNIP1 localizes to autophagosomes.** U2OS cells kept in either fed or starved (HBSS) conditions and treated with either vehicle (DMSO) or BafA1 for 8 h. Cells were fixed and stained with antibodies against endogenous TNIP1 (green), p62 (orange), and LC3 (purple) and imaged using the Zeiss LSM800 confocal microscope. Line-profile co-localization plots were made using the line-profile quantification tool in the Zen blue imaging software (Zeiss). Vertical axis represents measurements of fluorescent intensity and the horizontal axis the drawn distances. Scale bar = 10 μ m.

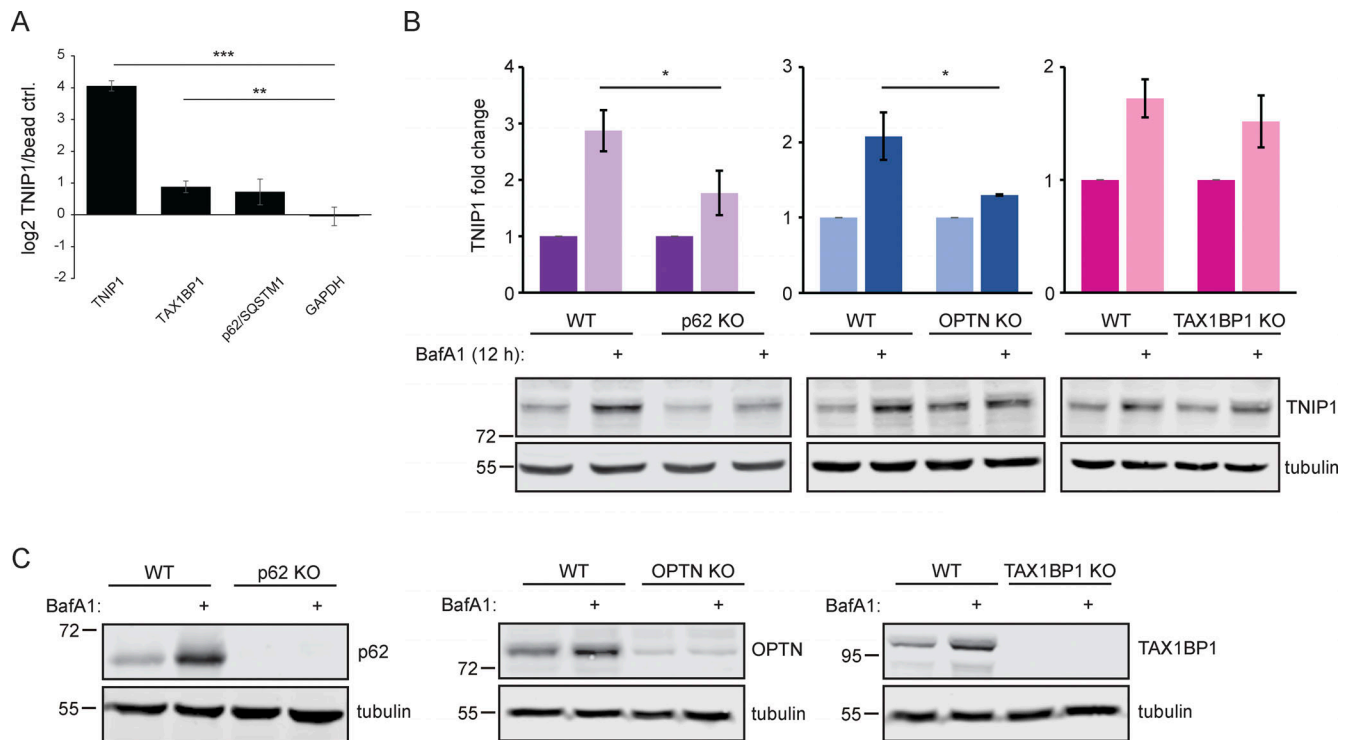


Figure S3. **Endogenous TNIP1 interacts with TAX1BP1 and p62/SQSTM1 under basal conditions.** (A) SILAC-based, IP-MS analyses of anti-TNIP1 immunoprecipitations identified TAX1BP1 and p62/SQSTM1 as enriched compared to negative control IPs using beads only. GAPDH is shown as negative control. Shown are average values of three biological replicates ($n = 3$). Error bars: SD, ** = $P < 0.01$, *** = $P < 0.001$, unpaired, two-sided t test. (B and C) Lysosomal turnover of TNIP1 is mediated by several SLRs. HeLa WT and HeLa p62, OPTN, and TAX1BP1 KO cells were either left untreated or treated with 200 nM BafA1 for 12 h. Shown are average values of three biological replicates. Error bars: SD, * = $P < 0.05$, unpaired, two-sided t test. Source data are available for this figure: SourceData FS3.

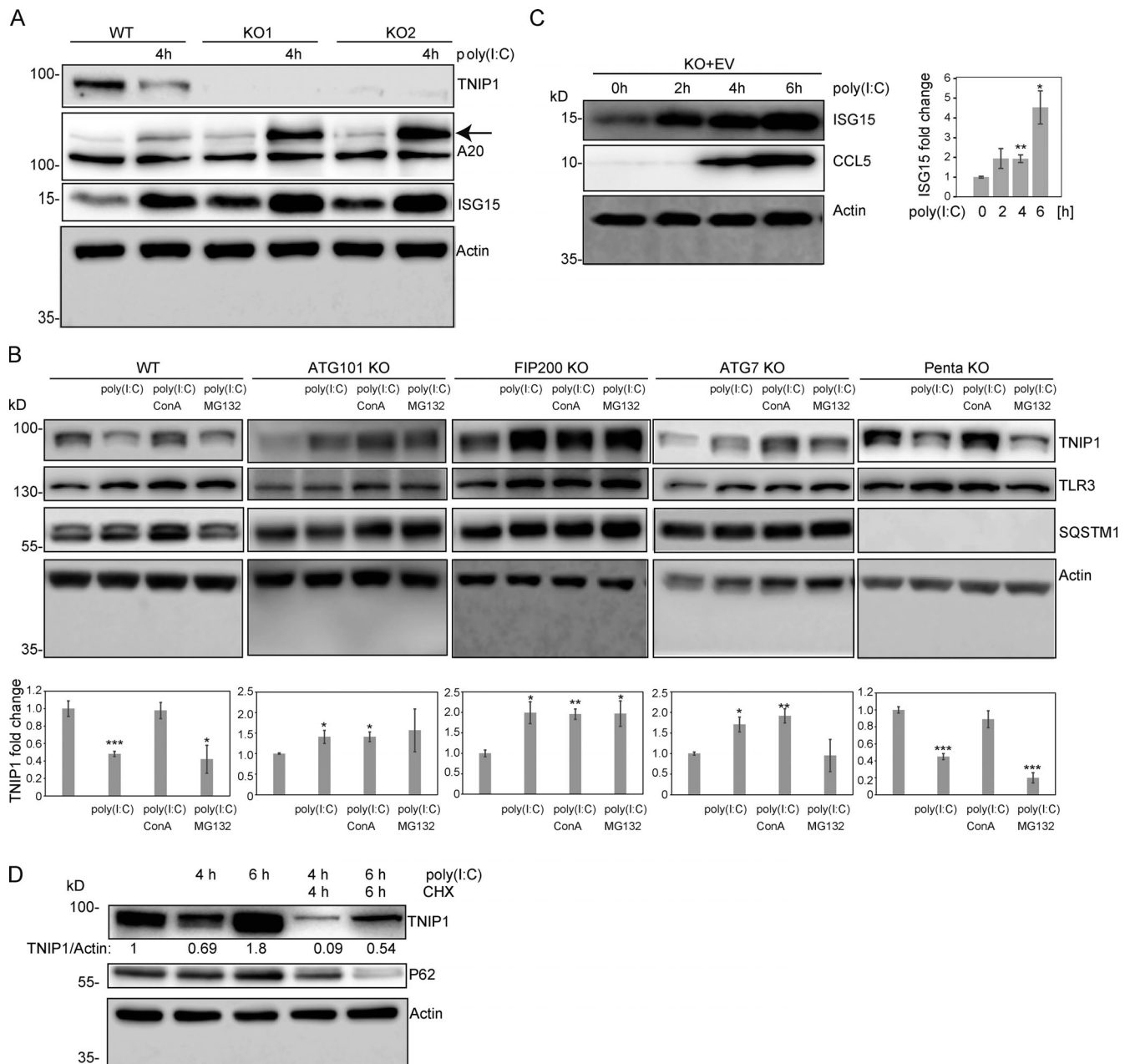


Figure S4. Regulation of TNIP1 protein abundance. (A) Reduction of TNIP1 correlates with an increase of ISG15 and TNFAIP3/A20 in HeLa cells. The increase of the TNIP1 interaction partner TNFAIP3 under poly(I:C) treatment indicates the existence of distinct TNIP1 pools, i.e., free and bound to TNFAIP3. Arrow marks A20 band. (B) Poly(I:C) treatment leads to an autophagy-dependent and SLR-independent lysosomal degradation of TNIP1. Whereas lysosomal inhibition by ConA treatment leads to a significant block of TNIP1 degradation in WT and pentaKO cells, proteasomal inhibition by MG132 treatment has no effect. In ATG101 KO, FIP200 KO and ATG7 KO, autophagy incompetent cell lines poly(I:C) does not lead to TNIP1 degradation. TLR3 and SQSTM1 are monitored as positive controls, actin as loading control. Shown are representative blots of three biological replicates each. Bar diagram shows quantification, error bars: SEM. * = $P < 0.05$, ** = $P < 0.01$, *** = $P < 0.001$, unpaired, two-sided t test. (C) TNIP1 KO cells transfected with an empty control vector (EV) do also respond to poly(I:C) treatment by an upregulation of ISG15 and CCL5 similar to KO cells transfected with a TNIP1 expression construct. This indicates that ISG15 and CCL5 abundances are not only regulated by TNIP1. Shown are representative blots of three biological replicates. Bar diagram shows quantification. Error bars represent SEM. * = $P < 0.05$, ** = $P < 0.01$, *** = $P < 0.001$; unpaired, two-sided t test. (D) Blockage of protein translation by cycloheximide (CHX) treatment reduced the time- and poly(I:C)-dependent increase of TNIP1 after 6 h of treatment indicating a regulation on translational level. Source data are available for this figure: SourceData FS4.

Provided online are Table S1, Table S2, Table S3, Table S4, Table S5, and Table S6. Table S1 shows UbiSite-proteomics approach to identify ubiquitination sites on proteins being potentially involved in autophagy. Table S2 shows HA-TNIP1 interactome. Table S3




shows RNA-Proteome correlation comparing WT and TNIP1 KO HeLa clones. Table S4 shows chemical reagents used in this study. Table S5 shows antibodies used in this study. Table S6 lists plasmids used in this study.

PAPER II

PAPER III

REVIEW

NBR1: The archetypal selective autophagy receptor

Nikoline Lander Rasmussen¹ , Athanasios Kournoutis¹, Trond Lamark¹ , and Terje Johansen¹ 

NBR1 was discovered as an autophagy receptor not long after the first described vertebrate autophagy receptor p62/SQSTM1. Since then, p62 has currently been mentioned in >10,000 papers on PubMed, while NBR1 is mentioned in <350 papers. Nonetheless, evolutionary analysis reveals that NBR1, and likely also selective autophagy, was present already in the last eukaryotic common ancestor (LECA), while p62 appears first in the early Metazoan lineage. Furthermore, yeast-selective autophagy receptors Atg19 and Atg34 represent NBR1 homologs. NBR1 is the main autophagy receptor in plants that do not contain p62, while most animal taxa contain both NBR1 and p62. Mechanistic studies are starting to shed light on the collaboration between mammalian NBR1 and p62 in the autophagic degradation of protein aggregates (aggrephagy). Several domains of NBR1 are involved in cargo recognition, and the list of known substrates for NBR1-mediated selective autophagy is increasing. Lastly, roles of NBR1 in human diseases such as proteinopathies and cancer are emerging.

The selective autophagy receptor NBR1

Selective autophagy consists of a set of evolutionarily conserved pathways for targeted lysosomal degradation of macromolecules, protein aggregates, lipid droplets, viral capsids, intracellular pathogens, and organelles. The different pathways of selective autophagy depend on either soluble or membrane-bound selective autophagy receptors (SARs; Lamark and Johansen, 2021). The first SAR discovered, p62/SQSTM1 (sequestosome-1), belongs to a family of soluble SARs including NBR1, CALCOCO1, CALCOCO2 (aka NDP52), TAX1BP1 (aka CALCOCO3), and OPTN (optineurin). This group of SARs, commonly referred to as sequestosome-1 like receptors (SLRs; Deretic, 2012), are typically characterized by the presence of (1) an LC3 interacting region (LIR) motif, (2) homo- or hetero-oligomerization domains, and (3) a C-terminal ubiquitin-binding domain for engaging ubiquitinated substrates (Johansen and Lamark, 2020; Nthiga et al., 2020). The SLR-LIR motifs bind to ATG8 family proteins anchored in the autophagosomal double membrane through a covalent conjugation to phosphatidylethanolamine (Lystad and Simonsen, 2019; Mizushima et al., 2011). Substrates and cargos for selective autophagy are usually labeled with ubiquitin or other “eat me” signals recognized by the ubiquitin-binding domain or other domains found in SLRs. When bound to cargo, some SLRs can themselves initiate autophagosome formation in situ by interacting with components of the core autophagy machinery (Chang et al., 2021; Goodall et al., 2022). Further, SLRs can facilitate the expansion of the autophagosome membrane (phagophore) by multivalent interactions with ATG8 proteins (Johansen and Lamark, 2020). The most studied SLR p62 forms

phase-separated bodies in cells that are called p62 bodies (Lamark and Johansen, 2021). The formation of p62 bodies depends on polymerization mediated by the N-terminal Phox/Bem1p (PB1) domain (Lamark et al., 2003; Wilson et al., 2003), with p62 forming helical filaments (Ciuffa et al., 2015; Jakobi et al., 2020), and is induced by binding of p62 to poly-ubiquitin, causing a phase separation (Sun et al., 2018; Zaffagnini et al., 2018). Phase separation of p62 filaments is also induced by increased p62 expression or by posttranslational modifications increasing the binding of p62 to ubiquitin (Lamark and Johansen, 2021).

NBR1 (neighbor of BRCA1 gene 1) was discovered as a selective autophagy receptor due to its interaction with and similarity in domain organization to p62 and direct binding to ATG8 proteins and ubiquitin (Kirkin et al., 2009; Waters et al., 2009). Mammalian NBR1 acts as a SAR involved in degrading protein aggregates (aggrephagy; Kirkin et al., 2009), peroxisomes (pexophagy; Deosaran et al., 2013), midbody remnants (Isakson et al., 2013; Kuo et al., 2011), focal adhesions (Kenific et al., 2016), and major histocompatibility complex (MHC) class I receptor (Yamamoto et al., 2020). In plants, NBR1 degrades protein aggregates upon heat-, oxidative-, salt-, and drought stress (Zhou et al., 2013; Zhou et al., 2014), viral capsids (Hafren et al., 2017), a viral RNA silencing suppressor (Hafren et al., 2018), and acts in defense against bacterial infections (Leong et al., 2022; Ustun and Hofius, 2018). In fungi, NBR1 homologs transport lysosomal enzymes from the cytoplasm into the vacuole as shown in the fission yeast *Schizosaccharomyces pombe* (Liu et al., 2015; Wang et al., 2021), and they act as a pexophagy receptor in the filamentous fungus *Sordaria macrospora* (Werner et al., 2019).

¹Autophagy Research Group, Department of Medical Biology, University of Tromsø-The Arctic University of Norway, Tromsø, Norway.

Correspondence to Terje Johansen: terje.johansen@uit.no.

© 2022 Rasmussen et al. This article is available under a Creative Commons License (Attribution 4.0 International, as described at <https://creativecommons.org/licenses/by/4.0/>).

Substrates of NBR1 in mammals, plants, and yeast are summarized in Fig. 1. In this review, we will elaborate on the roles of NBR1 in selective autophagy processes in plants, fungi, and mammals, and its roles in human disease. But first, we will focus on the domain structure and evolution of NBR1.

Domain structure of NBR1

Vertebrate NBR1 and p62 share an N-terminal PB1 domain, the ZZ zinc finger domain, LIR motif, and C-terminal UBA domains. In addition, NBR1 contains the four tryptophan (FW) domains involved in protein-protein interactions, two coiled-coil (CC) domains, and an amphipathic helix (AH) domain not found in p62 (Deosaran et al., 2013; Mardakheh et al., 2010; Svenning et al., 2011; Fig. 2 A). The PB1 domain is involved in interactions with other PB1 domain-containing proteins (notably p62, see below), while the CC1 domain mediates self-interaction. The UBA domain binds to ubiquitin and ubiquitinated cargo, while the LIR binds to ATG8 family proteins (Johansen and Lamark, 2020). Human NBR1 has two LIR motifs. Both bind ATG8 proteins in vitro, but only LIR1 binds strongly in cell extracts and is required for efficient autophagic degradation of NBR1 (Kirkin et al., 2009).

The FW domain was so named because it contains four highly conserved tryptophan (W) residues (Svenning et al., 2011). It is also referred to as NBR1-like or NBR1 domain (Kraft et al., 2010). Some bacterial proteins also contain FW domains, which precede the eukaryotic NBR1 that first appeared in protists (Marchbank et al., 2012; Svenning et al., 2011; Fig. 2 A). The FW domain is present in only one other eukaryotic protein called ILRUN (inflammation and lipid regulator with UBA-like and NBR1-like domains; Fig. 2 A). The FW domain of human NBR1 binds to microtubule-associated protein MAPIB and TAX1BP1 (Marchbank et al., 2012; Turco et al., 2021). The recent finding that the FW domain of the filamentous fungus *Chaetomium thermophilum* binds specifically to vacuolar α -mannosidase (Ams1) and delivers Ams1 to the vacuole by autophagy in the fission yeast *S. pombe* shows that this domain can be involved in cargo recognition (Zhang et al., 2022a).

The same group previously showed that the *S. pombe* NBR1 homolog uses its ZZ domains to transport aminopeptidases Ape4, Ape2, and Lap2, and Ams1 from the cytosol into the vacuole, analogous to Atg19 acting as a receptor in the biosynthetic cytoplasm to vacuole transfer (Cvt) pathway in *S. cerevisiae* (Liu et al., 2015; Wang et al., 2021; Fig. 1 B). Ams1 and Ape4 bind competitively to ZZ1. Lap2 and Ape2 bind to ZZ2 and ZZ3. Surprisingly, this Nbr1-mediated vacuolar targeting (NVT) pathway in *S. pombe* is not mediated by autophagy components but by endosomal-sorting complexes required for transport (ESCRTs) in a process similar to microautophagy (Hama et al., 2021; Wang et al., 2021). Interestingly, the ZZ domain of mammalian p62, but not that of mammalian NBR1, is also used for cargo recognition by binding to N-arginylated proteins (Chamolstad et al., 2017).

The AH domain of mammalian NBR1 was identified as a 22 amino-acid amphipathic α -helical structure based on secondary structure predictions (Mardakheh et al., 2010). It is located adjacent to the UBA domain and was initially called the

JUBA domain for juxta-UBA. Since JUBA and UBA are confusingly similar names both verbally and written, we propose to call this domain simply AH for amphipathic α -helix. Circular dichroism spectroscopy showed the AH domain to be an unfolded structure that folds into an α -helix in the presence of membranes containing phosphatidylinositol-phosphates (PIPs; Mardakheh et al., 2010). AH displayed no specificity toward a specific PIP. Both the AH and UBA domains are needed for the co-localization of NBR1 with LAMP2 (late endosomes; Mardakheh et al., 2010) and peroxisomes (Deosaran et al., 2013), suggesting AH is required for membrane localization of NBR1.

Evolution of NBR1: The archetypal soluble autophagy receptor

Autophagy-related (ATG) genes have experienced expansions and losses during the evolution of different eukaryotic lineages, enabling functional diversification and specialization. Remote homologs of ATG proteins and the evolutionarily conserved protein domains are found in bacteria and archaea. These were likely recruited into the developing autophagy pathway during eukaryogenesis (Zhang et al., 2021). Phylogenetic and biochemical analyses reveal the evolutionary relationship between NBR1 and p62. Using the presence of the FW domain to distinguish between p62 and NBR1 homologs, we found NBR1 orthologs to be distributed throughout the eukaryotic kingdom, while p62 is confined to the metazoans (Svenning et al., 2011; Fig. 2, B and C). Most non-metazoan organisms have only a single NBR1 homolog and no p62 homolog. Metazoans generally contain both NBR1 and p62, but NBR1 has been secondarily lost in some animal lineages including nematodes, insects, and crustaceans. Clearly, NBR1 preceded p62 in evolution, and p62 likely arose through gene duplication of the ancestral NBR1 gene, which happened early in the metazoan lineage (Fig. 2 C). This is illustrated by the fact that the choanoflagellate *Monosiga brevicollis* and the amoeban protist *Capsaspora owczarzaki*, representing the closest living unicellular relatives of metazoans (King et al., 2008; Ruiz-Trillo et al., 2004), have only a single NBR1 homolog and no p62 homolog (Svenning et al., 2011).

Autophagy is a very fundamental pathway appearing at the root of eukaryote evolution and is likely present in the last eukaryotic common ancestor (LECA; Zhang et al., 2021). LECA is defined as the ancestor of all existing eukaryotes, plus extinct post-LECA lineages. LECA likely arose 1.9–1.6 billion years ago, with all the main features of a eukaryotic cell (Spang et al., 2022). With a few exceptions like red algae, microsporidia, and the flagellate intestinal parasite *Giardia lamblia*, ATG genes and autophagy are found throughout eukaryotes (Zhang et al., 2021; Zhang et al., 2022b). Although gene loss and expansions occur in many lineages, the two conjugation systems with ATG8 and ATG12 are conserved in most eukaryotic clades (Zhang et al., 2022b). The origin of selective autophagy likely occurred with the first SAR, and NBR1 is the pioneer soluble SAR. None of the other vertebrate SARs have been found in protists or plants. Defining NBR1 homologs as proteins that as a minimum contain an FW domain and a PB1 or ZZ-type zinc finger domain, we find NBR1 homologs in five of the supergroups of the newly proposed tree of eukaryotes (Burki et al., 2020). Specifically, representatives of the TSAR supergroup (including Stramenopila,

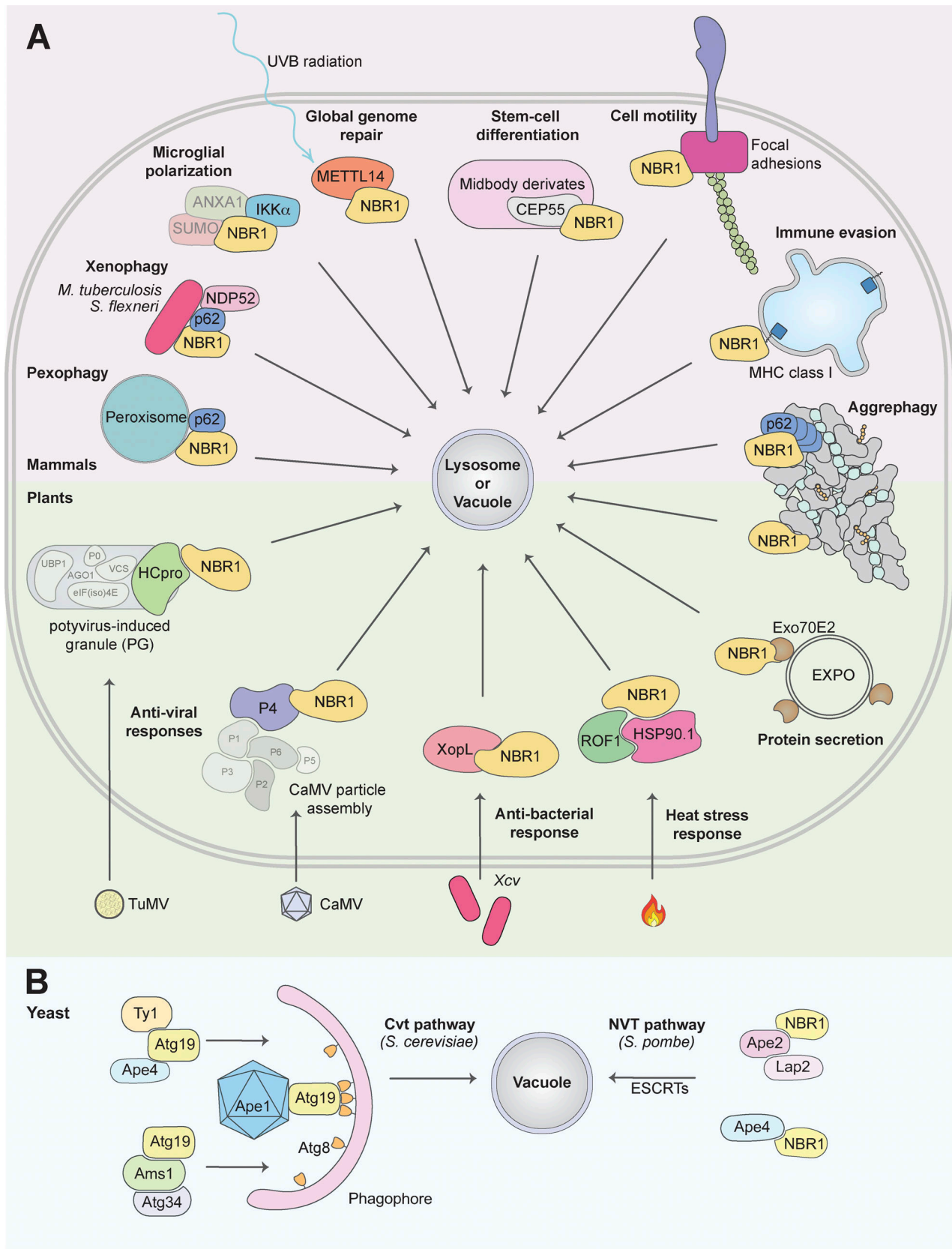


Figure 1. **NBR1 as a selective autophagy receptor in mammals, plants, and yeast.** Summary of identified substrates of NBR1-mediated selective autophagy, indicated by immediate vicinity to NBR1. This does not distinguish direct or indirect interaction. Transparent proteins are part of a complex. **(A)** In mammals, NBR1 has been shown to mediate the degradation of peroxisomes (pexophagy), bacteria (xenophagy), and protein aggregates (aggrephagy) in

conjunction with p62 (and NDP52 for xenophagy). Furthermore, NBR1 has been shown to affect several processes through selective autophagic degradation of the following substrates: the proinflammatory kinase IKK α , affects microglial polarization following ischemia (Li et al., 2021); METTL14 (methyltransferase-like 14) upon ultraviolet B radiation, consequently affecting global genome repair (Yang et al., 2021); the midbody protein CEP55 upon stem-cell differentiation (Kuo et al., 2011); turnover of focal adhesions, promoting cell motility; and MHC class I proteins in PDAC cells, promoting immune evasion. In plants, NBR1 regulates several plant stress responses: clearance of aggregates (aggrephagy), restricting TuMV infection by targeting the viral RNA silencing suppressor component HCpro; restricting CaMV infection by targeting the viral particle protein P4; targeting the bacteria effector protein XopL for degradation, restricting Xcv infection; promoting heat stress recovery by targeting ROF1 and HSP90.1; targeting Exo70E2, a marker for the exocyst-positive organelle (EXPO; Ji et al., 2020). **(B)** In *S. cerevisiae*, the NBR1 homolog Atg19 mediates the degradation of Ty1, Ape4, Ape1, and Ams1 through the Cvt pathway. The second NBR1 homolog Atg34, only targets Ams1. In *S. pombe*, the NBR1 homolog targets Ape2, Lap2, and Ape4 to the vacuole. This Nbr1-mediated vacuolar targeting (NVT) pathway is mediated by ESCRTs, not macroautophagy. Only references not cited in the main text are cited here.

Alveolata, and Rhizaria), Haptista (Haptophyta), Archaeplastida (Chloroplastida), Amorphea (including Apusomonada, Amoebozoa, and Ophisthokonta), and Discoba all have NBR1 homologs (Fig. 2 B). Opisthokonta includes animals, fungi, and some protist lineages that are most closely related to either animals or fungi. Chloroplastida includes green algae and land plants. All the remaining supergroup taxa mentioned represent protists (Burki et al., 2020). The lack of sequence data for some important species defining a few of the taxa presently precludes an exhaustive analysis. However, the coincident presence of important core ATG proteins makes it tempting to suggest that the ancestor NBR1 may have been present in LECA, representing the first SAR that evolved. Hence, selective autophagy may have originated in the LECA and co-evolved with unselective autophagy.

Apart from NBR1, ILRUN is the only other eukaryotic protein containing an FW domain (Fig. 2 A). It is not clear if there is a functional relationship between NBR1 and ILRUN. Human ILRUN is a 298 amino acid protein (formerly known as C6orf106) containing an N-terminal UBA-like domain (residues 23–64) and a central FW domain (residues 71–180). We traced the homologs of ILRUN protein in the evolution, guided by the eukaryotic tree of life, and found that ILRUN is present in all metazoans including the simplest metazoan *Trichoplax adhaerens* and the closest unicellular relatives to metazoans *Monosiga brevicollis* and *Capsaspora owczarzaki*. ILRUN homologs are also found in the Stramenopila of the TSAR supergroup, Haptophyta of the Haptista supergroup, and Apusomonada, but not the sister group Amoebozoa of the Amorphea supergroup (Fig. 2 B). Intriguingly, distinct from NBR1, ILRUN is not found in plants and fungi. This suggests a secondary loss of ILRUN in these taxa.

Atg19 and Atg34 are yeast NBR1 homologs

S. cerevisiae, *D. melanogaster*, and *C. elegans* are extremely valuable model organisms. However, due to long divergent evolution with gene duplications and loss they are often the “odd ones out” when it comes to sequence-based evolutionary studies of proteins. A seminal perspective article suggested that Atg19 is the NBR1 homolog in *S. cerevisiae* (Kraft et al., 2010). Acting as a receptor in the Cvt pathway, yeast Atg19 was the first selective autophagy receptor discovered (Leber et al., 2001; Scott et al., 2001). The primary cargo in the Cvt pathway is the precursor form of the vacuolar aminopeptidase 1 (preApe1), which forms a tetrahedral dodecameric structure that is recognized by the CC domain of Atg19. Atg19 recruits Atg8 via its C-terminal LIR (often called Atg8-family interaction motif [AIM] in yeast) and

the selective autophagy adapter Atg11. This Cvt complex recruits the core autophagy machinery to initiate membrane formation and expansion to form the Cvt vesicle, a special type of autophagosome only 150 nm in diameter (reviewed in Yamasaki and Noda, 2017). In addition to Ape1, Atg19 also transports the vacuolar aspartyl aminopeptidase Ape4, the vacuolar α -mannosidase Ams1, and even the Ty1 retrotransposon particle to the vacuole. Almost 10 yr after the discovery of Atg19, its paralog Atg34 was discovered (Suzuki et al., 2010). Atg19 and Atg34 have the same domain organization (Fig. 3 A) and show 31% overall sequence identity (49% similarity), but Atg34 can only target Ams1. Hence, Atg34 cannot compensate for Atg19 in the Cvt pathway (Yamasaki and Noda, 2017).

Atg19 has lost the ZZ zinc-finger domain and has no sequence similarity to NBR1 homologs in other phyla. However, Kraft, Peter, and Hofmann noted that Atg19 has the LIR domain and predicted that highly divergent PBI and NBR1 folds were present in *S. cerevisiae* Atg19, as well as a CC domain (Kraft et al., 2010). Their argument also rested on the evolutionary analysis of NBR1 with emphasis on fungal homologs, where some fungal lineages had retained NBR1 with PBI, ZZ, FW, LIR, and UBA domains although having two or three copies of the ZZ domain. Most fungi lost the UBA domain, and PBI and FW domains could not be identified by sequence conservation in evolved lineages such as *Saccharomyces*, but a similar fold was predicted, suggesting the presence of PBI-like and FW-like domains in *S. cerevisiae* Atg19 (Kraft et al., 2010; Fig. 3 A). The solution structures of the α -mannosidase binding domains (ABD) of Atg19 and Atg34 are solved (Watanabe et al., 2010). The Atg19 and Atg34 ABD structures are very similar, with a root mean square difference (RMSD) of 2.1 Å for 102 residues, forming an immunoglobulin-like β -sandwich fold with two β -sheets, each with four anti-parallel β -strands. The ABD of the NBR1 homolog of the filamentous fungus *C. thermophilum* has an FW domain very similar in structure to those found in human NBR1 and ILRUN (Zhang et al., 2022a). Structural comparison of FW domain structures of NBR1 and ILRUN with the ABD of Atg19 and Atg34 revealed the latter to be FW-like domains (Fig. 3 B). A VAST structural alignment search of the Protein Database with the Atg34 ABD revealed the human ILRUN FW domain as a structural homolog of the ABD. With the ABD of Atg19 and -34 being structurally homologous to FW domains, we asked if the N-terminal regions of these two yeast proteins may be PBI-like domains. Comparing the PBI domain structure of *Arabidopsis* NBR1 (Jakobi et al., 2020) to AlphaFold structure prediction with 90% confidence of the *S. cerevisiae* Atg34 N-terminal region

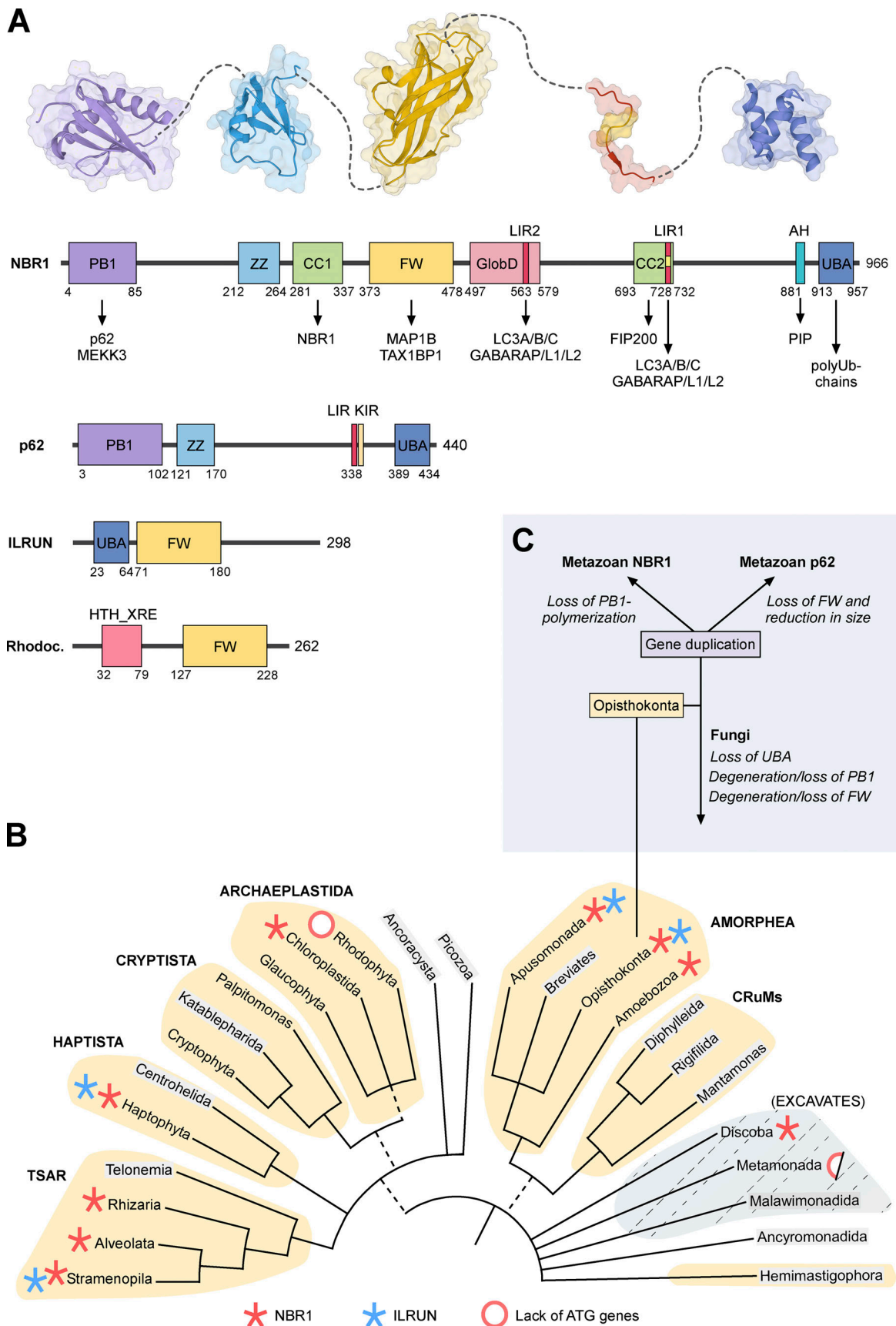


Figure 2. **Domain structure and evolution of NBR1.** (A) Domain architectures of human NBR1, p62, and ILRUN, and HTH-XRE (Helix-turn-helix XRE-family like protein) from *Rhodococcus fascians*. The amino acid positions of the domain borders and the length of the proteins are indicated by numbers below and to

the right of the cartoons, respectively. Structures of PB1, ZZ, FW, LIR, and UBA domains are shown above the NBR1 domain architecture. **(B)** Distribution of NBR1 (red asterisk) and ILRUN (blue asterisk) on The New Tree of Eukaryotes. Red ring, or half-red ring, indicates the lack of ATG genes in some clades. The colored groupings are the current “supergroups.” Multifurcations indicate unresolved branching orders among lineages while broken lines represent minor uncertainties about the monophyly of certain groups (Burki et al., 2020). We searched the NCBI Protein Database and the Conserved Domains Database to identify NBR1 and ILRUN homologs (Lu et al., 2020). The phylogenomic distribution was also determined using the SMART database (Letunic et al., 2006). The names of the groupings where sequence data were not available are indicated in gray. **(C)** The Ophisthokonta contains both the metazoans and fungi. The gene duplication and divergence of the ancestor NBR1 gene in the early metazoan lineage, and loss of UBA and loss or degeneration of PB1 domains in fungi are indicated.

(Jumper et al., 2021; Varadi et al., 2022) clearly suggest the presence of a PB1 domain in Atg34 (Fig. 3 C). In Atg19 the prediction is very uncertain, but the presence of a PB1-like domain is likely. Structure determinations of the N-terminal regions of Atg19 and Atg34 will give us clear answers. However, taken together, we suggest that Atg19 and Atg34 are clearly NBR1 homologs with PB1/PB1-like, CC, FW, and LIR domains (Fig. 3 A).

An early metazoan gene duplication created the paralogs p62/SQSTM1 and metazoan NBR1

The split of ancestor NBR1 into the current paralogs p62/SQSTM1 and NBR1 in vertebrates was likely initiated by a gene duplication very early in metazoan evolution (Svenning et al., 2011; Fig. 2 C). Further evolution led to one shortened paralog lacking the CC and FW domains (p62) and one full-length with a modified and monomeric PB1 domain (metazoan NBR1). The gain of an AH domain may have occurred before vertebrates evolved. To understand the functional consequence of the duplication event, it is important to relate it to the role of the PB1 domain in selective autophagy. PB1 is a ubiquitin-like domain that engages in homomeric or heteromeric PB1–PB1 interactions. The interaction involves two individual and oppositely charged binding surfaces. A negatively charged binding surface in one PB1 domain binds to a positively charged binding surface in the other (Jakobi et al., 2020; Lamark et al., 2003; Wilson et al., 2003). Individual PB1 domains may contain one or both binding surfaces. PB1 domains with both binding surfaces can result in homomeric polymerization of the PB1-containing protein, as seen for mammalian p62. Cryo-EM analyses demonstrated that the PB1 domain of p62 forms flexible helical polymers in vitro (Ciuffa et al., 2015). The PB1 domain constitutes the scaffold in p62 filaments, while the LIR and UBA domains are exposed (Ciuffa et al., 2015). We found that the plant ortholog from *Arabidopsis* (AtNBR1) has a PB1 domain that can homopolymerize (Svenning et al., 2011). The presence of a PB1 domain alone is not enough to predict self-interaction. Studies are therefore needed to determine how widespread polymerization is among non-metazoan NBR1 orthologs. Metazoan NBR1 orthologs have lost the basic binding surface resulting in a monomeric PB1 domain. To compensate, metazoan NBR1 and some fungal orthologs harbor a self-interacting CC domain, a domain absent in plant orthologs or p62. Despite the split of the ancestor NBR1 into p62 and NBR1 in metazoans, mammalian NBR1 remains attached to p62 via the acidic PB1 surface that is not mutated (Lamark et al., 2003). The only known interaction partners of mammalian NBR1 that bind via PB1–PB1 interactions are p62 (Lamark et al., 2003) and the kinase MEKK3 (Hernandez et al., 2014), and NBR1 is always recruited to p62 bodies.

We propose that the early metazoan gene duplication facilitated the evolution and divergence in domain structures, which allowed p62 and NBR1 to both tackle separate functions and collaborate on certain functions. The split into two proteins enabled different expression levels in cells and various tissues and different regulations by posttranslational modifications. The gene duplication enabled a deletion of domains from p62 streamlining it as an effective SAR facilitating p62 body formation, which requires high quantities of p62. NBR1 is less central in forming the scaffold of the p62 body, allowing the development of other functions such as gain of the AH domain enabling membrane binding. In humans, NBR1 is much less abundant in most cell types than p62, varying from 10 to almost 100-fold difference in protein levels (Cho et al., 2022; Wang et al., 2015). According to The Human Protein Atlas, both proteins are expressed in most tissues with little tissue specificity, but with particularly high levels of p62 in skeletal muscle and of NBR1 in late spermatids of the testis (Uhlen et al., 2015).

Plant NBR1 is polymeric, forms filaments similar to p62, and acts in stress responses

Arabidopsis NBR1 (AtNBR1) and mammalian p62 share the abilities of PB1 self-polymerization and helical filament formation, as well as LIR-ATG8 binding and UBA-ubiquitin interactions (Jakobi et al., 2020; Svenning et al., 2011). AtNBR1 forms cellular p62 bodies with a striking similarity to those formed by mammalian p62, and the formation of AtNBR1 bodies depends on PB1-mediated polymerization and UBA-mediated ubiquitin binding (Svenning et al., 2011). High-resolution cryo-EM studies of the purified PB1 domain of AtNBR1 revealed similar types of filamentous structures as seen for the human p62 PB1 domain (Jakobi et al., 2020). A tandem arginine motif that is absent in human NBR1, but present in p62 (R21/22) and AtNBR1 (R19/20), is important for stabilizing a filamentous structure and for the formation of p62/AtNBR1 bodies with ubiquitin (Jakobi et al., 2020; Lin et al., 2017). This strongly supports the conclusion that p62 bodies and AtNBR1 bodies are structurally very similar. Another common feature of p62 and AtNbr1 is that their degradation by autophagy depends on a polymeric PB1 domain (Svenning et al., 2011). In comparison, mammalian NBR1 has a monomeric PB1 domain, and its degradation by autophagy does not depend on its PB1 domain (Kirkin et al., 2009).

The roles of NBR1-mediated selective autophagy in plant stress responses have recently been excellently reviewed (Zhang and Chen, 2020; Fig. 1 A). AtNBR1 is involved in heat tolerance, modulation of plant heat memory, plant–pathogen interactions, and aggregophagy (autophagic degradation of protein aggregates) during abiotic stress tolerance (Young et al., 2019; Zhou et al.,

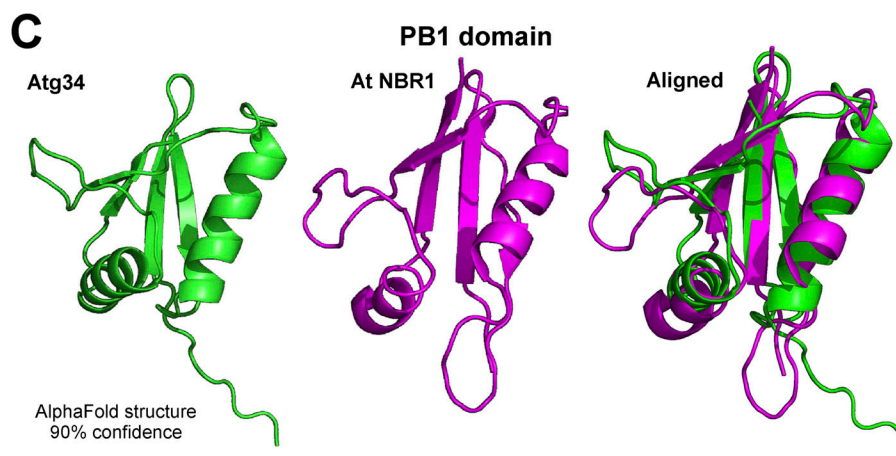
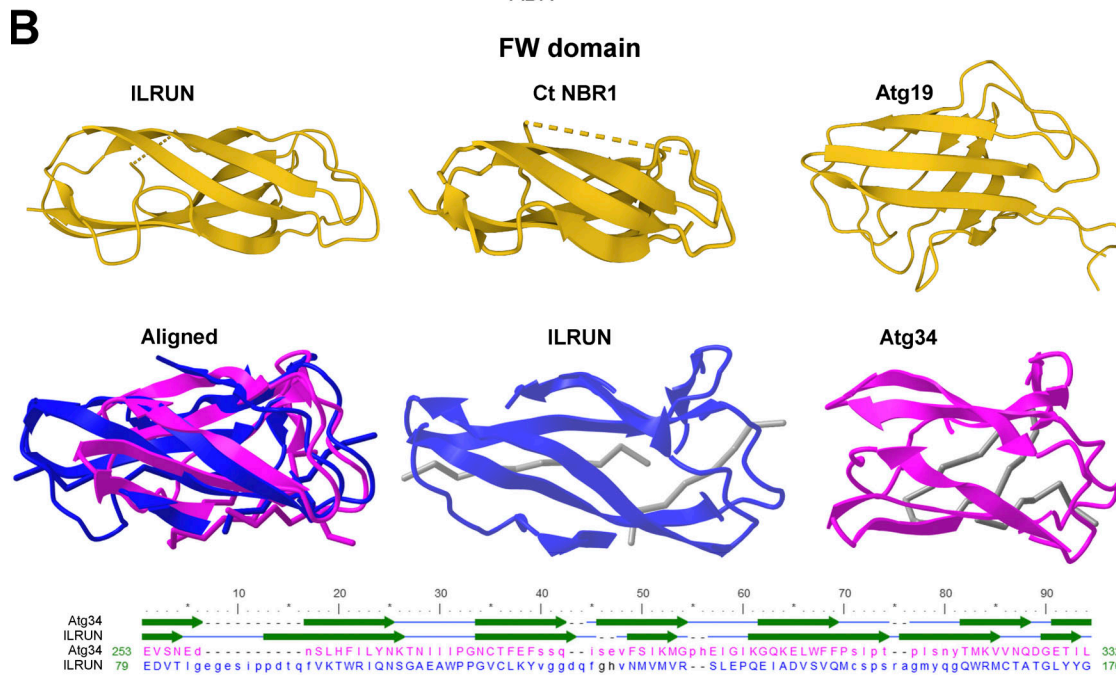
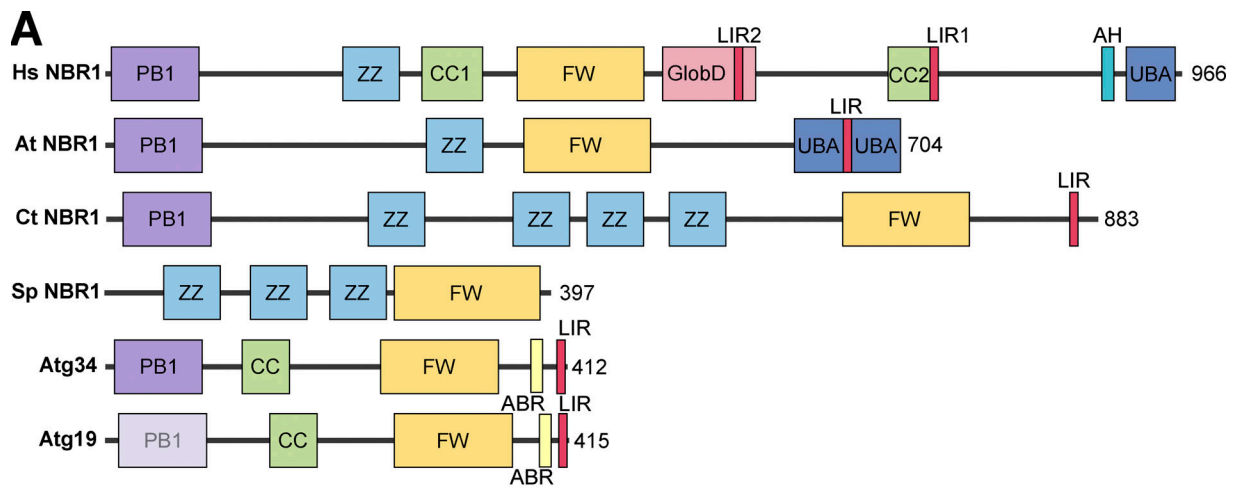


Figure 3. **The yeast Cvt receptor Atg19 and the paralog Atg34 are NBR1 homologs.** (A) Domain architecture of NBR1 homologs from humans, the plant *Arabidopsis thaliana*, the filamentous fungus *C. thermophilum*, fission yeast *S. pombe*, *S. cerevisiae* Atg19 and Atg34. (B) Comparison of FW domain structures between human ILRUN (PDB accession no. 6VHI), *C. thermophilum* (Ct NBR1; PDB accession no. 7VQO), and the ABD structures from yeast Atg19 (PDB accession no. 2KZB) and Atg34 (PDB accession no. 2KZK). Structural alignment of the ILRUN FW domain (blue) to the Atg34 ABD/FW domain (magenta) obtained

by a VAST search of the PDB database. A sequence alignment with positions of the structural elements (β strands) is shown below the structures. Despite only 7% sequence identity the alignment gives a root-mean-square deviation of 1.90 Å over a 60 amino acid sequence. **(C)** Atg34 contains a PB1 domain fold. The AlphaFold structure predicted with 90% confidence for the N-terminal domain of Atg34 (green) is a PB1 domain that can be structurally aligned to the solved structure (PDB accession no. 6TGN) of the PB1 domain of *Arabidopsis thaliana* (magenta). The structures were aligned using PyMol.

2013; Zhou et al., 2014). Upon high-temperature stress, plants require an equilibrium between poststress growth recovery and the establishment of heat stress memory (which relates to heat tolerance complexes being available during the early stages of a high-temperature event; Sedaghatmehr et al., 2019). The HSP90.1-ROF1 complex mediates the heat stress response through interaction with transcription factor HSF2A. A heat-responsive interaction between HSP90.1-ROF1 and HSF2A in the cytoplasm leads to nuclear translocation and activation of heat-responsive genes. AtNBR1-mediated selective autophagy of HSP90.1 and ROF1 mitigates the HSF2A-dependent response to high temperature (Thirumalaikumar et al., 2021). Consequently, the heat stress response is attenuated. The degradation of heat-responsive elements like HSP90.1 and ROF1 promotes recovery after heat stress but weakens heat stress memory.

Following viral infection, autophagy is often initiated to curtail a viral particle increase by delivering viruses or their components to the lysosomes for degradation, a process known as xenophagy. AtNBR1-dependent selective autophagic degradation of both non-assembled and particle-associated P4 (one of the six cauliflower mosaic virus [CaMV] viral proteins important for viral particle assembly) is ubiquitin-independent and restricts CaMV infection in a process resembling mammalian xenophagy (Hafren et al., 2017). Since particle functions are imperative for successful CaMV infection in plants, AtNBR1-mediated xenophagy counteracts infection establishment. Beyond targeting of non-assembled and particle-associated proteins, RNA silencing is regarded as the main antiviral defense mechanism in plants, and viral suppressors of RNA silencing (VSRs) have co-evolved to escape this mechanism (Boualem et al., 2016). AtNBR1 has been shown to degrade the viral RNA silencing suppressor helper component proteinase (HCpro) of the Turnip mosaic virus (TuMV) by targeting ubiquitinated potyvirus-induced RNA granules (PGs) for autophagic destruction (Hafren et al., 2018; Fig. 1 A).

Unlike viruses, bacteria generally do not enter plant cells due to the plant cell wall and turgor pressure. Instead, bacteria express effector proteins that can be translocated into the plant cells and they manipulate the host cell to promote infection (Khan et al., 2018). NBR1-mediated autophagy has been shown to counteract the pathogenic effect of the bacterial effector protein HopM1, thereby suppressing bacterial proliferation (Ustun et al., 2018). Recently, it was demonstrated that NBR1 directly targets and promotes the selective degradation of the effector protein XopL of the plant bacterium *Xanthomonas campestris* pv. *Vesicatoria* (Leong et al., 2022). XopL suppresses autophagy through its E3 ligase activity, while also being targeted by NBR1-mediated selective autophagy. Furthermore, NBR1 restricts oomycete *Phytophthora infestans* infection (Dagdas et al., 2018). These studies demonstrate the complexity of host-pathogen

interactions and an important role of NBR1 in counteracting infection in plants.

Aggrephagy—Roles of NBR1 in p62 bodies

Depletion of NBR1 inhibits the formation of p62 bodies (Kirkin et al., 2009). Human NBR1 binds to p62 by strong PB1-PB1 electrostatic interactions and competes with p62 polymerization, acting as a chain terminator. Hence, in vitro, the addition of NBR1 reduces filament length (Jakobi et al., 2020). The role of NBR1 may therefore be to regulate the length of p62 filaments in p62 bodies. By reducing filament length, NBR1 may promote the formation of p62 bodies since very long filaments are not easily packed into dynamic, phase-separated structures (Fig. 4 A). The addition of purified NBR1 increases in vitro phase separation of p62 upon mixing with ubiquitin (Zaffagnini et al., 2018). In mouse hepatocytes, the formation of p62 bodies is compromised by the loss of NBR1 and promoted by overexpression of NBR1 (Sanchez-Martin et al., 2020).

Using a combination of in vitro reconstitution assays and cell biological studies, NBR1 contributes to efficient cargo clustering in p62 bodies by bringing its high-affinity ubiquitin-binding UBA domain to the p62 filaments via PB1-PB1 interactions between NBR1 and p62 (Turco et al., 2021). NBR1 uses its FW domain to recruit TAX1BP1 to p62 filaments, and the core autophagy machinery component FIP200 of the ULK complex is recruited by both TAX1BP1 and by NBR1. The SKICH domain of TAX1BP1 (and NDP52) is known to bind to FIP200 (Ravenhill et al., 2019), while NBR1 binds to FIP200 via its CC2 domain (Turco et al., 2021; Fig. 4 B). Previously, it was shown that p62 bound to the C-terminal Claw domain of FIP200 (Turco et al., 2019). NBR1 also binds to the Claw domain, but much more strongly than p62, even somewhat stronger than TAX1BP1. However, TAX1BP1 is suggested to be the main recruiter of FIP200 to p62 bodies. The Claw domain in FIP200 is homologous to the C-terminal region of the yeast selective autophagy adaptor and Atg1 activator, Atg11 (Turco et al., 2019). The yeast NBR1 homolog, Atg19, recruits Atg11 by binding to this C-terminal region in Atg11 (Yorimitsu and Klionsky, 2005). Hence, the parallel here is clear between mammalian NBR1 and FIP200 and yeast Atg19 and Atg11. In contrast to p62 and NBR1, TAX1BP1 does not contribute directly to the formation of ubiquitin condensates in vitro (Turco et al., 2021) or in cells treated with puromycin that causes ubiquitinated protein aggregates to form in cells (Sarraf et al., 2020). However, TAX1BP1 is needed for the efficient autophagic degradation of these aggregates, and mice expressing a deletion mutant of TAX1BP1 that cannot bind ubiquitin show the accumulation of ubiquitin-conjugated proteins and Lipofuscin pathology (Sarraf et al., 2020). Upon ATG7-independent autophagy in K562 cells, NBR1 forms a heterotypic autophagy receptor complex with p62 and TAX1BP1 that requires TAX1BP1 to induce local autophagosome formation

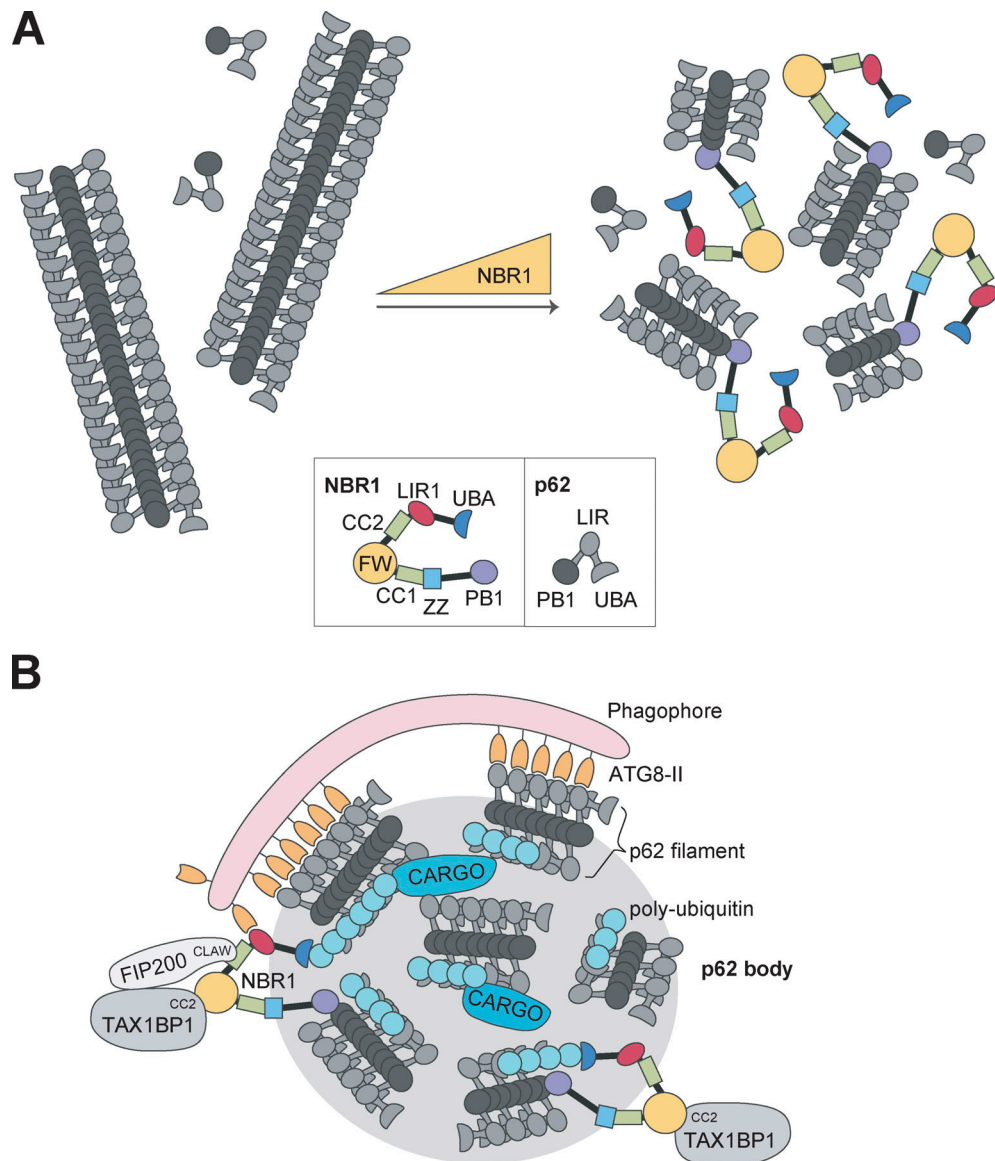


Figure 4. NBR1 collaborates with p62 in the formation of p62 bodies and with TAX1BP1 in the recruitment of core autophagy components to p62 bodies. (A) p62 forms long filaments in vitro as a result of PB1-mediated polymerization. Due to the monomeric nature of NBR1, it is hypothesized that NBR1 can act as a chain terminator of p62 filaments. With increasing amounts of NBR1 in vitro, the length of the p62 filaments is reduced. Shorter p62 filaments will likely form p62 bodies more easily. Therefore, a role for NBR1 in cells may be to promote p62 body formation by regulating p62 filament length. (B) The role for NBR1 in p62 body dynamics. NBR1 promotes p62 body formation by PB1-mediated regulation of p62 filament length and high-affinity ubiquitin binding. Furthermore, NBR1 facilitates autophagosome formation by recruiting TAX1BP1 and FIP200. FIP200 is recruited by direct binding between the FIP200 CLAW domain to the CC2 of NBR1. TAX1BP1 binds NBR1 FW domain via its CC2 domain and also recruits FIP200. NBR1 LIR1 also binds ATG8 proteins in the growing phagophore. In addition, NBR1 contains multiple domains that may be involved in cargo recruitment (UBA, ZZ, FW, AH).

(Ohnstad et al., 2020). TAX1BP1 binds to NBR1 via its CC2 domain. Taken together, these studies show that in human cells, a trio of SLRs work together for the efficient formation and degradation of p62 bodies. NBR1 affects p62 filament length by PB1 domain interactions, as well as recruitment of ubiquitinated cargo via the UBA domain, recruitment of TAX1BP1 via the FW domain, FIP200 via the CC2 domain, and ATG8s via the LIR1 domain (Fig. 4).

Phase separation of plant NBR1 has not been demonstrated experimentally. However, AtNBR1 ectopically expressed in HeLa cells or plant tissues form ubiquitin aggregates resembling those

formed by p62 (Svenning et al., 2011). We therefore believe that AtNBR1/p62 bodies represent a unique type of preautophagic structures or phagophore assembly sites (PAS) that are evolutionary conserved and formed in all eukaryotic cells expressing p62 or polymeric NBR1 orthologs.

A functionally distinct type of p62 bodies named dendritic aggresome-like induced structures (DALIS) are transiently formed by p62 in activated dendritic cells and involved in antigen processing (Lelouard et al., 2004; Lelouard et al., 2002). Ubiquitinated substrates recruited to DALIS, including defective ribosomal products (DRiPs), are either degraded by the

proteasome or by autophagy. NBR1 is not required for the formation of DALIS, but for their degradation by autophagy and antigen presentation via MHC class II, which may occur even in the absence of p62 (Arguello et al., 2016). In cells lacking NBR1, ubiquitinated substrates in DALIS are degraded by the proteasome, presumably depending on the solubilization of DALIS. Puromycin induction of p62 bodies in HeLa cells involving recruitment of ubiquitinated DRiPs into p62 bodies is highly dependent on NBR1 (Kirkin et al., 2009). While the degradation of p62 does not depend on NBR1, ubiquitinated proteins in p62 bodies are not degraded by autophagy in cells lacking NBR1 (Kirkin et al., 2009).

NBR1 is efficiently degraded by ATG7- and ATG8-dependent autophagy independent of p62 (Kirkin et al., 2009), but also ATG7-independent autophagy pathways exist for NBR1. The SLRs p62, NBR1, TAX1BP1, and NDP52 are degraded by endosomal microautophagy in response to acute starvation (Mejlvang et al., 2018). Degradation of NBR1 is in this case partially ATG7-independent. ATG7-independent degradation of NBR1 and TAX1BP1 requires direct interaction of NBR1 with TAX1BP1 (Ohnstad et al., 2020) and also depends on a SKICH-mediated binding of TAX1BP1 to FIP200 (Ravenhill et al., 2019; Thurston et al., 2016). Hence, the SLR-dependent recruitment of FIP200 allows ATG8-independent autophagy to occur to degrade NBR1 in the absence of functional conjugation machinery mediating lipidation of ATG8s (Ohnstad et al., 2020).

Pexophagy

NBR1 acts as a receptor for pexophagy in mammalian cells (Deosaran et al., 2013; Fig. 1 A). Interestingly, the NBR1 homolog in the filamentous ascomycete *Sordaria macrospora* is required for pexophagy, and human NBR1 can rescue growth defects under stress conditions when the fungal protein is lost (Werner et al., 2019). In *Arabidopsis*, pexophagy occurs independently of AtNBR1 (Young et al., 2019). We found that the amphipathic alpha-helix (AH) located immediately N-terminal to the UBA domain as well as the UBA, LIR, and CC domains of mammalian NBR1 are required for pexophagy. Coincident binding of the AH and UBA domains directs NBR1 to ubiquitinated peroxisomes and targets them for selective autophagy. Electron microscopy studies revealed that aggregates of overexpressed NBR1 contain clusters of 50-nm vesicles together with peroxisomes, autophagosomes, and some larger vesicle structures (possibly late endosomes; Deosaran et al., 2013). Endogenous p62 is recruited to NBR1 vesicle aggregates via its direct binding to NBR1. Its presence has a positive effect on NBR1-mediated pexophagy. However, pexophagy occurs also in the absence of p62, and p62 overexpression does not induce pexophagy (Deosaran et al., 2013).

Activation of the hypoxia-inducible factor HIF-2 α augments NBR1-mediated pexophagy, and peroxisome numbers are reduced in VHL-deficient human clear cell renal cell carcinomas with elevated levels of HIF-2 α (Walter et al., 2014). Overexpression of the peroxisomal membrane protein PEX3 increases NBR1-mediated pexophagy, but it is not ubiquitination of PEX3 as such that leads to increased pexophagy (Yamashita et al., 2014). SQSTM1/p62 was required only for the clustering of

peroxisomes. The peroxisomal E3 ubiquitin ligase peroxin 2 (PEX2) is upregulated upon amino acid starvation and rapamycin treatment. PEX2 expression induces ubiquitination of PEX5 and PMP70 on peroxisomes and boosts NBR1-dependent pexophagy (Sargent et al., 2016).

Xenophagy

Several soluble SLRs are involved in the autophagic clearance of invading pathogens, a process known as xenophagy (Goodall et al., 2022; Lamark and Johansen, 2021). Invading bacteria exposed in the cytosol become tagged with ubiquitin chains and sequestered into autophagosomes by ubiquitin-binding SLRs (Goodall et al., 2022). NBR1, NDP52, and p62 are recruited to intracytosolic *Mycobacterium tuberculosis* (Manzanillo et al., 2013) and *Shigella flexneri* (Mostowy et al., 2011; Fig. 1 A). In the case of *S. flexneri* infection, NBR1 is necessary to recruit p62 and NDP52; yet the mechanism and functional significance of this remains elusive (Mostowy et al., 2011). Upon infection with *M. tuberculosis*, both NBR1 and p62 are recruited in a parkin2-dependent manner (Manzanillo et al., 2013). NBR1, but not p62, can also be recruited by the HECT E3 ligase Smurf1 to *M. tuberculosis* (Franco et al., 2017). Mice depleted of either parkin2 or Smurf1 are more sensitive to *M. tuberculosis* infection, suggesting that both E3 ligases are important for the recruitment of SLRs and subsequent xenophagy (Franco et al., 2017; Manzanillo et al., 2013). Furthermore, the *M. tuberculosis* surface protein Rv1468c binds polyubiquitin chains and recruits SLRs, including NBR1, in a UBA-dependent manner (Chai et al., 2019). NBR1 is also recruited to group A Streptococcus (GAS)-containing vesicles in a Tollip-dependent manner. Tollip knockout prevents the recruitment of NBR1, NDP52, and TAX1BP1 to GAS-containing vesicles, yet p62 recruitment is unaffected (Lin et al., 2020).

Viruses utilize various strategies to manipulate host cell autophagy to their advantage (Liu et al., 2022). One such strategy involves NBR1-mediated autophagic degradation of the antiviral adaptor protein MAVS (Zeng et al., 2021). The basic polymerase 1 (PB1, not to be confused with the PB1 domain) of the H7N9 strain of influenza A virus promotes K27-polyubiquitination of MAVS and specifically recruits NBR1 to mediate enhanced MAVS degradation by autophagy, which further facilitates viral replication. Interestingly, the autophagic degradation of MAVS is dependent on ATG7, but does not require components of the ULK-complex. Some viruses, like Coxsackievirus, also counter the antiviral activity of both p62 and NBR1 by encoding proteases that cleave p62 and NBR1, releasing C-terminal fragments exerting dominant negative effects on endogenous p62 and NBR1 (Shi et al., 2014).

NBR1 and human disease

Proteinopathies

The giant protein titin acts as a scaffold for the assembly of the sarcomere and signaling complexes in muscle cells. Titin contains a serine/threonine kinase domain (TK) involved in mechanosensing (Puchner et al., 2008). NBR1 interacts with TK and recruits p62 and the E3 ligase MURF2 in active muscle, thereby regulating mechanical signaling and muscle gene transcription

(Lange et al., 2005). Analysis of two unrelated families with hereditary myopathy with early respiratory failure identified a mutation in the NBR1-interaction site within TK that disrupts NBR1 binding. NBR1 was more diffusely localized, p62 accumulated in many patient muscle samples, and MURF2 showed more nuclear localization, suggesting disruption of the NBR1-p62-MURF2 complex.

NBR1 function in aggrephagy may link it to diseases characterized by the accumulation of misfolded proteins. One such disease is sporadic inclusion body myositis (sIBM), a progressive degenerative myopathy that is the most common skeletal myopathy in older people. Pathological features of this disease include the accumulation of rimmed vacuoles (hence the name “inclusion body”) and misfolded protein aggregates in muscle fiber cells, indicating defects in autophagy and lysosomal degradation. Biopsies and cultured cells from sIBM patients show an increase in NBR1 protein, and NBR1 accumulation alongside p62 and LC3 in the ubiquitin-positive aggregates that are characteristic of this disease (D’Agostino et al., 2011). NBR1 is phosphorylated by GSK3B at Thr586, which promotes NBR1-mediated degradation of ubiquitinated proteins and prevents the formation of misfolded aggregates (Nicot et al., 2014). Meanwhile, in sIBM patient biopsies, NBR1 phosphorylation is reduced. This, in turn, prevents the clearance of ubiquitinated substrates, instead leading to the accumulation of misfolded proteins. NBR1 is also accumulated in Lewy bodies in Parkinson’s disease and glial cytoplasmic inclusions in multiple system atrophy (Odagiri et al., 2012). We also reported early on that NBR1 colocalized with p62 and ubiquitin in Mallory bodies in the liver of a patient with alcoholic steatohepatitis (Kirkin et al., 2009). However, given the cooperation of NBR1 and p62 in p62 bodies, it is often hard to distinguish NBR1-specific pathological effects.

NBR1 and cancer

Data from the Human Protein Atlas show that NBR1 mRNA is expressed in most cancers with low-cancer specificity (Uhlen et al., 2017). Recently, whole exome sequencing on germline DNA from a family presenting with different subtypes of renal cell carcinoma (RCC) identified a frameshift mutation in NBR1 (Adolphe et al., 2021). The mutation results in the expression of a truncated form of NBR1 that no longer includes LIR and UBA domains. While this does not affect the ability of NBR1 to interact with itself and with p62, overexpression of the truncated NBR1 delays the turnover of p62 and peroxisomes. The overexpression of truncated NBR1 increases the proliferation capacity of renal cancer cells compared with cells overexpressing WT NBR1. Exactly how NBR1 may affect RCC development is unclear and will require further studies. Some rare cases of RCC present with eosinophilic cytoplasmic inclusions, which are aggregates associated with membrane-bound, electron-dense organelles (Yu et al., 2018). These aggregates contain p62, NBR1, and other autophagy markers, and maybe the result of defects in autophagy. Strikingly, these aggregates are surrounded by clusters of peroxisomes only when NBR1 is present. While these inclusions are relatively rare in RCC, their presence is generally associated with larger tumors (Yu et al., 2018). However, the exact effects

of these inclusions and clustering of peroxisomes on tumor progression are not known.

In recent years, several comprehensive studies have revealed potentially unique roles for NBR1 in cancer development, independent of p62. In migrating cells, focal adhesions (FAs) are continuously assembled and disassembled to allow cell protrusion, adhesion, and contraction. NBR1 has a specific role as a selective autophagy receptor in the turnover of FAs at the leading edge of the cell during cell migration (Kenific et al., 2016; Fig. 1 A). Knockdown of NBR1, but not other SLRs, inhibited cell migration and increased FA lifetime. NBR1 localizes to FAs and recruits autophagosomes to FAs at the leading edge of the cell, targeting FAs for autophagosomal degradation and thereby promoting cell migration. This process may be hijacked by cancer cells to facilitate cancer metastasis. A more recent study investigated the role of autophagy in different stages of breast cancer development in a mouse model (Marsh et al., 2020). As expected, impairment of autophagy led to an accumulation of NBR1 and p62. Intriguingly, the accumulation of NBR1, but not p62, promoted the development of an aggressive subpopulation of tumor cells. Injection of tumor cells overexpressing NBR1 led to metastatic outgrowth, while overexpression of p62 did not. Knockdown of NBR1 in the autophagy-deficient cells reversed the metastatic phenotype otherwise observed upon autophagy inhibition alone. Even in autophagy-competent cells, the ectopic overexpression of NBR1 was sufficient to promote tumor metastasis. These results suggest that aberrant accumulation of NBR1 can promote metastatic outgrowth during breast cancer progression.

NBR1 plays a role in the immune evasion of pancreatic cancer cells. Cytotoxic T cells can detect and eliminate cancerous cells that present tumor antigens via MHC class I molecules on their surface. Consequently, many cancers evade the immune system through mutations or loss of MHC class I molecules. In pancreatic ductal adenocarcinomas (PDACs), MHC class I surface expression is often downregulated, but rarely due to mutations. In PDAC cells, MHC class I molecules are being degraded by NBR1-mediated selective autophagy, effectively preventing them from reaching the cell surface (Yamamoto et al., 2020; Fig. 1 A). Inhibition of autophagy increases both the total and cell surface expression of MHC class I in PDAC cells and further leads to increased antigen presentation, T-cell infiltration, and tumor cell killing. Of the SLRs tested, NBR1 was found to co-precipitate with MHC class I proteins, while p62, NDP52, TAX1BP1, and OPTN did not co-precipitate. Knockdown of NBR1 increases the total and surface levels of MHC class I molecules. Altogether, this supports a role for NBR1 in targeting MHC class I molecules for autophagic degradation, facilitating immune evasion of PDAC cells. More studies are required to probe for possible direct or indirect roles of NBR1 and other SLRs on the turnover of MHC class I in different normal and cancer cells.

Possible autophagy-independent roles of NBR1

NBR1 has been implicated in processes with no obvious link to autophagy, including the downregulation of receptor tyrosine kinases and inhibition of ERK1/2 (Mardakheh et al., 2010; Mardakheh et al., 2009). Several PBI domain-containing

proteins are implicated in the differentiation of activated T cells, including NBR1 and p62 (Martin et al., 2006; Yang et al., 2010). NBR1 is required for proper differentiation of T helper 2 cells. Whether this relates to the function of NBR1 as an autophagy receptor or potentially autophagy-independent functions is not known. NBR1 also acts as a regulator of JNK signaling and adipose tissue inflammation by engaging in a PB1–PB1 interaction with MEKK3 (Hernandez et al., 2014). Furthermore, p62 and NBR1 regulate PPAR γ –RXR α heterodimerization to control thermogenesis in brown adipocytes. NBR1 represses the activity of PPAR γ when p62 is inactivated. (Huang et al., 2021). NBR1 has been shown to deliver IL-12 to late endosomes in intestinal myeloid cells (Merkley et al., 2022).

NBR1 is reported to interact with activated p38 and limit its activity (Kim et al., 2019; Whitehouse et al., 2010). In mice, the expression of a truncated version of NBR1 that is unable to bind p38 and mitigate its activity results in an age-dependent increase in bone mass (Whitehouse et al., 2010). Furthermore, loss of NBR1 in both transformed and non-transformed cell lines causes cellular senescence because of p38-induced ER stress (Kim et al., 2019). Whether or not this negative regulation of p38 requires autophagy is not clear.

Concluding remarks and future questions/perspectives

NBR1 is the archetypal autophagy receptor, likely present as early as in the latest eukaryotic common ancestor. Gene duplication in the early metazoan lineage and subsequent molecular evolution gave rise to mammalian NBR1 and the much more studied paralog p62. Studies of NBR1 homologs in plants, fungi, and mammals are beginning to shed light on some of the unique roles of NBR1, gradually bringing it out of the shadow of p62. Structural and functional comparisons clearly suggest that yeast Atg19 and Atg34 are NBR1 homologs. NBR1 plays a central role in pexophagy in mammals, while its role in xenophagy is far better understood in plants than in mammals. Exciting new information has come from studies on the collaboration between p62, TAX1BP1, and NBR1 in the recruitment of core autophagy components to p62 bodies to facilitate autophagosome formation. Here, NBR1 plays a much more central role than anticipated. Important p62-independent roles of NBR1 in cancer metastasis and immune evasion in cancer have been revealed. NBR1 also has autophagy-independent roles in regulating signaling pathways and immune cell differentiation.

NBR1 is understudied and future research must address this. In future studies, a deeper understanding of the evolution and interplay between NBR1 and p62 may reveal further functions of NBR1, not only as a SAR but also in regulating the dynamics of p62 bodies. Very likely, new autophagic substrates unique to NBR1 will be discovered. It will be important to penetrate more mechanisms of pexophagy and xenophagy involving NBR1. Studies of fungal NBR1 homologs ask the question if there are analogous roles of mammalian NBR1 in pathways similar to the Cvt and NVT pathways. Further elucidation of pathophysiological roles of NBR1 in human disease is required to evaluate NBR1 as a potential target for therapeutic strategies in cancer and proteinopathies.

Acknowledgments

The authors thank all researchers who contributed data and discoveries mentioned here. We apologize to colleagues whose work was not cited due to space limitations.

Research in the lab of T. Johansen is supported by grant 190214 from Norwegian Cancer Society and grant 249884 from The Research Council of Norway to T. Johansen.

The authors declare no competing financial interests.

Submitted: 17 August 2022

Revised: 3 October 2022

Accepted: 3 October 2022

References

- Adolphe, F., S. Ferlicot, V. Verkarre, K. Posseme, S. Couve, P. Garnier, N. Droin, M. Deloger, B. Job, S. Giraud, et al. 2021. Germline mutation in the NBR1 gene involved in autophagy detected in a family with renal tumors. *Cancer Genet.* 258–259:51–56. <https://doi.org/10.1016/j.cancerogen.2021.07.003>
- Arguello, R.J., M. Reverendo, E. Gatti, and P. Pierre. 2016. Regulation of protein synthesis and autophagy in activated dendritic cells: Implications for antigen processing and presentation. *Immunol. Rev.* 272: 28–38. <https://doi.org/10.1111/imr.12427>
- Boualem, A., C. Dogimont, and A. Bendahmane. 2016. The battle for survival between viruses and their host plants. *Curr. Opin. Virol.* 17:32–38. <https://doi.org/10.1016/j.coviro.2015.12.001>
- Burki, F., A.J. Roger, M.W. Brown, and A.G.B. Simpson. 2020. The new tree of eukaryotes. *Trends Ecol. Evol.* 35:43–55. <https://doi.org/10.1016/j.tree.2019.08.008>
- Cha-Molstad, H., J.E. Yu, Z. Feng, S.H. Lee, J.G. Kim, P. Yang, B. Han, K.W. Sung, Y.D. Yoo, J. Hwang, et al. 2017. p62/SQSTM1/Sequestosome-1 is an N-recognition of the N-end rule pathway which modulates autophagosome biogenesis. *Nat. Commun.* 8:102. <https://doi.org/10.1038/s41467-017-00085-7>
- Chai, Q., X. Wang, L. Qiang, Y. Zhang, P. Ge, Z. Lu, Y. Zhong, B. Li, J. Wang, L. Zhang, et al. 2019. A Mycobacterium tuberculosis surface protein recruits ubiquitin to trigger host xenophagy. *Nat. Commun.* 10:1973. <https://doi.org/10.1038/s41467-019-09955-8>
- Chang, C., L.E. Jensen, and J.H. Hurley. 2021. Autophagosome biogenesis comes out of the black box. *Nat. Cell Biol.* 23:450–456. <https://doi.org/10.1038/s41556-021-00669-y>
- Cho, N.H., K.C. Cheveralls, A.D. Brunner, K. Kim, A.C. Michaelis, P. Raghavan, H. Kobayashi, L. Savy, J.Y. Li, H. Canaj, et al. 2022. OpenCell: Endogenous tagging for the cartography of human cellular organization. *Science.* 375:eabi6983. <https://doi.org/10.1126/science.abi6983>
- Ciuffa, R., T. Lamark, A.K. Tarafder, A. Guesdon, S. Rybina, W.J. Hagen, T. Johansen, and C. Sachse. 2015. The selective autophagy receptor p62 forms a flexible filamentous helical scaffold. *Cell Rep.* 11:748–758. <https://doi.org/10.1016/j.celrep.2015.03.062>
- D'Agostino, C., A. Nogalska, M. Cacciottolo, W.K. Engel, and V. Askanas. 2011. Abnormalities of NBR1, a novel autophagy-associated protein, in muscle fibers of sporadic inclusion-body myositis. *Acta Neuropathol.* 122: 627–636. <https://doi.org/10.1007/s00401-011-0874-3>
- Dagdas, Y.F., P. Pandey, Y. Tumbas, N. Sanguankiatichai, K. Belhaj, C. Dugan, A.Y. Leary, M.E. Segretin, M.P. Contreras, Z. Savage, et al. 2018. Host autophagy machinery is diverted to the pathogen interface to mediate focal defense responses against the Irish potato famine pathogen. *Elife.* 7:e37476. <https://doi.org/10.7554/eLife.37476>
- Deosaran, E., K.B. Larsen, R. Hua, G. Sargent, Y. Wang, S. Kim, T. Lamark, M. Jauregui, K. Law, J. Lippincott-Schwartz, et al. 2013. NBR1 acts as an autophagy receptor for peroxisomes. *J. Cell Sci.* 126:939–952. <https://doi.org/10.1242/jcs.114819>
- Deretic, V. 2012. Autophagy as an innate immunity paradigm: Expanding the scope and repertoire of pattern recognition receptors. *Curr. Opin. Immunol.* 24:21–31. <https://doi.org/10.1016/j.coi.2011.10.006>
- Franco, L.H., V.R. Nair, C.R. Scharn, R.J. Xavier, J.R. Torrealba, M.U. Shiloh, and B. Levine. 2017. The ubiquitin ligase Smurf1 functions in selective autophagy of Mycobacterium tuberculosis and anti-tuberculous host

- defense. *Cell Host Microbe*. 22:421–423. <https://doi.org/10.1016/j.chom.2017.08.005>
- Goodall, E.A., F. Kraus, and J.W. Harper. 2022. Mechanisms underlying ubiquitin-driven selective mitochondrial and bacterial autophagy. *Mol. Cell*. 82:1501–1513. <https://doi.org/10.1016/j.molcel.2022.03.012>
- Hafren, A., J.L. Macia, A.J. Love, J.J. Milner, M. Drucker, and D. Hofius. 2017. Selective autophagy limits cauliflower mosaic virus infection by NBRI-mediated targeting of viral capsid protein and particles. *Proc. Natl. Acad. Sci. USA*. 114:E2026–E2035. <https://doi.org/10.1073/pnas.1610687114>
- Hafren, A., S. Ustun, A. Hochmuth, S. Svenning, T. Johansen, and D. Hofius. 2018. Turnip mosaic virus counteracts selective autophagy of the viral silencing suppressor HCpro. *Plant Physiol*. 176:649–662. <https://doi.org/10.1104/pp.17.01198>
- Hama, Y., S. Zhang, and N. Mizushima. 2021. ZZ domains keep cytosol to vacuole delivery whiZZing along. *EMBO J*. 40:e108777. <https://doi.org/10.15252/emj.2021108777>
- Hernandez, E.D., S.J. Lee, J.Y. Kim, A. Duran, J.F. Linares, T. Yajima, T.D. Muller, M.H. Tschop, S.R. Smith, M.T. Diaz-Meco, and J. Moscat. 2014. A macrophage NBRI-MEKK3 complex triggers JNK-mediated adipose tissue inflammation in obesity. *Cell Metabol*. 20:499–511. <https://doi.org/10.1016/j.cmet.2014.06.008>
- Huang, J., J.F. Linares, A. Duran, W. Xia, A.R. Saltiel, T.D. Muller, M.T. Diaz-Meco, and J. Moscat. 2021. NBRI is a critical step in the repression of thermogenesis of p62-deficient adipocytes through PPAR γ . *Nat. Commun*. 12:2876. <https://doi.org/10.1038/s41467-021-23085-0>
- Isakson, P., A.H. Lystad, K. Breen, G. Koster, H. Stenmark, and A. Simonsen. 2013. TRAF6 mediates ubiquitination of KIF23/MKLP1 and is required for midbody ring degradation by selective autophagy. *Autophagy*. 9:1955–1964. <https://doi.org/10.4161/auto.26085>
- Jakobi, A.J., S.T. Huber, S.A. Mortensen, S.W. Schultz, A. Palara, T. Kuhm, B.K. Shrestha, T. Lamark, W.J.H. Hagen, M. Wilmanns, et al. 2020. Structural basis of p62/SQSTM1 helical filaments and their role in cellular cargo uptake. *Nat. Commun*. 11:440. <https://doi.org/10.1038/s41467-020-14343-8>
- Ji, C., J. Zhou, R. Guo, Y. Lin, C.H. Kung, S. Hu, W.Y. Ng, X. Zhuang, and L. Jiang. 2020. AtNBRI is a selective autophagic receptor for AtExo70E2 in Arabidopsis. *Plant Physiol*. 184:777–791. <https://doi.org/10.1104/pp.20.00470>
- Johansen, T., and T. Lamark. 2020. Selective autophagy: ATG8 family proteins, LIR motifs and cargo receptors. *J. Mol. Biol*. 432:80–103. <https://doi.org/10.1016/j.jmb.2019.07.016>
- Jumper, J., R. Evans, A. Pritzel, T. Green, M. Figurnov, O. Ronneberger, K. Tunyasuvunakool, R. Bates, A. Zidek, A. Potapenko, et al. 2021. Highly accurate protein structure prediction with AlphaFold. *Nature*. 596:583–589. <https://doi.org/10.1038/s41586-021-03819-2>
- Kenific, C.M., S.J. Stehbens, J. Goldsmith, A.M. Leidal, N. Faure, J. Ye, T. Wittmann, and J. Debnath. 2016. NBRI enables autophagy-dependent focal adhesion turnover. *J. Cell Biol*. 212:577–590. <https://doi.org/10.1083/jcb.201503075>
- Khan, M., D. Seto, R. Subramaniam, and D. Desveaux. 2018. Oh, the places they'll go! A survey of phytopathogen effectors and their host targets. *Plant J*. 93:651–663. <https://doi.org/10.1111/tpj.13780>
- Kim, H.S., Y. Kim, M.J. Lim, Y.G. Park, S.I. Park, and J. Sohn. 2019. The p38-activated ER stress-ATF6 α axis mediates cellular senescence. *FASEB J*. 33:2422–2434. <https://doi.org/10.1096/fj.201800836R>
- King, N., M.J. Westbrook, S.L. Young, A. Kuo, M. Abedin, J. Chapman, S. Fairclough, U. Hellsten, Y. Isogai, I. Letunic, et al. 2008. The genome of the choanoflagellate *Monosiga brevicollis* and the origin of metazoans. *Nature*. 451:783–788. <https://doi.org/10.1038/nature06617>
- Kirkin, V., T. Lamark, Y.S. Sou, G. Bjorkoy, J.L. Nunn, J.A. Bruun, E. Shvets, D.G. McEwan, T.H. Clausen, P. Wild, et al. 2009. A role for NBRI in autophagosomal degradation of ubiquitinated substrates. *Mol. Cell*. 33:505–516. <https://doi.org/10.1016/j.molcel.2009.01.020>
- Kraft, C., M. Peter, and K. Hofmann. 2010. Selective autophagy: Ubiquitin-mediated recognition and beyond. *Nat. Cell Biol*. 12:836–841. <https://doi.org/10.1038/ncb0910-836>
- Kuo, T.C., C.T. Chen, D. Baron, T.T. Onder, S. Loewer, S. Almeida, C.M. Weismann, P. Xu, J.M. Houghton, F.B. Gao, et al. 2011. Midbody accumulation through evasion of autophagy contributes to cellular reprogramming and tumorigenicity. *Nat. Cell Biol*. 13:1214–1223. <https://doi.org/10.1038/ncb2332>
- Lamark, T., and T. Johansen. 2021. Mechanisms of selective autophagy. *Annu. Rev. Cell Dev. Biol*. 37:143–169. <https://doi.org/10.1146/annurev-cellbio-120219-035530>
- Lamark, T., M. Perander, H. Outzen, K. Kristiansen, A. Øvervatn, E. Michaelsen, G. Bjørkøy, and T. Johansen. 2003. Interaction codes within the family of mammalian Phox and Bem1p domain-containing proteins. *J. Biol. Chem*. 278:34568–34581. <https://doi.org/10.1074/jbc.M303221200>
- Lange, S., F. Xiang, A. Yakovenko, A. Vihola, P. Hackman, E. Rostkova, J. Kristensen, B. Brandmeier, G. Franzen, B. Hedberg, et al. 2005. The kinase domain of titin controls muscle gene expression and protein turnover. *Science*. 308:1599–1603. <https://doi.org/10.1126/science.1110463>
- Leber, R., E. Silles, I.V. Sandoval, and M.J. Mazon. 2001. Yol082p, a novel CVT protein involved in the selective targeting of aminopeptidase I to the yeast vacuole. *J. Biol. Chem*. 276:29210–29217. <https://doi.org/10.1074/jbc.M101438200>
- Lelouard, H., V. Ferrand, D. Marguet, J. Bania, V. Camosseto, A. David, E. Gatti, and P. Pierre. 2004. Dendritic cell aggresome-like induced structures are dedicated areas for ubiquitination and storage of newly synthesized defective proteins. *J. Cell Biol*. 164:667–675. <https://doi.org/10.1083/jcb.200312073>
- Lelouard, H., E. Gatti, F. Cappello, O. Gresser, V. Camosseto, and P. Pierre. 2002. Transient aggregation of ubiquitinated proteins during dendritic cell maturation. *Nature*. 417:177–182. <https://doi.org/10.1038/417177a>
- Leong, J.X., M. Rafféiner, D. Spinti, G. Langin, M. Franz-Wachtel, A.R. Guzman, J.G. Kim, P. Pandey, A.E. Minina, B. Macek, et al. 2022. A bacterial effector counteracts host autophagy by promoting degradation of an autophagy component. *EMBO J*. 41:e110352. <https://doi.org/10.15252/emj.202110352>
- Letunic, I., R.R. Copley, B. Pils, S. Pinkert, J. Schultz, and P. Bork. 2006. SMART 5: Domains in the context of genomes and networks. *Nucleic Acids Res*. 34:D257–D260. <https://doi.org/10.1093/nar/gkj079>
- Li, X., Q. Xia, M. Mao, H. Zhou, L. Zheng, Y. Wang, Z. Zeng, L. Yan, Y. Zhao, and J. Shi. 2021. Annexin-A1 SUMOylation regulates microglial polarization after cerebral ischemia by modulating IKK α stability via selective autophagy. *Sci. Adv*. 7:eabc5539. <https://doi.org/10.1126/sciadv.abc5539>
- Lin, C.Y., T. Nozawa, A. Minowa-Nozawa, H. Toh, M. Hikichi, J. Iibushi, and I. Nakagawa. 2020. Autophagy receptor Tollip facilitates bacterial autophagy by recruiting galectin-7 in response to group A Streptococcus infection. *Front. Cell. Infect. Microbiol*. 10:583137. <https://doi.org/10.3389/fcimb.2020.583137>
- Lin, Q., Q. Dai, H. Meng, A. Sun, J. Wei, K. Peng, C. Childress, M. Chen, G. Shao, and W. Yang. 2017. The HECT E3 ubiquitin ligase NEDD4 interacts with and ubiquitylates SQSTM1 for inclusion body autophagy. *J. Cell Sci*. 130:3839–3850. <https://doi.org/10.1242/jcs.207068>
- Liu, X.M., L.L. Sun, W. Hu, Y.H. Ding, M.Q. Dong, and L.L. Du. 2015. ESCRTs cooperate with a selective autophagy receptor to mediate vacuolar targeting of soluble cargos. *Mol. Cell*. 59:1035–1042. <https://doi.org/10.1016/j.molcel.2015.07.034>
- Liu, Y., T. Zhou, J. Hu, S. Jin, J. Wu, X. Guan, Y. Wu, and J. Cui. 2022. Targeting selective autophagy as a therapeutic strategy for viral infectious diseases. *Front. Microbiol*. 13:889835. <https://doi.org/10.3389/fmicb.2022.889835>
- Lu, S., J. Wang, F. Chitsaz, M.K. Derbyshire, R.C. Geer, N.R. Gonzales, M. Gwadz, D.I. Hurwitz, G.H. Marchler, J.S. Song, et al. 2020. CDD/SPARCLE: The conserved domain database in 2020. *Nucleic Acids Res*. 48:D265–D268. <https://doi.org/10.1093/nar/gkz991>
- Lystad, A.H., and A. Simonsen. 2019. Mechanisms and pathophysiological roles of the ATG8 conjugation machinery. *Cells*. 8:973. <https://doi.org/10.3390/cells8090973>
- Manzanillo, P.S., J.S. Ayres, R.O. Watson, A.C. Collins, G. Souza, C.S. Rae, D.S. Schneider, K. Nakamura, M.U. Shiloh, and J.S. Cox. 2013. The ubiquitin ligase parkin mediates resistance to intracellular pathogens. *Nature*. 501:512–516. <https://doi.org/10.1038/nature12566>
- Marchbank, K., S. Waters, R.G. Roberts, E. Solomon, and C.A. Whitehouse. 2012. MAP1B interaction with the FW domain of the autophagic receptor Nbr1 facilitates its association to the microtubule network. *Int. J. Cell Biol*. 2012:208014. <https://doi.org/10.1155/2012/208014>
- Mardakheh, F.K., G. Auciello, T.R. Dafforn, J.Z. Rappoport, and J.K. Heath. 2010. Nbr1 is a novel inhibitor of ligand-mediated receptor tyrosine kinase degradation. *Mol. Cell Biol*. 30:5672–5685. <https://doi.org/10.1128/MCB.00878-10>
- Mardakheh, F.K., M. Yekezare, L.M. Machesky, and J.K. Heath. 2009. Spred2 interaction with the late endosomal protein NBRI down-regulates fibroblast growth factor receptor signaling. *J. Cell Biol*. 187:265–277. <https://doi.org/10.1083/jcb.200905118>
- Marsh, T., C.M. Kenific, D. Suresh, H. Gonzalez, E.R. Shamir, W. Mei, A. Tankka, A.M. Leidal, S. Kalavacherla, K. Woo, et al. 2020. Autophagic degradation of NBRI restricts metastatic outgrowth during mammary tumor progression. *Dev. Cell*. 52:591–604.e6. <https://doi.org/10.1016/j.devcel.2020.01.025>

- Martin, P., M.T. Diaz-Meco, and J. Moscat. 2006. The signaling adapter p62 is an important mediator of T helper 2 cell function and allergic airway inflammation. *EMBO J.* 25:3524–3533. <https://doi.org/10.1038/sj.emboj.7601250>
- Mejlvang, J., H. Olsvik, S. Svenning, J.A. Bruun, Y.P. Abudu, K.B. Larsen, A. Brech, T.E. Hansen, H. Brenne, T. Hansen, et al. 2018. Starvation induces rapid degradation of selective autophagy receptors by endosomal microautophagy. *J. Cell Biol.* 217:3640–3655. <https://doi.org/10.1083/jcb.201711002>
- Merkley, S.D., S.M. Goodfellow, Y. Guo, Z.E.R. Wilton, J.R. Byrum, K.C. Schwalm, D.L. Dinwiddie, R.R. Gullapalli, V. Deretic, A. Jimenez Hernandez, et al. 2022. Non-autophagy role of Atg5 and NBR1 in unconventional secretion of IL-12 prevents gut dysbiosis and inflammation. *J. Crohn's Colitis.* 16:259–274. <https://doi.org/10.1093/ecco-jcc/jjab144>
- Mizushima, N., T. Yoshimori, and Y. Ohsumi. 2011. The role of Atg proteins in autophagosome formation. *Annu. Rev. Cell Dev. Biol.* 27:107–132. <https://doi.org/10.1146/annurev-cellbio-092910-154005>
- Mostoway, S., V. Sancho-Shimizu, M.A. Hamon, R. Simeone, R. Brosch, T. Johansen, and P. Cossart. 2011. p62 and NDP52 proteins target intracytosolic Shigella and Listeria to different autophagy pathways. *J. Biol. Chem.* 286:26987–26995. <https://doi.org/10.1074/jbc.M111.223610>
- Nicot, A.S., F. Lo Verso, F. Ratti, F. Pilot-Storck, N. Streichenberger, M. Sandri, L. Schaeffer, and E. Goillot. 2014. Phosphorylation of NBR1 by GSK3 modulates protein aggregation. *Autophagy.* 10:1036–1053. <https://doi.org/10.4161/auto.28479>
- Nthiga, T.M., B. Kumar Shrestha, E. Sjøttem, J.A. Bruun, K. Bowitz Larsen, Z. Bhujabal, T. Lamark, and T. Johansen. 2020. CALCOCO1 acts with VAMP-associated proteins to mediate ER-phagy. *EMBO J.* 39:e103649. <https://doi.org/10.15252/embj.2019103649>
- Odagiri, S., K. Tanji, F. Mori, A. Kakita, H. Takahashi, and K. Wakabayashi. 2012. Autophagic adapter protein NBR1 is localized in Lewy bodies and glial cytoplasmic inclusions and is involved in aggregate formation in alpha-synucleinopathy. *Acta Neuropathol.* 124:173–186. <https://doi.org/10.1007/s00401-012-0975-7>
- Ohnstad, A.E., J.M. Delgado, B.J. North, I. Nasa, A.N. Kettenbach, S.W. Schultz, and C.J. Shoemaker. 2020. Receptor-mediated clustering of FIP200 bypasses the role of LC3 lipidation in autophagy. *EMBO J.* 39:e104948. <https://doi.org/10.15252/embj.2020104948>
- Puchner, E.M., A. Alexandrovich, A.L. Kho, U. Hensen, L.V. Schafer, B. Brandmeier, F. Grater, H. Grubmuller, H.E. Gaub, and M. Gautel. 2008. Mechanoenzymatics of titin kinase. *Proc. Natl. Acad. Sci. USA.* 105:13385–13390. <https://doi.org/10.1073/pnas.0805034105>
- Ravenshill, B.J., K.B. Boyle, N. von Muhlinen, C.J. Ellison, G.R. Masson, E.G. Otten, A. Foeglein, R. Williams, and F. Randow. 2019. The cargo receptor NDP52 initiates selective autophagy by recruiting the ULK complex to cytosol-invading bacteria. *Mol. Cell.* 74:320–329.e6. <https://doi.org/10.1016/j.molcel.2019.01.041>
- Ruiz-Trillo, I., Y. Inagaki, L.A. Davis, S. Sperstad, B. Landfald, and A.J. Roger. 2004. Capsaspora owczarzakii is an independent opisthokont lineage. *Curr. Biol.* 14:R946–R947. <https://doi.org/10.1016/j.cub.2004.10.037>
- Sanchez-Martin, P., Y.S. Sou, S. Kageyama, M. Koike, S. Waguri, and M. Komatsu. 2020. NBR1-mediated p62-liquid droplets enhance the Keap1-Nrf2 system. *EMBO Rep.* 21:e48902. <https://doi.org/10.15252/embr.201948902>
- Sargent, G., T. van Zutphen, T. Shatseva, L. Zhang, V. Di Giovanni, R. Bandsma, and P.K. Kim. 2016. PEX2 is the E3 ubiquitin ligase required for pexophagy during starvation. *J. Cell Biol.* 214:677–690. <https://doi.org/10.1083/jcb.201511034>
- Sarraf, S.A., H.V. Shah, G. Kanfer, A.M. Pickrell, L.A. Holtzclaw, M.E. Ward, and R.J. Youle. 2020. Loss of TAX1BP1-directed autophagy results in protein aggregate accumulation in the brain. *Mol. Cell.* 80:779–795.e10. <https://doi.org/10.1016/j.molcel.2020.10.041>
- Scott, S.V., J. Guan, M.U. Hutchins, J. Kim, and D.J. Klionsky. 2001. Cvt19 is a receptor for the cytoplasm-to-vacuole targeting pathway. *Mol. Cell.* 7:1131–1141. [https://doi.org/10.1016/s1097-2765\(01\)00263-5](https://doi.org/10.1016/s1097-2765(01)00263-5)
- Sedaghatmehr, M., V.P. Thirumalaikumar, I. Kamranfar, A. Marmagne, C. Masclaux-Daubresse, and S. Balazadeh. 2019. A regulatory role of autophagy for resetting the memory of heat stress in plants. *Plant Cell Environ.* 42:1054–1064. <https://doi.org/10.1111/pce.13426>
- Shi, J., G. Fung, P. Piesik, J. Zhang, and H. Luo. 2014. Dominant-negative function of the C-terminal fragments of NBR1 and SQSTM1 generated during enteroviral infection. *Cell Death Differ.* 21:1432–1441. <https://doi.org/10.1038/cdd.2014.58>
- Spang, A., T.A. Mahendrarajah, P. Offre, and C.W. Stairs. 2022. Evolving perspective on the origin and diversification of cellular life and the virosphere. *Genome Biol. Evol.* 14:evac034. <https://doi.org/10.1093/gbe/evac034>
- Sun, D., R. Wu, J. Zheng, P. Li, and L. Yu. 2018. Polyubiquitin chain-induced p62 phase separation drives autophagic cargo segregation. *Cell Res.* 28:405–415. <https://doi.org/10.1038/s41422-018-0017-7>
- Suzuki, K., C. Kondo, M. Morimoto, and Y. Ohsumi. 2010. Selective transport of alpha-mannosidase by autophagic pathways: Identification of a novel receptor, Atg34p. *J. Biol. Chem.* 285:30019–30025. <https://doi.org/10.1074/jbc.M110.143511>
- Svenning, S., T. Lamark, K. Krause, and T. Johansen. 2011. Plant NBR1 is a selective autophagy substrate and a functional hybrid of the mammalian autophagic adapters NBR1 and p62/SQSTM1. *Autophagy.* 7:993–1010. <https://doi.org/10.4161/auto.7.9.16389>
- Thirumalaikumar, V.P., M. Gorka, K. Schulz, C. Masclaux-Daubresse, A. Sampathkumar, A. Skirycz, R.D. Vierstra, and S. Balazadeh. 2021. Selective autophagy regulates heat stress memory in Arabidopsis by NBR1-mediated targeting of HSP90.1 and ROF1. *Autophagy.* 17:2184–2199. <https://doi.org/10.1080/15548627.2020.1820778>
- Thurston, T.L., K.B. Boyle, M. Allen, B.J. Ravenhill, M. Karpiyevich, S. Bloor, A. Kaul, J. Noad, A. Foeglein, S.A. Matthews, et al. 2016. Recruitment of TBK1 to cytosol-invading Salmonella induces WIPI2-dependent antibacterial autophagy. *EMBO J.* 35:1779–1792. <https://doi.org/10.15252/embj.201694491>
- Turco, E., A. Savova, F. Gere, L. Ferrari, J. Romanov, M. Schuschnig, and S. Martens. 2021. Reconstitution defines the roles of p62, NBR1 and TAX1BP1 in ubiquitin condensate formation and autophagy initiation. *Nat. Commun.* 12:5212. <https://doi.org/10.1038/s41467-021-25572-w>
- Turco, E., M. Witt, C. Abert, T. Bock-Bierbaum, M.Y. Su, R. Trapannone, M. Sztacho, A. Danieli, X. Shi, G. Zaffagnini, et al. 2019. FIP200 Claw domain binding to p62 promotes autophagosome formation at ubiquitin condensates. *Mol. Cell.* 74:330–346.e11. <https://doi.org/10.1016/j.molcel.2019.01.035>
- Uhlen, M., L. Fagerberg, B.M. Hallstrom, C. Lindskog, P. Oksvold, A. Mardinnoglu, A. Sivertsson, C. Kampf, E. Sjostedt, A. Asplund, et al. 2015. Proteomics. Tissue-based map of the human proteome. *Science.* 347:1260419. <https://doi.org/10.1126/science.1260419>
- Uhlen, M., C. Zhang, S. Lee, E. Sjostedt, L. Fagerberg, G. Bidkhorji, R. Benfeitas, M. Arif, Z. Liu, F. Edfors, et al. 2017. A pathology atlas of the human cancer transcriptome. *Science.* 357:eaan2507. <https://doi.org/10.1126/science.aan2507>
- Ustun, S., A. Hafren, Q. Liu, R.S. Marshall, E.A. Minina, P.V. Bozhkov, R.D. Vierstra, and D. Hofius. 2018. Bacteria exploit autophagy for proteasome degradation and enhanced virulence in plants. *Plant Cell.* 30:668–685. <https://doi.org/10.1105/tpc.17.00815>
- Ustun, S., and D. Hofius. 2018. Anti- and pro-microbial roles of autophagy in plant-bacteria interactions. *Autophagy.* 14:1465–1466. <https://doi.org/10.1080/15548627.2018.1475817>
- Varadi, M., S. Anyango, M. Deshpande, S. Nair, C. Natassia, G. Yordanova, D. Yuan, O. Stroe, G. Wood, A. Laydon, et al. 2022. AlphaFold protein structure database: Massively expanding the structural coverage of protein-sequence space with high-accuracy models. *Nucleic Acids Res.* 50:D439–D444. <https://doi.org/10.1093/nar/gkab1061>
- Walter, K.M., M.J. Schonenberger, M. Trotschmuller, M. Horn, H.P. Elsasser, A.B. Moser, M.S. Lucas, T. Schwarz, P.A. Gerber, P.L. Faust, et al. 2014. Hif-2 α promotes degradation of mammalian peroxisomes by selective autophagy. *Cell Metabol.* 20:882–897. <https://doi.org/10.1016/j.cmet.2014.09.017>
- Wang, M., C.J. Herrmann, M. Simonovic, D. Szklarczyk, and C. von Mering. 2015. Version 4.0 of PaxDb: Protein abundance data, integrated across model organisms, tissues, and cell lines. *Proteomics.* 15:3163–3168. <https://doi.org/10.1002/pmic.201400441>
- Wang, Y.Y., J. Zhang, X.M. Liu, Y. Li, J. Sui, M.Q. Dong, K. Ye, and L.L. Du. 2021. Molecular and structural mechanisms of ZZ domain-mediated cargo selection by Nbr1. *EMBO J.* 40:e107497. <https://doi.org/10.15252/embj.2020107497>
- Watanabe, Y., N.N. Noda, H. Kumeta, K. Suzuki, Y. Ohsumi, and F. Inagaki. 2010. Selective transport of alpha-mannosidase by autophagic pathways: Structural basis for cargo recognition by Atg19 and Atg34. *J. Biol. Chem.* 285:30026–30033. <https://doi.org/10.1074/jbc.M110.143545>
- Waters, S., K. Marchbank, E. Solomon, C. Whitehouse, and M. Gautel. 2009. Interactions with LC3 and polyubiquitin chains link nbr1 to autophagic protein turnover. *FEBS Lett.* 583:1846–1852. <https://doi.org/10.1016/j.febslet.2009.04.049>
- Werner, A., B. Herzog, O. Voigt, O. Valerius, G.H. Braus, and S. Poggeler. 2019. NBR1 is involved in selective pexophagy in filamentous ascomycetes and can be functionally replaced by a tagged version of its human

- homolog. *Autophagy*. 15:78–97. <https://doi.org/10.1080/15548627.2018.1507440>
- Whitehouse, C.A., S. Waters, K. Marchbank, A. Horner, N.W.A. McGowan, J.V. Jovanovic, G.M. Xavier, T.G. Kashima, M.T. Cobourne, G.O. Richards, et al. 2010. Neighbor of Brca1 gene (Nbr1) functions as a negative regulator of postnatal osteoblastic bone formation and p38 MAPK activity. *Proc. Natl. Acad. Sci. USA*. 107:12913–12918. <https://doi.org/10.1073/pnas.0913058107>
- Wilson, M.I., D.J. Gill, O. Perisic, M.T. Quinn, and R.L. Williams. 2003. PBI domain-mediated heterodimerization in NADPH oxidase and signaling complexes of atypical protein kinase C with Par6 and p62. *Mol. Cell*. 12:39–50. [https://doi.org/10.1016/s1097-2765\(03\)00246-6](https://doi.org/10.1016/s1097-2765(03)00246-6)
- Yamamoto, K., A. Venida, J. Yano, D.E. Biancur, M. Kakiuchi, S. Gupta, A.S.W. Sohn, S. Mukhopadhyay, E.Y. Lin, S.J. Parker, et al. 2020. Autophagy promotes immune evasion of pancreatic cancer by degrading MHC-I. *Nature*. 581:100–105. <https://doi.org/10.1038/s41586-020-2229-5>
- Yamasaki, A., and N.N. Noda. 2017. Structural biology of the Cvt pathway. *J. Mol. Biol.* 429:531–542. <https://doi.org/10.1016/j.jmb.2017.01.003>
- Yamashita, S.i., K. Abe, Y. Tatemichi, and Y. Fujiki. 2014. The membrane peroxin PEX3 induces peroxisome-ubiquitination-linked pexophagy. *Autophagy*. 10:1549–1564. <https://doi.org/10.4161/aut.29329>
- Yang, J.Q., H. Liu, M.T. Diaz-Meco, and J. Moscat. 2010. NBR1 is a new PBI signalling adapter in Th2 differentiation and allergic airway inflammation in vivo. *EMBO J*. 29:3421–3433. <https://doi.org/10.1038/emboj.2010.214>
- Yang, Z., S. Yang, Y.H. Cui, J. Wei, P. Shah, G. Park, X. Cui, C. He, and Y.Y. He. 2021. METTL14 facilitates global genome repair and suppresses skin tumorigenesis. *Proc. Natl. Acad. Sci. USA*. 118:e2025948118. <https://doi.org/10.1073/pnas.2025948118>
- Yorimitsu, T., and D.J. Klionsky. 2005. Atg11 links cargo to the vesicle-forming machinery in the cytoplasm to vacuole targeting pathway. *Mol. Biol. Cell*. 16:1593–1605. <https://doi.org/10.1091/mbc.e04-11-1035>
- Young, P.G., M.J. Passalacqua, K. Chappell, R.J. Llinas, and B. Bartel. 2019. A facile forward-genetic screen for Arabidopsis autophagy mutants reveals twenty-one loss-of-function mutations disrupting six ATG genes. *Autophagy*. 15:941–959. <https://doi.org/10.1080/15548627.2019.1569915>
- Yu, Z., J. Ma, X. Li, Y. Liu, M. Li, L. Wang, M. Zhao, H. He, Y. Zhang, Q. Rao, et al. 2018. Autophagy defects and related genetic variations in renal cell carcinoma with eosinophilic cytoplasmic inclusions. *Sci. Rep.* 8:9972. <https://doi.org/10.1038/s41598-018-28369-y>
- Zaffagnini, G., A. Savova, A. Danieli, J. Romanov, S. Tremel, M. Ebner, T. Peterbauer, M. Sztacho, R. Trapannone, A.K. Tarafder, et al. 2018. p62 filaments capture and present ubiquitinated cargos for autophagy. *EMBO J*. 37:e98308. <https://doi.org/10.15252/embj.201798308>
- Zeng, Y., S. Xu, Y. Wei, X. Zhang, Q. Wang, Y. Jia, W. Wang, L. Han, Z. Chen, Z. Wang, et al. 2021. The PBI protein of influenza A virus inhibits the innate immune response by targeting MAVS for NBR1-mediated selective autophagic degradation. *PLoS Pathog.* 17:e1009300. <https://doi.org/10.1371/journal.ppat.1009300>
- Zhang, J., Y.Y. Wang, Z.Q. Pan, Y. Li, J. Sui, L.L. Du, and K. Ye. 2022a. Structural mechanism of protein recognition by the FW domain of autophagy receptor Nbr1. *Nat. Commun.* 13:3650. <https://doi.org/10.1038/s41467-022-31439-5>
- Zhang, S., Y. Hama, and N. Mizushima. 2021. The evolution of autophagy proteins - diversification in eukaryotes and potential ancestors in prokaryotes. *J. Cell Sci.* 134:jcs233742. <https://doi.org/10.1242/jcs.233742>
- Zhang, S., E. Yazaki, H. Sakamoto, H. Yamamoto, and N. Mizushima. 2022b. Evolutionary diversification of the autophagy-related ubiquitin-like conjugation systems. *Autophagy*:1–16. <https://doi.org/10.1080/15548627.2022.2059168>
- Zhang, Y., and Z. Chen. 2020. Broad and complex roles of NBR1-mediated selective autophagy in plant stress responses. *Cells*. 9:2562. <https://doi.org/10.3390/cells9122562>
- Zhou, J., J. Wang, Y. Cheng, Y.J. Chi, B. Fan, J.Q. Yu, and Z. Chen. 2013. NBR1-mediated selective autophagy targets insoluble ubiquitinated protein aggregates in plant stress responses. *PLoS Genet.* 9:e1003196. <https://doi.org/10.1371/journal.pgen.1003196>
- Zhou, J., J. Wang, J.Q. Yu, and Z. Chen. 2014. Role and regulation of autophagy in heat stress responses of tomato plants. *Front. Plant Sci.* 5:174. <https://doi.org/10.3389/fpls.2014.00174>

